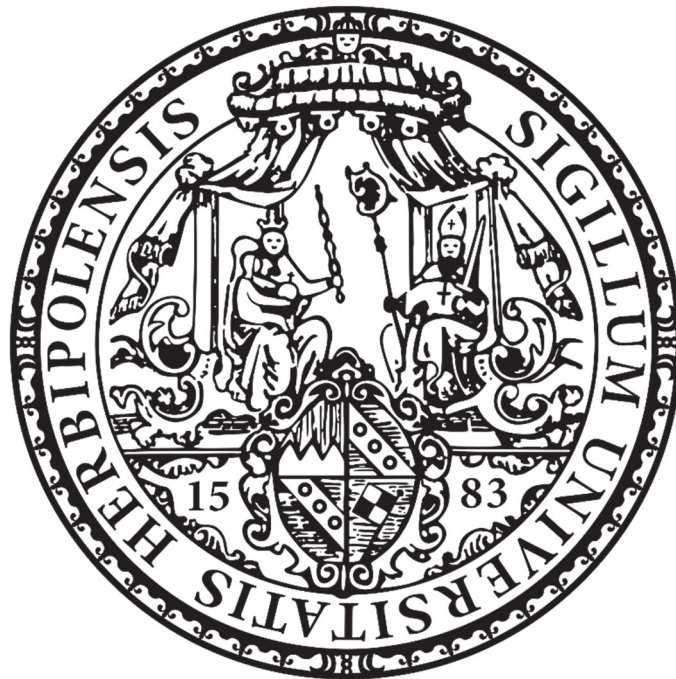


# Synthesis of Analogues and Hybrid Ligands of Pilocarpine for the Study of Muscarinic Receptor Dynamics



Dissertation

zur Erlangung des naturwissenschaftlichen Doktorgrades  
der Julius-Maximilians-Universität Würzburg

vorgelegt von

**Christine Silvia Heinz**

aus Thüngen

Würzburg 2022





Eingereicht bei der Fakultät für Chemie und Pharmazie am:

.....

Gutachter der schriftlichen Arbeit

1. Gutachter: .....

2. Gutachter: .....

Prüfer des öffentlichen Promotionskolloquiums

1. Prüfer: .....

2. Prüfer: .....

3. Prüfer: .....

Datum des öffentlichen Promotionskolloquiums

.....

Doktorurkunde ausgehändigt am

.....



## Acknowledgment

This work has been carried out under supervision of Prof. Dr. Ulrike Holzgrabe at the chair of Medicinal Chemistry at the Institute of Pharmacy and Food Chemistry of the Julius-Maximilians-University Würzburg. I gratefully thank her for the possibility to work in her group on this challenging and interesting topic, and for the possibility to work very independently on my research topic while supporting my work with expert advice.

I would like to thank Jun.-Prof. Dr. Marcel Bermudez for the computational basis of the project on pilocarpine analogues and his openness to discussions on the topic.

I thank my cooperation partner Prof. Dr. Carsten Hoffmann and his group members Dr. Michael Kauk, Carolin Grosse and Natasha Jaiswal for the pharmacological testing and helpful discussions about interpretation of the results.

I am grateful to Jun.-Prof. Dr. Oliver Scherf-Clavel for the training on the semipreparative HPLC and his spontaneous support whenever HPLC problems arose.

I would like to acknowledge my current and former colleagues for training on various techniques, NMR and LC-MS measurements, helpful discussions on research problems and a comfortable working atmosphere – including coffee, tea, lunch and ice breaks: Lina, Flo, Dani, Jogi, Miri, Nils, Jens, Nina, Lu, Christine E., Christiane, Alex, Curd, Antonio, Anja, Paul, Niclas, Nicolas, Klaus, Patrick, Markus, Jonas U., Jonas W., Joseph, Emilie, Theresa, Cristian, Nelson, Mohamed, Sylvia, Rasmus, Sebastian, Adrian, Liling, Laura, Lukas, Ruben, and Joshua; and the technical support team Christoph, Matthias and Karl as well as the secretaries Martina and Frau Möhler for solving the daily technical and bureaucratic problems.

I would also like to thank my internship students Christine Sternstein and Angela Münch for their synthetic work and the discussions about synthetic problems.

Further, many thanks to the team of the 5<sup>th</sup> semester for the uncomplicated way of working together and always being there to help each other: Prof. Dr. Petra Högger, Klaus, Dani, Theresa, Max, Jasmin, Silke, Renate, Eva-Maria.

Last but not least, I thank my family for supporting me at all stages of this work and on the whole journey leading there.



# Table of Contents

<b>1</b>	<b>Introduction.....</b>	<b>1</b>
1.1	Muscarinic Acetylcholine Receptors (mAChRs).....	1
1.1.1	Physiological Role of mAChRs .....	1
1.1.2	mAChRs as Important Drug Targets .....	3
1.1.3	Structure and Function of mAChRs .....	5
1.1.4	Allosteric Modulation of mAChRs .....	7
1.1.5	Dualsteric Ligands for mAChRs.....	9
1.2	Pilocarpine as a Partial Agonist of mAChRs.....	12
1.2.1	Discovery and Clinical Use of Pilocarpine.....	12
1.2.2	Partial Agonism of Pilocarpine .....	13
1.2.3	Structure–Activity Relationships of Pilocarpine .....	15
1.2.4	The Putative Binding Pose of Pilocarpine.....	17
1.2.5	Pharmacological Studies of Ternary Complexes with Pilocarpine .....	18
<b>2</b>	<b>Aim of the Work .....</b>	<b>20</b>
<b>3</b>	<b>Hybrid Ligands with Pilocarpine Analogues as Orthosteric Moiety .....</b>	<b>21</b>
3.1	Design of the Pilocarpine-Based Hybrid Ligands .....	21
3.2	Synthesis of the Pilocarpine-Based Hybrid Compounds .....	22
3.2.1	Synthesis of Pilocarpine Analogues as Orthosteric Fragments of Hybrid Compounds and as Orthosteric Reference Compounds.....	22
3.2.2	Synthesis of Hybrid Molecules with Pilocarpine Analogues as Orthosteric Moiety.....	33
3.3	Stability of Pilocarpine and the Hybrid Ligands.....	37
3.4	Protonation State of the Orthosteric Fragments and the Hybrid Compounds at Physiological pH .....	39
3.5	Pharmacological Evaluation of the Orthosteric Fragments and the Hybrid Compounds .....	41
3.5.1	The Mini-G NanoBRET Assay .....	41
3.5.2	Results of the Mini-G NanoBRET Assay.....	42
3.5.3	Discussion of the Effects of Hybrid Formation in Pilocarpine-Based Hybrid Ligands .....	47

<b>4</b>	<b>Synthesis of Pilocarpine Analogues for the Study of Pilocarpine's Binding Mode in mAChRs ..</b>	<b>53</b>
4.1	Synthesis of Diastereomeric Mixtures of Pilocarpine Analogues and Approaches to their Separation.....	53
4.1.1	Methylation of Racemic Desmethyl Pilocarpine.....	53
4.1.2	Synthesis of Pilocarpine Analogues by Radical Cyclisation .....	54
4.1.3	Synthesis of Diastereomeric Mixtures of Pilocarpine Analogues by a Michael-Addition-Alkylation Reaction.....	57
4.1.4	Trials to Separate the Diastereomers and Enantiomers of the Pilocarpine Analogues by Chiral HPLC .....	63
4.1.5	Trials to Separate the Diastereomers and Enantiomers of the Pilocarpine Analogues by Fractional Crystallisation .....	65
4.2	Diastereoselective Synthesis of Pilocarpine Analogues .....	67
4.2.1	Tested Diastereoselective Synthesis of Pilocarpine Analogue <b>31c</b> by Heterogenous Hydrogenation of an Exocyclic Double Bond .....	67
4.2.2	Diastereospecific Synthesis of Racemic Pilocarpine Analogues by Hydrogenation of an Endocyclic Double Bond .....	69
<b>5</b>	<b>Summary .....</b>	<b>78</b>
<b>6</b>	<b>Zusammenfassung .....</b>	<b>82</b>
<b>7</b>	<b>Experimental .....</b>	<b>86</b>
7.1	General Methods and Techniques.....	86
7.1.1	Chemicals .....	86
7.1.2	Thin Layer Chromatography (TLC).....	86
7.1.3	Flash Column Chromatography.....	86
7.1.4	Purification by Preparative HPLC.....	86
7.1.5	LC–MS Analysis.....	87
7.1.6	NMR Spectroscopy .....	88
7.1.7	FT-IR Spectroscopy .....	88
7.1.8	Purity Determination.....	88
7.1.9	Melting Point Determination .....	91
7.1.10	Determination of Specific Optical Rotation .....	91



7.1.11	Vacuum Pumps.....	92
7.1.12	Degasification of Solvents .....	92
7.1.13	Cooling Baths.....	92
7.2	Synthesis of the Aldehyde Precursors .....	92
7.2.1	Synthesis of a Regioisomeric Mixture of 1-Benzyl-1 <i>H</i> -imidazole-4/5-carbaldehyde ( <b>40/42</b> ) <sup>[83]</sup> .....	92
7.2.2	Synthesis of 1-Benzyl-1 <i>H</i> -imidazole-5-carbaldehyde ( <b>40</b> ) .....	93
7.2.3	Synthesis of 1-Methyl-1 <i>H</i> -imidazole-5-carbaldehyde ( <b>37</b> ) .....	96
7.3	Synthesis of Pilocarpine Analogues as Orthosteric Moieties and References .....	98
7.3.1	Generation of Pilocarpine as a free base ( <b>2</b> ) <sup>[81]</sup> .....	98
7.3.2	Preparation of Isopilocarpine ( <b>15</b> ) .....	99
7.3.3	Attempted Stereospecific Synthesis of Pilocarpine and Pilosinine .....	101
7.3.4	Synthesis of the Racemic Simplified Analogue of Pilosinine ( <b>35</b> ).....	106
7.4	Synthesis of the Hybrid Ligands.....	112
7.4.1	Synthesis of the Allosteric Moiety with Linker ( <b>64</b> ) .....	112
7.4.2	Synthesis of <i>rac-N</i> -Desmethyl-Pilosinine-6-Naph ( <b>69</b> ) .....	115
7.4.3	Synthesis of Pilosinine-6-Naph ( <b>70</b> ).....	116
7.4.4	General Procedure for the Synthesis of the Pilo-n-Naph Hybrids ( <b>33a-c</b> ).....	117
7.4.5	General Procedure for the Synthesis of the Isopilo-n-Naph Hybrids ( <b>34a-c</b> ).....	119
7.5	Synthesis of Pilocarpine Analogues for the Study of Pilocarpine's Binding Mode in mAChRs....	122
7.5.1	Attempted Nonstereospecific Synthesis by Radical Ring Closure.....	122
7.5.2	Nonstereospecific Synthesis by Conjugate Addition to 3(2 <i>H</i> )-Furanone .....	124
7.5.3	Attempted Stereospecific Synthesis by Hydrogenation of an Exocyclic Double Bond .....	134
7.5.4	Stereospecific Synthesis by Hydrogenation of an Endocyclic Double Bond .....	138
7.6	Stability of Pilocarpine .....	152
<b>8</b>	<b>References</b> .....	<b>153</b>
<b>9</b>	<b>Appendix</b> .....	<b>163</b>



## Abbreviations

AC	adenylyl cyclase
AcCoA	acetyl coenzyme A
ACh	acetylcholine
AChE	acetylcholineesterase
AIBN	azobisisobutyronitrile
ATP	adenosine triphosphate
BHT	2,6-di-tert-butyl-4-methylphenol
BQCAD	benzyl quinolone carboxylic acid derivative
BRET	bioluminescence resonance energy transfer
cAMP	cyclic adenosine monophosphate
CCh	carbachol
ChAT	choline acetyltransferase
COPD	chronic obstructive pulmonary disease
DCC	<i>N,N'</i> -dicyclohexylcarbodiimide
de	diastereomeric excess
DMAP	4-dimethylaminopyridine
DMPU	<i>N,N'</i> -dimethylpropyleneurea
$E_{\max}$	efficacy
GDP	guanosine diphosphate
GPCR	G protein-coupled receptor
GTP	guanosine triphosphate
HD	$\alpha$ -helical domain
HEKt cell	human embryonic kidney cell expressing SV40 large T antigen
HEPES	2-[4-(2-hydroxyethyl)piperazin-1-yl]ethane-1-sulfonic acid
HMBC	heteronuclear multiple bond correlation (NMR)
HWE	Horner-Wadsworth-Emmons
IP <sub>3</sub>	inositol triphosphate
iper	iperoxo
isopilo	isopilocarpine
KHMDS	potassium bis(trimethylsilyl)amide
LDA	lithium diisopropylamide
LiHMDS	lithium bis(trimethylsilyl)amide
mAChR	muscarinic acetylcholine receptor

MCh	methacholine
M <sub>x</sub>	subtype x of mAChR
nAChR	nicotinic acetylcholine receptor
naph	naphthalimidopropylamino
NES	nuclear export sequence
NLuc	NanoLuciferase
NMS	<i>N</i> -methylscopolamine
PhFI	phenylfluorenyl
phth	phthalimidopropylamino
PI	phosphatidylinositol
pilo	pilocarpine
PLC	phospholipase C
PVDF	polyvinylidene fluoride
qNMR	quantitative NMR
sco	scopolamine
S <sub>N</sub> 2	nucleophilic substitution of second order
TM	transmembrane helix
TMEDA	tetramethylenediamine
V	Venus protein
VAcHT	vesicular acetylcholine transporter

# 1 Introduction

## 1.1 Muscarinic Acetylcholine Receptors (mAChRs)

### 1.1.1 Physiological Role of mAChRs

Muscarinic Acetylcholine Receptors are present in the synapses of the central and the peripheral nervous system. In the central nervous system, they are involved in the regulation of temperature or vascular tonus, learning processes, and memory, for example. Within the peripheral nervous system, mAChRs are found in all preganglionic neurons of the autonomous nervous system, in motoneurons and in postganglionic neurons of the parasympathetic nervous system.<sup>[1]</sup> In smooth muscles, for example, signals coming from motoneurons activate mAChRs to increase cellular  $\text{Ca}^{2+}$  levels leading to muscle contraction.<sup>[2]</sup>

mAChRs are class A G protein-coupled receptors (GPCRs). The general mode of action first involves receptor activation by the binding of the neurotransmitter acetylcholine (1) as the endogenous agonist (Figure 1). The activated receptor activates a heterotrimeric G protein recruited to the intracellular part of the receptor, triggering an exchange of G protein-bound GDP to GTP. This leads to dissociation of the G protein from the receptor and of the GTP-bound  $\text{G}_\alpha$  subunit from the  $\text{G}_{\beta\gamma}$  subunits. The two different parts of the G protein, but mainly the  $\text{G}_\alpha$  subunit, are responsible for activating effectors which propagate the signalling cascade within the cell.<sup>[3]</sup>

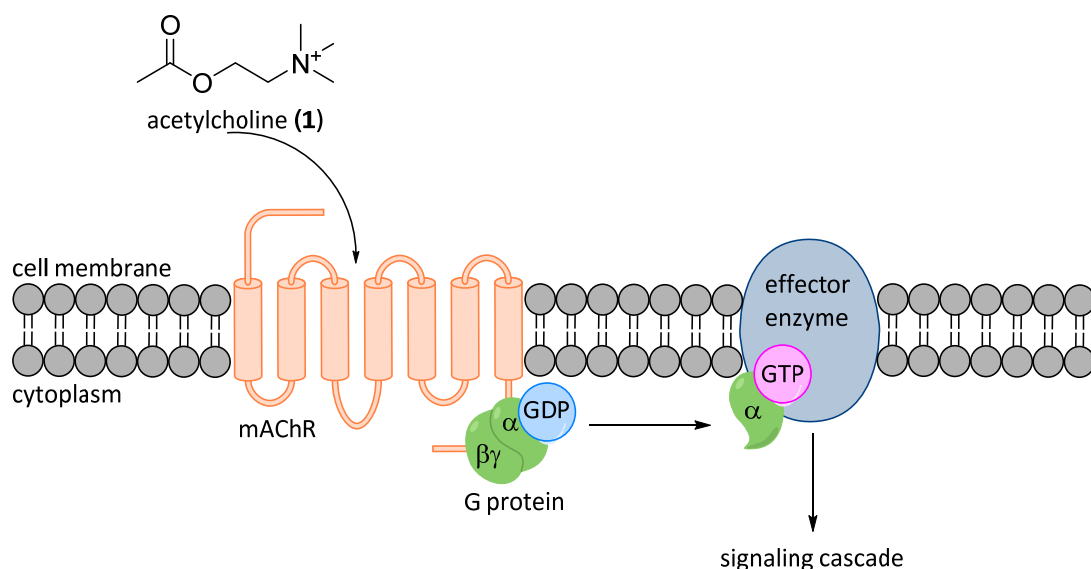


**Figure 1:** Signal transduction by mAChRs. Binding of the neurotransmitter acetylcholine to the mAChR activates the receptor, leading to recruitment of the G protein followed by an exchange of G protein-bound GDP to GTP. Subsequent dissociation of the  $\text{G}_\alpha$  subunit activates the effector enzymes and initiates the intracellular signalling cascade.

The mAChRs are a family of five different receptor subtypes,  $\text{M}_1$  to  $\text{M}_5$ . The receptors of the odd numbered subtypes ( $\text{M}_1$ ,  $\text{M}_3$  and  $\text{M}_5$ ) are coupled to the  $\text{G}_{q/11}$  family of G proteins, which activate

phospholipase C to produce the second messengers inositol triphosphate (IP<sub>3</sub>) and diacylglycerol (DAG) by the cleavage of phosphatidylinositol 4,5-bisphosphate (PIP<sub>2</sub>) (Figure 2). IP<sub>3</sub> leads to an increase of the Ca<sup>2+</sup> concentration within the cell. In contrast, the even numbered subtypes (M<sub>2</sub> and M<sub>4</sub>) are coupled to G<sub>i/o</sub> proteins. The activated G<sub>i/o</sub> protein inhibits adenylyl cyclase leading to reduced cyclisation of ATP to cyclic adenosine monophosphate (cAMP), which is involved in the regulation of protein kinase A (PKA) and cAMP-gated channels.<sup>[1a, 4]</sup>

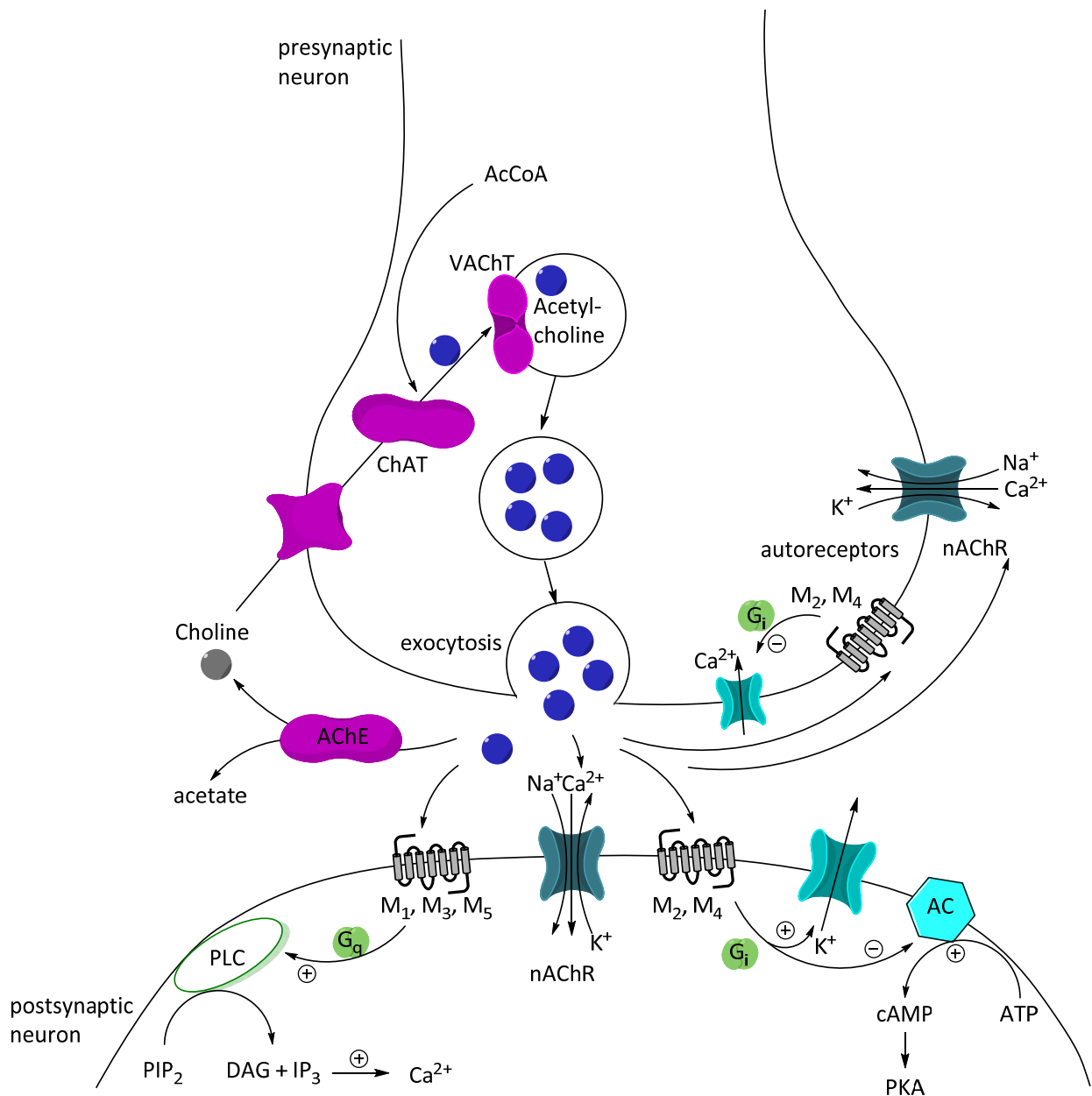


**Figure 2:** Representation of the processes involved in signal transduction over the synaptic cleft (adapted by permission from Springer Nature Customer Service Centre GmbH: Springer, Pharmakologie und Toxikologie by Freissmuth, M., Offermanns, S., Böhm, S.; Copyright 2016). AcCoA: acetyl coenzyme A, nAChR: nicotinic acetylcholine receptor, AChE: acetylcholine esterase, ChAT: choline acetyltransferase, VACHT: vesicular acetylcholine transporter, PLC: phospholipase C, AC: adenylyl cyclase.

In the context of signal transduction in a cholinergic synapse, activation of mAChRs by acetylcholine plays different roles (Figure 2). When an action potential reaches the synapse, the neurotransmitter

acetylcholine (**1**) is released from vesicles in the presynaptic neuron into the synaptic cleft and binds to mAChRs. This leads to receptor activation and induces a longer lasting depolarisation of the postsynaptic membrane having a neuromodulating effect. In contrast, a fast synaptic transmission is assured by activation of ion channels, the nicotinic acetylcholine receptors, located at the postsynaptic membrane.

Various factors can end the signalling cascade. mAChRs in the presynaptic membrane, so-called autoreceptors, are part of a negative feedback cycle to inhibit neurotransmitter release. Additionally, the remaining acetylcholine is hydrolysed by the acetylcholine esterase in the synaptic cleft, and the mAChRs are desensitised by phosphorylation, followed by the recruitment of  $\beta$ -arrestin resulting in endocytosis.<sup>[3]</sup>

### 1.1.2 mAChRs as Important Drug Targets

mAChR activation can be influenced by small synthetic molecules. Full agonists activate the receptor with a similar efficacy to the endogenous agonist acetylcholine. Partial agonists activate the receptor with less efficacy than acetylcholine. Competitive antagonists bind to the receptor and inhibit activation by agonists but do not have any effect on their own. Inverse agonists reduce the receptor's basal activity (Figure 3).<sup>[5]</sup>

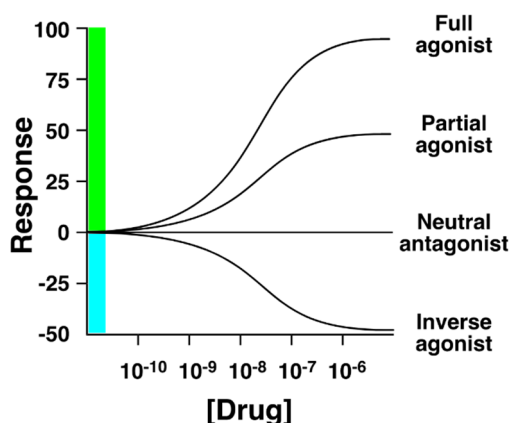


**Figure 3:** Possible dose response curves for the effects of ligands (drugs) on receptor activation. The response level is set to zero for the constitutive activity of the receptor, i.e. the signal obtained without ligand. (Adapted from <sup>[6]</sup> with permission by the Creative Commons Attribution-Share Alike 4.0 International licence.)

Due to their widespread physiological distribution and implication in various fundamental processes, mAChRs seem to be very promising targets for the treatment of several diseases. This includes applications in the central nervous system for the treatment of Alzheimer's disease, Parkinson's disease, schizophrenia or drug addiction as well as peripheral applications to treat obesity, COPD, xerostomia or type-2-diabetes.<sup>[7]</sup>

Currently approved drugs include the mAChR partial agonist pilocarpine (**2**) and several mAChR antagonists. For example, atropine (**3**) and scopolamine (**4**) are used topically as eyedrops for the

## Introduction

inactivation of the ciliary muscle. Atropine (**3**) is also used as an antidote against poisoning with phosphororganic substances in pesticides or nerve agents. The antagonist butylscopolaminium bromide (**7**) is applied as spasmolytic drug, and the antagonist biperiden (**5**) is used in the treatment of Parkinson's disease. The antagonist tiotropiumbromide (**6**) is a topical long term treatment of COPD.<sup>[1a, 8]</sup>

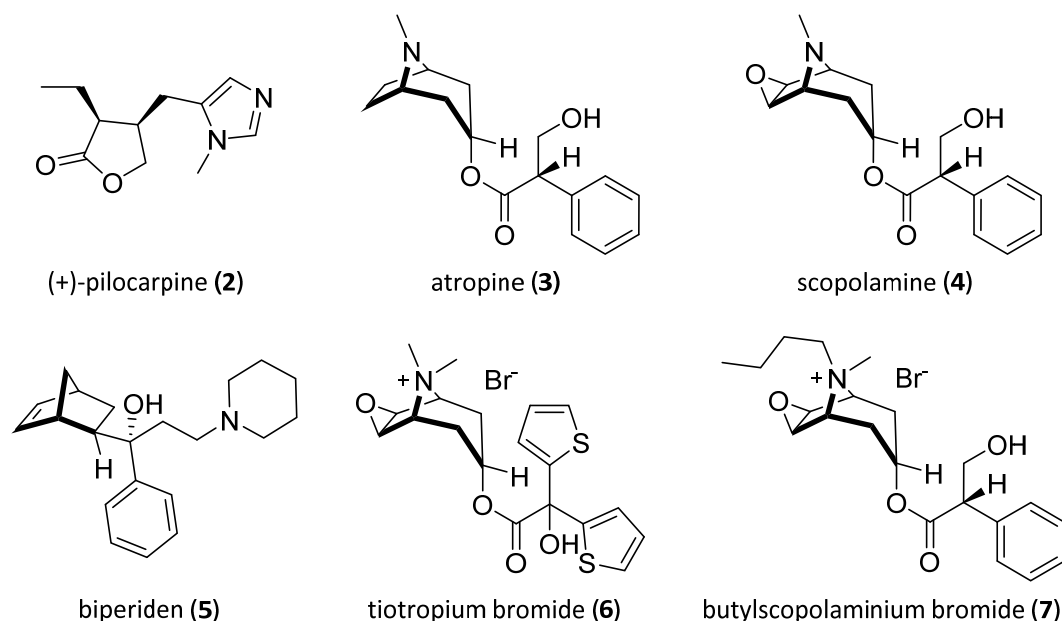


**Figure 4:** Structures of currently approved drugs which target mAChRs.

One major drawback of systemic application of general muscarinic agonists or antagonists is a wide range of side effects due to the wide physiological distribution of mAChRs. mAChR antagonists can cause side effects such as mouth dryness, fever, tachycardia, obstipation, mydriasis, or delirium. In contrast, mAChR agonists can provoke bradycardia, hypotony, bronchoconstriction, sweating or emesis.<sup>[8-9]</sup>

Most tissues express more than one subtype of the receptor. However, some subtypes have been identified to have predominant locations or roles (Table 1). For this reason, it is implied that subtype selective ligands may provide better therapeutic profiles (Table 2).

**Table 1:** Predominant expression and roles of the different subtypes of mAChRs.

Receptor subtype	Predominant expression/roles
M <sub>1</sub>	central nervous system (cortex, striatum, hippocampus), cognition <sup>[10]</sup>
M <sub>2</sub>	heart rate, temperature regulation, learning memory <sup>[7]</sup>
M <sub>3</sub>	exocrine gland secretion, smooth muscles contractility, pupil dilation, food intake, weight gain <sup>[7]</sup>
M <sub>4</sub>	wound healing, modulation of dopamine activity in motor tracts <sup>[11]</sup>
M <sub>5</sub>	tone of cerebral blood vessels, modulation of central dopamine function <sup>[11]</sup>

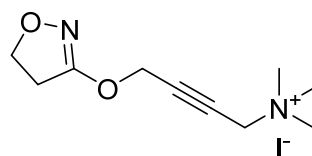


**Table 2:** Examples of potential therapeutic uses of mAChR subtype-selective compounds (adapted from<sup>[7]</sup>).

Clinical condition	Drug
Alzheimer's disease	M <sub>1</sub> , M <sub>5</sub> or mixed M <sub>1</sub> /M <sub>5</sub> agonist, M <sub>2</sub> antagonist
Sjogren's syndrome	M <sub>1</sub> , M <sub>3</sub> or mixed M <sub>1</sub> /M <sub>3</sub> agonist
Schizophrenia	M <sub>1</sub> , M <sub>4</sub> or mixed M <sub>1</sub> /M <sub>4</sub> agonist
Parkinson's disease	M <sub>1</sub> , M <sub>4</sub> or mixed M <sub>1</sub> /M <sub>4</sub> antagonist
Type-2-diabetes	M <sub>3</sub> agonist (peripherally acting)
Obesity	M <sub>3</sub> antagonist (peripherally acting)
COPD	M <sub>3</sub> antagonist
Drug addiction and withdrawal	M <sub>5</sub> antagonist

### 1.1.3 Structure and Function of mAChRs

Since 2012, all five receptor subtypes have been crystallised in their inactive conformation in complex with antagonists.<sup>[12]</sup> Additionally, the M<sub>2</sub> receptor was crystallised in its active conformation<sup>[13]</sup> in complex with iperoxo (**8**) (Figure 5), a superagonist, and structures of both the active M<sub>1</sub> and the active M<sub>2</sub> receptors were obtained by cryogenic electron microscopy.<sup>[14]</sup> This library allows for deductions about the mechanism of receptor activation and about the differences between the receptor subtypes to further ease the search for subtype selective ligands.



iperoxo iodide (**8**)

**Figure 5:** Structure of the superagonist iperoxo.

The common structure of all mAChRs includes a highly conserved core of seven transmembrane helices (TM) which are linked by three intracellular and three extracellular loops (Figure 6a). An additional helix 8 is located in the cytoplasm. The N-terminus is found on the extracellular side, the C-terminus on the intracellular side of the membrane. The transmembrane helices are arranged to create a hydrophilic channel which is only interrupted by three conserved hydrophobic residues: L<sup>2.46</sup>, L<sup>4.43</sup>, I<sup>6.40</sup> (Ballesteros-Weinstein numbers<sup>[15]</sup>) (Figure 6b). The orthosteric binding site, i.e. the binding site of the endogenous ligand acetylcholine, is located inside this central channel towards the extracellular side within a highly conserved region (Figure 6a). A second binding site, known as the common allosteric binding site or the extracellular vestibule, is positioned in an extracellular receptor region which is less conserved between subtypes.<sup>[12a, 12c]</sup> The receptor interacts with the G protein via another allosteric binding site in the cytosol.

## Introduction

The main interactions with the orthosteric ligand are formed with the side chains of TM3-7 including hydrogen bonds with D<sup>6.52</sup> and a charge-charge interaction with D<sup>3.32</sup>. These interactions orient the ligand within the binding site. Additionally, the amine or ammonium function of the ligand is enclosed by aromatic residues forming a lid, referred to as the tyrosin-lid, over the ligand resulting in distinct separation of the orthosteric site from the allosteric site (Figure 6c).<sup>[12a]</sup>

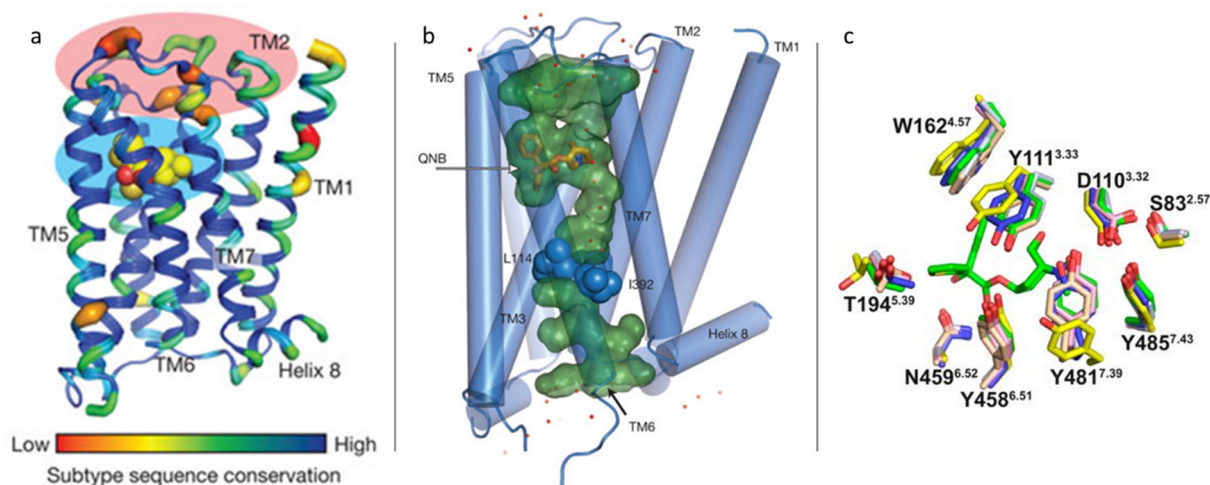


**Figure 6:** a) The M<sub>3</sub> acetylcholine receptor with highlighted regions of the orthosteric (blue) and the common allosteric binding site (red). The allosteric site marks the extracellular part, helix 8 the intracellular part of the receptor. The structure is coloured by sequence conservation among the five mAChR subtypes. (Reprinted with permission by Springer Nature Customer Service Centre GmbH: Nature<sup>[12b]</sup> Copyright 2012) b) The aqueous channel within the mAChRs. The channel is interrupted by hydrophobic residues (blue spheres), water molecules are shown as red dots. The antagonist QNB is represented in the orthosteric site. (Reprinted with permission by Springer Nature Customer Service Centre GmbH: Nature<sup>[12a]</sup> Copyright 2012) c) Overlay of the residues of the orthosteric site of M<sub>1</sub>.tiotropium (peach), M<sub>2</sub>.NMS (blue), M<sub>2</sub>.AF-DX384 (yellow), M<sub>3</sub>.tiotropium (grey), M<sub>4</sub>.tiotropium (pink) and M<sub>5</sub>.tiotropium (green). The antagonist tiotropium (6) is shown as crystallised in M<sub>5</sub>.tiotropium.<sup>[12d]</sup> (Copyright 2019 National Academy of Sciences)

Comparison of the active and the inactive receptor conformation reveals that during activation an inward movement of TM5 and 6 and a slight rotation of TM3 occurs along with a decrease in size of the orthosteric binding pocket (Figure 7a). The binding mode of the agonist ligand, however, is still dominated by the same interactions as in the inactive conformation. In the active state, the tyrosine-lid between the orthosteric and the allosteric site is completely closed (Figure 7b and d). These changes at the orthosteric site induce a size reduction of the allosteric site (Figure 7c) and an outward movement of TM5 and 6 in the intracellular region, which creates a cavity to accommodate the C-terminus of the G protein.<sup>[13]</sup>

As the orthosteric binding site is highly conserved between the receptor subtypes, subtype selective ligands targeting solely this particular site are difficult to design. Preferences for one or another subtype can result from slight differences within the binding pocket or kinetic selectivity, as observed for tiotropium (6). Before binding to or dissociation from the receptor, tiotropium binds to the extracellular vestibule. Due to different allosteric binding modes, dissociation in this model is slower from M<sub>3</sub> than from M<sub>2</sub> explaining a selectivity for M<sub>3</sub> despite similar affinities.<sup>[12b]</sup>

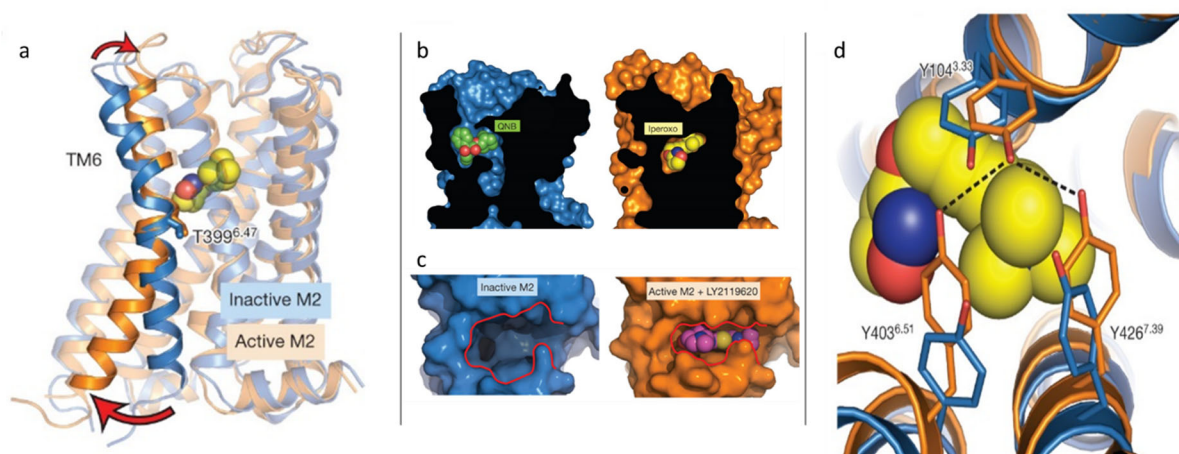


**Figure 7:** a) TM6 switches position from the inactive to the active conformation thus creating the G protein binding site and decreasing the size of the orthosteric binding site. b) Cross section through the orthosteric site of an inactive (left) and an active (right) M<sub>2</sub> receptor. The active receptor orthosteric binding site is closed off by the tyrosine lid. c) The size of the allosteric binding site is decreased in the active M<sub>2</sub> receptor in comparison to the inactive M<sub>2</sub> receptor. d) The tyrosine lid is stabilised by hydrogen bonds in the active receptor conformation.<sup>[13]</sup> (Reprinted with permission by Springer Nature Customer Service Centre GmbH: Nature <sup>[13]</sup> Copyright 2012)

#### 1.1.4 Allosteric Modulation of mAChRs

A molecule which binds to the allosteric site can modulate the receptor's response to an orthosteric ligand. The modulator can influence either affinity or efficacy of the orthosteric probe or both. An increase in affinity or efficacy is referred to as positive allosteric modulation, while negative allosteric modulation results in a decrease in affinity or efficacy. In dose-response curves, modulation of affinity is reflected by a horizontal shift of the curve (Figure 8). Modulation of efficacy shifts the maximum receptor response to higher or lower values<sup>[16]</sup> and combinations of both effects can be observed.<sup>[17]</sup> Neutral allosteric ligands do not have any influence on the receptor's response. However, they might compete with other positive or negative allosteric modulators for the common allosteric binding site.<sup>[16, 18]</sup>

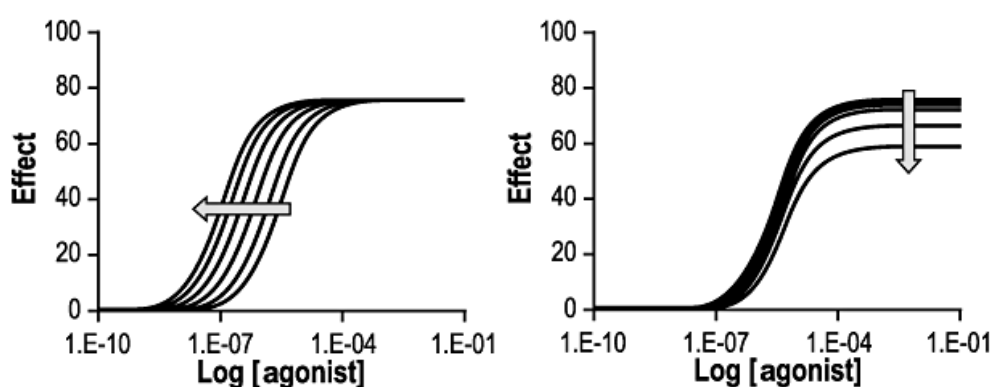


**Figure 8:** The effect of positive binding cooperativity (left) and negative activation cooperativity in allosteric modulation (right) on dose response curves. (Adapted with permission by John Wiley & Sons, Inc.: British Journal of Pharmacology<sup>[19]</sup> Copyright 2012)

The mechanism behind allosteric modulation is thought to rely on a stabilising or destabilising effect of various possible receptor conformations. Positive binding cooperativity results when the orthosteric

## Introduction

and the allosteric ligand stabilise the same conformation in which the binding interaction with the receptor is optimised for both molecules.<sup>[18a, 19]</sup> The allosteric modulator might contribute to the stabilisation of one receptor conformation by stabilising parts of the extracellular loops in a fixed geometry.<sup>[18a]</sup> In the M<sub>4</sub> receptor, a network of residues, the so-called “cooperativity network”, links the orthosteric and the allosteric binding sites.<sup>[12c]</sup> The residues along the extracellular loop 2 and in the interface between both binding sites energetically relate both sites to mediate cooperativity.

As a result, allosteric modulators show strong probe dependency.<sup>[19]</sup> One molecule can simultaneously be positive or negative allosteric modulator depending on which orthosteric ligand is bound. Naphmethonium (**9**), for example, shows negative binding cooperativity in combination with acetylcholine (**1**), but positive binding cooperativity with pilocarpine (**2**).<sup>[17]</sup>

Another result of the supposed various specific receptor conformations induced by different couples of allosteric and orthosteric ligands is biased signalling. In many cases, receptors activate more than one signalling cascade, i.e. they either activate more than one specific G protein or recruit  $\beta$ -arrestin in addition to the usual G protein activation.<sup>[20]</sup> Allosteric ligands have been observed to introduce a bias into the system specific equilibrium between the different signalling pathways.<sup>[21]</sup> A possible explanation for this observation is, that the allosteric modulator induces an active receptor conformation, which is slightly different to the active receptor conformation without an allosteric modulator. This results in a differential recruitment of G protein or  $\beta$ -arrestin on the intracellular level. These findings promise possible allosteric drugs, which provoke less side effects than orthosteric drugs.<sup>[19, 22]</sup>

As the common allosteric binding site is less conserved than the orthosteric binding site, receptor subtype selective allosteric modulators are known. In most cases, the exact mechanism responsible for selectivity remains unclear. However, some M<sub>1</sub> selective positive allosteric modulators are thought to occupy a cryptic pocket. Computational simulations have shown that this pocket is open most often in M<sub>1</sub> allosteric sites but preferably closed in the other receptor subtypes.<sup>[23]</sup> Studies of the M<sub>2</sub> receptor have identified the so called <sup>172</sup>EDGE<sup>175</sup> sequence, a very polar sequence in the extracellular loop of M<sub>2</sub>, to greatly influence the subtype selectivity for M<sub>2</sub>.<sup>[16-17, 24]</sup>

In general, allosteric modulators provide therapeutic advantages over orthosteric ligands. The aim of less side effects can be reached due to subtype selectivity and probe dependency of the allosteric modulation. Allosteric modulators only have an effect in presence of the orthosteric ligand which preserves physiological temporal patterns of signalling and reduces side effects, and the ceiling effect due to modulation, instead of activation, reduces the risks in case of an overdose.<sup>[16, 19]</sup>

### 1.1.5 Dualsteric Ligands for mAChRs

Recent attempts to overcome the challenge of subtype selectivity while applying knowledge of allosteric modulation have led to the design of dualsteric ligands. Dualsteric ligands bind to both receptor binding sites simultaneously. The idea was to link an allosteric modulator via a linking unit to an orthosteric ligand (Figure 9a). The allosteric modulator should convey subtype selectivity whereas the orthosteric ligand activates or blocks the receptor. This concept corresponds to the message-address principle of Schwyzer.<sup>[16, 25]</sup>

The first and most studied dualsteric ligands target the M<sub>2</sub> receptor. They consist of a phthalimidopropylamino (phth) or naphthalimidopropylamino (naph) moiety derived from the M<sub>2</sub> selective negative allosteric modulators W84 (**10**) or naphmethonium (**9**), an alkyl linker chain and iperoxo (iper) (**8**), an unselective superagonist of mAChRs<sup>[26]</sup> (Figure 10a–c). These ligands provided proof of concept by showing the expected dualsteric binding mode, agonistic properties due to the orthosteric moiety and subtype selectivity for the M<sub>2</sub> receptor due to the selective allosteric moiety.<sup>[25b, 27]</sup> The hybrid ligands were partial agonists which can partly be explained by the additional flexibility conveyed by the alkyl linker. The degree of partial agonism was found to be tunable by the choice of linker length and flexibility, which strongly influences whether the ligand is bound dualsterically or in a purely allosteric binding mode. The more the dualsteric binding mode prevails, the more receptor response was observed (Figure 9b).<sup>[28]</sup>

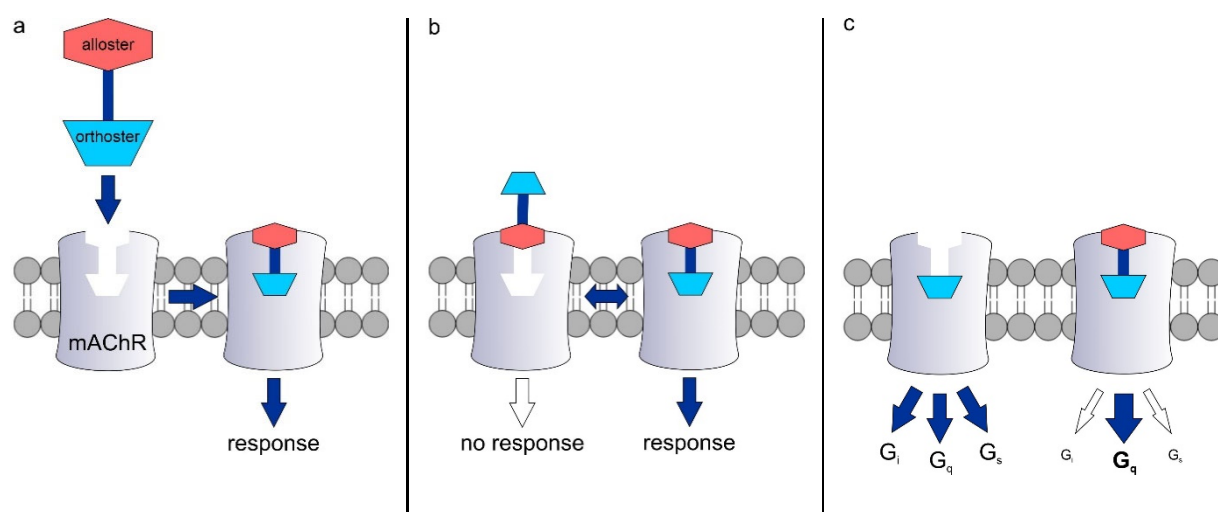


**Figure 9:** a) The general design of a dualsteric ligand consists of an allosteric and an orthosteric ligand of the mAChR connected by a linker. The orthosteric moiety (blue) binds to the orthosteric binding site at the center of the receptor while the allosteric moiety binds to the allosteric vestibule in the extracellular region of the receptor. b) Dualsteric ligands can bind in a purely allosteric mode and in a dualsteric mode. Only the dualsteric binding mode leads to receptor activation which is the reason for partial agonism of some dualsteric agonists. c) Receptors activated with a dualsteric ligand can show signalling bias. The dualsteric ligand only activates a specific signalling pathway whereas the corresponding orthosteric ligand alone activates several possible signalling pathways.

## Introduction

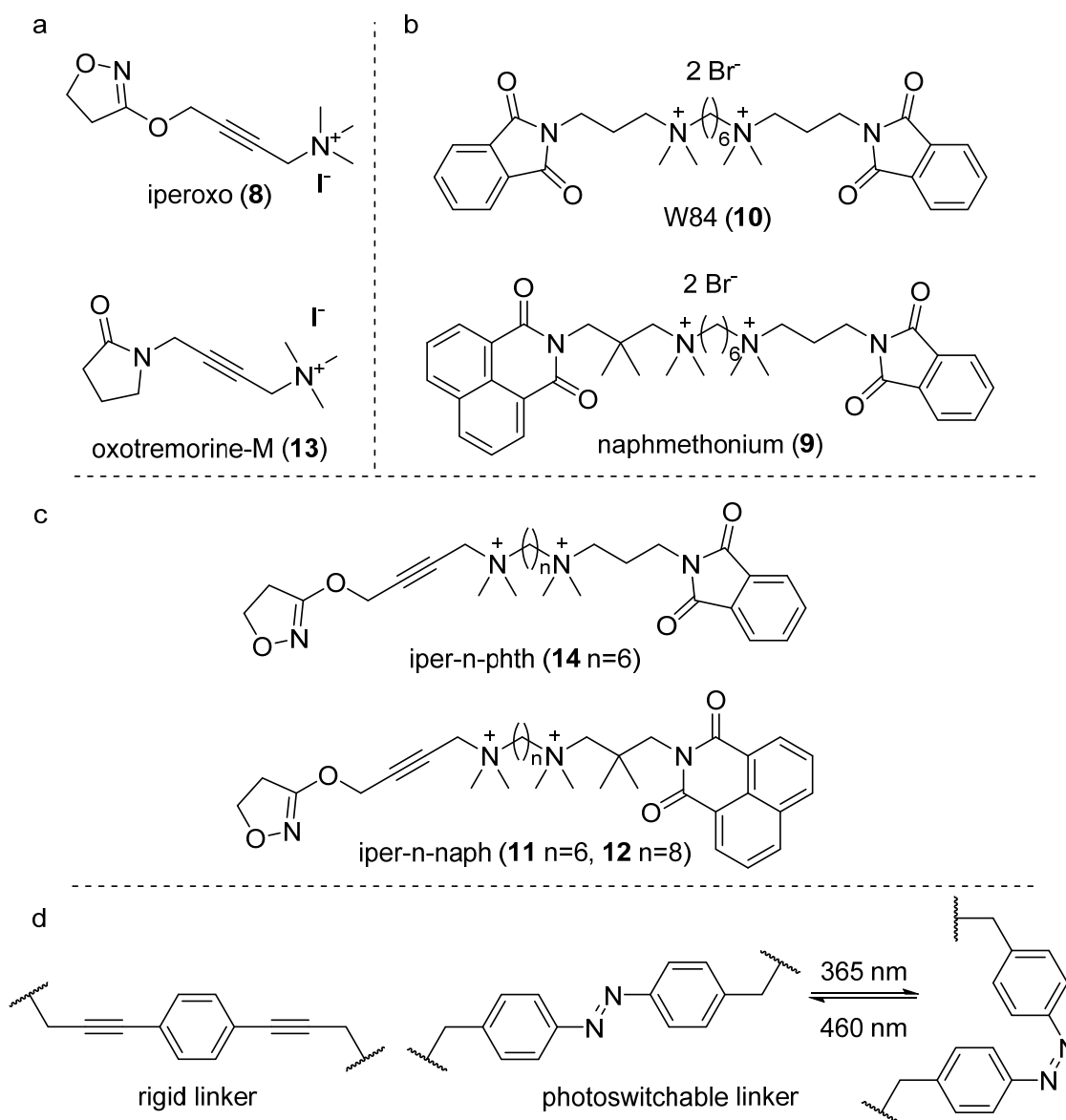


**Figure 10:** Exemplary structures of a) mAChR agonists, b) M<sub>2</sub> selective negative allosteric modulators, c) dualsteric ligands with alkyl chain linkers, d) other linkers than alkyl chains.

After the successful development of the first series of M<sub>2</sub> selective dualsteric ligands consisting of an agonist and a negative allosteric modulator, various other combinations have been created and characterized. Subtype selective dualsteric antagonists have been obtained from combinations of antagonists and allosteric modulators,<sup>[29]</sup> further subtype selective partial agonists were obtained from full agonists linked to allosteric modulators.<sup>[30]</sup>

Other features of the dualsteric ligands resemble those observed for allosteric modulators. For example, signalling bias was observed. Iperoxo (**8**) leads to activation of the G<sub>q</sub>, G<sub>i</sub> and the G<sub>s</sub> coupled pathways at the M<sub>2</sub> receptor. In contrast, iper-6-naph (**11**) only activates G<sub>i</sub> coupled pathways. Computational modelling showed that iperoxo is firmly bound in the orthosteric pocket inducing a forced position of the allosteric moiety, thus hindering complete closure of the allosteric vestibule. This effect is less pronounced with a longer linker in iper-8-naph, correlating to the observed reduced

## Introduction

G<sub>i</sub> bias of iper-8-naph (**12**) (Figure 9c).<sup>[31]</sup> Similar investigations at the M<sub>1</sub> receptor revealed a hierarchy of G protein binding: G<sub>q</sub> was still activated when short linkers were used and conformational changes due to receptor activation were minor. G<sub>i</sub> requires full binding pocket closure which was obtained with longer linkers while G<sub>s</sub> lies in between.<sup>[32]</sup>

Signalling bias was also reported at the M<sub>1</sub> receptor for various hybrid molecules with a benzyl quinolone carboxylic acid derivative (BQCAd) as allosteric moiety.<sup>[30a]</sup> In this case, the positioning of the orthosteric moiety, especially the ammonium group of the ligand, is controlled by a defined binding pose of BQCAd in the allosteric vestibule and linker length. Depending on the type of orthosteric ligand both G protein and  $\beta$ -arrestin were recruited or only G protein activation occurred.

In summary, dualsteric ligands combine the properties of orthosteric and allosteric ligands and have proven to be useful pharmacological tools for the investigation of receptor activation and signalling selectivity. The possibility to address specific receptor subtypes more selectively and to select specific signalling pathways offers approaches in the search of novel drugs showing fewer side effects.

In some cases, promising results for an in vivo application have indeed been found. The same dualsteric ligands **11** and **14** have shown context-sensitive signalling as they provoke less signalling in cAMP rich cellules than in a context of low cAMP concentrations. This led to reduced cardiac depression and better tolerability in vivo compared to the orthosteric agonist oxotremorine-M (**13**).<sup>[33]</sup> Additionally, peripheral antinociceptive properties without severe side effects<sup>[34]</sup> and cytotoxic effects on glioblastoma cancer stem cells<sup>[35]</sup> were shown. Another study showed that replacement of the hexamethylene linker of iper-6-phth (**14**) by a photoswitchable linker with an azo group (Figure 10d) led to compounds with variable geometry, which allowed to control cardiac function by external light irradiation.<sup>[36]</sup>

That these preliminary studies of dualsteric agonists have the potential to lead to pharmaceutical applications has been demonstrated with antagonistic dualsteric ligands: revefenacin (Yupelri) by Theravance/Mylan showing kinetic selectivity for the M<sub>3</sub> receptor<sup>[37]</sup> has been approved by the FDA for the inhalative treatment of COPD<sup>[38]</sup> and bafenterol by Theravance/GSK, a bifunctional compound with characteristic M<sub>2</sub>/M<sub>3</sub> antagonism and  $\beta$ 2-adrenegic agonism,<sup>[39]</sup> has completed clinical phase II studies for the same indication.<sup>[39]</sup>

## 1.2 Pilocarpine as a Partial Agonist of mAChRs

### 1.2.1 Discovery and Clinical Use of Pilocarpine

Pilocarpine<sup>1</sup> (**2**) is an imidazole alkaloid, which is produced as secondary metabolite in plants of the genus *Pilocarpus* of the rutaceae family (Figure 11). Several species such as *Pilocarpus jaborandi*, *Pilocarpus pennatifolius* or *Pilocarpus microphyllus* belong to the genus, all of them occurring in South America, mostly in Brazil. Many of the *Pilocarpus* species are commonly named “jaborandi”, a name supposedly originating from the Tupí word “jaborandi” (“which causes slobbering”).<sup>[40]</sup> As an extract, the roots of the jaborandi plants provoke increased sweating, salivation and urination. The South American indigenous people used it as an antidote to cure poisoning. The use as a treatment of ophthalmitis, spasm, catarrhal diseases, gonorrhoea and urinary calculus was also reported.<sup>[40]</sup> The plant was brought to Europe by Coutinho, a Brazilian physician, around the year 1874.<sup>[41]</sup> Soon afterwards, jaborandi infusions were used for a wide range of indications including fever, intoxications, neurosis, renal disease, stomatitis, influenza, and pneumonia.<sup>[40]</sup>

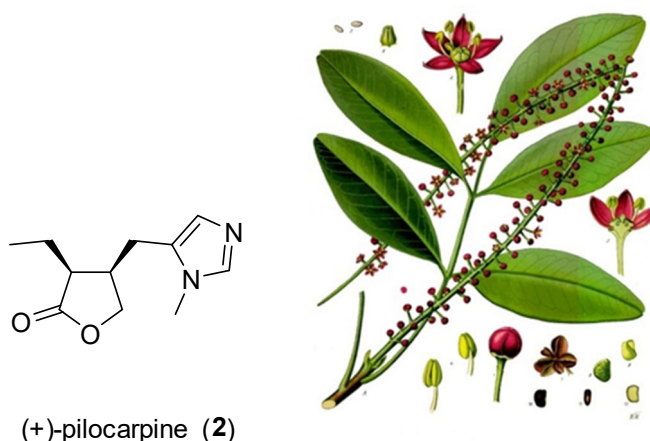


**Figure 11:** Structure of pilocarpine and a schematic representation of the *Pilocarpus pennatifolius* plant characteristics.<sup>[8]</sup>

Around the same time (1875), extraction of pilocarpus leaves or bark yielded one major alkaloid component which was named pilocarpine and identified to be responsible for the pharmacological effects of pilocarpus by Gerrard and Hardy independently.<sup>[42]</sup> The constitution of the molecule was elucidated by the year 1902 through the work of Jowett and Pinner<sup>[43]</sup>, and the stereoinformation was determined as (3*S*,4*R*) in 1966 by Hill and Barcza<sup>[44]</sup> and confirmed by X-ray crystallographic data in 1968.<sup>[45]</sup> However, the knowledge of the structure did not lead to synthetic production of pilocarpine

<sup>1</sup> For the ease of reading, the name pilocarpine is used for the naturally occurring compound, i.e. the (3*S*,4*R*)-enantiomer of pilocarpine, also designated as (+)-pilocarpine. The enantiomer or the racemic mixture will be marked as (-)-pilocarpine or racemic pilocarpine, respectively.



because synthesis proved difficult and not competitive with the extraction process from *P. jaborandi* leaves.<sup>[45]</sup>

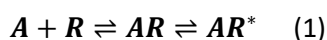
Over time, application of pilocarpine decreased. In some cases, this was due to the simple fact that pilocarpine was completely useless for the original indication, and in other cases, new drugs were more efficient or selective. In Germany, the parasympathomimetic drug pilocarpine (**2**) or its hydrochloride salt are only approved as eyedrops for the treatment of glaucoma and ocular hypertension and as film coated tablets for the treatment of xerostomia in the context of Sjogren's syndrome or radiation therapy.<sup>[46]</sup> In research, pilocarpine (**2**) is commonly used to induce epilepsy in mouse studies<sup>[47]</sup> and as an agonist of mAChRs.

### 1.2.2 Partial Agonism of Pilocarpine

After discovery of pilocarpine, its parasympathomimetic properties were soon established. Experiments investigating the effect of pilocarpine on different glands such as those for tear production,<sup>[48]</sup> sweating or salivation,<sup>[49]</sup> or on isolated tissue<sup>[50]</sup> were carried out.

After the determination of the five different mAChR subtypes, competition binding experiments and FRET studies were conducted to investigate the subtype specific receptor interactions of different agonists and antagonists. There is no published study which investigated pilocarpine's properties at all receptor subtypes, M<sub>1</sub> to M<sub>5</sub>, using the same techniques. For this reason, data from different studies are difficult to compare and are sometimes found to be contradictory. One study investigated concentration response curves of pilocarpine at the receptors M<sub>1</sub> to M<sub>4</sub> in comparison to the full agonist Carbachol (Table 3).<sup>[51]</sup> Comparable data for the M<sub>5</sub> receptor is known.<sup>[52]</sup> Pilocarpine was shown to have a lower potency of 1-2 logarithmic units than Carbachol at all receptors. At the same time, the maximum effect obtained at high concentrations of pilocarpine varies a lot between the different receptor subtypes. This means that pilocarpine is a partial agonist when observing phosphatidylinositol (PI) hydrolysis at the M<sub>3</sub> and the M<sub>5</sub> receptor or cAMP accumulation at the M<sub>2</sub> receptor. However, the general assumption of pilocarpine being a partial agonist did not hold true for PI hydrolysis experiments at M<sub>1</sub> or cAMP accumulation experiments at M<sub>4</sub>, where Pilocarpine is a full agonist. Comparisons of the intrinsic relative activity at the receptors M<sub>1-4</sub> found a selectivity of pilocarpine for M<sub>1</sub> and M<sub>3</sub> relative to M<sub>2</sub> and M<sub>4</sub>, which results from the higher potency of pilocarpine at M<sub>1</sub> and M<sub>3</sub>.<sup>[51]</sup>

A mechanistical explanation for pilocarpine being a partial agonist has not been determined. General possible reasons can be derived from a simplified description of receptor activation:



## Introduction

These equations suppose that receptor activation happens after binding of the agonist A to the receptor R to form the inactive agonist receptor complex AR. AR then undergoes conformational changes to the active complex AR\* (Equation 1). This active receptor complex can bind a G protein to form a complex with the activated G protein AR\*G\* (Equation 2).

**Table 3:** Potency (pEC<sub>50</sub>) and efficacy (E<sub>max</sub>) of pilocarpine (Pilo) in comparison to the full agonist Carbachol (CCh) at the different receptor subtypes. M<sub>1</sub>, M<sub>3</sub> and M<sub>5</sub> data were determined by measurement of PI hydrolysis stimulation, M<sub>2</sub> and M<sub>4</sub> data was determined by measurement of inhibition of forskolin-stimulated cAMP accumulation in CHO cells. <sup>a</sup> Data taken from<sup>[51]</sup>, <sup>b</sup> Data taken from<sup>[53]</sup>, <sup>c</sup> Data taken from<sup>[52]</sup>.

Receptor Subtype	E <sub>max</sub> (Pilo)/E <sub>max</sub> (CCh)	pEC <sub>50</sub> Pilocarpine	pEC <sub>50</sub> Carbachol
M <sub>1</sub> <sup>a</sup>	119%	5.24 ± 0.05	5.86 ± 0.02
M <sub>2</sub> <sup>a</sup>	55%	4.76 ± 0.06	6.65 ± 0.07
M <sub>3</sub> <sup>b</sup>	40%	5.54 ± 0.07	5.96 ± 0.02
M <sub>4</sub> <sup>a</sup>	94%	5.01 ± 0.12	6.63 ± 0.05
M <sub>5</sub> <sup>c</sup>	31%	5.16 ± 0.06	5.76 ± 0.09

Partial agonism is shown by a lowered proportion of AR\*G\* compared to activation by a full agonist. Each step before activation of the G protein can be responsible for partial agonism: the efficacy of G protein activation may be reduced or the driving force of isomerisation of AR to AR\* might be weaker.<sup>[54]</sup> In cases of partial agonists, the affinity for the active and the inactive receptor states may be similar so that the equilibrium is not pronouncedly shifted to the activated receptor state as seen for a full agonist or to the inactivated receptor state as with competitive antagonists.<sup>[55]</sup> Alternatively, the efficacy of G protein activation by the AR\* complex may be influenced by the partial agonist provoking a different activated receptor conformation than a full agonist. This receptor conformation might have less affinity to the G protein or induces less activation of the G protein.<sup>[56]</sup>

Another possible cause of partial agonism is the existence of more than one binding pose of the orthosteric ligand. If one binding pose is agonistic and another pose does not lead to receptor activation, the ratio of occupancy of each binding pose will determine the maximum measured effect of the ligand.<sup>[28b]</sup>

Additionally, pilocarpine was observed to be a biased agonist for at least three of the five receptor subtypes. In a study, which observed G<sub>i</sub> and G<sub>s</sub> coupling at the M<sub>2</sub> and the M<sub>4</sub> receptors separately (Table 4), pilocarpine turned out to be a full agonist at the M<sub>4</sub> for G<sub>i</sub> activation and a partial agonist at the M<sub>4</sub> when observing G<sub>s</sub> activation.<sup>[57]</sup> At the M<sub>2</sub> receptor, pilocarpine is a partial agonist for both pathways, still showing a bias towards the G<sub>i</sub> coupling. At the M<sub>3</sub> receptor in cells without overexpressed levels of M<sub>3</sub>, pilocarpine activates the β-arrestin pathway but not G<sub>q</sub>.<sup>[58]</sup> In the latter case, pilocarpine was an antagonist, which abolished carbachol-induced G<sub>q</sub> activation.

**Table 4:** Efficacy of pilocarpine (Pilo) in comparison to the full agonist Methacholine (MCh) when studying  $G_i$  activation and  $G_s$  activation separately.  $G_i$  activation was studied as the inhibition of Forskolin-stimulated adenylate cyclase.  $G_s$  activation was studied as the enhancement of Forskolin-stimulated adenylate cyclase after incubation with pertussis toxin which inhibits the  $G_i$  pathway.<sup>[57]</sup>

Receptor Subtype	$G_i$	$G_s$
	$I_{\max}(\text{Pilo})/I_{\max}(\text{MCh})$	$E_{\max}(\text{Pilo})/E_{\max}(\text{MCh})$
$M_2$	$54.7 \pm 5.7$	$9.7 \pm 5.1$
$M_4$	$90.5 \pm 7.1$	$35.3 \pm 3.1$

### 1.2.3 Structure–Activity Relationships of Pilocarpine

Between the 1970 and 2000, many analogues of pilocarpine (**2**) were synthesised, a broad variety of them were pharmacologically tested and their activities were compared to the parent compound. This led to a better understanding of the structural requirements for agonistic activity of pilocarpine-like compounds. The investigations can be sorted into three main categories: variation of the lactone core, variation of the imidazole moiety, and the role of the ethyl group attached to the lactone (Figure 12).

Variation of the lactone core includes exchanges of the carbonyl group for  $\text{CH}_2$ <sup>[59]</sup>,  $\text{C}=\text{S}$  and  $\text{CHOH}$ <sup>[60]</sup>, as well as replacement of the ether oxygen with  $\text{CH}_2$ <sup>[61]</sup>,  $\text{S}$ ,  $\text{NH}$ , or  $\text{NMe}$ <sup>[60]</sup>. In all cases, a complete or partial loss of muscarinic activity was observed leading to the conclusion that both oxygen atoms are essential for hydrogen bond formation. The carbonyl group seems to play a primary role in comparison to the ether oxygen because changes in this position have a bigger impact on muscarinic activity. The observation, that an inverted lactone with the carbonyl function at position 5 instead of position 2 is inactive, points to the same conclusion.<sup>[62]</sup> A ring extension to a 6 or 7 membered lactone leads to a complete loss of activity<sup>[63]</sup> as well as the lactone opening in a hydrolysis reaction.<sup>[64]</sup>

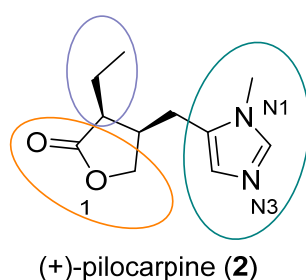


**Figure 12:** Illustration of the structural groups of pilocarpine (**2**) which were investigated by structure–activity relationships. Studies concerning the ethyl group are mostly based on the naturally occurring congeners of pilocarpine. Isopilocarpine (**15**) is the C3 epimer of pilocarpine with much less activity than pilocarpine<sup>[62, 64]</sup> indicating a strong influence of the configuration of the C3 stereocentre. In pilosinine (**16**), the ethyl group is missing and in pilosine (**17**), the ethyl group is replaced by a much larger hydroxy(phenyl)methyl group (Figure 13a). Both substances show a strongly reduced muscarinic

activity.<sup>[62]</sup> By replacing the CH group at position 3 with a nitrogen atom, a compound with similar pharmacological behaviour as pilocarpine was obtained.<sup>[65]</sup> In this oxazolidinone compound the effect of a replacement of ethyl by methyl and propyl has been investigated, leading to a reduced efficacy of the propyl derivative and to an almost complete loss of activity for the methyl derivative.<sup>[66]</sup> Altogether, the size of the ethyl group might be optimum to achieve both binding and efficacy of the molecule.

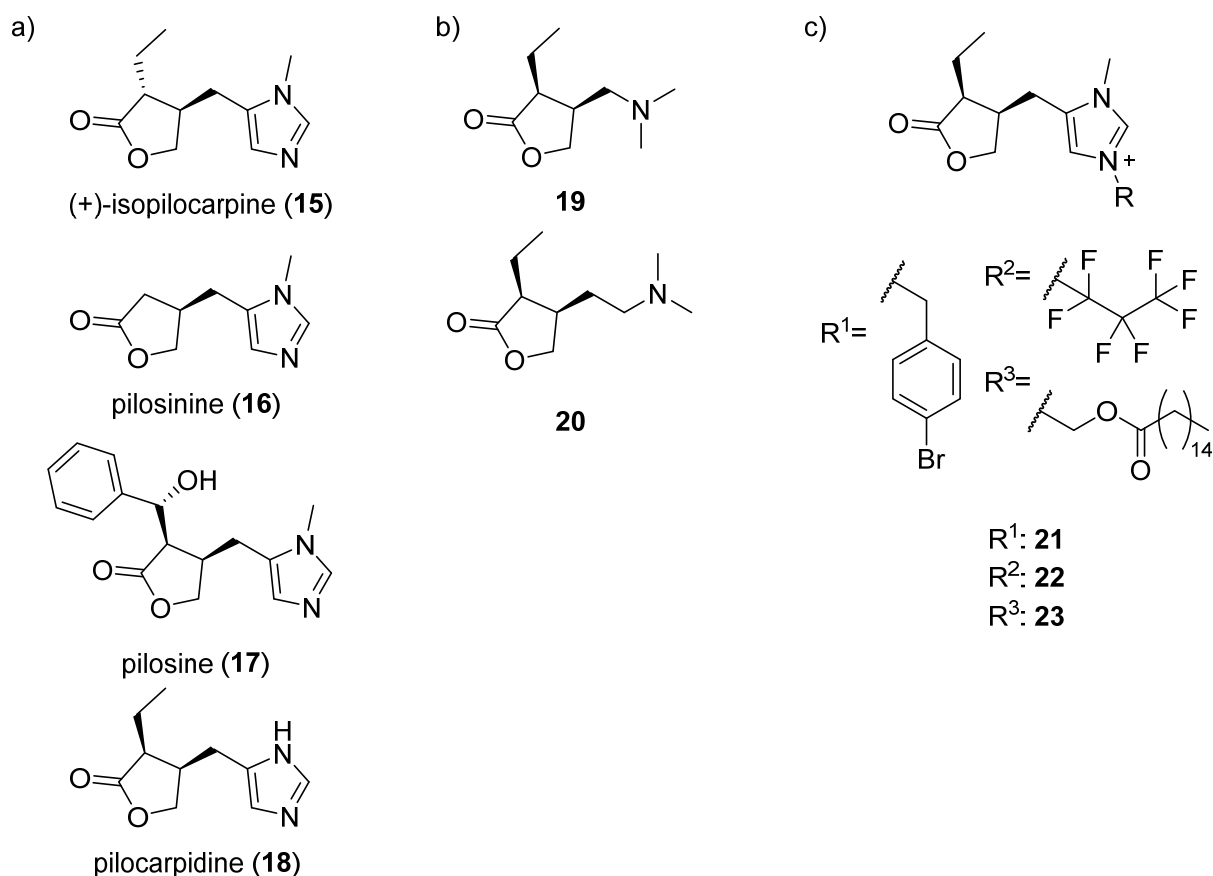


**Figure 13:** a) Naturally occurring congeners of pilocarpine are less active than pilocarpine. b) Two partially agonistic substances in which the imidazole has been replaced by open chain tertiary amines retain low muscarinic agonism.<sup>[67]</sup> c) Examples of residues attached to pilocarpine by quaternisation of the imidazole moiety with R<sup>1</sup> yielding a muscarinic antagonist<sup>[68]</sup>, R<sup>2</sup> leads to an agonist<sup>[69]</sup> and R<sup>3</sup> to a prodrug<sup>[70]</sup>.

The study of the imidazole moiety revealed that an exchange of imidazole to a 4-pyrimidyl group is tolerated with a slight loss of muscarinic activity.<sup>[61]</sup> Weak activity was equally retained when replacing the imidazole by open chain tertiary amines (**19**, **20**, Figure 13b).<sup>[67]</sup> The imidazole was also retained while the substitution pattern was investigated. A missing methyl group as observed in pilocarpidine (**18**) produces very weak muscarinic activity whereas a methyl substitution only at N3 leads to a complete loss of activity.<sup>[62]</sup> A loss of activity at pH above 9 indicates that protonation of the imidazole plays a crucial role.<sup>[45]</sup> Quaternisation of the imidazole core (molecules **21–23**) creates a permanent delocalised positive charge of the heterocycle. Depending on the residues used for quaternisation, agonists, antagonists or prodrugs can be obtained (Figure 13c). Aromatic residues such as 4-bromobenzyl (**21**) or 3,4-dichlorobenzyl lead to antagonism<sup>[68]</sup>, short perfluorinated alkyl chains

(**22**) lead to agonists.<sup>[69]</sup> Quaternisation of the imidazole with a residue that can be cleaved by enzymatic activity leads to prodrugs. The residue of molecule **23**, for example can be cleaved by esterases. The resulting  $\alpha$ -hydroxylammonium salt spontaneously decomposes to liberate pilocarpine.<sup>[70]</sup>

In summary, the lactone moiety is essential for muscarinic activity and the ethyl group in the *S*-configuration seems to be optimum for good receptor agonism. The imidazole moiety, in contrary, tolerates some careful modifications.

### 1.2.4 The Putative Binding Pose of Pilocarpine

The putative binding pose of pilocarpine at the orthosteric site of mAChRs relies on findings from point mutation studies and computational docking studies. Most publications agree about an essential hydrogen bond or ion–ion interaction of the imidazole moiety of pilocarpine with a conserved aspartate residue, D<sup>3.32</sup>, on helix 3.<sup>[60b, 71]</sup> Thus, the protonated imidazole moiety is placed similarly to the ammonium group in acetylcholine (**1**) or iperoxo (**8**), which has been analysed in crystal structures<sup>[13]</sup> (Figure 14).

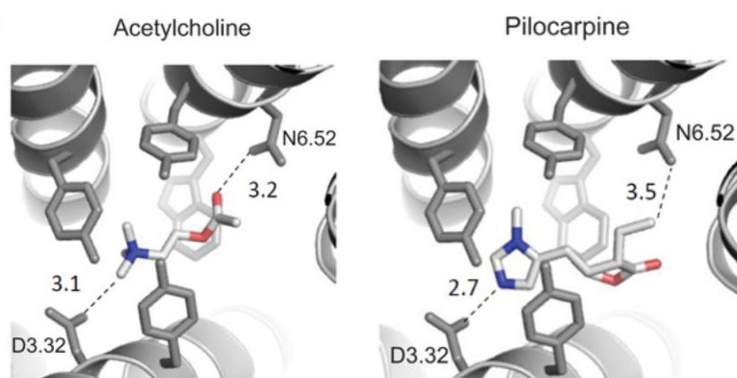


**Figure 14:** Docked binding poses of acetylcholine (**1**) and pilocarpine (**2**) to the orthosteric binding pocket of the M<sub>3</sub> receptor. (From<sup>[71a]</sup>. Reprinted with permission from AAAS.)

Shapiro et al. have proposed a vertical binding pose along TM3 of the M<sub>1</sub> receptor. In this case, the lactone moiety of pilocarpine is bound by S<sup>3.39</sup> and S<sup>3.36</sup> pointing towards the intracellular space.<sup>[60b]</sup> This seems improbable due to a range of other publications preferring a horizontal binding mode, which would explain receptor activation by pilocarpine inducing the inward movement of TM6 at the orthosteric site.<sup>[71a-c]</sup>

The exact interaction patterns of pilocarpine with the different receptor subtypes varies in literature. In general, it was observed that the cation– $\pi$  or  $\pi$ – $\pi$  stacking interactions of the protonated imidazole with the tyrosine lid (Y<sup>6.51</sup> and Y<sup>3.33</sup>)<sup>[71c, 72]</sup> and a tryptophan residue (W<sup>4.57</sup> or W<sup>6.48</sup>)<sup>[71b, 71c, 72]</sup> in the active site play a role in stabilising the hydrogen bond of D<sup>3.32</sup> with the imidazole moiety. Alternatively – and in contrast to the binding of acetylcholine (**1**) – the interaction with only one aromatic residue was

proposed due to the planar charge distribution in the protonated imidazole ring.<sup>[17]</sup> Additionally, the ethyl group interacts hydrophobically with residues from TM5 and TM6<sup>[71c]</sup> and a hydrogen bond of the lactone group with N<sup>6.52</sup> has been suggested.<sup>[71c, 72]</sup> Furthermore, mutations of D<sup>3.26</sup>, L<sup>3.29</sup> and V<sup>3.40</sup> in the M<sub>4</sub> receptor altered the affinity of pilocarpine for the mutated receptor showing an important involvement of those residues in the binding of pilocarpine.<sup>[71d]</sup>

Recent computational analysis of pilocarpine binding to the M<sub>2</sub> receptor used the dynophore approach.<sup>[73]</sup> This approach uses dynamic pharmacophores to observe the predicted dynamic interactions between ligand and binding pocket over a certain period of time. The results show that the imidazole and the carbonyl function of pilocarpine are found at the same position during the whole observation time. The ethyl substituent at lactone C-3, however, switches between two binding modes, which suggests the existence of binding mode ensembles for pilocarpine at the M<sub>2</sub> receptor. Bermudez proposes two binding poses of pilocarpine, one leading to receptor activation and the other being antagonistic. This might be an explanation for the partial agonism observed with pilocarpine.<sup>[73]</sup>

### 1.2.5 Pharmacological Studies of Ternary Complexes with Pilocarpine

Some pharmacological studies of allosteric modulators and their probe dependent effects include pilocarpine as an exemplary partial agonist in addition to common full agonists of mAChRs. As a result, pilocarpine has been studied together with naphmethonium (**9**)<sup>[17]</sup>, brucine (**24**)<sup>[74]</sup>, (-)-eburnamonine (**25**)<sup>[74]</sup>, alcuronium (**26**)<sup>[75]</sup> or LY2033298 (**27**)<sup>[76]</sup> at the M<sub>2</sub> receptor and with ML380 (**28**) or ML375 (**29**)<sup>[77]</sup> at the M<sub>5</sub> receptor (Figure 10 and Figure 15).

In all cases, the maximum response of pilocarpine has been altered positively for known positive allosteric modulators or negatively for known negative allosteric modulators. In contrast, full agonists did not show any changes of the maximum response. This might point to a difference in active receptor conformations between pilocarpine and full agonists.<sup>[76]</sup>

The positive allosteric modulator LY2033298 (**27**) and the negative allosteric modulator ML375 (**29**) had no influence on the potency of pilocarpine, whereas the positive allosteric modulator ML380 (**28**) increased the potency of pilocarpine. Interestingly, the negative allosteric modulator naphmethonium (**9**) increased the potency of pilocarpine but decreased the potency of acetylcholine. A possible explanation could be that naphmethonium as a negative allosteric modulator stabilises the inactive receptor conformation. Acetylcholine would only have a low affinity to the inactive receptor whereas pilocarpine as a partial agonist has good affinity for both receptor conformations. As the binding cooperativity of pilocarpine with naphmethonium is similar to that of the antagonist *N*-methylscopolamine (NMS, **30**) with naphmethonium, it was concluded that the allosteric site of the

pilocarpine-bound inactive receptor state takes a similar conformation as the NMS-bound inactive receptor state.<sup>[17]</sup>

Noteworthy, these studies showed that the maximum response of pilocarpine in the presence of ML375 (**29**), alcuronium (**26**) or LY2033298 (**27**), negative allosteric modulators, could be abolished completely at high concentrations of modulator. This could be understood as a conversion to antagonists. Indeed, pilocarpine was shown to be a competitive antagonist of oxotremorine-M (**13**) in the presence of alcuronium.<sup>[75]</sup>

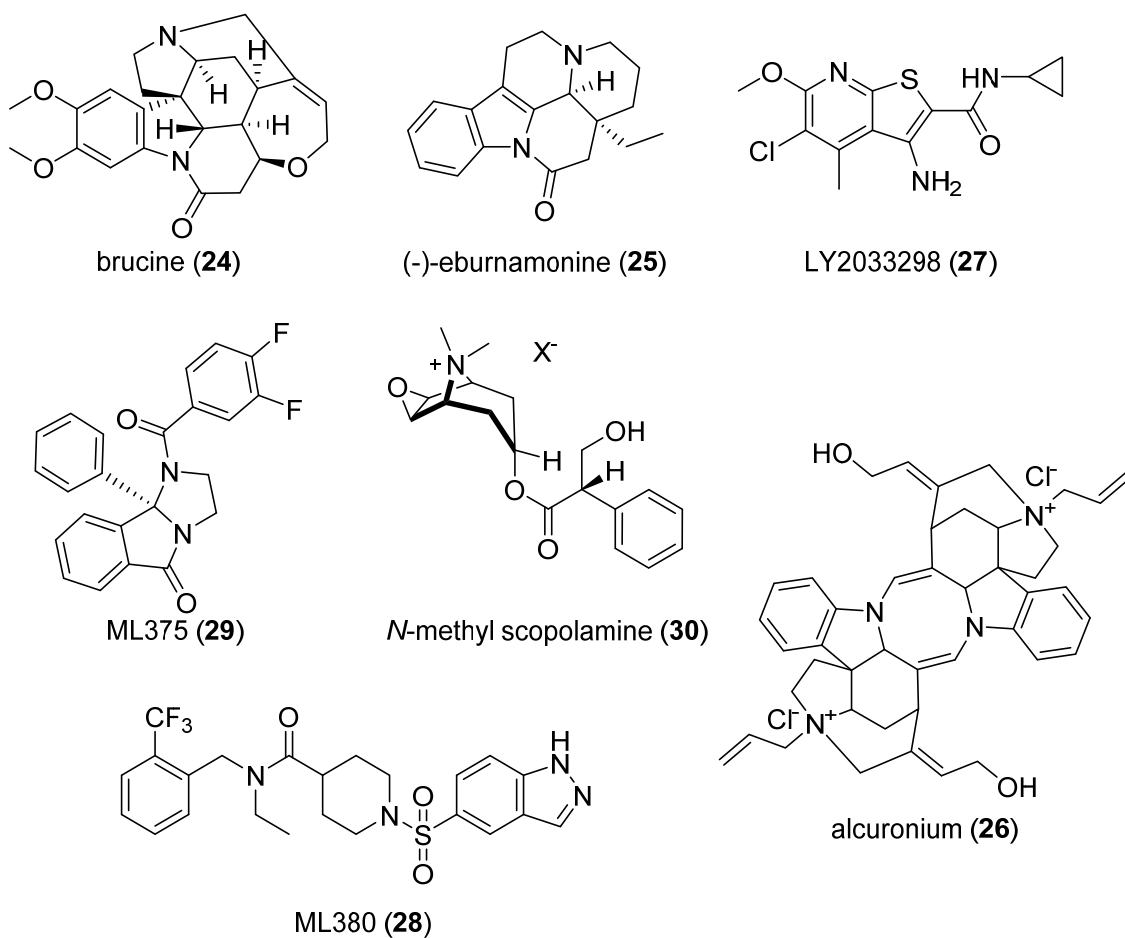


**Figure 15:** Structures of allosteric modulators that have been studied in ternary complexes with pilocarpine.

## 2 Aim of the Work

This work was subdivided into two projects. The first project aimed for the synthesis of hybrid molecules of an allosteric modulator with pilocarpine or pilocarpine-like orthosters. In previous studies, agonistic dualsteric ligands were based on full agonists or superagonists.<sup>[27, 28b, 29d, 30, 36b, 78]</sup> In contrast, the new dualsteric ligands in this work would be based on a partial agonist as orthosteric moiety. To investigate which position of pilocarpine is appropriate to attach the linker without losing the ability to activate the receptor, we aimed for the synthesis of pilocarpine hybrid molecules with different linker attachment positions (Figure 16).

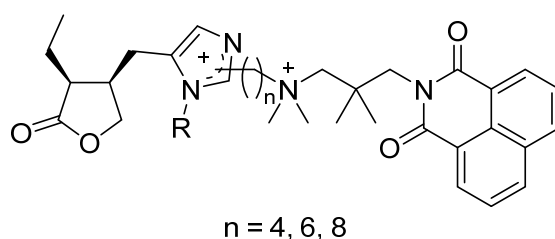


**Figure 16:** General structure of the targeted hybrid molecules with  $R^1 = \text{H, Me}$ .

The second project aimed for a better understanding of pilocarpine's binding pose in the orthosteric binding site of mAChRs and the molecular basis for its partial agonism. As described previously (Chapter 1.2.4), the ethyl group of pilocarpine might switch between two distinct binding poses. One of the binding poses is assumed to be agonistic while the other binding pose is assumed to be antagonistic. The ratio of occupancy would determine the efficacy of pilocarpine similarly to what has been described for ligand binding ensembles of dualsteric ligands.<sup>[28a]</sup> This hypothesis was experimentally challenged. As the binding pocket for the ethyl group in the putative antagonistic binding mode is larger than the binding pocket used in the agonistic binding mode, replacement of the ethyl group by a larger residue should lead to a less efficient partial agonist and a smaller residue would increase efficacy. For this reason, we aimed for the synthesis and pharmacological evaluation of a series of pilocarpine analogues with residues of different size at lactone position 3, molecules **16** ( $R = \text{H}$ , pilosinine), **31a** ( $R = \text{Me}$ ), **31c** ( $R = \text{Pr}$ ) and **31d** ( $R = \text{Bu}$ ) (Figure 17).

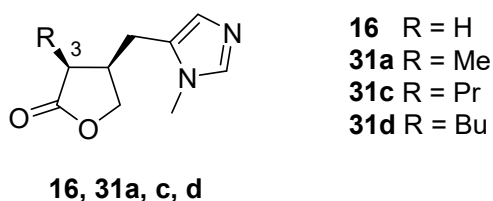


**Figure 17:** General structure of the targeted pilocarpine analogues.



### 3 Hybrid Ligands with Pilocarpine Analogues as Orthosteric Moiety

#### 3.1 Design of the Pilocarpine-Based Hybrid Ligands

To obtain a pilocarpine-based hybrid ligand the following aspects needed to be considered:

- the choice of a pilocarpine-related orthosteric moiety
- the linker attachment point
- the choice of the allosteric moiety
- the type of linker and its length

The position of the linker should not interfere with the main interactions of pilocarpine (**2**) with the receptor binding site. The structure-activity relationship for pilocarpine (Chapter 1.2.3) shows that the lactone moiety and its substitution pattern is crucial and optimised for receptor activation. This means that the linker needs to be attached to the imidazole moiety. This coincides with the supposed proximity of the imidazole to the entrance of the orthosteric binding site when pilocarpine is bound to the receptor (Chapter 1.2.4). Attachment of the linker at the imidazole moiety would therefore lead to a dualsteric ligand which corresponds to the putative geometric requirements in the receptor.

From a synthetic point of view the two nitrogen atoms can be suitable attachment points due to their nucleophilic nature. Thus, the linker could be either connected to N<sup>3</sup> as an additional substituent or instead of the methyl substituent at N<sup>1</sup> (Figure 18). The first option holds the risk of obtaining antagonists when the imidazole is quaternised with larger residues. The second option might be difficult to achieve due to preferred substitution at N<sup>3</sup> of 5-substituted 1*H*-imidazoles.

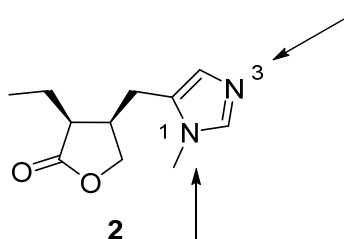


**Figure 18:** Possible positions for linker attachment to pilocarpine (**2**).

To minimize unknown factors, a naphmethonium (**9**) fragment, a thoroughly investigated allosteric moiety, was chosen for the synthesis of the new dualsteric ligands.<sup>[27, 28b, 31a]</sup> An additional reason for the choice of naphmethonium was the study of Jäger et al.<sup>[17]</sup> providing pharmacological data for the ternary complex of the M<sub>2</sub> receptor with naphmethonium and pilocarpine. Positive binding cooperativity between naphmethonium and pilocarpine was observed and led to an increase in pilocarpine potency while negative activation cooperativity induced a decrease of efficacy

(Chapter 1.2.5). It was considered to be interesting to investigate if those effects can be reproduced with dualsteric ligands.

An alkyl linker chain was chosen, which can penetrate the tyrosine lid without impeding its closure<sup>[28a, 30b]</sup> and is flexible enough to allow for optimum binding of the orthosteric moiety. The length of six methylene units has proven to be a good starting point when investigating binding of dualsteric ligands with naphmethonium fragments at the M<sub>2</sub> receptor.<sup>[28a]</sup>

According to the above-mentioned considerations, molecules **32** and **33** were defined as first target compounds for this study (Figure 19).

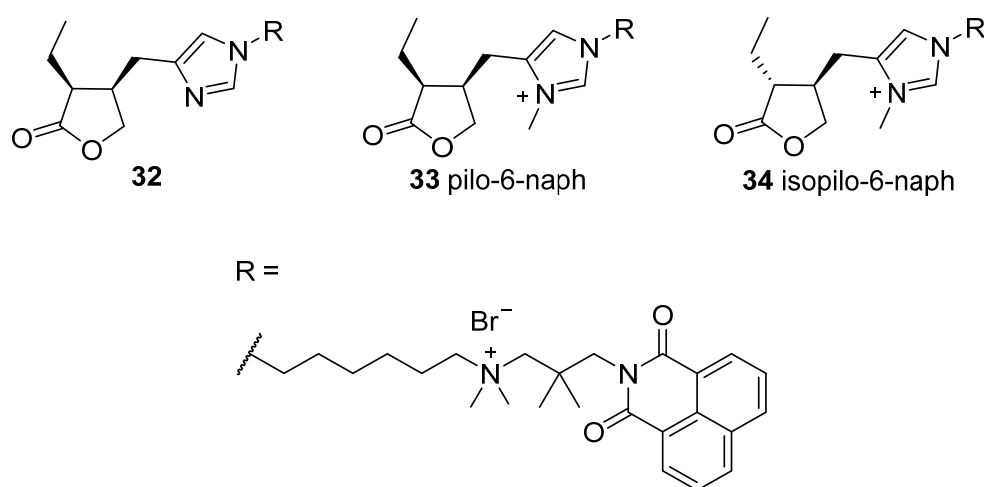


Figure 19: Target hybrid molecules **32**, **33** and **34**.

The first synthesis of a hybrid compound of pilocarpine led to the formation of the isopilocarpine hybrid due to facile epimerisation at the lactone C-3. Bearing in mind that isopilocarpine is less potent than pilocarpine<sup>[60b, 62, 79]</sup> and was coupled to a naphmethonium fragment, an alloster with supposed strong negative cooperativity, the isopilocarpine hybrid (**34**) was added to the list of target compounds with the intention to provide a negative control.

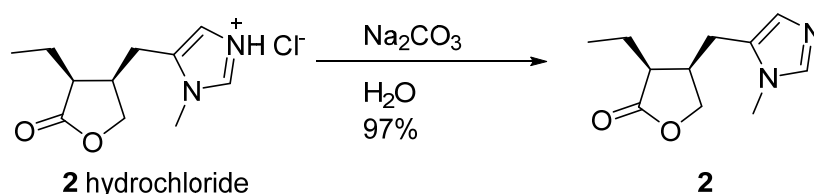
## 3.2 Synthesis of the Pilocarpine-Based Hybrid Compounds

### 3.2.1 Synthesis of Pilocarpine Analogues as Orthosteric Fragments of Hybrid Compounds and as Orthosteric Reference Compounds

For the synthesis of the target hybrid molecules **32**, **33** and **34**, pilocarpidine (**18**), pilocarpine (**2**), and isopilocarpine (**15**), respectively, were used as the orthosteric moiety of the hybrid ligand. Pilocarpine is commercially available as the hydrochloride or as the nitrate salt and only needed to be deprotonated to the free base. Isopilocarpine (**15**) could be easily obtained from pilocarpine (**2**). Pilocarpidine (**18**), however, needed to be synthesised, as it was neither commercially available nor was it accessible from pilocarpine.

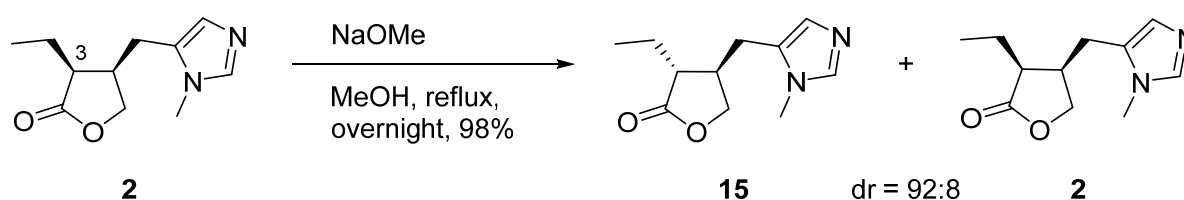
## Liberation of Pilocarpine (**2**) from its Salts and Synthesis of Isopilocarpine (**15**)

Pilocarpine (**2**) was liberated from its commercially available salts by deprotonation. The  $pK_a$  value of pilocarpine is given as 7.03.<sup>[80]</sup> For the generation of a 100-fold excess of the free base to the protonated form, the pH needed to be adjusted to two logarithmic units above the  $pK_a$ . The pilocarpine salt was dissolved in water, the pH adjusted to > 9 by addition of  $Na_2CO_3$  and the free base was isolated by extraction from the aqueous layer with chloroform (Scheme 1).<sup>[81]</sup>



**Scheme 1:** Liberation of pilocarpine from its hydrochloride salt.

Isopilocarpine (**15**) can be obtained from pilocarpine (**2**) by epimerisation of the labile stereocentre at the lactone C-3. Epimerisation takes place under basic conditions due to enolization of the lactone (Scheme 2). The reprotonation under thermodynamic conditions leads mainly to the more stable isopilocarpine. This reaction takes place in competition to lactone hydrolysis. Water-free conditions were chosen and sodium methoxide was used as a base to avoid product loss by hydrolysis or the need for recyclisation in acidic aqueous solution.<sup>[81]</sup> The competing lactone opening reaction leads to the formation of a methyl ester which spontaneously recyclises to the desired lactone. The product was obtained in excellent yields. It was composed of isopilocarpine with 6–11% pilocarpine as impurity. This amount of pilocarpine might correspond to the relative thermodynamic stabilities of both epimers.



**Scheme 2:** Epimerisation of pilocarpine (**2**) to provide isopilocarpine (**15**).<sup>[81]</sup>

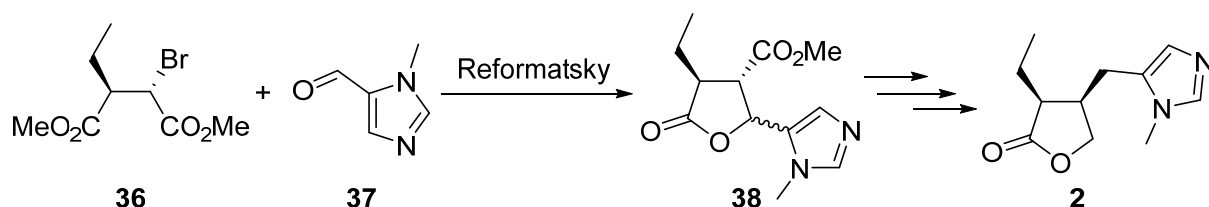
## Attempted Enantioselective Synthesis of Pilocarpidine (**18**) and its Simplified Analogue Demethylated Pilosinine (**35**)

As a first approach to synthesise enantiopure pilocarpidine (**18**), the synthetic route of Dener et al.<sup>[82]</sup> was adapted. The route relies on the synthesis of the enantiopure diester **36** and a nearly stereospecific Reformatsky reaction to link the lactone precursor to the imidazole moiety **37** (Scheme 3a). To obtain pilocarpidine (**18**) instead of the published pilocarpine (**2**), the methyl substituent at the imidazole was

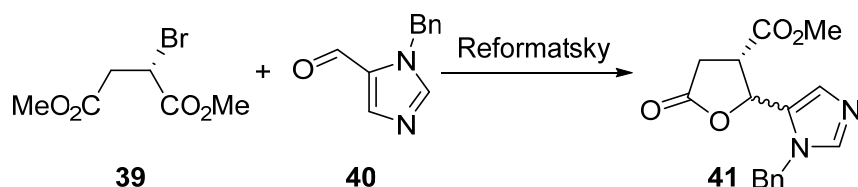
replaced by a benzyl protecting group throughout the synthesis to be removed by hydrogenolysis as the final step to provide pilocarpidine (**18**).

The synthesis of **18** was approached in two ways. The synthesis of the lactone precursor **36** was investigated in parallel to test reactions for the Reformatsky reaction with a simplified diester **39** lacking the ethyl substituent (Scheme 3b).

a)



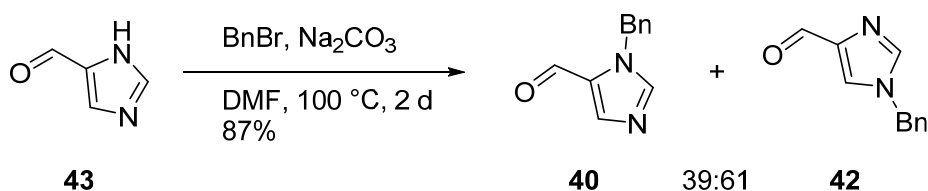
b)



**Scheme 3:** a) The Reformatsky reaction as the key step of the enantioselective synthesis of pilocarpine (**2**) by Dener et al.<sup>[82]</sup>  
b) Test reaction for the modified Reformatsky reaction.

#### Test Reactions for the Reformatsky Reaction with a Simplified Diester

The aldehyde precursor **40/42** was synthesised as a mixture of benzylation regioisomers in one step. Commercially available 1*H*-imidazole-5-carbaldehyde (**43**) was stirred with benzyl bromide and Na<sub>2</sub>CO<sub>3</sub> in DMF at 100 °C for 2 d (Scheme 4).<sup>[83]</sup> The product was isolated by extraction as a 39:61 mixture of the 1,5- and the 1,4-substituted regioisomers **40/42**, respectively, with a yield of 87%. As the benzyl group was planned to be removed at the end of the synthesis, it was not important which nitrogen of the imidazole carried the benzyl substituent.

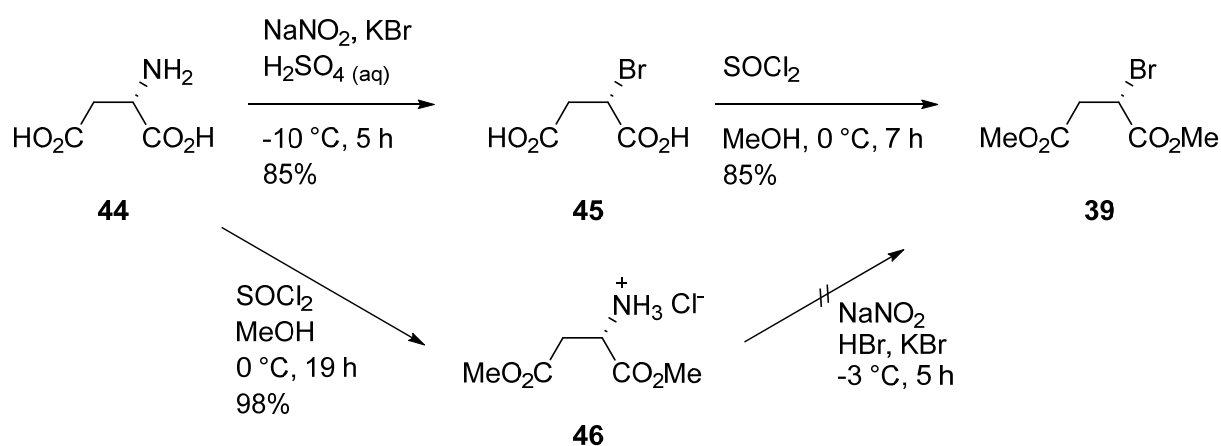


**Scheme 4:** Benzylation of 1*H*-imidazole-5-carbaldehyde (**43**) provides a regioisomeric mixture of protected imidazoles **40** and **42**.<sup>[83]</sup>

For Reformatsky test reactions, a simplified diester precursor **39** was synthesised (Scheme 5). The simplified precursor lacking the ethyl group became available in two steps: bromination of *L*-aspartate (**44**) by diazotisation followed by esterification of **45**.

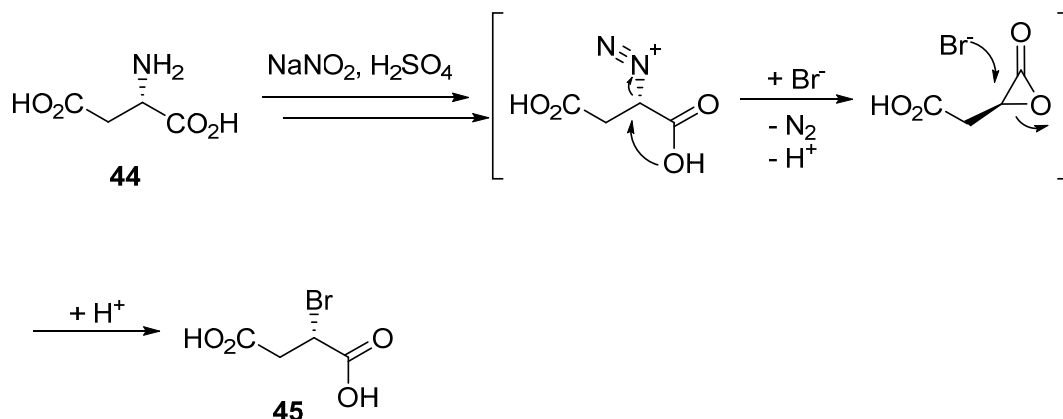
For the bromination reaction<sup>[82, 84]</sup> the starting material **44** was dissolved in diluted sulfuric acid and KBr was added. At  $-10\text{ }^{\circ}\text{C}$ , sodium nitrite was slowly added. After stirring for 5 h and warming to RT, the mixture was extracted with ethyl acetate. The desired brominated product **45** was obtained in 85% yield.

Twofold esterification of compound **45** was achieved by activation of the carboxylic acids with thionyl chloride in dry methanol at  $0\text{--}20\text{ }^{\circ}\text{C}$  (Scheme 5). Andrews and Hardwicke<sup>[85]</sup> have observed a thermal racemisation of dimethyl (-)-bromosuccinate (**39**) so that esterification methods involving reflux conditions were to be avoided. The method used here produced the diester **39** without significant racemisation.



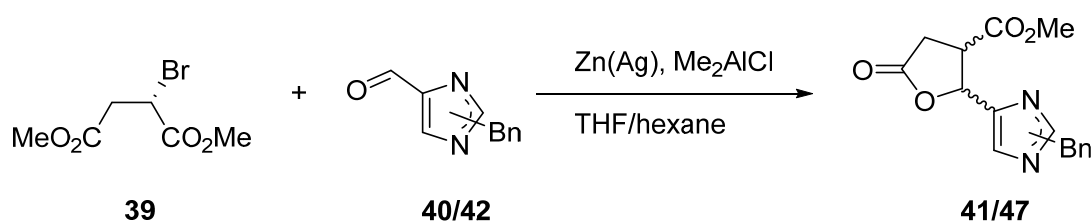
**Scheme 5:** Synthesis of the simplified diester precursor **39** for Reformatsky test reactions.

The alternative route starting with esterification of **44** followed by bromination of the resulting diester **46** was not successful. The bromination reaction produced a mixture of many uncharacterized compounds. This underlines the importance of the adjacent carboxylic acid for the success of the reaction resulting from a double  $\text{S}_{\text{N}}2$  mechanism which also explains retention at the stereocentre (Scheme 6).<sup>[86]</sup>



**Scheme 6:** Schematic representation of the double  $\text{S}_{\text{N}}2$  mechanism after diazotization of L-aspartate (**44**) responsible for retention of the configuration at the stereocentre.<sup>[86]</sup>

With precursor **39**, the Reformatsky reaction was tested. In a Reformatsky reaction, the  $\alpha$ -bromo ester is transformed into an organozinc compound by insertion of zinc into the carbon-bromine bond, which is in equilibrium with the zinc enolate.<sup>[87]</sup> The so-formed Reformatsky reagent can react in a nucleophilic addition with the imidazole aldehyde **40/42** (Scheme 7). The resulting alcoholate spontaneously reacts to the lactone **41** in an intramolecular esterification reaction.<sup>[82]</sup> When an enolate with a chiral centre (such as the enolate of **36**) is used, stereoselectivity can be observed as the reaction is supposed to progress via a Zimmerman-Traxler-like transition state involving both starting materials chelated by zinc and the Lewis acid.<sup>[82, 88]</sup>



**Scheme 7:** Test reaction for the key Reformatsky reaction using the simplified diester precursor **39**.

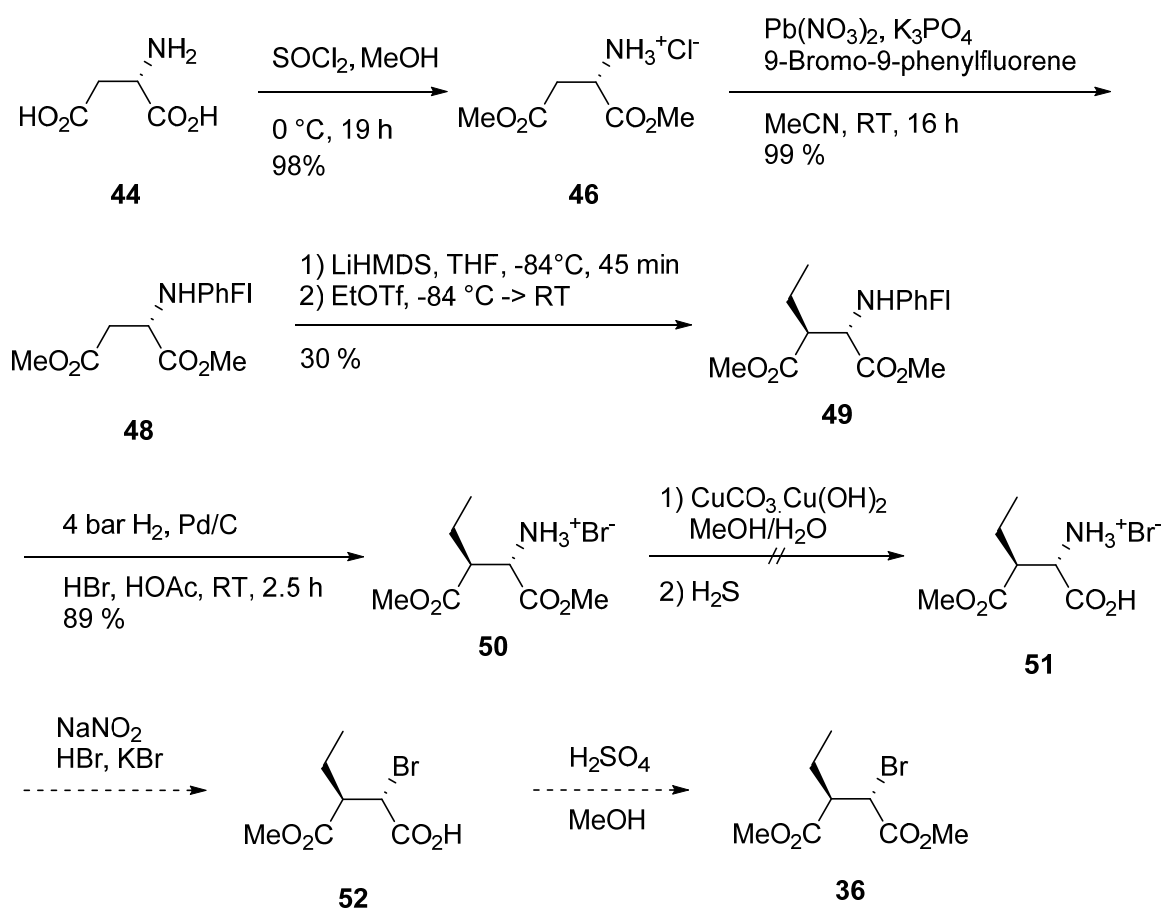
Following the procedure of Dener et al.<sup>[82]</sup>, a zinc/silver couple (prepared according to Rousseau and Conia<sup>[89]</sup>) and a catalytic amount of copper(I) bromide were suspended in dry THF and dimethyl aluminium chloride was added. After stirring for 20 minutes, the mixture was cooled to  $-8\text{ }^{\circ}\text{C}$  and a 1:1 mixture of the starting materials **39** and **40/42** dissolved in dry THF was added. The reaction was stirred at  $-8\text{ }^{\circ}\text{C}$  for 2 h and at RT for 30 minutes. TLC and LC-MS controls of the reaction did not show any conversion, which did not improve with longer reaction times. However, when tried with a mixture of 1- and 3-methyl-1*H*-imidazole-5-carbaldehyde, the product was formed and could be isolated. It was concluded that the synthetic approach of the Reformatsky reaction was not adaptable to the synthesis of pilocarpidine and work proceeded with an alternative synthetic approach.

A later retrial of the test reaction yielded a crude mixture of lactone **41**, its benzylation regioisomer **47** and the ring-opened analogue in 63% crude yield. A possible explanation for the earlier failure of the reaction could be the use of a batch of supposedly dry THF which was not dry. It could have been of interest to pursue this synthetic route.

#### Enantioselective Synthesis of Diester **36** as Lactone Precursor

In parallel to the Reformatsky test reactions, the synthesis of the elaborated lactone precursor **36** was approached (Scheme 8). The synthesis of diester **36** starts with *L*-aspartic acid (**44**). First, both acidic functions were transformed to the methyl ester by addition of thionyl chloride to a solution of *L*-aspartic acid in methanol at  $0\text{ }^{\circ}\text{C}$ . The product was crystallised in diethylether to produce the hydrochloride of the diester **46** as white crystals with a yield of 98%.<sup>[90]</sup>

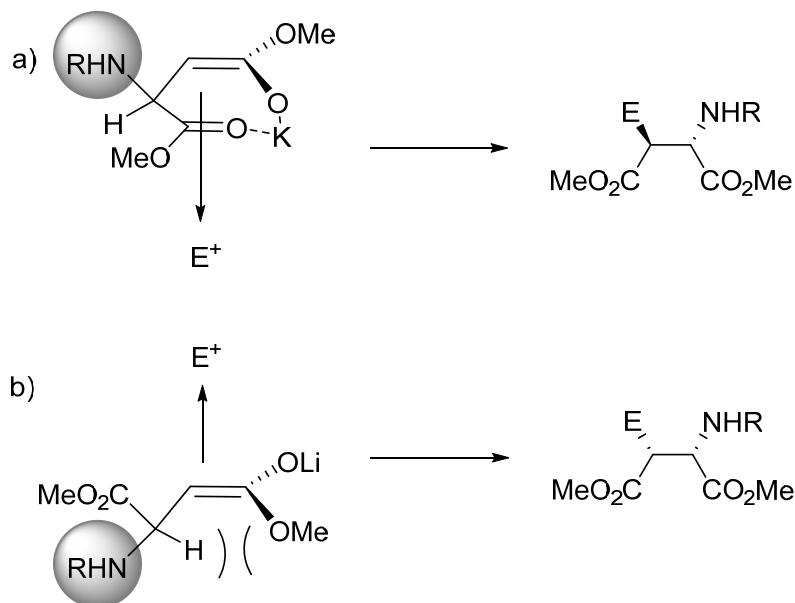
Then, the amine group of **46** was protected with a sterically demanding 9-phenyl-9-fluorenyl protecting group. The starting material was stirred with anhydrous lead nitrate, potassium phosphate and 9-bromo-9-phenylfluorene in dry acetonitrile at RT overnight.<sup>[90]</sup> In this reaction the halogenophilic lead nitrate activates the bromo substituent as a leaving group<sup>[91]</sup> and potassium phosphate neutralises HCl from the hydrochloride salt and the HBr liberated during the reaction. After complete conversion, the solid salts were removed by filtration and the subsequent acidic extractions removed any unreacted starting material. After purification by column chromatography, the fully protected aspartate **48** was obtained with 80–99% yield.



**Scheme 8:** Attempted synthetic route to the enantiopure diester **36** as lactone precursor.<sup>[82]</sup>

Next, the ethyl residue was introduced. The bulky 9-phenyl-9-fluorenyl substituent favours  $\beta$ -deprotonation of **48** in competition to  $\alpha$ -deprotonation when a sterically demanding base is used.<sup>[91]</sup> Diastereoselectivity of the subsequent alkylation can be influenced by the choice of the enolate counter ion in combination with the steric bulk of the nitrogen protecting group (Scheme 9).<sup>[92]</sup> The creation of a chelated potassium enolate intermediate would be prerequisite to obtain the desired diastereomer during ethylation of **48** (Scheme 9a). An open lithium enolate intermediate would lead to opposite inductive effects (Scheme 9b). For that reason, Wolf and Rapoport<sup>[93]</sup> used KHMDS to deprotonate **48**. However, at the time when the reaction was to be carried out, KHMDS was not

commercially available and LiHMDS was used out of necessity, accepting the expected formation of a diastereomeric mixture. A switch to KHMDS would be possible once it became available.



**Scheme 9:** Rationale to explain stereoselectivity during alkylation of a protected *L*-aspartate with R = 9-phenyl-9-fluorenyl such as **48**. a) Conformational arrangement of the enolate intermediate induced by chelation of the potassium counterion. b) Preferred conformational arrangement of the enolate intermediate with the nonchelating lithium counterion defined by 1,3-allylic strain. In both cases, alkylation with the electrophile E<sup>+</sup> is expected to take place on the sterically less hindered face opposite to the bulky 9-phenyl-9-fluorenyl substituent leading to **49** or its epimer.<sup>[92]</sup>

LiHMDS was added to a solution of **48** in dry THF at  $-84\text{ }^{\circ}\text{C}$ . After stirring for 45 minutes, ethyl triflate was added in one portion and the reaction mixture was allowed to warm to RT. After acidic workup, the crude product **49** was crystallised from methanol with 22% yield. Column chromatography of the mother liquor provided another 20% yield of a diastereomeric mixture and 30% of the starting material was recovered. Comparison of the optical rotation and proton NMR spectra to literature data<sup>[82, 93]</sup> revealed that the crystallised product was the desired (2*S*,3*S*)-configured product with 10% (2*S*,3*R*)-configured product as impurity. As expected, the published formation of less than 2% of the (3*R*)-configured byproduct<sup>[82]</sup> was not reached with LiHMDS (Scheme 9). The incomplete conversion of **48** can be explained by overestimated concentration of the base or the solvent containing residual water.

After ethylation of the protected *L*-aspartate **48**, the 9-phenyl-9-fluorenyl group was removed by hydrogenation of **49** with palladium on activated charcoal in a mixture of methanol, acetic acid and aqueous HBr.<sup>[82]</sup> A hydrogen pressure of 4 bar over 2.5 h at RT was sufficient to achieve complete conversion. After catalyst removal by filtration and extraction, the product **50** was obtained as an orange to brown oil in almost quantitative yield.

For selective hydrolysis of the  $\alpha$ -methyl ester, the hydrobromide **50** was dissolved in a mixture of water and methanol and stirred with an excess of basic copper carbonate at RT for a week.<sup>[82]</sup> The resulting copper complex and excess of copper carbonate were to be destroyed by precipitation of copper as



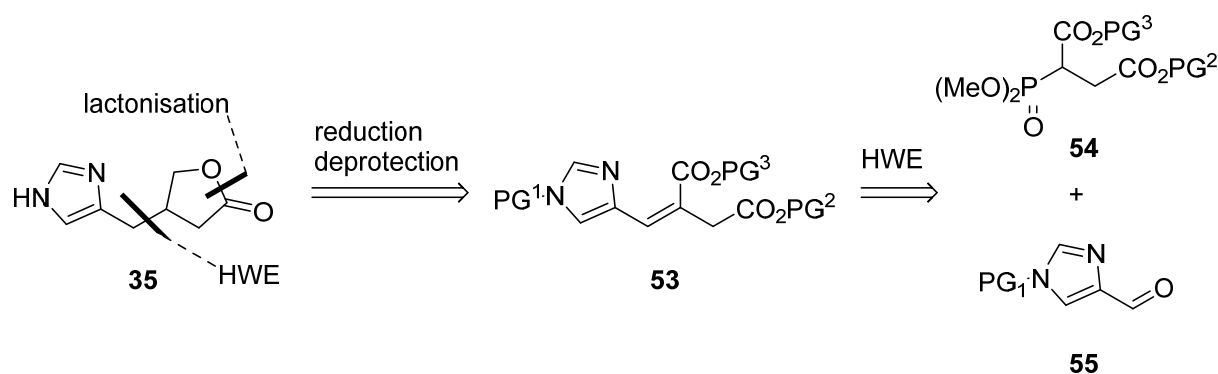
copper sulfide.<sup>[82]</sup> This precipitation was attempted in two ways. First, hydrogen sulfide was produced in situ by addition of thioacetamide<sup>[94]</sup> or sodium sulfide and acid. Alternatively, hydrogen sulfide was produced in a separate flask by slow addition of aqueous HCl to an aqueous solution of sodium sulfide. The liberated hydrogen sulfide was fed into the reaction mixture. In all cases, the desired product **51** was formed, but could not be isolated as a pure compound.

The bromination by diazotisation of the amine only takes place with a neighbouring acid, not with an ester. For this reason, the ester hydrolysis was required. Alternative saponification procedures to hydrolyse one or both esters could have been tried, but in parallel it turned out, that the Reformatsky reaction did not work in the test reactions. The synthesis of the lactone precursor was abandoned at this point.

### Synthesis of Racemic Desmethyl Pilocarpine (**35**)

After failure of the Reformatsky reaction and difficulties with the stereoselective introduction of the ethyl substituent at C-3 of the lactone, the decision to first synthesise a racemic desmethyl analogue of pilosinine **35** was taken. This molecule has one stable stereocenter, but no labile stereocenter in  $\alpha$ -position to the lactone carbonyl.

The idea was to modify the already attempted synthesis by replacing the Reformatsky reaction which links the lactone to the imidazole fragment of the target molecule. Similar to earlier synthetic approaches by Compagnone and Rapoport<sup>[95]</sup> a Horner–Wadsworth–Emmons (HWE) reaction with consecutive reduction of the newly formed double bond should create the methylene bridge between lactone and imidazole moieties (Scheme 10).



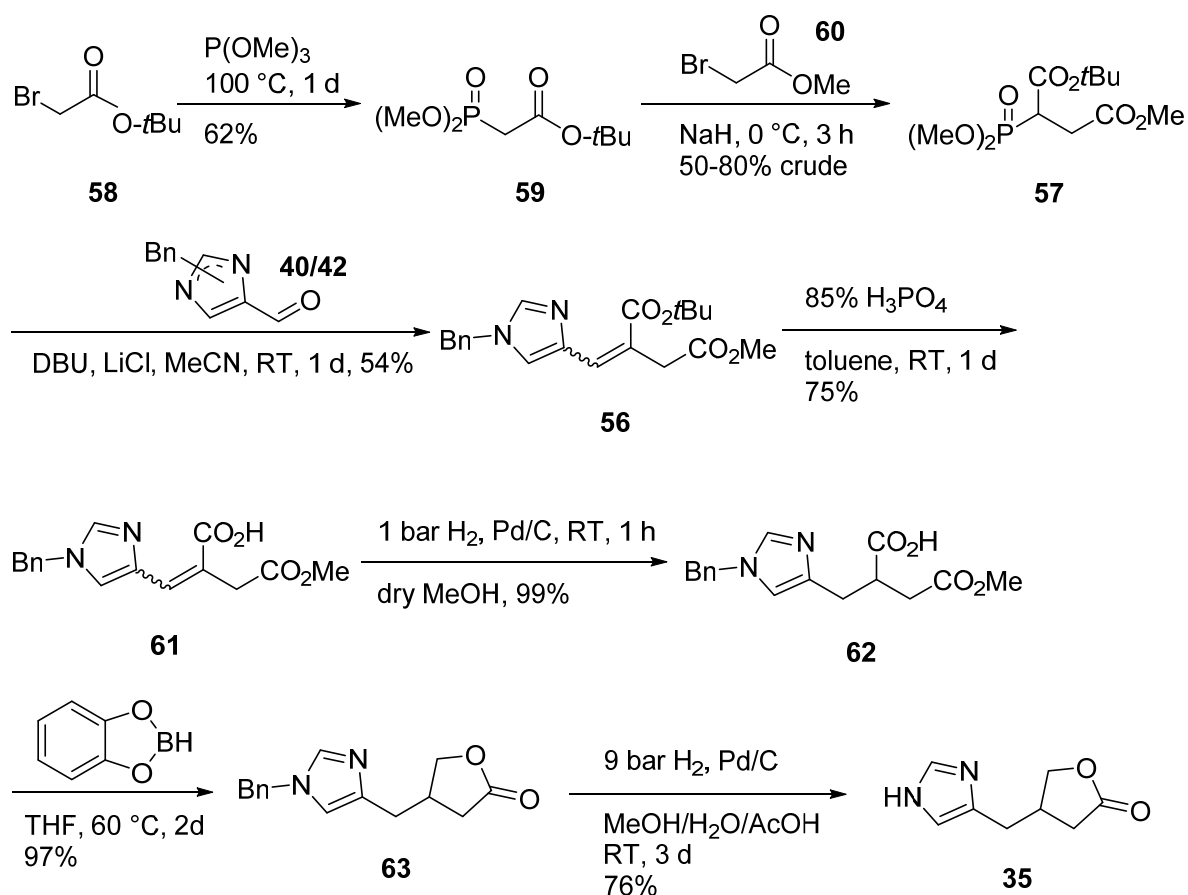
**Scheme 10:** Retrosynthesis of racemic desmethyl pilosinine **35** with PG: protecting group.

The lactone moiety was planned to be synthesised from two orthogonally protected carboxylic acid functions. Methyl and *tert*-butyl esters are orthogonal as the *tert*-butyl ester can be hydrolysed at an acidic pH of 1–4 and the methyl ester can be cleaved in basic conditions or transesterified by a nucleophilic attack.<sup>[96]</sup> The choice of the position of both groups causes the need to reduce a carboxylic acid to the alcohol in presence of an ester or the need to reduce an ester to the alcohol in presence of

a carboxylic acid. Methods for both cases exist.<sup>[96]</sup> The first option was chosen in the hope that deprotection of the methyl ester would not be necessary as the lactone formation would be spontaneous.

The basic imidazole nitrogen should be protected throughout the whole synthetic route and deprotected in the last step (PG<sup>1</sup> in Scheme 10). A benzyl group was chosen as it is stable to acidic and basic conditions. Its hydrogenolytic removal requires long reaction times and a relatively high hydrogen pressure of 10 bar.<sup>[96]</sup> No influence was expected with reference to which nitrogen carries the protecting group.

These considerations led to a synthetic route starting from commercially available starting materials to the final compound with a total of 7 linear steps (Scheme 11).



**Scheme 11:** Synthetic route to the racemic demethylated analogue of pilosinine **35**.

#### Synthesis of Intermediate **56** by a HWE Reaction

The phosphonate precursor **57** for the HWE reaction was synthesised in two steps according to Hellwinkel<sup>[97]</sup> and Wang et al.<sup>[98]</sup> The commercially available *tert*-butyl 2-bromoacetate (**58**) was reacted in a neat mixture with 1 equivalent of trimethylphosphite at 100 °C to form the corresponding phosphonate **59** in a Michaelis-Arbuzov reaction. When the <sup>1</sup>H NMR of the reaction mixture showed that one of the starting materials was consumed, the remaining other starting material and low-level

byproducts were distilled off at 35 °C at a pressure of  $5.2 \times 10^{-2}$  mbar. A distillation of the product was possible at 77–80 °C but not necessary for purification. The yields were about 60%. When reaction batches with more than 26 mmol starting material were attempted, the reaction profile changed, and the distillation did not provide pure product.

The resulting phosphonate **59** was racemically alkylated by a sequence of deprotonation of the  $\alpha$ -position with sodium hydride followed by addition of methyl 2-bromoacetate (**60**). The crude product **57** was extracted from the reaction mixture. The mineral oil introduced with the sodium hydride separated from the product by formation of a distinct layer which was pipetted off to leave the product with a yield between 50 and 80%. The resulting product was used without further purification.

The benzyl imidazole carboxaldehyde as second starting material of the HWE reaction was provided as a mixture of regioisomers **40/42** by direct benzylation of 4(5)-imidazole carboxaldehyde (**43**)<sup>[83]</sup> (p. 24) or as pure 3,4-substituted imidazole (**40**) in 4 steps.<sup>[99]</sup> As the 3,4-substituted imidazole products were more water soluble and led to difficult workup in later synthesis steps, the mixture of 3,4- and 1,4-substituted imidazoles was preferred.

For the HWE reaction under standard conditions, the phosphonate **57** was deprotonated with sodium hydride in dry THF at 0 °C followed by addition of the aldehyde **40/42**.<sup>[100]</sup> The yields of this reaction were only 30%. Milder conditions with DBU and lithium chloride in dry acetonitrile at RT<sup>[101]</sup> were applied and led to improved yields of up to 54%. Analysis of the reaction showed that the 1,4-substituted imidazole **42** was completely converted while the conversion of the 3,4-substituted imidazole **40** was not complete. Additionally, the 3,4-substituted starting material and product coeluted during column chromatography but the 1,4-substituted product was obtained pure. Under these conditions and the starting material containing 40% of the 3,4-substituted compound, a maximum yield of 60% was expected. The reaction was not further optimised as higher yields would only be obtained by a different composition of the starting material. The configuration of the newly formed double bond was not determined as this was not of importance for the suite of the synthetic route.

#### Formation of the Lactone **63** and Final Deprotection

The *tert*-butyl protecting group of **56** was removed by stirring the molecule in a biphasic system of 85% aqueous phosphoric acid and toluene overnight at RT.<sup>[102]</sup> After extraction of the reaction mixture, the product **61** was obtained as a solid in good yields of 75%. During the reaction a white insoluble solid precipitated and affected stirring so that on larger scale the reaction needed more time to complete. Yields decreased on larger scale probably due to inclusion of the product into the solid byproduct. A scale of 2.8 mmol was good to handle.

The double bond of **61** was hydrogenated at this stage of the synthetic route to avoid hydroboration during the reduction step of the carboxylic acid with borane. Application of atmospheric pressure hydrogen atmosphere to a mixture of the starting material in dry methanol and 10% palladium on activated charcoal led to a complete reduction of the double bond within few hours. Debenzylation as a side reaction was not observed. Consequently, product **62** was isolated in almost quantitative yields. The use of a chiral catalyst for an asymmetric hydrogenation could be a possibility if the product was to be synthesised enantioselectively but was not tried in this work.

The reduction of the carboxylic acid of **62** in presence of an ester requires mild reduction reagents.<sup>[103]</sup> Reactions using the borane–THF complex did not lead to reduction, the borane–dimethyl sulfide complex, however, provided the desired lactone **63** in 35% yield and catechol borane yielded up to 97% of the product. The five-membered lactone **63** was spontaneously formed in this reaction, the intermediate alcohol in presence of the methyl ester was not found. The lactone was isolated and purified by column chromatography.

The benzyl protecting group of **63** was removed by hydrogenolysis. Oxidative debenzylation would not be compatible with the other functional groups of the molecule (Table 5, entry 6). A standard hydrogenation procedure with 10% palladium on activated charcoal with up to 15 bar hydrogen pressure did not lead to conversion (entry 1). A range of conditions was tested (Table 5) until addition of acetic acid to a methanolic solution of the starting material **63** led to a successful reaction with 10% palladium on activated charcoal and 7 bar hydrogen (entry 7). The product **35** was isolated in its protonated form as an acetate salt by filtration and removal of the solvents. The free base was obtained after column chromatography on basic aluminium oxide of activity II–III with yields of 76%.

**Table 5:** Conditions screened for the debenzylation of **63**. The reactions were stirred for 1 d if not otherwise mentioned. The reactions were analysed by two TLCs on silica with 10% MeOH/DCM. One plate was stained with Dragendorff's reagent to detect the starting material **65** and the other with Gibbs reagent to detect the product **35**.

	Conditions	Result
1	15 bar H <sub>2</sub> , Pd/C, DCM	Starting material
2	4 bar H <sub>2</sub> , Pd/C, MeOH, HCl, 2 d	Starting material and presumed product
3	Pd/C, Et <sub>3</sub> SiH, THF <sup>[104]</sup>	Starting material
4	Pd/C, NH <sub>4</sub> COOH <sup>[105]</sup>	Starting material and presumed product
5	AlCl <sub>3</sub> , toluene <sup>[106]</sup>	Starting material
6	KOtBu, DMSO, O <sub>2</sub> <sup>[107]</sup>	Many spots (decomposition)
7	7 bar H <sub>2</sub> , Pd/C, MeOH, AcOH, 3 d <sup>[108]</sup>	Presumed product

This newly developed synthesis of the racemic desmethyl analogue of pilosinine **35** comprises seven steps in the longest linear sequence with an overall yield of 14%. The product, a colourless oil, was analysed to be 95% pure by qNMR.

### 3.2.2 Synthesis of Hybrid Molecules with Pilocarpine Analogues as Orthosteric Moiety

The initial plan aimed at the synthesis of hybrid molecules of pilocarpine (**2**) and pilocarpidine (**18**). Additionally, hybrids of isopilocarpine (**15**) should be produced as presumed inactive references. As the synthesis of pilocarpidine (**18**) was not achieved, the simplified analogue desmethyl pilosinine (**35**) was used instead. For a direct comparison of the influence of the imidazole methyl substituent, pilosinine (**16**) was added to the set of orthosteric fragments. As a result, four different orthosteric fragments were used to synthesise hybrid molecules with naphmethonium fragments (Figure 20).

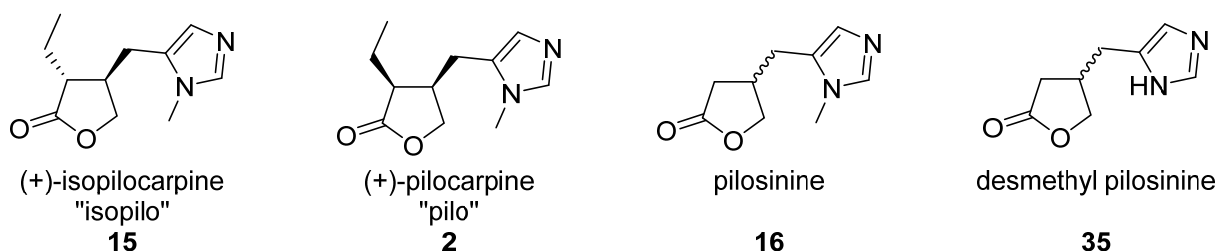
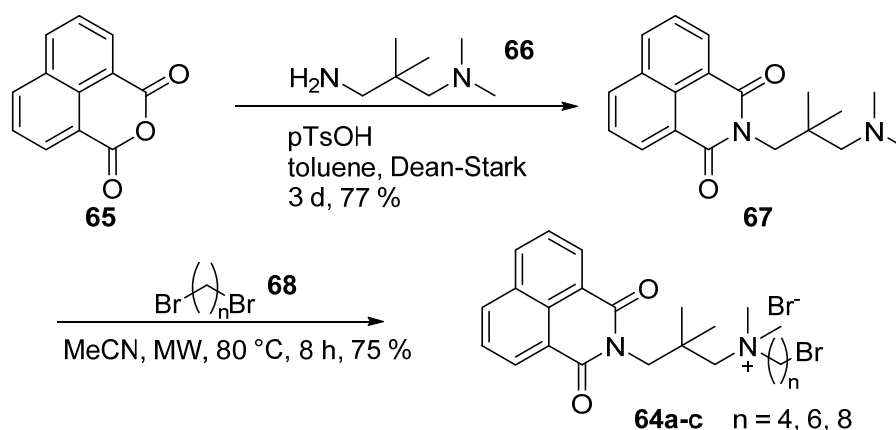


**Figure 20:** Orthosteric fragments as starting materials for hybrid molecules.

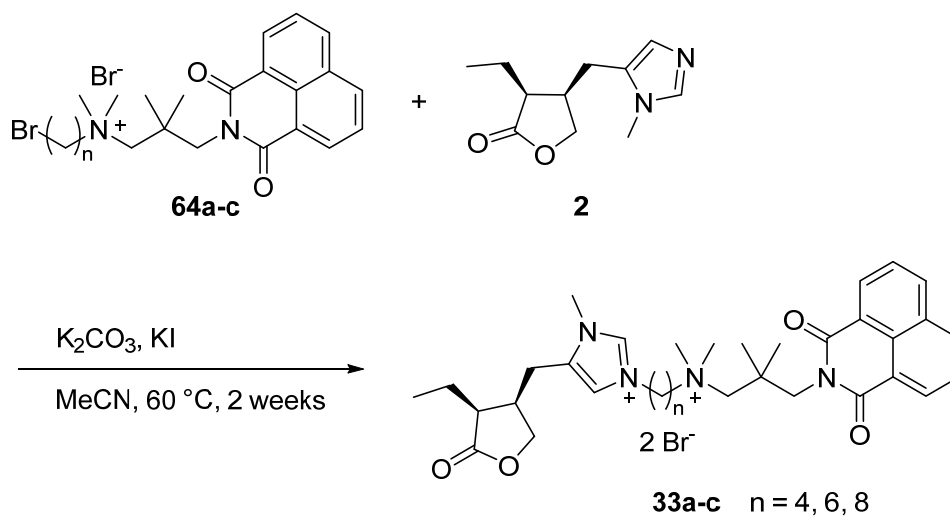
The synthesis of the hybrid molecules relies on well established procedures for the synthesis of the naphmethonium fragment connected to a methylene linker **64a–c** (Scheme 12).<sup>[30b, 109]</sup> 1,8-naphthalic anhydride **65** was reacted under acidic catalysis with the amine **66** to form the allosteric moiety **67** in 77% yield. The linker was attached by a microwave reaction of **67** with an excess of the dibromo alkane **68a–c** with the appropriate chain length and acetonitrile as solvent. The respective molecules **64a–c** were obtained after column chromatography on alumina (activity II–III) in 75% yield.

The four orthosteric fragments were linked to **64a–c** in a nucleophilic substitution reaction, similarly to previous syntheses of dualsteric ligands such as iper-6-naph (**11**).<sup>[27, 31b]</sup> For the linkage of the orthosteric fragment to **64a–c**, both reactants were dissolved in acetonitrile or DMF. Potassium carbonate and a catalytic amount of potassium iodide were added (Scheme 13). Pilocarpine (**2**), isopilocarpine (**15**) and pilosinine (**16**) share the same methyl substituent at the N<sup>1</sup> position of the imidazole whereas **35** is not substituted. The missing substitution directly translates into higher nucleophilicity of **35** compared to the methylated imidazoles. Indeed, the reaction of **35** with **64** was complete after 10 h at 60 °C when heated in the microwave, whereas the other reactions were stirred for 1–2 weeks at 60 °C in a sealed tube and were not significantly accelerated by microwave irradiation.

Hybrid Ligands with Pilocarpine Analogues as Orthosteric Moiety



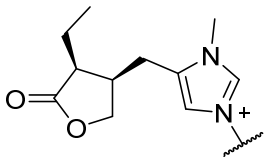
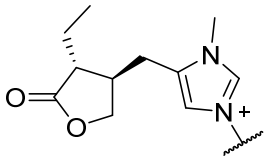
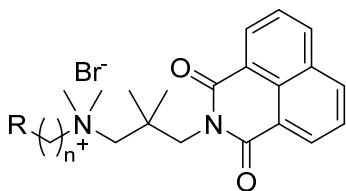
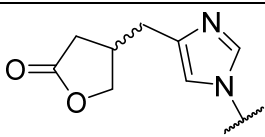
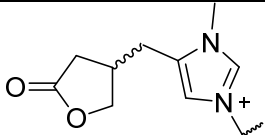
**Scheme 12:** Synthesis of the naphmethonium moiety connected to the bromoalkyl linker (**64a-c**) with  $n = 4, 6, 8$ .



**Scheme 13:** Exemplary scheme for the synthesis of the hybrid ligands **33a-c**. The other hybrid ligands were obtained in the same fashion.

The isolation and purification of the dualsteric compounds was challenging. Reverse phase flash chromatography on a C18 column with acidic mobile phase yielded purified **69** (Table 6), but the other compounds were not obtained in sufficient purity as the longer reaction times also led to more impurities in the reaction mixture. Furthermore, pilo-6-naph (**33b**) isomerised to isopilo-6-naph (**34b**) when chromatographed with acidic additive to the mobile phase. In this way the isopilo-6-naph (**34b**) was first obtained. Without the use of an acidic additive in the mobile phase, product peaks were broader and a separation by flash chromatography was not possible due to insufficient column efficiency. Purification by preparative HPLC on an NX-C18 column with water and methanol as the mobile phase was successful. This can be explained by the use of a slightly different stationary phase and a higher theoretical plate number resulting from a smaller particle size of the stationary phase and an increased column length compared to the flash conditions.

**Table 6:** Overview of the synthesised hybrid molecules.

R	Molecule	n	Name
 "pilo"	<b>33a</b>	4	Pilo-4-naph
	<b>33b</b>	6	Pilo-6-naph
	<b>33c</b>	8	Pilo-8-naph
 "isopilo"	<b>34a</b>	4	Isopilo-4-naph
	<b>34b</b>	6	Isopilo-6-naph
	<b>34c</b>	8	Isopilo-8-naph
	 <b>69</b>	6	Desmethyl-pilosinine-6-naph
	 <b>70</b>	6	Pilosinine-6-naph

NMR analysis of the target molecules confirmed the attachment point of the linker. For each molecule, the  $^1\text{H}/^{13}\text{C}$  HMBC spectrum shows cross peaks between the linker protons and the two unsubstituted imidazole carbons and not to the quaternary imidazole carbon, which confirms a substitution at the  $\text{N}^3$  position (Figure 21). The molecules with a methyl substituent at  $\text{N}^1$  position additionally show cross peaks between the protons of the methyl group and the imidazole carbons at positions 2 and 4.

Additionally, the  $^1\text{H}$  NMR spectra of **33b**, **34a–c** and **70** show broadened singlets with lowered integral values for the proton at imidazole position 2. The effect appears strongest in the spectrum measured in methanol- $\text{d}_4$  of isopilo-6-naph (**34b**), where this peak only integrates for 0.15 relative to the other signals with an integral of approximately 1 per proton. A measurement of isopilo-6-naph (**34b**) in acetonitrile- $\text{d}_3$  shows an integral of 0.65 (Figure 22). At the same time,  $^{13}\text{C}$  chemical shifts for the carbon at position 2 were determined from the  $^1\text{H}/^{13}\text{C}$  HMBC spectra due to a missing peak in the  $^{13}\text{C}$  NMR spectrum of **33b** and **34b**. All those observations lead to the assumption, that the mentioned carbon and proton signals appear reduced due to the quadrupole moment of the two neighbouring nitrogen atoms. The dipole–quadrupole interaction is known to shorten the spin-lattice-relaxation time of the observed nucleus, leading to a less intense and broadened signal.<sup>[110]</sup>

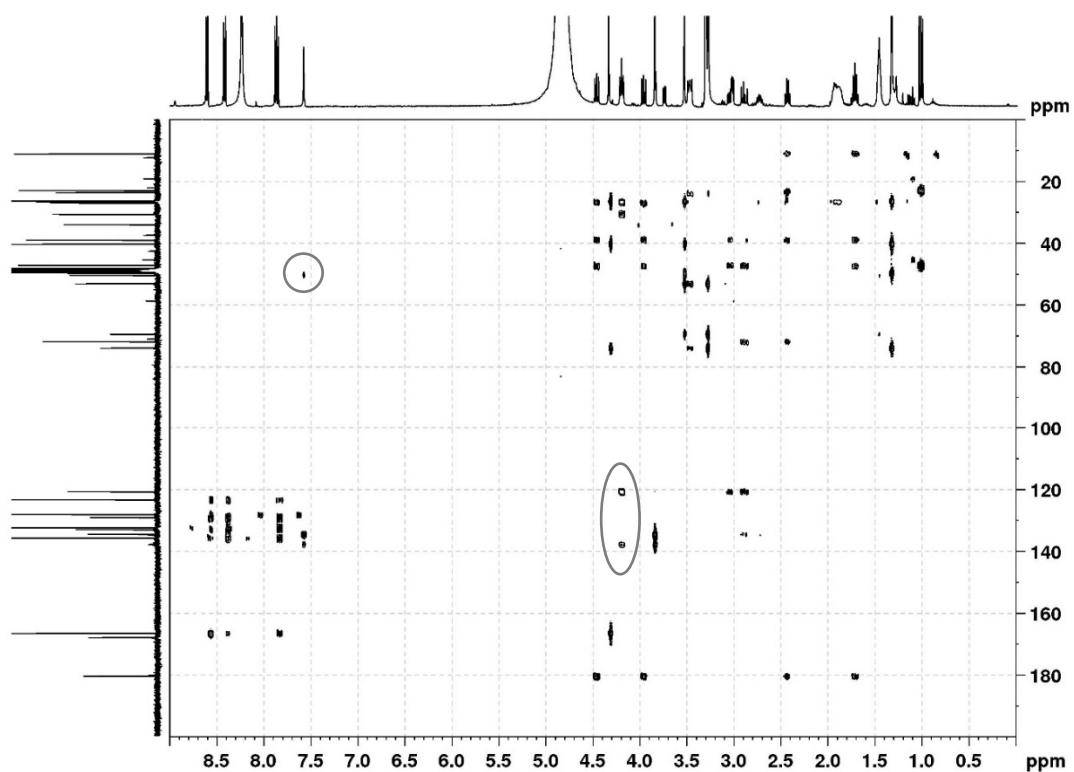


**Figure 21:** Exemplary  $^1\text{H}/^{13}\text{C}$  HMBC spectrum of isopilo-6-naph (**34b**) with highlighted cross-peaks between linker and the two unsubstituted imidazole positions.

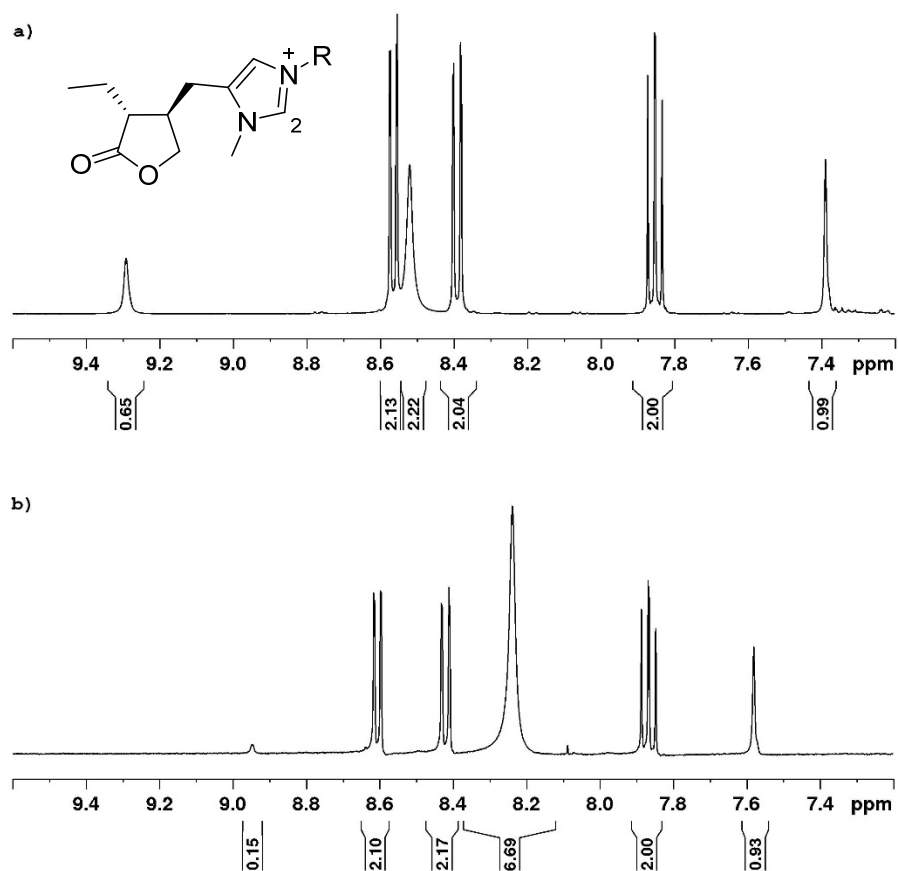


**Figure 22:**  $^1\text{H}$  NMR spectra of the aromatic region of **34b** measured in a) acetonitrile- $\text{d}_3$  and b) methanol- $\text{d}_4$ . The signals at 9.29 (a) and 8.95 ppm (b) correspond to the imidazole proton at position 2.



Taken together, a series of hybrid molecules with four different orthosteric moieties has been synthesised and purified (Table 6). The orthosteric moieties show differences in the lactone ring substitution pattern. The ethyl group can be missing or found either *cis*- or *trans*-configured related to the substituent in position 4. Other differences concern the methyl substitution of the imidazole, which can be missing or present. A comparison of pharmacological results may lead to information about the influence of the ethyl group and the quaternisation of the imidazole on the hybrid molecule's efficacy and affinity.

### 3.3 Stability of Pilocarpine and the Hybrid Ligands

During the synthesis of the pilocarpine hybrid compounds, epimerisation and lactone hydrolysis was observed as unwanted degradation reaction (Figure 23). In particular, hydrolysis readily occurs in basic aqueous media.<sup>[111]</sup> To avoid an impact of degradation on pharmacological test results, the stability of pilocarpine under the pharmacological test conditions was evaluated.

The following references were prepared according to the European Pharmacopoeia<sup>[112]</sup>:

- A sample of commercial pilocarpine hydrochloride in water (10 mg/mL)
- A sample of the hydrolysis products composed of pilocarpic acid (**71**) with isopilocarpic acid (**72**) as byproduct, produced by heating pilocarpine hydrochloride (10 mg/mL) with ammonia

Additionally, the buffer commonly used for pharmacological tests with mAChR was prepared.<sup>[28b]</sup> The buffer composition was 10mM 4-(2-hydroxyethyl)-1-piperazineethanesulfonic acid (HEPES) with 10 mM magnesium chloride and 100 mM sodium chloride at pH 7.4.<sup>[28b]</sup>

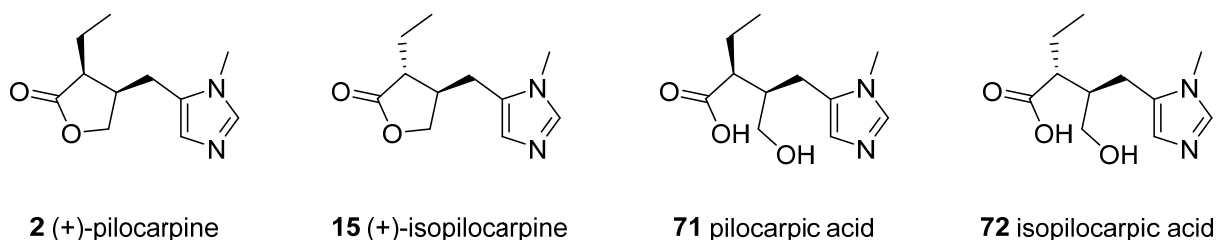


**Figure 23:** Pilocarpine and its epimerisation and hydrolysis products.

Both reference samples and the undiluted HEPES buffer were analysed to check whether the RP18-HPLC method proposed in the European Pharmacopoeia<sup>[112]</sup> was suitable for the analysis of the degradation of pilocarpine. These first measurements (Figure 24, bottom four chromatograms) showed that the buffer peak did not overlap with the analytes of interest and the hydrolysis products were well separated from the main peak. However, an impurity in the commercial sample of pilocarpine hydrochloride was observed in front of the main peak but not completely resolved from the main peak (Figure 25). This peak presumably corresponds to isopilocarpine as described in the

European Pharmacopoeia.<sup>[112]</sup> Altogether, the method was considered to be sufficient to deliver qualitative results.

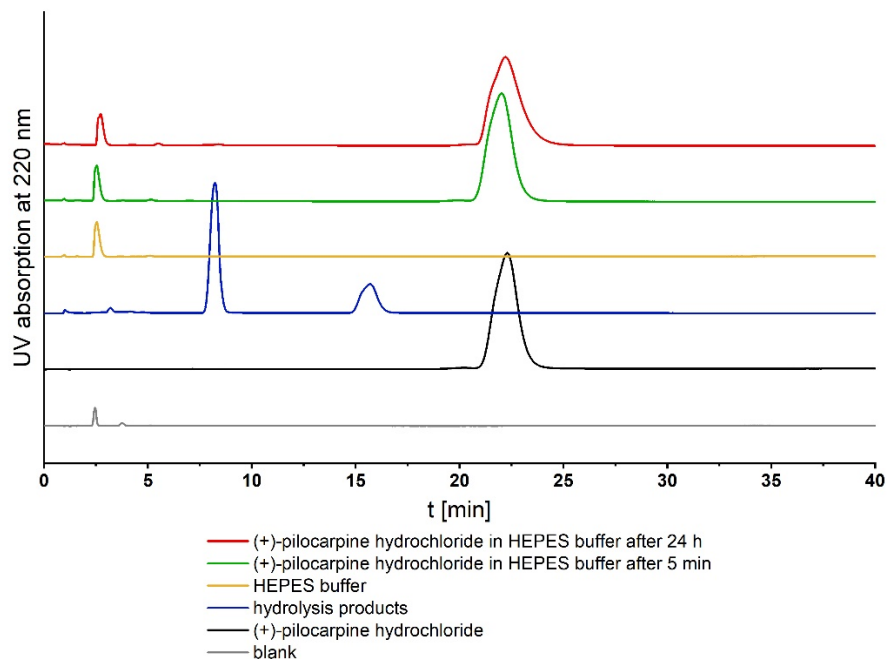


**Figure 24:** Chromatograms of the references and the stability samples of pilocarpine (**2**). The shape of the peaks of the sample after 24 h is altered compared to the sample after 5 minutes as the column was not fully equilibrated when the 24-hour sample was injected. The column ran dry due to a failure of the computer connection overnight.

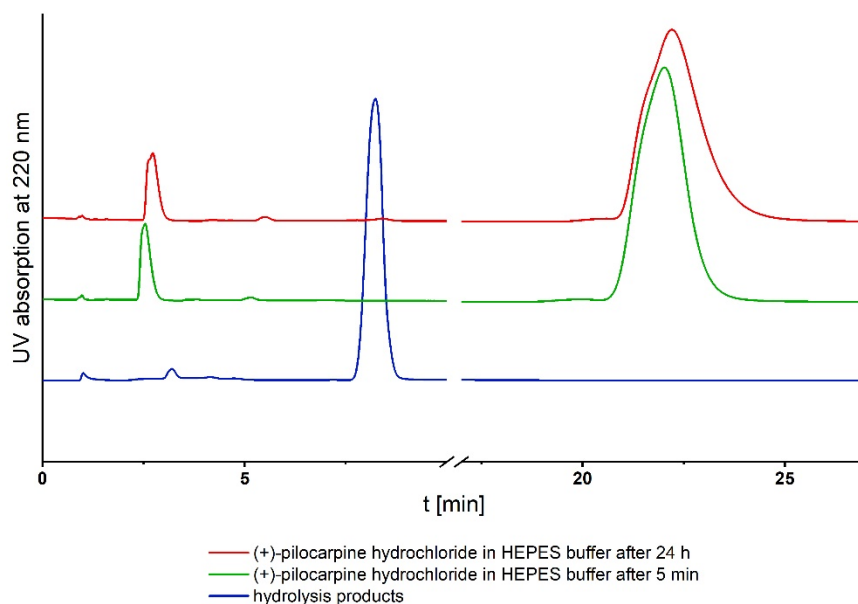


**Figure 25:** Details of the stability analysis of pilocarpine and the main hydrolysis product of pilocarpine (**2**). The initial analysis of pilocarpine and the analysis after 24 h at RT differ in a small peak with the retention time of the main hydrolysis product. The stability samples do not show any peaks in the region of the axis break.

For the qualitative stability evaluation, 10 mg of pilocarpine hydrochloride were dissolved in 10 mL of the HEPES buffer. This mixture was analysed 5 min and 24 h after preparation. The first chromatogram of the solution shows no change in comparison to an overlay of the chromatograms of the reference

pilocarpine sample with the HEPES buffer reference (Figure 24). After 24 h at RT, a peak of 0.3% peak area at a retention time of 15.7 min, appeared as an impurity (Table 7). The peak of the isopilocarpine impurity was not increased.

**Table 7:** Retention times of the peaks in the reference samples using the methods of the European Pharmacopoeia and integrals of the corresponding peaks in the stability sample.

Peak	Retention time [min]	Integral [a.u.]	
		after 5 min	after 24 h
Pilocarpine ( <b>2</b> )	22.3	4769	4705
Isopilocarpine ( <b>15</b> )	20.0	60	32
Pilocarpic acid ( <b>71</b> )	8.2	–	14
Isopilocarpic acid ( <b>72</b> )	15.7	–	–
HEPES	2.5	Not of concern	

As conclusion, pilocarpine's stability in HEPES buffer at a pH of 7.4 and RT is sufficient for pharmacological tests for at least 24 h. The lactone moiety is the instable part of pilocarpine. The lactone is unchanged in the hybrid molecules so that the same stability can be expected in the case of the hybrid ligands.

Usual handling of the compounds involves dissolution in the buffer and aliquotation of the solution to avoid several cycles of freezing and thawing before use. The pharmacological experiments are usually carried out within one working day. In this context, there is no concern about degradation affecting the test results. In case the stock solution is not aliquoted directly after preparation, the solution would undergo regular cycles of freezing and thawing. To avoid hydrolysis in these cases, dimethyl sulfoxide should be used as solvent for the stock solution.

### 3.4 Protonation State of the Orthosteric Fragments and the Hybrid Compounds at Physiological pH

Acetylcholine (**1**), iperoxo (**8**) and most other agonists of mAChRs have a permanently positively charged nitrogen which is crucial for the interaction with the orthosteric binding site and receptor activation. Pilocarpine (**2**) is not constitutively positively charged, but protonation of the imidazole is possible under physiological conditions. For this reason, it is important to be aware of possible variabilities in the protonation state of the orthosteric fragments and hybrid compounds.

The fraction of protonated versus unprotonated species in solution can be determined with the Henderson–Hasselbalch equation

$$\text{pH} = \text{pK}_a - \log_{10} \frac{[\text{HA}^+]}{[\text{A}]}$$

with  $[\text{HA}^+]$  representing the concentration of the protonated form of the substance and  $[\text{A}]$  the concentration of the free base. The  $\text{pK}_a$  value and the target pH need to be known.

Pilocarpine (**2**), Isopilocarpine (**15**) and Pilosinine (**16**)<sup>1</sup> are structurally very similar concerning the imidazole moiety which is important for protonation. As an example for all three compounds, pilocarpine's experimental  $\text{pK}_a$  values were extracted from literature with values of 7.03<sup>[80]</sup> and 6.78<sup>[80]</sup>. At a physiological pH of 7.4 the ratio of protonated to unprotonated species results as 43 and 24%, respectively (Table 8). Less than half of the available pilocarpine is protonated under physiological conditions.

**Table 8:** Calculated values of  $[\text{HA}^+]/[\text{A}]$  at a physiological pH of 7.4 for the  $\text{pK}_a$  values of the specified compounds.

Compound	$\text{pK}_a$	$[\text{HA}^+]/[\text{A}]$
pilocarpine ( <b>2</b> )	7.03 <sup>[80]</sup>	43%
pilocarpine ( <b>2</b> )	6.78 <sup>[113]</sup>	24%
desmethyl pilosinine ( <b>35</b> )	7.12 <sup>[114]</sup>	52%
desmethyl-pilosinine-6-naph ( <b>69</b> )	7.00 <sup>[114]</sup>	40%

Desmethyl pilosinine (**35**), however, presents a different substitution pattern at the imidazole moiety which might influence the proton affinity. For this reason, the  $\text{pK}_a$  value of **35** was predicted using ACD prediction tools in the SiriusT3Control software.<sup>[114]</sup> The  $\text{pK}_a$  was predicted as 7.12 which correlates with a fraction of protonated **35** of 52% at pH = 7.4. As shown in the case of pilocarpine, a small difference in the  $\text{pK}_a$  values can result in a big difference of the protonated fraction due to the change from logarithmic units to a linear scale. Therefore, the predicted value needs to be handled with care. As the published measured values for pilocarpine are quite far apart, a measurement of the  $\text{pK}_a$  value of demethylated pilosinine would not in every case promise a more accurate result than the predicted  $\text{pK}_a$ . If the  $\text{pK}_a$  prediction can be trusted, the fractions of protonated and unprotonated species of desmethyl pilosinine **35** are equal. In comparison to pilocarpine, slightly more protonation takes place.

In the case of the hybrid ligands of pilocarpine, isopilocarpine and pilosinine (**33**, **34** and **71**), the question of protonation does not arise. These hybrid ligands are constitutively charged at the imidazole moiety. The hybrid of desmethylated pilosinine (**69**), however, is not quaternised at the imidazole. Its

<sup>1</sup> To ease the understanding of the following discussions, an overview of the synthesised molecules is provided in the unfoldable appendix.

$pK_a$  was predicted with 7.00<sup>[114]</sup> which corresponds to a protonated fraction of 40% at pH = 7.4. This is similar to the supposed protonation state of pilocarpine.

Taken together, a big difference between the hybrid ligands with a constitutive charge at the imidazole moiety (**33**, **34** and **70**) and the protonatable molecules **2**, **15**, **16**, **35** and **69** exists. Given the case that the protonation state at physiological pH correctly represents the conditions at the receptor binding site, the protonatable molecules would be expected to be much less active than those with a constitutive charge. Their protonated fraction is at maximum 50% of the total available concentration. This might contribute to the explanation of pilocarpine's partial agonism.

### 3.5 Pharmacological Evaluation of the Orthosteric Fragments and the Hybrid Compounds

#### 3.5.1 The Mini-G NanoBRET Assay

Mini-G proteins were originally developed for structural studies of activated GPCRs<sup>[115]</sup> and then adapted to the study of receptor activation in living cells.<sup>[116]</sup> Under natural circumstances, an activated GPCR binds to a corresponding heterotrimeric G protein via its  $\alpha$  subunit, which initiates the signalling cascade. Mini-G proteins were developed as simplified versions of the  $G_s\alpha$  subunit of the  $G_s$  protein (Figure 26): The  $\alpha$  subunit has been deprived of the membrane anchor, the binding domain for the  $\beta$  and the  $\gamma$  subunit, and the  $\alpha$ -helical domain (HD). Additionally, GPCR binding was uncoupled from guanine nucleotide release, and mutations conveying protein stability were introduced. Further, at the new N terminus, a Venus protein (V) was attached, which is a more pH and chloride ion tolerant analogue of the yellow fluorescing protein. Finally, a nuclear export sequence (NES) was added to ensure the mini-G protein is found in the cytoplasm where it can interact with the GPCRs. The mini- $G_s$  protein was shown to bind to the activated GPCR similarly to the complete G protein.<sup>[116b]</sup>

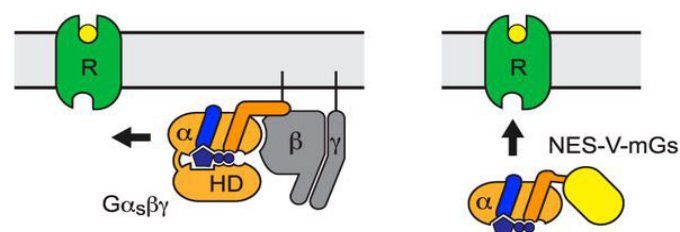


**Figure 26:** Schematic comparison of a complete G protein consisting of  $G\alpha_s\beta\gamma$  (left) and a simplified mini- $G\alpha_s$  protein (right) binding to the GPCR (R) in the cell membrane.<sup>[116b]</sup> (Reprinted under the terms of Creative Commons Attribution license 4.0 (CC-BY). Created by Wan et al.<sup>[116b]</sup>, Copyright © 2018, Elsevier)

Once the viable mini- $G\alpha_s$  was obtained, other mini-G proteins mimicking the other G protein classes were created as chimera between the mini- $G\alpha_s$  and the subfamily specific binding sequence. Those

chimeric mini-G proteins were called mini-G $\alpha_{si}$  and mini-G $\alpha_{sq}$ . All newly created mini-G proteins behaved analogously to the complete G proteins.<sup>[116b]</sup>

To build a bioluminescence resonance energy transfer (BRET) assay based on the mini-G proteins, the receptors to be studied were fused to a luciferase (Figure 27). In the case of the work of our cooperation partners, NanoLuciferase (NLuc) was used (analogous to the Renilla luciferase used by Wan et al.<sup>[116b]</sup>), hence the name NanoBRET for the assay. NLuc generates bioluminescence at 460 nm when converting furimazine to furimamide in the presence of oxygen.<sup>[117]</sup> When a Venus protein is close to the luciferase, i.e. when the mini-G protein is bound to the receptor, this Venus protein can be excited by the bioluminescence and thus fluoresce at 528 nm.<sup>[118]</sup> Detection of the emitted fluorescence allows for quantitation of binding of the mini-G protein to the receptor, which means quantitation of the active-state receptor.

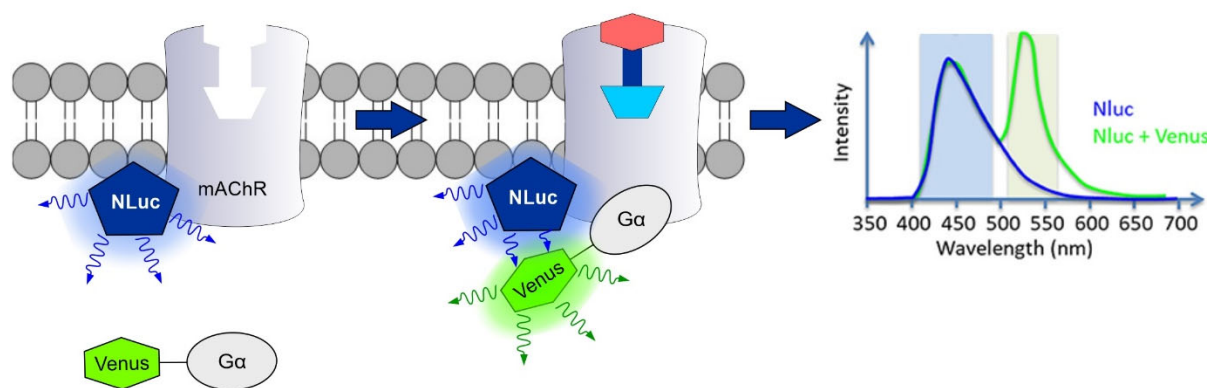


**Figure 27:** The NanoBRET assay relies on detection of spacial proximity between the NLuc at the receptor C-terminus and the Venus protein carried by the mini-G protein. Spacial proximity occurs when the receptor is activated and binds the mini-G protein. This induces a BRET signal between the NLuc and the Venus protein which can be detected by measurement of light emission at 528 nm, the wavelength of fluorescence emission of the Venus protein. (Emission spectra reprinted under the terms of Creative Commons Attribution license 4.0 (CC-BY). Created by Chastagnier et al.<sup>[119]</sup>, Copyright © 2018, Frontiers Media S.A.)

The assay was set up in HEKt cells and measured in 96 well plates. Each substance, i.e. the four orthosteric fragments, the hybrid compounds with a linker of six methylene units and the reference acetylcholine (**1**), were studied in triplicate measurements in seven concentrations at each receptor subtype. The results were normalised to the mini-G protein recruitment of acetylcholine at a concentration of 10  $\mu$ M.

### 3.5.2 Results of the Mini-G NanoBRET Assay

#### Pharmacological Activity of the Orthosteric Fragments

Comparison of the dose-response curves of the orthosteric fragments to the reference acetylcholine (**1**) shows that none of the orthosters is a full agonist at any receptor subtype (Figure 28). Amongst the orthosteric fragments, pilocarpine (**2**) displays the highest efficacy at all receptor

subtypes but with different levels compared to acetylcholine (**1**). At the M<sub>1</sub> receptor, a high efficacy of 81% compared to acetylcholine (**1**) was measured (Table 9). At the M<sub>3</sub> receptor, the efficacy was reduced to 54% of G protein recruitment compared to acetylcholine (**1**) and was even lower at the M<sub>2</sub>, M<sub>4</sub> and M<sub>5</sub> receptors.

The pEC<sub>50</sub> values show that pilocarpine (**2**) generally has a lower potency than acetylcholine (**1**) (Table 10). The pEC<sub>50</sub> values of **2** were highest at the M<sub>1</sub> and the M<sub>5</sub> receptors showing a higher affinity for these receptor subtypes than for M<sub>2-4</sub>. The lowest pEC<sub>50</sub> value was observed at M<sub>4</sub> with approximately one log unit difference to the M<sub>1</sub> receptor.

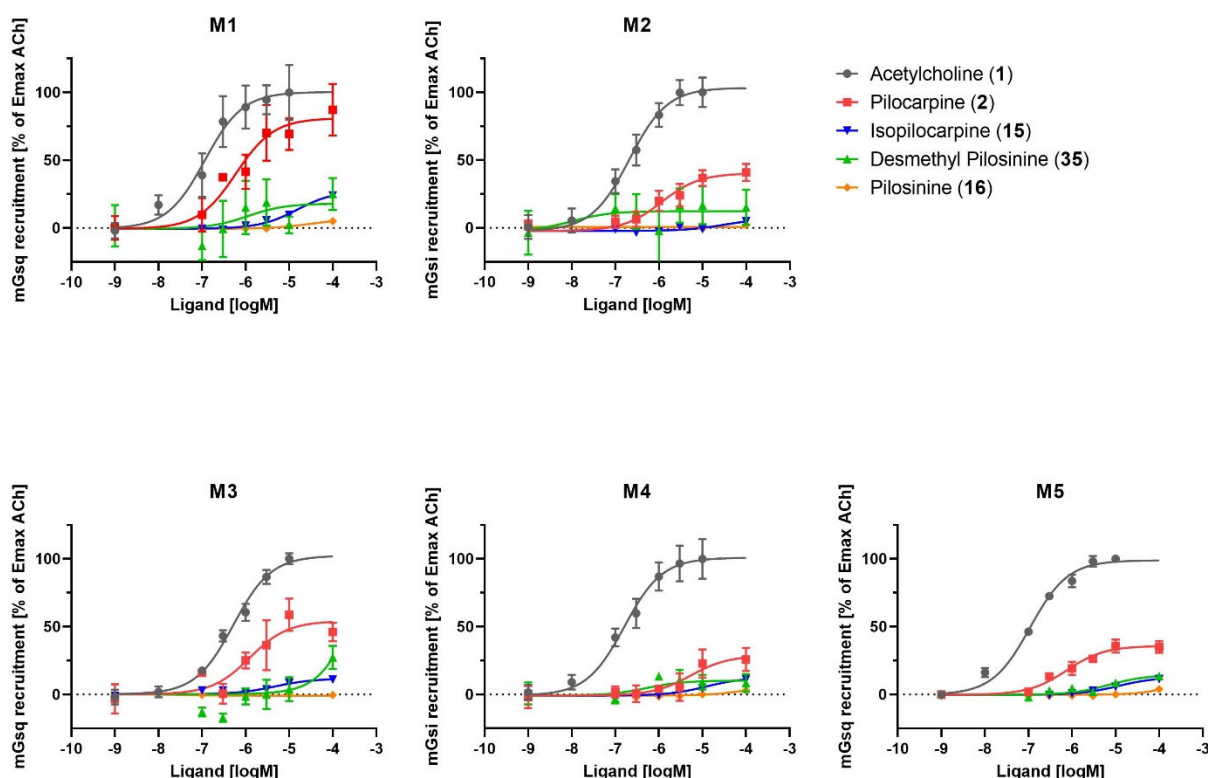


**Figure 28:** Results of the mini-G protein recruitment assays of the orthosteric fragments at the receptors M<sub>1-5</sub>. Results are normalised to the mini-G protein recruitment of acetylcholine (**1**) at a concentration of 10 μM. The experiments were performed in triplicates except for **2** and **35** at M<sub>1,3,4,5</sub> (once) and **35** at M<sub>2</sub> (duplicates).

**Table 9:** Efficacy of the orthosteric ligands compared to acetylcholine (ACh, **1**). The data of the dose-response curves was fitted with a four-parameter model with a fixed Hill slope of 1 and a common minimum value for all data sets. The efficacy was calculated by comparison of the maximum value of the fitted curve to the value of acetylcholine at 10 μM. Missing numbers are due to either a lack of activity or ambiguous fitting results. \* experiment was performed in duplicates; \* experiment was performed once

E <sub>max</sub> in % of E <sub>max</sub> ACh	M <sub>1</sub>	M <sub>2</sub>	M <sub>3</sub>	M <sub>4</sub>	M <sub>5</sub>
Pilocarpine ( <b>2</b> )	81*	40	54*	29*	36*
Isopilocarpine ( <b>15</b> )	28	7	12	13	13
Pilocarpine ( <b>16</b> )	7	1	-	8	-
Desmethyl Pilocarpine ( <b>35</b> )	18*	12 <sup>+</sup>	-*	10*	15*

**Table 10:** pEC<sub>50</sub> values for the orthosteric ligands and acetylcholine (**1**). The data of the dose-response curves was fitted with a four-parameter model with a fixed Hill slope of 1 and a common minimum value for all data sets. The efficacy was calculated by comparison of the maximum value of the fitted curve to the value of acetylcholine at 10 μM. Missing numbers are due to either a lack of activity or ambiguous fitting results. † experiment was performed in duplicates; \* experiment was performed once

pEC <sub>50</sub>	M <sub>1</sub>	M <sub>2</sub>	M <sub>3</sub>	M <sub>4</sub>	M <sub>5</sub>
Acetylcholine ( <b>1</b> )	6.93 ± 0.15	6.68 ± 0.11	6.28 ± 0.18	6.79 ± 0.07	6.96 ± 0.05
Pilocarpine ( <b>2</b> )	6.22 ± 0.21*	5.94 ± 0.25	5.90 ± 2.11*	5.27 ± 0.37*	6.12 ± 0.18*
Isopilocarpine ( <b>15</b> )	4.82 ± 0.49	4.51 ± 2.56	5.36 ± 1.59	4.91 ± 0.56	4.93 ± 0.36
Pilosinine ( <b>16</b> )	-	-	-	-	-
Desmethyl Pilosinine ( <b>35</b> )	5.96 ± 3.02*	7.97 ± 2.45 <sup>†</sup>	-*	6.29 ± 0.93*	5.15 ± 0.48*

Our results for pilocarpine's efficacy and potency should be considered in the context of published data sets. Earlier studies measured phosphatidylinositol (PI) hydrolysis at M<sub>1</sub>, M<sub>3</sub> and M<sub>5</sub> and the inhibition of forskolin-stimulated cAMP accumulation at M<sub>2</sub> and M<sub>4</sub>, i.e. the downstream signals of the GPCR pathway, as an indirect measurement of receptor activation (Chapter 1.2.2, Table 3).<sup>[51-53]</sup> In contrast, our experiments detect G protein recruitment directly at the receptor. In the experiments used in <sup>[51-53]</sup>, full agonism of pilocarpine was observed in comparison to the full agonist carbachol at M<sub>1</sub> and M<sub>4</sub><sup>[51-53]</sup> whereas pilocarpine was found to be a partial agonist at all receptor subtypes in our experiments with the highest efficacies at M<sub>1</sub> and M<sub>3</sub>. Our E<sub>max</sub> values are 38% lower at M<sub>1</sub> and 65% lower at M<sub>4</sub>. Comparison of the pEC<sub>50</sub> values leads to additional differences. Literature described pilocarpine as relatively potent at M<sub>1</sub>, M<sub>3</sub> and M<sub>5</sub>, but reported only weak potency at the M<sub>2</sub> receptor.<sup>[51-53]</sup> Our data suggests a higher potency at M<sub>1</sub> and M<sub>5</sub>, but at M<sub>2</sub> and M<sub>3</sub> they are similar and weaker than at M<sub>1</sub> and M<sub>5</sub>.

In contrast to the above cited full agonism of pilocarpine (**2**) at M<sub>1</sub>,<sup>[51]</sup> dynamic mass redistribution experiments,<sup>[120]</sup> measurement of calcium release<sup>[121]</sup> or again quantification of PI hydrolysis<sup>[58]</sup> revealed that pilocarpine was a partial agonist at M<sub>1</sub>, which is in line with our experiments. Of course, signal amplification can have a high impact on the outcome of the experiments when measurements of the downstream signals are carried out. Additionally different levels of receptor expression might hinder comparability of the results. Our measurements exclude the effects of signal amplification, however, differences in receptor expression cannot be excluded.

Isopilocarpine (**15**) proved to be a weak partial agonist with highest measured efficacies of 28% compared to acetylcholine at the M<sub>1</sub> receptor. The efficacy at the other receptor subtypes was below 15% (Table 9). Additionally, the affinity of isopilocarpine (**15**) was reduced compared to pilocarpine (**2**) at all receptor subtypes with the least differences of a half log unit at M<sub>3</sub> and M<sub>4</sub>, respectively (Table 10). At the other receptors, the affinity of isopilocarpine (**15**) was decreased by more than one



log unit compared to pilocarpine (**2**). Our data set for isopilocarpine (**15**) corresponds to the earlier literature data. Its lower efficacy compared to pilocarpine is in line with observations that isopilocarpine (**15**) induces less shrinkage of the ciliary processes<sup>[48]</sup> and less PI turnover in rat hippocampus<sup>[122]</sup> than pilocarpine (**2**). Similarly, the decreased potency of isopilocarpine compared to pilocarpine agrees to the reported tenfold reduction in affinity at the bovine ciliary muscle muscarinic receptors (mainly M<sub>3</sub>).<sup>[79]</sup>

Pilosinine (**16**) did not show any efficacy at any receptor subtype of more than 10% compared to acetylcholine (**1**) at concentrations up to 100 µM. The decreasing efficacies from pilocarpine (**2**) over isopilocarpine (**15**) to pilosinine (**16**) at all receptor subtypes show that the ethyl group at the lactone C-3 conveys activity and even better if the ethyl group is *cis*- instead of *trans*-configured related to the neighbouring substituent at the lactone. These results explain the 50- to 100-year-old macroscopic observations such as reduction of heart rate<sup>[123]</sup> in animals or measurements of the intra-ocular pressure<sup>[124]</sup> in humans leading to the conclusion that the lactone and the ethyl group of pilocarpine (**2**), including the stereoinformation, are optimised for receptor activation.<sup>[62]</sup>

The demethylated analogue of pilosinine (**35**) had an efficacy in the range of 10 to 20%, which is similar to the efficacy of isopilocarpine (**15**) and slightly higher than that of pilosinine (**16**). Thus, the methyl group at the imidazole seems to lower the efficacy. Whether this is a result of a different protonation behaviour or different interactions with the orthosteric binding site remains to be determined. Interestingly, the potency of desmethyl pilosinine (**35**) is higher than the potency of acetylcholine (**1**) at M<sub>2</sub> and higher than the potency of pilocarpine (**2**) at M<sub>4</sub>.

### Pharmacological Activity of the Hybrid Ligands

The pharmacological study of the hybrid ligands shows that the hybrids of pilocarpine and isopilocarpine, **33b** and **34b**, induced receptor activation at all receptor subtypes and that the hybrids of pilosinine derivatives, **70** and **69**, clearly activate at least one receptor subtype (M<sub>2</sub> and M<sub>1,2,4</sub>) (Figure 29). For this reason, we assume receptor binding of all the tested hybrid compounds. Thus, the choice of the linker attachment point to the orthosteric fragment seems appropriate and to not interfere critically with ligand binding.

A closer look at the data reveals, that at all receptor subtypes, the isopilocarpine hybrid (**34b**) displayed a higher efficacy than the other hybrid ligands in this test series, albeit the highest observed efficacy was only 46% compared to acetylcholine (**1**) at the M<sub>1</sub> receptor (Table 11). Pilo-6-naph (**33b**) induced G protein recruitment of about 20% compared to acetylcholine (**1**) at the M<sub>1</sub>, M<sub>2</sub> and M<sub>4</sub> receptors and almost did not activate the M<sub>3</sub> and M<sub>5</sub> receptors. This is significantly less activation compared to **34b**. Thus, a *trans*- instead of a *cis*-substitution pattern at the lactone of the hybrid ligand improved the capability to activate the receptor. As pilosinine-6-naph (**70**) is virtually inactive at all receptor

subtypes, a lack of the ethyl group in **70** leads to a reduced activity compared to the isopilocarpine and the pilocarpine hybrids, **34b** and **33b** respectively.

Due to a lack of significant activation of the receptors by **69** and **70** (only **69** induces some receptor activation at M<sub>1</sub> and M<sub>2</sub>), conclusions about the influence of the methyl substituent at the imidazole of the hybrids cannot be drawn. Additionally, none of the studied hybrid ligands turned out to be a subtype selective ligand.

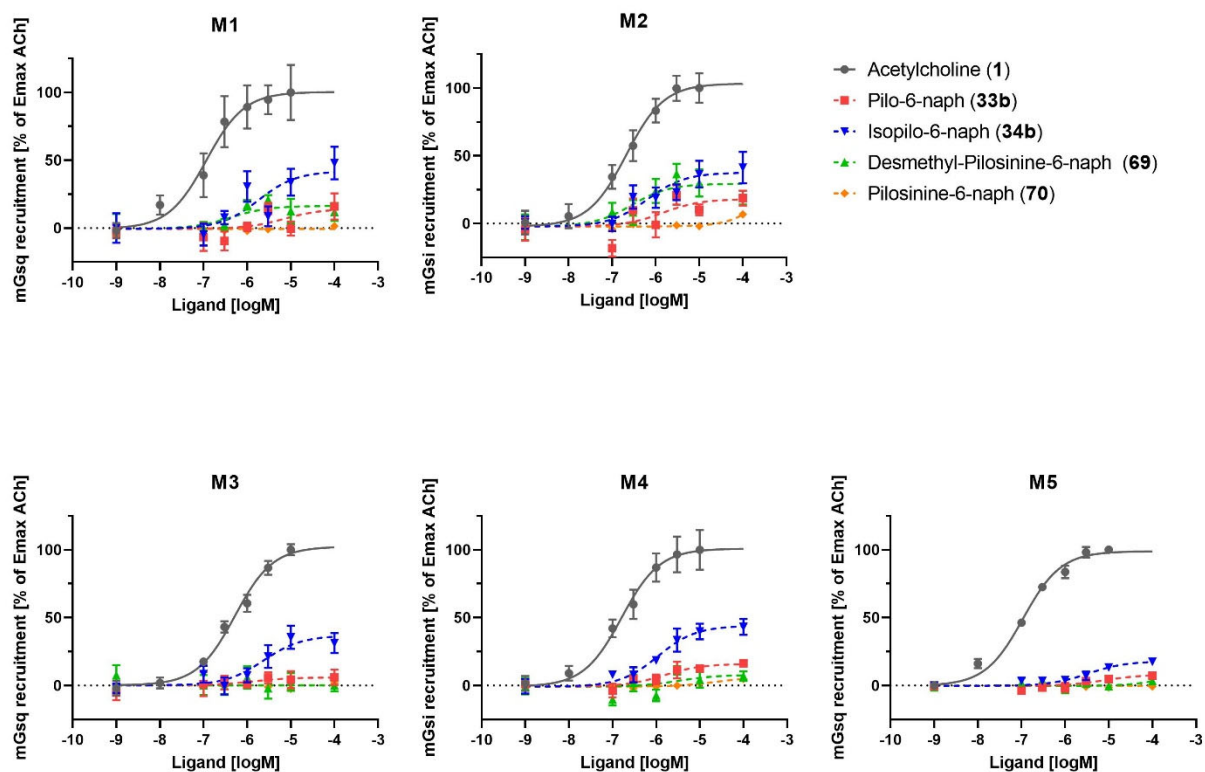


**Figure 29:** Results of the mini-G protein recruitment assays of the hybrid molecules at the receptors M<sub>1-5</sub>. Results are normalised to the mini-G protein recruitment of acetylcholine (**1**) at a concentration of 10  $\mu$ M. All experiments were performed in triplicates except for **33b**, **34b**, **69** at M<sub>1,3,4,5</sub> (duplicates).

**Table 11:** Efficacy of the hybrid ligands compared to acetylcholine (**1**). The data of the dose-response curves was fitted with a four-parameter model with a fixed Hill slope of 1 and a common minimum value for all data sets. The efficacy was calculated by comparison of the maximum value of the fitted curve to the value of acetylcholine at 10  $\mu$ M. Missing numbers are due to either a lack of activity or ambiguous fitting results. \* experiment was performed in duplicates.

<b>E<sub>max</sub> in % of E<sub>max</sub> ACh</b>	<b>M<sub>1</sub></b>	<b>M<sub>2</sub></b>	<b>M<sub>3</sub></b>	<b>M<sub>4</sub></b>	<b>M<sub>5</sub></b>
Pilo-6-naph ( <b>33b</b> )	19 <sup>+</sup>	18	6 <sup>+</sup>	16 <sup>+</sup>	8 <sup>+</sup>
Isopilo-6-naph ( <b>34b</b> )	46 <sup>+</sup>	38	37 <sup>+</sup>	44 <sup>+</sup>	18 <sup>+</sup>
Pilosinine-6-naph ( <b>70</b> )	-	-	-	6	-
Desmethyl-pilosinine-6-naph ( <b>69</b> )	16 <sup>+</sup>	29	- <sup>+</sup>	8 <sup>+</sup>	- <sup>+</sup>

**Table 12:** pEC<sub>50</sub> values for the hybrid ligands and acetylcholine (**1**). The data of the dose-response curves was fitted with a four-parameter model with a fixed Hill slope of 1 and a common minimum value for all data sets. The efficacy was calculated by comparison of the maximum value of the fitted curve to the value of acetylcholine at 10 μM. Missing numbers are due to either a lack of activity or ambiguous fitting results. † experiment was performed in duplicates.

pEC <sub>50</sub>	M <sub>1</sub>	M <sub>2</sub>	M <sub>3</sub>	M <sub>4</sub>	M <sub>5</sub>
Pilo-6-naph ( <b>33b</b> )	5.15 ± 1.91 <sup>†</sup>	5.84 ± 0.56	5.87 ± 1.23 <sup>†</sup>	5.82 ± 0.43 <sup>†</sup>	5.09 ± 0.61 <sup>†</sup>
Isopilo-6-naph ( <b>34b</b> )	5.79 ± 0.29 <sup>†</sup>	6.20 ± 0.27	5.63 ± 1.61 <sup>†</sup>	5.96 ± 0.16 <sup>†</sup>	5.47 ± 0.25 <sup>†</sup>
Pilosinine-6-naph ( <b>70</b> )	-	-	-	4.65 ± 1.43	-
Desmethyl-pilosinine-6-naph ( <b>69</b> )	6.37 ± 0.80 <sup>†</sup>	6.56 ± 0.33	- <sup>†</sup>	5.50 ± 0.86 <sup>†</sup>	- <sup>†</sup>

### 3.5.3 Discussion of the Effects of Hybrid Formation in Pilocarpine-Based Hybrid Ligands

A large variety of hybrid compounds between orthosteric agonists and antagonists with an allosteric moiety has been investigated in earlier studies with the aim to create ligands which are able to simultaneously bind to the orthosteric and allosteric binding sites of mAChRs and, in the case of agonists, activate them (Chapter 1.1.5). At the same time many hybrids retained the subtype selectivity patterns of their allosteric moiety promising insights into the origin of subtype selectivity which might be exploited to create therapies with reduced side effects.<sup>[16, 25b, 25c, 120, 125]</sup> Additionally observed signalling bias contributes further options to optimise drug selectivity.<sup>[18b, 31a, 32, 126]</sup>

High affinity of hybrid compounds was obtained when a hybrid of two high affinity moieties perfectly fits the geometric requirements of the receptor. In the case of a well-designed ligand, an increased affinity compared to the affinities of the allosteric and orthosteric fragments due to an extended binding mode can be achieved.<sup>[127]</sup> When the orthosteric fragment was a full or superagonist, high efficacy was reached as seen with iper-8-naph,<sup>[31a]</sup> for example. Both efficacy and affinity can be influenced by the allosteric fragment of the hybrid ligand similarly to the effects known as cooperativity effects between separate orthosters and allosteric modulators.<sup>[16]</sup> A positive influence on the affinity is expected when both fragments of the hybrid stabilise the same receptor conformation. For example, in the high-affinity dualsteric antagonist THRX-160209 (Figure 30) both the negative allosteric modulator 4-aminobenzylpiperidine and the orthosteric antagonist 3-benzhydryl pyrrolidine preferably bind to the inactive receptor conformation of M<sub>2</sub>.<sup>[127]</sup> Negative cooperativity results from a mismatched case as in iper-6-naph (**11**)<sup>[25b]</sup> and allosteric quenching of the intrinsic activity of the orthosteric moiety tetramethylammonium was observed with the hybrid partial agonist McN-A-343.<sup>[128]</sup>

The hybridisation of pilocarpine analogues with a naphmethonium fragment led to varied changes in affinity and efficacy (Figure 31, Figure 32). Isopilocarpine (**15**) profited from hybridisation especially at the M<sub>2</sub> and M<sub>4</sub> receptors whereas the pilocarpine hybrid **33b** showed reduced potency and efficacy except for the M<sub>4</sub> receptor. Desmethyl-pilosinine-6-naph (**69**) equally showed reduced affinity at the

M<sub>2</sub> receptor compared to the corresponding orthoster **35**. The behaviour of pilo-6-naph (**33b**) partly contrasts the findings of studies of ternary complexes of the M<sub>2</sub> receptor with naphmethonium (**9**) and pilocarpine (**2**). Naphmethonium (**9**) was shown to increase the potency and decrease the efficacy of pilocarpine.<sup>[17]</sup> As a partial agonist, pilocarpine (**2**) is thought to bind to both the active and the inactive receptor state the latter being stabilised by the allosteric modulator naphmethonium (**9**). This facilitates binding of pilocarpine (**2**) in presence of naphmethonium (**9**), but also stabilises the inactive receptor conformation.<sup>[17]</sup> A possible explanation for the low potency of pilo-6-naph (**33b**) is that the hybrid is not able to adopt a binding pose which ensures all interactions of the corresponding fragments in the ternary complex and that the naphmethonium fragment of the hybrid only contains one half of its parent compound so that the observations of the ternary complex cannot be transferred. A low efficacy of pilo-6-naph was expected due to the only partial agonism of pilocarpine and a negative influence of the naphmethonium fragment. A binding pose with impaired binding interactions due to hybrid formation might have an additional impact on the efficacy.

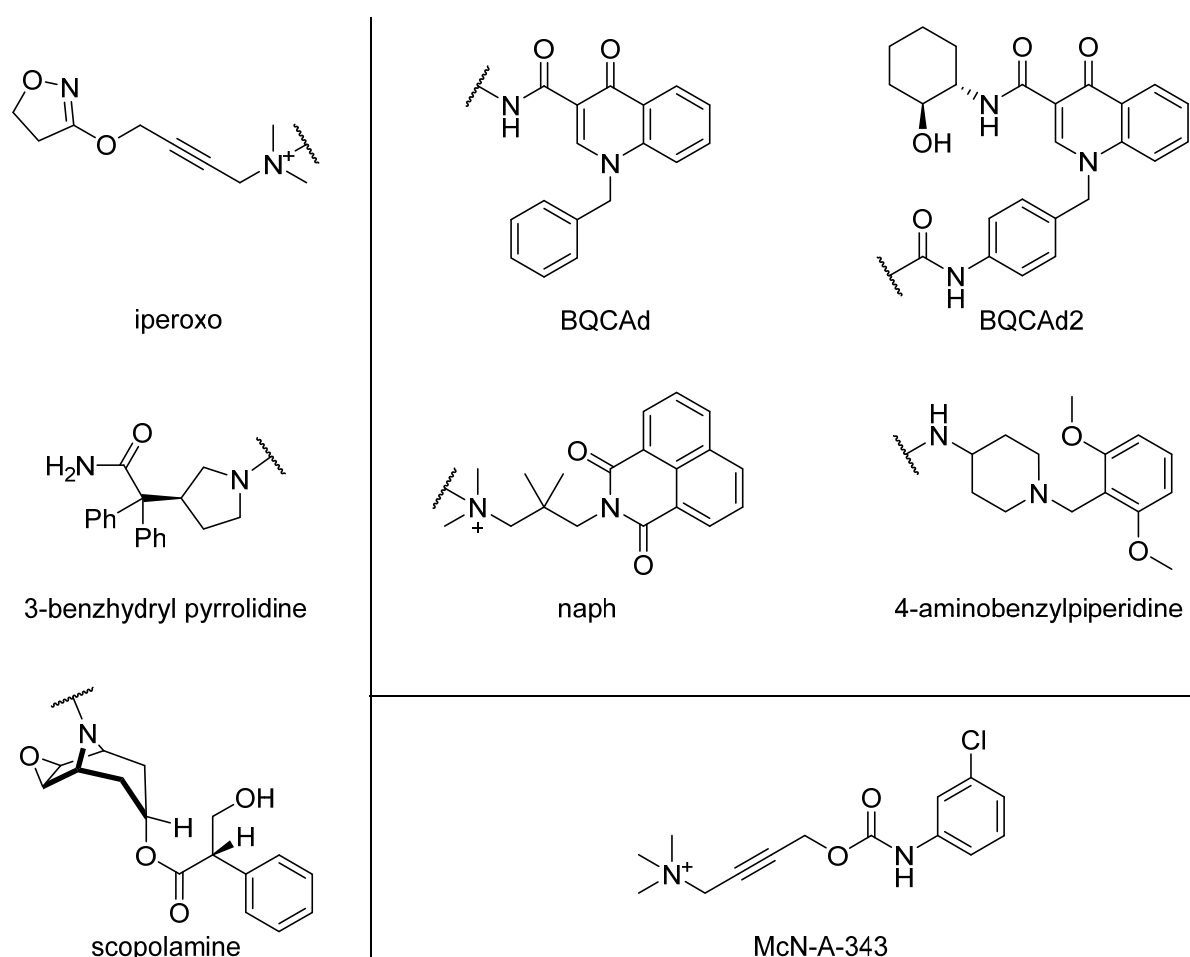


**Figure 30:** Structures of the orthosteric moieties iperoxo, 3-benzhydryl pyrrolidine and scopolamine, the allosteric moieties BQCAAd, BQCAAd2, 4-aminobenzylpiperidine and naph and the hybrid ligand McN-A-343. Orthosteric and allosteric moieties are linked in various combinations by an alkyl chain of *n* methylene units to obtain the respective hybrid ligands.

## Hybrid Ligands with Pilocarpine Analogues as Orthosteric Moiety

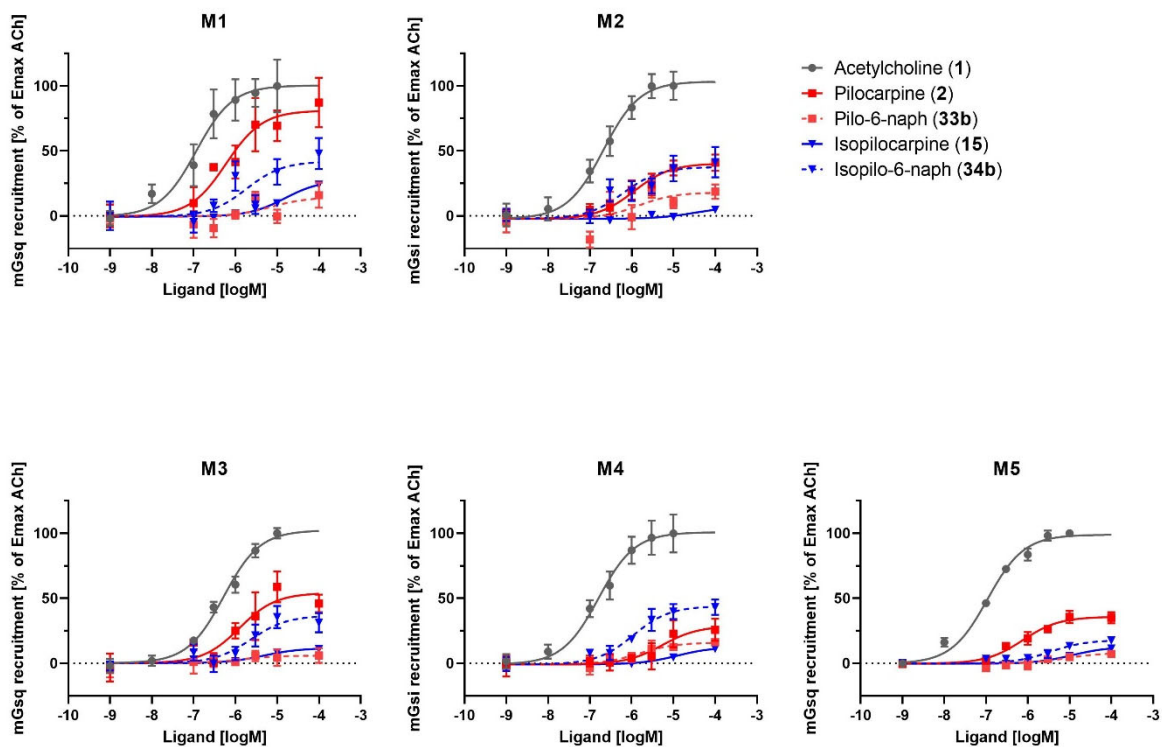


**Figure 31:** Results of the mini-G protein recruitment assays of pilocarpine (2), isopilocarpine (15) and their hybrids 33b and 34b at the receptors M<sub>1-5</sub>. Results are normalised to the mini-G protein recruitment of acetylcholine (1) at a concentration of 10  $\mu$ M. Experiments were performed in triplicates except for 2 at M<sub>1,3,4,5</sub> (once) and 33b, 34b at M<sub>1,3,4,5</sub> (duplicates).

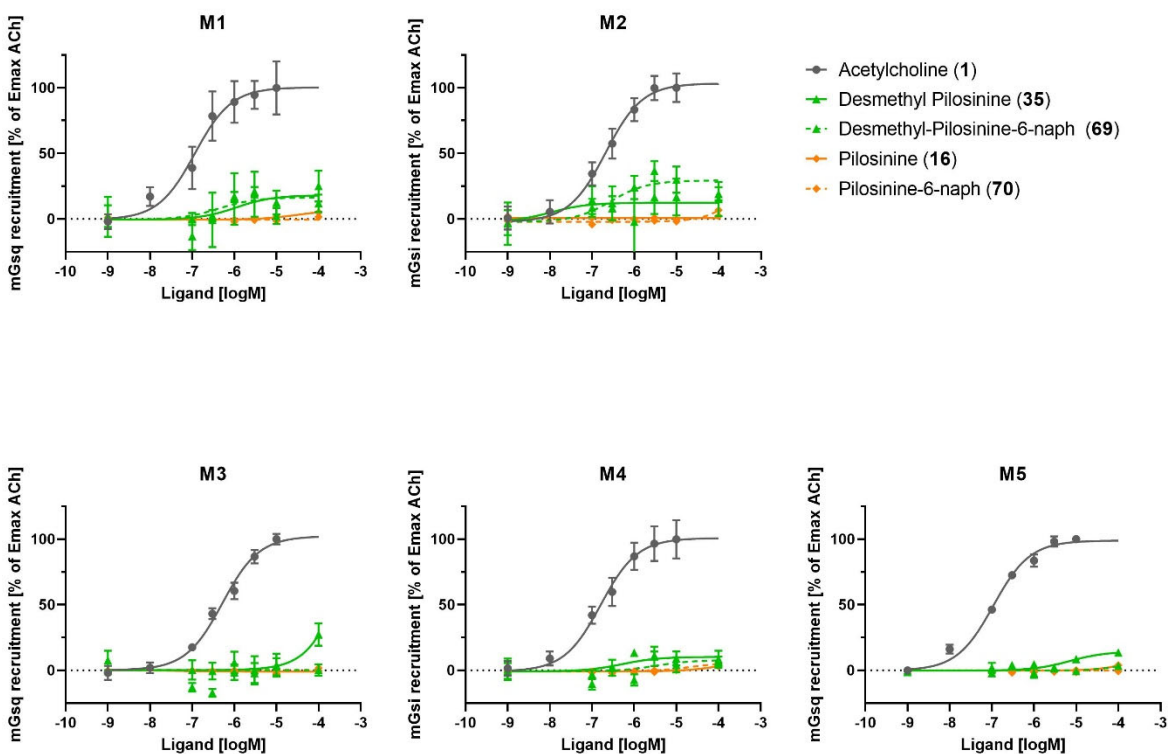


**Figure 32:** Results of the mini-G protein recruitment assays of pilosinine (16), demethylated pilosinine (35) and their hybrids 69 and 70 at the receptors M<sub>1-5</sub>. Results are normalised to the mini-G protein recruitment of acetylcholine (1) at a concentration of 10  $\mu$ M. Experiments were performed in triplicates except for 35 at M<sub>1,3,4,5</sub> (once) and 69 at M<sub>1,3,4,5</sub> and 35 at M<sub>2</sub> (duplicates).

Especially the linker length was found to have a strong influence on affinity and efficacy of earlier dualsteric ligands. A short linker length can restrict the fit of both fragments of the hybrid ligand to the respective binding sites. In the case of iper-n-naph at the M<sub>1</sub><sup>[32]</sup> and the M<sub>2</sub><sup>[31a]</sup> receptor and iper-n-BQCA2 (Figure 30) at all receptor subtypes<sup>[129]</sup>, the orthosteric moiety was shown to dominate the binding pose of the hybrid so that a shorter linker leads to an increased steric hinderance of receptor closure due to the steric bulk of the allosteric moiety. In contrast to the iper-n-naph and iper-n-BQCA2 hybrids, the binding pose of various BQCA2 hybrids at the M<sub>1</sub> receptor was dominated by the allosteric moiety so that the linker length determined the position of the orthosteric moiety, especially of the quaternary ammonium.<sup>[30a]</sup> Additionally, the nature and length of the linker of iper-n-naph influences the equilibrium of ligand binding ensembles between the dualsteric and purely allosteric binding pose of the hybrid, thus having a big influence on the hybrid's efficacy.<sup>[28a]</sup> As each of the hybrids has a different binding pose the linker lengths cannot be directly compared. This is the reason, why each study determined the optimum linker length for the specific experimental setting. In all cases, linker lengths of six to eight methylene units led to the best affinities and efficacies. Therefore, the investigation of the pilocarpine hybrids with a longer linker, for example eight methylene units (**33c**), would be of interest to determine whether the linker length is responsible for the observed reduced affinities and efficacies of pilo-6-naph.

In contrast to pilo-6-naph (**33b**), isopilo-6-naph (**34b**) at all receptor subtypes shows increased efficacies compared to its corresponding orthoster, although both orthosters **15** and **35** are weaker partial agonists than pilocarpine (**2**). In these cases, the effect of naphmethonium (**9**) on the dose–response curve of the orthosteric fragment in a ternary complex is not known. However, the data suggests a gain of affinity and efficacy of the hybrid ligand. Thus, the isopilocarpine hybrid **34b** seems to better fit the binding pocket and profit from stronger binding interactions to the active receptor conformation leading to better receptor activation than the pilocarpine hybrid **33b**. Pharmacological testing of the isopilo-8-naph hybrid (**34c**) will reveal if a longer linker can lead to an even stronger agonistic ligand.

The influence of an allosteric modulator on receptor activation is strongly probe dependent.<sup>[125a]</sup> However, in ternary complexes with full agonists and in hybrids with agonists as orthosteric fragments, naphmethonium (**9**) and its fragments have always had a strong negative influence<sup>[27]</sup> which reduced the efficacies of partial agonists as seen with pilocarpine (**2**) and decreased the potency of full agonists such as acetylcholine (**1**).<sup>[17]</sup> In hybrids with the antagonists atropine and scopolamine (sco) as orthosteric fragments, hybridisation with naphmethonium increased the potency of the hybrids compared to the orthoster alone.<sup>[109]</sup> As observed with isopilo-6-naph (**34b**), the naphmethonium fragment can also have a positive effect on receptor activation in agonistic hybrids (**34b**). With the hybrids iper-6-naph, pilo-6-naph (**33b**), isopilo-6-naph (**34b**) and sco-6-naph we have a series of

hybrids with a common allosteric moiety and linker but big differences in orthosteric activity ranging from superagonist over weak partial agonist to antagonist. At the M<sub>2</sub> receptor, the potency of iper-6-naph was reduced,<sup>[25b]</sup> pilo-6-naph unchanged and isopilo-6-naph and sco-6-naph<sup>[109]</sup> increased related to the corresponding orthosters. The interaction of the naphmethonium fragment seems to less hinder or better improve binding of the hybrid to the receptor the weaker the orthosteric agonists are, approaching the interactions between antagonist and naphmethonium.

Many hybrids of full agonists and antagonists were synthesised in order to obtain subtype selectivity.<sup>[130]</sup> For this reason a subtype selective allosteric moiety was attached to the orthosteric ligand. Indeed, iper-n-naph and iper-n-phth showed some M<sub>2</sub> selectivity<sup>[25b]</sup> which means that the hybrid retained the selectivity profile of the respective allosteric fragment. Analogously, BQCA fragments provide M<sub>1</sub> selectivity, but an iper-n-BQCA<sub>2</sub> hybrid was designed to a M<sub>2</sub>/M<sub>4</sub> selectivity by shortening of the linker length.<sup>[129]</sup> In case of a superagonist as orthosteric moiety leading to an orthosterically dominated binding pose, a shorter linker leads to a higher steric bulk in the allosteric vestibule hindering closure of the orthosteric binding site.<sup>[31a, 32]</sup> The result is a reduction in G<sub>q</sub> activation primarily shown by reduced efficacy at the G<sub>q</sub> coupled receptors M<sub>1</sub>, M<sub>3</sub> and M<sub>5</sub> leading to some selectivity for M<sub>2</sub> and M<sub>4</sub>.<sup>[31a, 129]</sup> As no subtype selectivity of the pilocarpine-based hybrids for M<sub>2</sub>/M<sub>4</sub> was observed, this source of selectivity was not exploited in this study. However, the increase of efficacy observed for isopilo-6-naph (**34b**) compared to isopilocarpine (**15**) was most pronounced and the decrease of efficacy of pilo-6-naph (**33b**) was least at the M<sub>2</sub> and M<sub>4</sub> receptors, which represents the selectivity pattern of naphmethonium (**9**). This points to an influence of the allosteric moiety on the interaction with the different receptor subtypes which is not sufficient to induce significant receptor subtype selectivity. This is probably due to subtype specific interactions with the allosteric binding sites similar to naphmethonium (**9**) alone, but the binding pose is supposedly not dominated by the orthosteric fragment.

In contrast to the binding poses of iper-n-naph, the binding pose of BQCA<sub>2</sub> hybrids with various orthosteric moieties at the M<sub>1</sub> receptor was dominated by the allosteric moiety.<sup>[30a]</sup> The binding pose of the orthosteric moieties was predefined by the positioning of the quaternary ammonium suspended on the linker. The resulting binding pose lacked optimum fit of the interactions between orthosteric moiety and the respective binding pocket. However, as long as the quaternary ammonium of the orthosteric moiety was correctly positioned, partial agonists with robust receptor activation were obtained. This was demonstrated by reduction of the orthosteric fragment to a tetramethylammonium unit<sup>[30a]</sup> or in the case of the dualsteric agonist McN-A-343.<sup>[128]</sup> The structure–activity relationship changed between pilocarpine analogues and their hybrids. Isopilocarpine (**15**) is less active than pilocarpine (**2**), but isopilo-6-naph (**34b**) induces more receptor activation than pilo-6-naph (**33b**). Apparently, the orthosteric pilocarpine-like moiety of the hybrids interacts in a different way with the

orthosteric binding site than the corresponding orthosters. As discussed above, the selectivity pattern of the allosteric naphmethonium fragment shows an influence on  $pEC_{50}$  and  $E_{max}$  of the hybrid ligands which might result from a binding pose of the naphmethonium moiety which is similar to that of naphmethonium (**9**). Therefore we suggest, that the binding pose of the hybrid ligands based on pilocarpine-like orthosters is dominated by the allosteric moiety similarly to the findings with the BQCAd hybrids.<sup>[30a]</sup> This would not be surprising given the relatively low affinity of pilocarpine (**2**) compared to naphmethonium (**9**) at the  $M_2$  receptor.<sup>[25b]</sup>



## 4 Synthesis of Pilocarpine Analogues for the Study of Pilocarpine's Binding Mode in mAChRs

The hypothesis of two distinct binding modes of pilocarpine in the orthosteric site of mAChRs leading to pilocarpine's partial agonism (Chapter 2) was to be challenged experimentally.

The targeted experimental tool compounds **16** and **31a–d** differ from pilocarpine in the size of the alkyl substituent R at the lactone C-3 (Figure 33). The compounds to test should be at least diastereomerically pure, enantiomeric purity would be better.

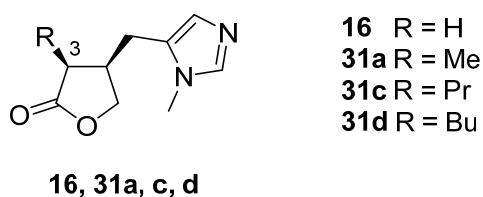
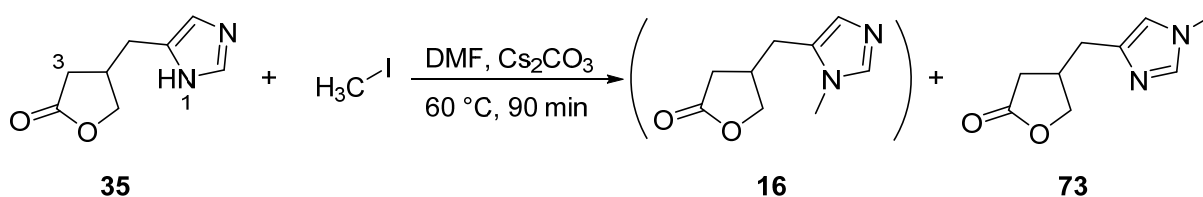


**Figure 33:** Targeted analogues of pilocarpine to study the binding pose in the orthosteric binding site of muscarinic receptors.

### 4.1 Synthesis of Diastereomeric Mixtures of Pilocarpine Analogues and Approaches to their Separation

#### 4.1.1 Methylation of Racemic Desmethyl Pilocarpine

A first synthetic approach to the target molecules was based on the already synthesised racemic desmethyl pilosinine (**35**) as starting material (Chapter 3.2.1). This route requires methylation of the imidazole at N-1 and stereoselective alkylation of the lactone at C-3.<sup>[131]</sup> Methylation should be the first step, because the acidic proton of the nonalkylated imidazole **35** would interfere with the deprotonation of the lactone C-3 needed for alkylation.



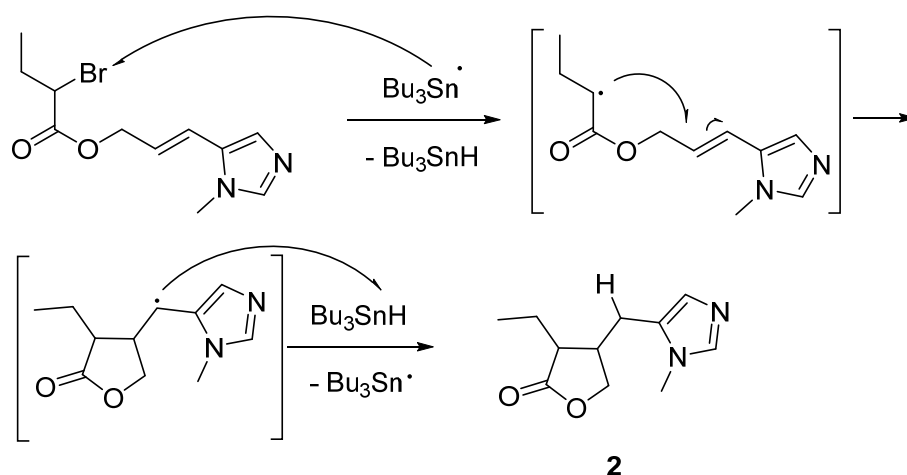
**Scheme 14:** Methylation of the imidazole moiety of **35**.<sup>[132]</sup>

The methylation reaction of the imidazole moiety of **35** (Scheme 14) yielded mainly the N<sup>3</sup>-methylated product **73** instead of the desired N<sup>1</sup>-methylated product **16**. An attempt to protect the N<sup>3</sup> with a trityl or a *para*-nitrobenzylsulfonyl group failed due to insufficient reactivity of the protected intermediate. Consequently, the methylation of demethylated racemic pilosinine **35** was abandoned.

An adaptation of the synthesis pathway leading to racemic desmethyl pilosinine **35** (Chapter 3.2.1) replacing the benzyl protected imidazole by methyl imidazole was abandoned due to low yields of only 25% in the HWE reaction combined with the suspension of commercial availability of catechol borane. The attempts to produce reactive catechol borane from catechol and borane–THF complex failed.

#### 4.1.2 Synthesis of Pilocarpine Analogues by Radical Cyclisation

Due to the failure to produce pilocarpine analogues using the above developed route, the synthetic approach to pilocarpine proposed by Belletire and Mahmoodi<sup>[81]</sup> was tested (Scheme 15). The synthetic route is based on a radical cyclisation reaction to form the lactone moiety. The advantage of the resulting 7-step synthetic route (Scheme 16) is a late introduction of the alkyl substituent at lactone C-3. The *cis/trans* ratio of the product pilocarpine (**2**), however, was reported to be only 1:4. The amount of *cis*-product would have to be increased by kinetic epimerisation as proposed by Compagnone.<sup>[95]</sup>



**Scheme 15:** Mechanism of the radical cyclisation reaction leading to the desired lactone of pilocarpine (**2**).<sup>[81]</sup>

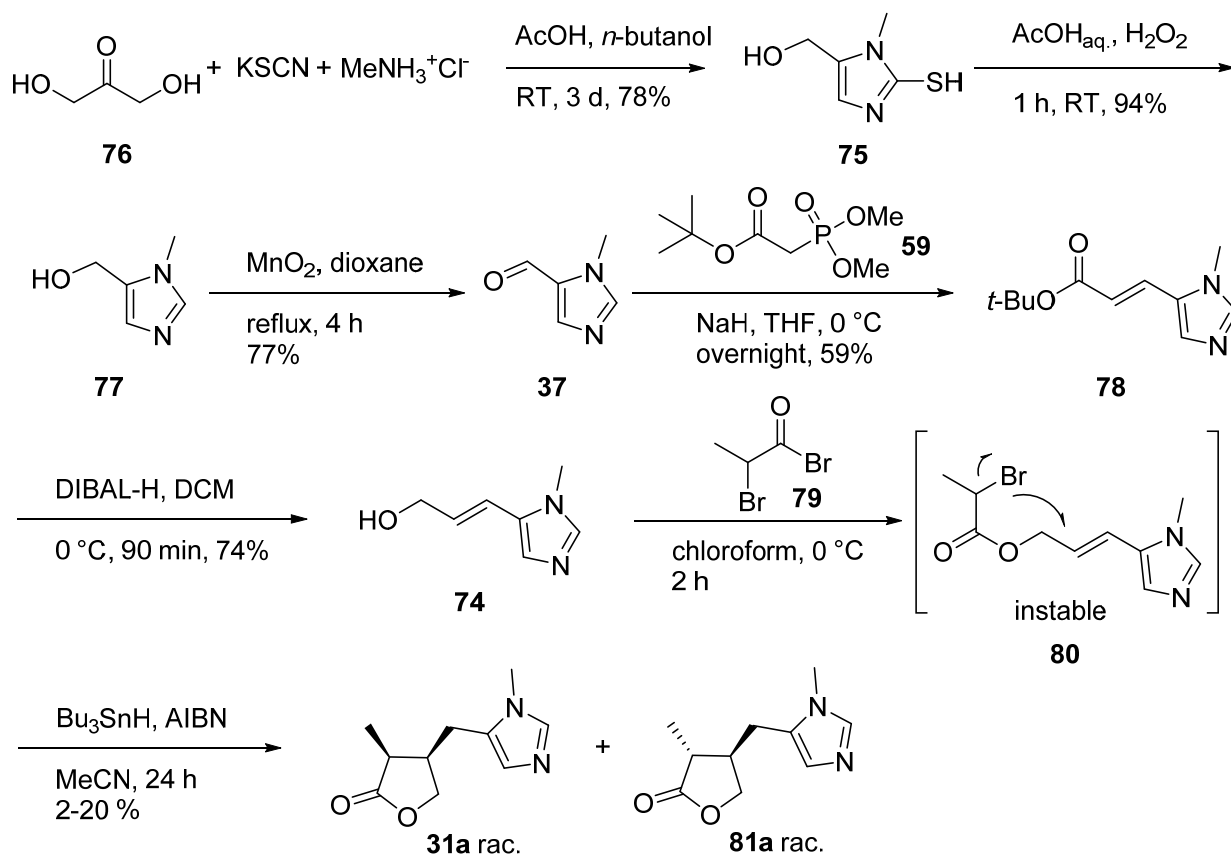
The alcohol precursor **74** to the radical cyclisation reaction was synthesised in 25% yield over 5 steps which were all scalable to gram-scale (Scheme 16). First, the imidazole **75** was made from dihydroxyacetone (**76**) or its dimer, potassium thiocyanate and methylammonium chloride by a Marckwald imidazole synthesis.<sup>[82]</sup> The starting materials were stirred in *n*-butanol and acetic acid at RT for 3 d. The product was isolated by filtration to yield 78% of a white powder. Addition of water to the reaction mixture or washes of the filter cake with water<sup>[82]</sup> led to a decrease in yield without purity benefit. Washing with diethyl ether was sufficient.

The thiol group of **75** was removed by oxidation with hydrogen peroxide in glacial acetic acid.<sup>[99a]</sup> After residual peroxide was destroyed with sodium sulfite, the mixture was adjusted to pH 9–10 and continuously extracted with ethyl acetate to recover the product **77** in 94% yield.

Oxidation of **77** with manganese(IV) oxide in 1,4-dioxane produced the desired aldehyde **37** after 4 h at reflux.<sup>[82]</sup> The mixture was filtered through celite and evaporation of the solvent provided the product **37** in 77% yield as a yellow oil which crystallised when cooled to RT.

The aldehyde precursor **37** was reacted in an HWE reaction with *tert*-butyl 2-(dimethoxyphosphoryl)-acetate **59** (Chapter 3.2.1). The phosphonate **59** was deprotonated with sodium hydride in dry THF at 0 °C. Two hours later, the aldehyde **37** dissolved in dry THF was added, and the reaction was stirred overnight. After quenching with water, the product was extracted with diethyl ether. A single isomer of product **78** was isolated in a standard work up procedure in 59% yield. <sup>1</sup>H NMR shows a coupling between the olefinic protons of 15.9 Hz which strongly points to an *E*-configured double bond.

The resulting *tert*-butyl ester **78** was reduced with diisobutylaluminium hydride which was added slowly to the solution of the ester **78** in dry dichloromethane. After complete conversion, the reaction was quenched with water and dilute NaOH solution, and evaporated to dryness. The solid residue containing the product and aluminium oxide was boiled in ethanol and filtered while warm. The filtrate was evaporated and purified by column chromatography to provide the product **74** as a yellow oil in 74% yield.



**Scheme 16:** Synthesis pathway to the diastereomeric mixture of the methyl analogue of pilocarpine **31a/81a** relying on a radical cyclisation to form the lactone moiety.<sup>[81]</sup>

The alcohol **74** was esterified with 2-bromopropanoyl bromide at 0 °C in dry chloroform. After stirring for 1 h, the TLC showed a spot-to-spot conversion of the alcohol. The reaction was worked up at a pH of 9. When the product was isolated after normal workup, however, the ester **80** could not be obtained, as it was unstable as a dry compound. In a reaction with bromoacetyl bromide, an NMR analysis revealed that the degradation product showed a strongly deshielded imidazole proton at 9.08 ppm, which is usually seen in quaternised or protonated imidazoles. Additionally,  $^1\text{H}/^{13}\text{C}$  HMBC cross peaks were observed between two imidazole carbon atoms and the  $\alpha\text{-CH}_2$  group. This suggests that the compound cyclised or oligomerised spontaneously by a nucleophilic substitution of the bromide by the imidazole. Belletire and Mahmoodi<sup>[81]</sup> proposed oligomers as the degradation product (Figure 34). However, the NMR did not resolve different sets of peaks representing different lengths of oligomers. In case of a Z-configured double bond the cyclisation product would be possible, but the coupling constant between the olefinic protons of 16.0 Hz suggests an E-configuration of the double bond. Oligomerisation remains the most probable explanation for the instability of **80**. Degradation was avoided by removal of the solvent at RT and addition of dry and degassed acetonitrile as reaction solvent for the cyclisation reaction when most solvent was evaporated.

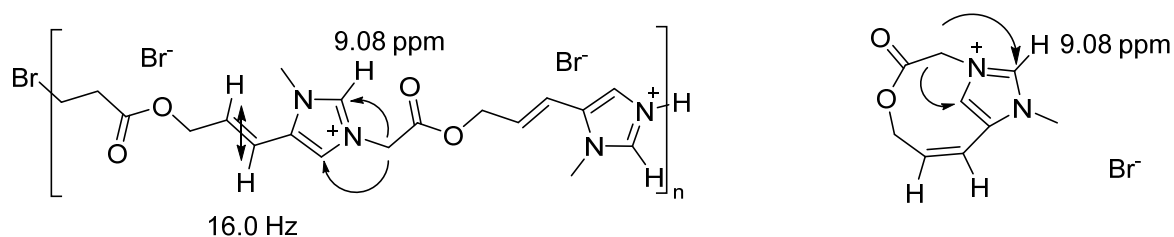


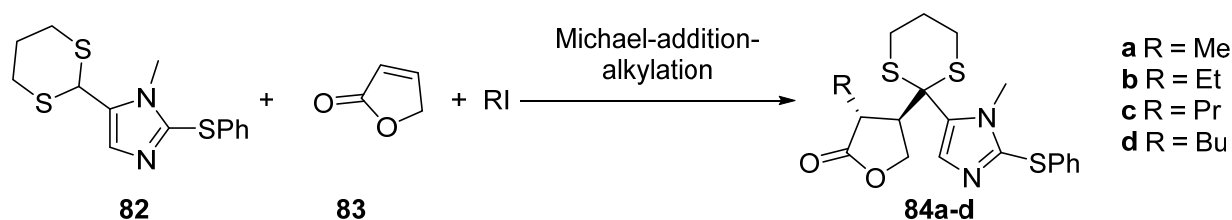
**Figure 34:** Possible degradation products after drying the unstable intermediate **80**. NMR characteristics (measured in methanol- $d_4$ ) leading to the structural assignment are shown. The arrows represent cross signals from the  $^1\text{H}/^{13}\text{C}$  HMBC spectrum the double arrow shows a coupling constant.

The solution of the ester **80** in dry and degassed acetonitrile was mixed with tributyltin hydride and a catalytic amount of azobisisobutyronitrile (AIBN) as radical initiator. This mixture was slowly added to refluxing dry and degassed acetonitrile over 5 h. After complete addition, the reaction was refluxed for additional 19 h. When the reaction was carried out without alkylation at the  $\alpha$ -carbon, the debrominated product was obtained instead of the cyclisation product. Apparently, the stability of the primary radical was not sufficient to undergo a cyclisation reaction. In case of the propionic ester analogue, cyclisation was observed in competition with debromination. After isolation by extractions and column chromatography, samples of the diastereomeric mixture of the target analogue **31a/81a** with a yield between 2% and 24% were obtained and a sample of the debrominated byproduct with a yield of 36% was obtained. The diastereomeric mixture showed a *cis/trans* ratio of 25:75 determined by  $^1\text{H}$  NMR. The quantities of **31a/81a** obtained as a sum of several experiments were sufficient to try epimerisation, but insufficient for separation of the diastereomers. Due to the low and not

reproducible yields and a lack of applicability to the acetic ester analogue, another synthetic route was needed.

#### 4.1.3 Synthesis of Diastereomeric Mixtures of Pilocarpine Analogues by a Michael-Addition-Alkylation Reaction

After failure to produce the desired pilocarpine analogues by radical cyclisation, another approach proposed by Braun et al.<sup>[133]</sup> and Heywang<sup>[134]</sup> in combination with the epimerisation procedure of Compagnone<sup>[95]</sup> was chosen. The forenamed propose a Michael-addition-alkylation reaction to link the imidazole moiety to the lactone (Scheme 17). In the same reaction, alkylation of the lactone can be achieved to yield the *trans*-substituted lactones **84a–d** which are closely related to the target molecules. Desulfurisation of **84a–d** should lead to isopilocarpine analogues and kinetic racemisation should epimerise most of the isopilocarpine analogues to the *cis*-configured products<sup>[95]</sup>.

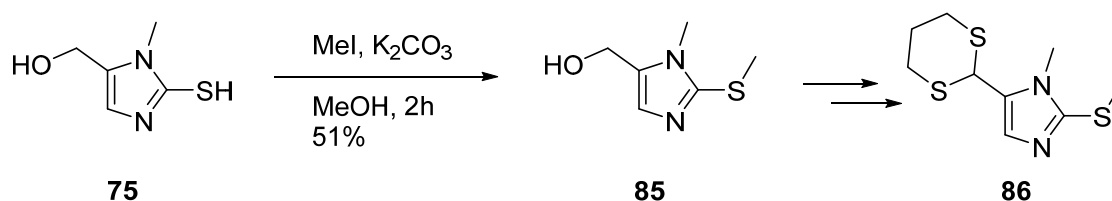


**Scheme 17:** The Michael-addition-alkylation reaction inspired by Braun's synthesis of isopilocarpine (with R = Et, **15**).<sup>[133]</sup>

#### Synthesis of the Dithiane Intermediate **82**

The choice of the dithiane precursor was important for the success of the Michael-addition-alkylation reaction. First attempts followed Heywang's patent<sup>[134]</sup> and used the unprotected 1-methyl-1*H*-imidazole 5-carboxaldehyde (**37**). The reaction did not yield any product and various undesired products were formed, probably due to the acidity of the imidazole at position 2.

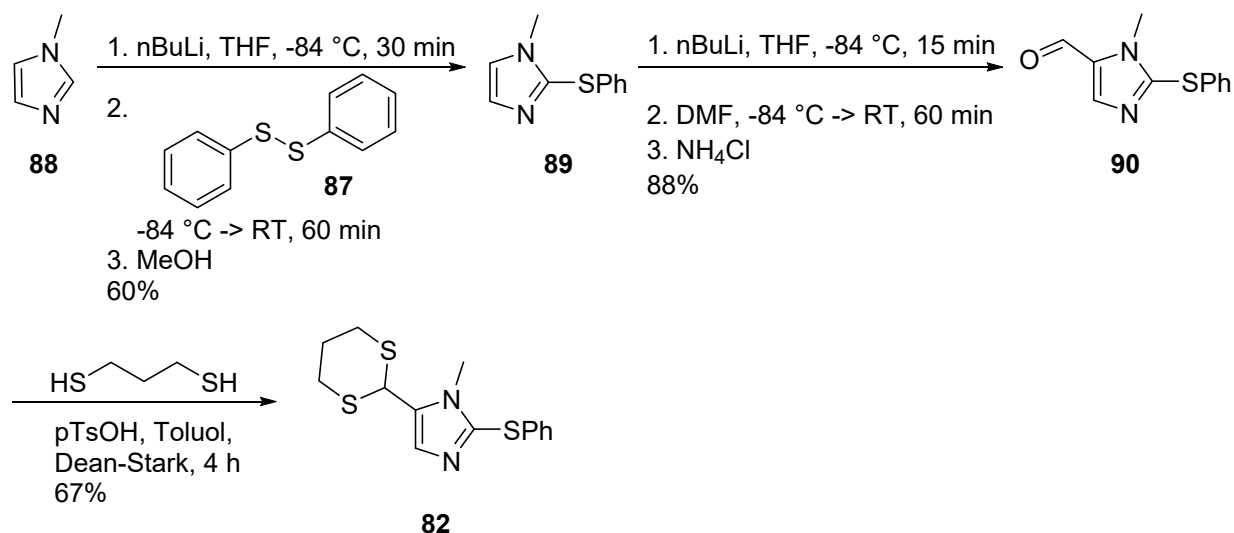
For this reason, a protecting group needed to be introduced at this position. Any sulfur-based protecting group was thought to be suitable as it would be removed in the step of the dithiane reduction. A methyl thioether **85** was easily accessible from the already available imidazole **75** (Scheme 18).<sup>[135]</sup> However, after oxidation of **85** to the aldehyde and dithiane formation, the Michael-addition-alkylation reaction of **86** failed probably due to the reactivity of the methyl thioether.



**Scheme 18:** Synthesis of the methylthioether protected dithiane precursor **86**.<sup>[135]</sup>

Instead of the methyl thioether, the phenyl thioether proposed by Braun et al.<sup>[133]</sup> was prepared (Scheme 19). As a reagent for the first step, diphenyl disulfide (**87**) was synthesised from thiophenol by an oxidation with hydrogen peroxide and catalytic amounts of potassium iodide.<sup>[136]</sup> The reaction was complete after 60 min. After reduction of excess peroxides with sodium sulfite, the pure compound **87** was obtained in 60% yield by phase separation and evaporation of the solvents.

At  $-84\text{ }^{\circ}\text{C}$ , 1-methyl-1*H*-imidazole (**88**) was protected by deprotonation with *n*-butyl lithium in dry THF followed by addition of diphenyl disulfide (**87**).<sup>[137]</sup> The reaction was quenched with dilute hydrochloric acid and was extracted with cyclohexane to remove the thiophenol byproduct. Then, the aqueous phase was adjusted to a pH of 9 and the product **89** was extracted with dichloromethane with a yield of 88%. No further purification was required. In this reaction, the addition of an excess of *n*-butyl lithium should be avoided as this leads to a second substitution at position 5 of the imidazole. Both compounds can be separated by normal phase column chromatography, but the use of no to little excess *n*-butyl lithium is recommended to avoid purification steps.



Scheme 19: Synthesis of the dithiane intermediate **82**.

Formylation at position 5 of **89** was achieved by another deprotonation with *n*-butyl lithium at  $-84\text{ }^{\circ}\text{C}$  followed by addition of dry DMF as formylating agent.<sup>[138]</sup> The product **90** was not pure, but nevertheless carried through the next step to avoid large scale column chromatography.

The aldehyde **90** was dissolved in toluene, *para*-toluenesulfonic acid and propane-1,3-dithiol were added. The mixture was refluxed using a Dean-Stark apparatus for 4 h to form the dithiane.<sup>[134]</sup> More than one equivalent of the *para*-toluenesulfonic acid was required to quantitatively protonate the starting material and to leave an excess to catalyse the thioacetal formation. The reaction mixture was washed with sodium hydroxide solution to remove excess dithiol and *para*-toluenesulfonic acid. After evaporation of the extraction solvent, the compound **82** was purified by recrystallisation from a

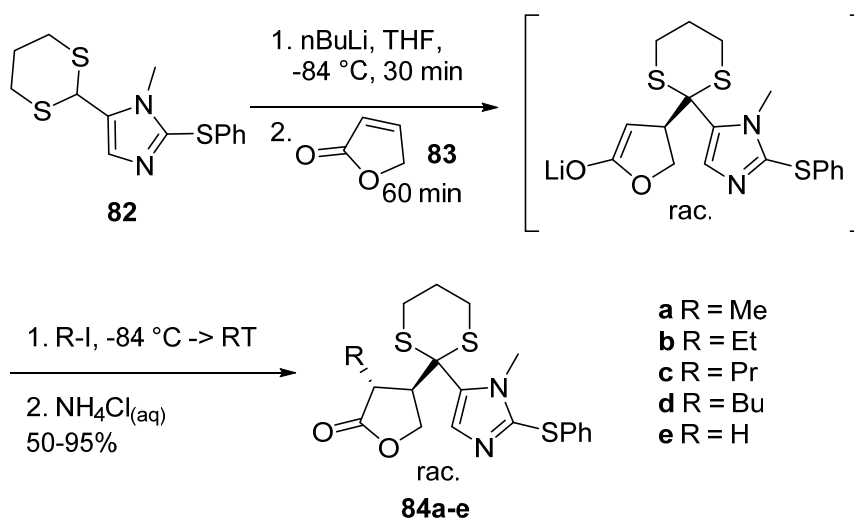
mixture of *n*-hexane and ethylacetate. As a result, the dithiane precursor **82** was obtained in three steps with an overall yield of 36%.

### The Michael-Addition-Alkylation Reaction

The dithiane **82**, commercially available furan-2(5*H*)-one (**83**) and iodoalkanes were reacted in a one-pot Michael-addition-alkylation reaction to construct the *trans*-substituted  $\gamma$ -butyrolactone at the core of isopilocarpine analogues.<sup>[133]</sup> Dithiane formation of an aldehyde leads to an umpolung so that the dithiane can be deprotonated and then attack the Michael system. The resulting enolate can be quenched with either water or alkylating reagents such as iodoalkanes to yield the *trans*-alkylated products **84a–d** (Scheme 20).

The dithiane **82** was deprotonated with *n*-butyllithium at  $-84\text{ }^{\circ}\text{C}$  in dry THF. After 30 minutes, furan-2(5*H*)-one (**83**) was added. When TLC showed a complete conversion of the dithiane **82** (after approximately 1 h), the iodoalkane was added. Earlier addition of the iodoalkane directly alkylated the dithiane **82**. The reaction mixture was warmed to RT over 1–5 h and conversion was monitored by TLC. Complete alkylation was reached faster with shorter alkyl chains than with longer alkyl chains. Then, the reaction was quenched with aqueous ammonium chloride solution and extracted with ethyl acetate. In case of a slow reaction due to very slow warming of the reaction mixture the reaction was not prolonged overnight, because an overnight reaction produced decomposition and lower yields than incomplete reactions.

For the synthesis of **16** (R = H, Figure 33), the reaction was quenched with saturated aqueous ammonium chloride solution instead of the addition of iodoalkane. This provided the unalkylated product **84e**.



**Scheme 20:** One-pot Michael-addition-alkylation reaction to build up the isopilocarpine-like scaffold.<sup>[133]</sup>

Purification of the reaction products **84a–e** was possible by flash chromatography if the alkylation step was complete or almost complete. High amounts of the unalkylated intermediate **84e** were not separable from the product due to very similar retention of both compounds. Additionally, the mixture should not be loaded onto the column as a solid depot on silica. Long contact of the product to silica during rotary evaporation of the solution with silica led to product decomposition. The same effect was observed when TLC spots were dried with heat prior to elution and all reaction components stayed at the baseline. Instead, the crude product was dissolved in a small amount of dichloromethane and deposited on the column as a concentrated solution. The described optimisations led to yields of 90–95% for the compounds **84a, b** and **e**. In the case of longer alkyl chains (**84c** and **d**) the yields varied between 50 and 80%.

With the good accessibility of the *trans*-substituted  $\gamma$ -butyrolactones with linear alkyl substituents, the introduction of branched residues such as isopropyl and isobutyl was tested. In these cases, the problem of a very slow alkylation reaction in competition with the formation of degradation products overnight became important and the products were not obtained. To accelerate the alkylation, two approaches were chosen:

- Addition of *N,N,N',N'*-tetramethylethylenediamine (TMEDA)<sup>[139]</sup> or *N,N'*-dimethylpropyleneurea (DMPU)<sup>[140]</sup> to increase the enolate reactivity by chelation of the lithium counter ion.
- Use of isopropyl methanesulfonate as more reactive alkylating agent due to the better leaving group.

All combinations of methanesulfonate and/or complexing agents failed to yield the isopropyl derivative. The complexing agents led to even more decomposition and elimination of the dithiane. Consequently, the synthesis of analogues with branched alkyl chains was abandoned at this point.

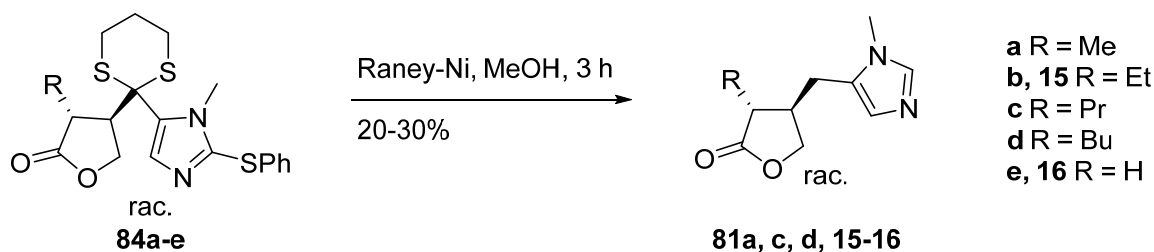
### Deprotection by Desulfurization

Having successfully linked lactone, imidazole moiety and linear alkyl substituents, all sulfuric groups of **84a–e** were removed with Raney nickel. Freshly prepared Raney nickel was decanted and washed with three portions of methanol, then with dry methanol (Scheme 21). This suspension of Raney nickel in dry methanol was added to a solution of the respective starting material **84a–e** in dry methanol and the mixture was refluxed for 3 h.<sup>[133]</sup> More of the suspension of Raney nickel was added until the conversion was complete. Then, the suspension was filtered through cotton and the filter cake washed with methanol. If Raney nickel was not completely removed after the first filtration, the solvent was evaporated, and the residue suspended in dichloromethane and filtered again. The products **15–16** and **81a, c, d** were purified by preparative HPLC. At the end of this step, the alkylated products **15** and



**81a, c, d** contained 8–10% of the related *cis*-isomers. The nonalkylated product **16** is racemic pilosinine with a purity of 95%. **16** was used for pharmacological experiments.

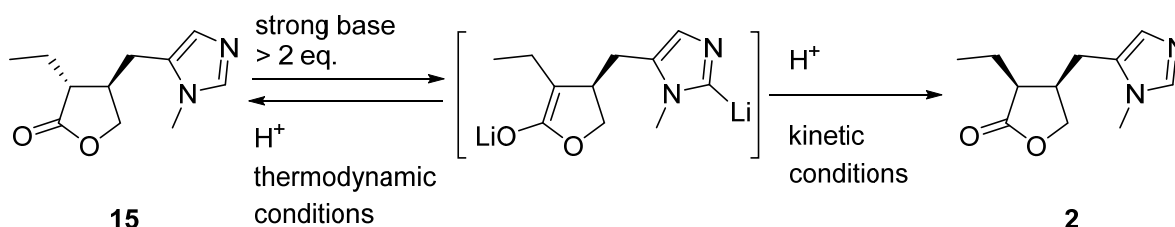
The yields of the desulfurisation were low with 20–30%. One reason might be the loss of product by decomposition during the reaction. Sometimes an amine smell was noticed when opening the reaction flask. Supposedly the imidazole moiety was reduced and decomposed by Raney nickel.



**Scheme 21:** Deprotection of the Michael-addition-alkylation product with Raney nickel to provide isopilocarpine analogues.

### Epimerisation of the Isopilocarpine Analogues

The isopilocarpine analogues **81a, c, d** differ from the targeted pilocarpine analogues **31a, c, d** in the configuration of the stereocenter at lactone position 3. Deprotonation at this position leads to a loss of stereoinformation due to the formation of a planar enolate. The conditions of the reprotonation of the enolate define the stereochemical outcome of the deprotonation–reprotonation experiment. Thermodynamic conditions would lead to the more stable product, in this case the isopilocarpine analogue. Kinetic conditions lead to the pilocarpine analogues as the kinetic product (Scheme 22).<sup>[141]</sup> Kinetic conditions include low temperatures and the choice of sterically hindered weak acids. Compagnone and Rapoport<sup>[95]</sup> published a successful kinetically controlled epimerisation of isopilocarpine to pilocarpine. Protonation with benzoic acid, aqueous Na<sub>2</sub>SO<sub>4</sub> and 2,4,6-tribromophenol resulted in *cis/trans* ratios of 55:45, but with 2,6-di-*tert*-butyl-4-methylphenol (BHT) they obtained a ratio of 75:25 (according to <sup>1</sup>H NMR).



**Scheme 22:** Possible outcomes of a deprotonation–reprotonation experiment of isopilocarpine (**15**).

The published protocol was applied to the isopilocarpine analogues. A solution of the isopilocarpine analogue was added to 3 equivalents of LDA in dry THF at –84 °C. After stirring for 2 h, a solution of 9 equivalents BHT was added in one shot and the mixture was slowly warmed to RT. Then, dilute hydrochloric acid was added, and the reaction was worked up. The product mixture always showed a

*cis/trans* ratio of about 57:43. One single reaction with the propyl analogue **31c/81c** yielded a ratio close to the published ratio.

The *cis/trans* ratio can be easily determined by  $^1\text{H}$  NMR measurements (Figure 35). All analogues show the same pattern for the lactone  $\text{CH}_2$  protons between 4.40 and 3.80 ppm. The inner two signals correspond to the pilocarpine analogue and the outer signals to the isopilocarpine analogues. The ratio between the integrals is the *cis/trans* ratio.

With the aim to improve the *cis/trans* ratio of the epimerisation, different parameters of the reaction were studied. To investigate the success of the deprotonation step, isopilocarpine (**15**) was deprotonated with 2.5 equivalents of lithium diisopropylamide (LDA) at  $-84^\circ\text{C}$ . After 3 h, the compound was reprotated with  $\text{D}_2\text{O}$ . The  $^1\text{H}$  NMR spectrum of the crude product (Figure 36) revealed a 90% decrease of the integral of the imidazole proton at the imidazole position 2 and an 80% decrease of the integral representing the proton at lactone position 3 due to reprotation with a deuterium instead of a proton. Additionally, 26% epimerisation to pilocarpine (**2**) was observed. Apparently 80–90% of the molecules were deprotonated, which supposedly is sufficient to yield higher diastereomeric ratios than 57:43 if the right kinetic reprotation conditions are chosen. The epimerisation ratio observed after reprotation with  $\text{D}_2\text{O}$  was expected to correspond to the diastereomeric ratio observed under thermodynamic conditions.

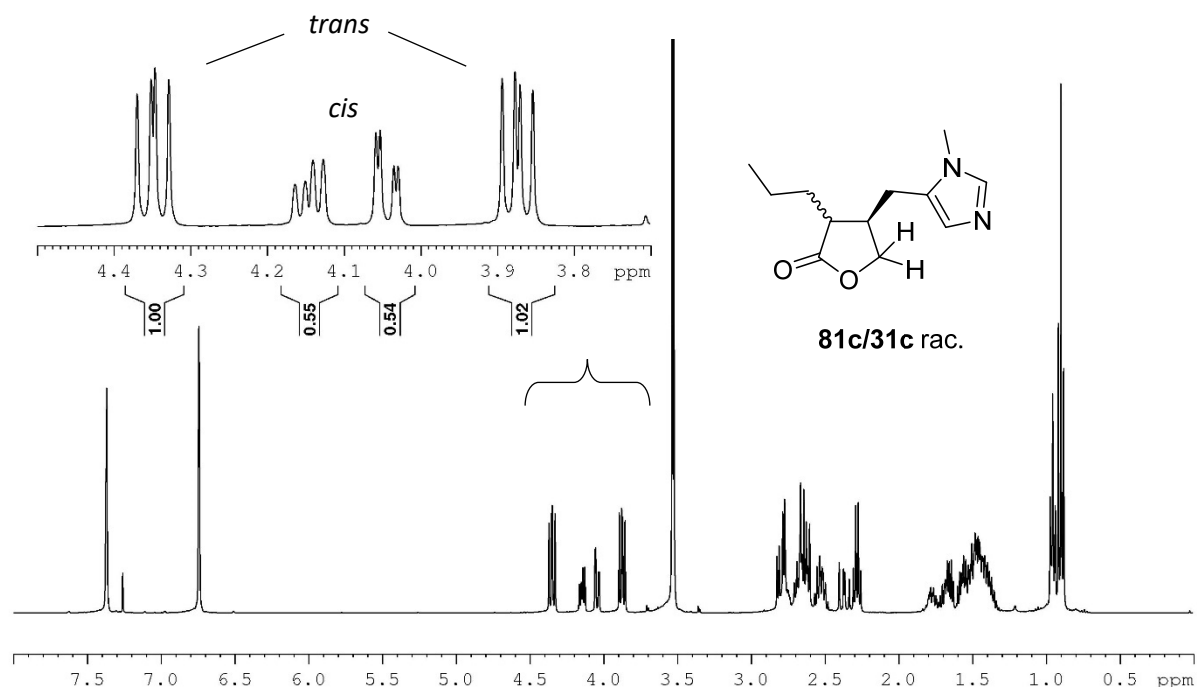


**Figure 35:**  $^1\text{H}$  NMR spectrum of a *cis/trans* mixture of the pilocarpine analogues **31c/81c** ( $\text{R} = \text{Pr}$ ) measured in  $\text{CDCl}_3$ . The signals between 4.40 and 3.80 ppm correspond to the lactone  $\text{CH}_2$ . The signals at 4.15 ppm and 4.05 ppm show the protons of the *cis*-diastereomer, the signals at 4.40 ppm and 3.92 ppm belong to the *trans*-diastereomer. The *cis/trans* ratio in this example is 35/65.

Another qualitative observation showed that reprotonation with BHT is slow. When reactions were injected with BHT and 1 h later with 2 M HCl at low temperatures, the yield of *cis*-product was always lower than in reactions which were quenched with HCl only after reaching RT.

Studying the epimerisation reaction did not lead the way to a more selective kinetic protonation procedure. The literature results could not be reproduced reliably. The same result was found by Bühne.<sup>[142]</sup> Nevertheless, the diastereomeric mixtures of pilocarpine and isopilocarpine analogues were purified by preparative non-chiral HPLC before attempting to further separate the mixture.

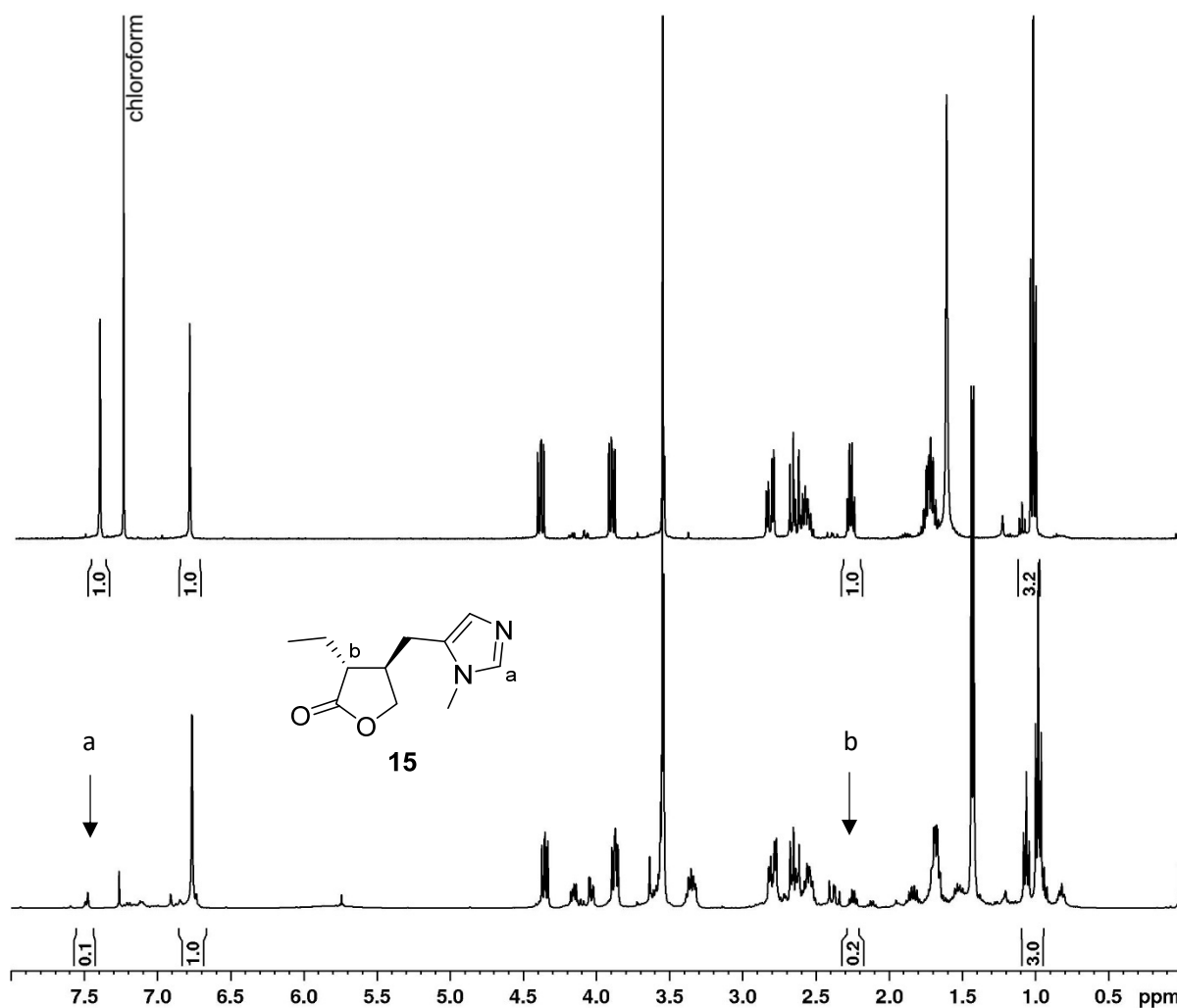


**Figure 36:** <sup>1</sup>H NMR spectra of isopilocarpine (**15**) (above) and isopilocarpine after deprotonation with 2.50 equivalents of LDA and reprotonation with D<sub>2</sub>O (below) measured in CDCl<sub>3</sub>. The peaks at 7.42 ppm (a) and 2.32–2.26 ppm (b) were reduced 80–90% due to reprotonation with a deuterium instead of a proton.

#### 4.1.4 Trials to Separate the Diastereomers and Enantiomers of the Pilocarpine Analogues by Chiral HPLC

The criterium for the purity of the target compounds **16** and **31a, c, d** was at least diastereomeric purity, if possible enantiomeric purity. The first approach to a separation of the diastereomeric mixtures was the use of chiral HPLC. With chiral chromatography, prediction of a suitable stationary

phase is elusive. For this reason, all six analytical chiral columns available in the working group were screened: Lux<sup>®</sup> i-amylose-1, Lux<sup>®</sup> amylose-2, Lux<sup>®</sup> cellulose-1, Lux<sup>®</sup> cellulose-3, Lux<sup>®</sup> cellulose-4, and Lux<sup>®</sup> i-cellulose-5.

First trials with the cellulose-1 column revealed that neutral reversed-phase conditions did not lead to any separation whereas neutral normal phase conditions showed a separation but overlapping broad peaks. When 0.1% diethylamine was added to the mobile phase, the peak form was narrowed, and separation improved due to the basicity of the analytes. Acidic additives were not tested to avoid a charged imidazole. Good conditions were found with mobile phase systems of *n*-hexane/isopropanol and 0.1% diethylamine.

For that reason, all columns were tested with this mobile phase but varying ratios of the solvents depending on the stationary phase. The samples used in this experiment were the isopilocarpine analogues **81a–e** containing 8–10% of the pilocarpine analogues. All isomers were present and an attribution of *cis*- or *trans*-configuration was possible related to the peak areas.

As all the peaks were close to one another, it was clear that a preparative separation of all four isomers would not be possible in a single method. Consequently, the problem was simplified to two isomers at a time. First the mixture of *trans*-enantiomers would be separated. Afterwards epimerisation of each enantiomer would yield a pair of diastereomers which would be separated in a second run. The results (Table 13) show, that no single column can resolve all the necessary mixtures. A combination of i-amylose-1 and cellulose-1, however, would presumably allow all separations. Unfortunately, only the preparative cellulose-1 column was available at the institute so that the separation of the diastereomers by preparative chiral HPLC was not possible in this project. The result of this screening was still useful for analytical purposes.

**Table 13:** Screening results for six 4.6x250 mm Lux<sup>®</sup> columns. All columns were run at 0.5 mL/min of *n*-hexane/isopropanol/0.1% diethylamine (described by % IPA). Column 1 indicates the separability of the *trans*-enantiomers and column 2 shows the separability of the corresponding *cis*- and *trans*-diastereomers after epimerisation. Separation was rated as good (✓) if the retention time differs in more than 2.0 minutes. The brackets indicate that the enantiomers are well separated one from another but not from the diastereomers. A question mark indicates that separation depends on the peak attribution which would only be known after the epimerisation reaction of the pure enantiomers.

R Column	H	Me		Et		Pr		Bu		Eluent % IPA
		1	2	1	2	1	2	1	2	
i-Amylose-1	✓	✓	?	✓	✓	✓	?	✓	?	20
Amylose-2	✗	✗	✗	✗	✗	✗	✗	✗	✗	50
Cellulose-1	✗	✗	✓	✓	✓	(✓)	✗	✓	✓	60
Cellulose-3	✗	✗	✗	✗	✗	(✓)	✗	(✓)	✗	60
Cellulose-4	✗	(✓)	✗	(✓)	✗	(✓)	✗	(✓)	✗	60
i-Cellulose-5	✗	✗	✗	✗	✗	✗	✗	✗	✗	95

#### 4.1.5 Trials to Separate the Diastereomers and Enantiomers of the Pilocarpine Analogues by Fractional Crystallisation

For the evaluation of a possible separation of the diastereomers by fractional crystallisation, the first crystallisations were carried out with a mixture of the commercial (+)-pilocarpine (**2**) and easily accessible (+)-isopilocarpine (**15**). Literature suggested fractional crystallisation of the nitrate or chloride salts.<sup>[131, 143]</sup> The enantiomers of tartaric acid and *para*-O,O'-toluoyltartaric acid were also tested (Table 14). At a scale of 60 mg for each crystallisation, a mixture of (+)-pilocarpine (**2**) and (+)-isopilocarpine (**15**) was dissolved in ethanol and 0.5 equivalents of the acid to test was added. Ethanol was added until complete dissolution of all components was achieved at reflux conditions. After slow cooling to  $-20\text{ }^{\circ}\text{C}$ , the mother liquor was pipetted off and the crystals were recrystallised one or more times in ethanol. The resulting crystals were analysed by  $^1\text{H}$  NMR and the diastereomeric excess of (+)-pilocarpine (**2**) in the crystals was compared to the diastereomeric excess of the free base before crystallisation (entry 1 in Table 14). This experiment showed that the hydrochloride salt did not crystallise. Crystallisations with tartaric acids and *L-para*-O,O'-toluoyl-tartaric acid did not change diastereomeric excess of (+)-pilocarpine (**2**) related to the original mixture of free bases, but the nitrate salt showed a significant increase in the diastereomeric excess of (+)-pilocarpine (**2**) after one recrystallisation. The effect was more pronounced after four recrystallisations. Thus, the diastereomers of pilocarpine can be separated by several recrystallisations as the nitrate.

**Table 14:** Results of the (attempted) fractional crystallisation and recrystallisation of different salts of a mixture of (+)-pilocarpine (**2**) and (+)-isopilocarpine (**15**). The diastereomeric excess (de) was determined by  $^1\text{H}$  NMR, comparing the integrals of the lactone  $\text{CH}_2$ .

salt	crystallisation step	integral	integral	de
		isopilocarpine	pilocarpine	
1 Free base	Before crystallisation	1.00	1.18	0.1
2 Hydrochloride	No crystallisation achieved	–	–	–
3 Nitrate	1 <sup>st</sup> recrystallisation	1.00	1.9	0.3
4 Nitrate	4 <sup>th</sup> recrystallisation	1.00	5.1	0.7
5 D-Tartrate	1 <sup>st</sup> recrystallisation	1.00	1.22	0.1
6 L-Tartrate	1 <sup>st</sup> recrystallisation	1.00	1.24	0.1
7 L-Toluoyltartrate	1 <sup>st</sup> recrystallisation	1.00	1.12	0.1

Consequently, the mixtures of **81a/31a** (R = Me) and **81c/31c** (R = Pr) containing all four diastereomers were crystallised as nitrates with the aim to obtain diastereomerically pure crystals. However, when a 1:1 mixture of the methyl-substituted diastereomers was fractionally crystallised, after 11 recrystallisations a diastereomeric excess of the *cis*-isomer of only 0.2 was reached. This experiment

showed that a separation of the diastereomers was not possible in mixtures of all four isomers of the methyl substituted analogue **81a/31a** due to very low enrichment of one pair of enantiomers. The same experiment with a propyl substituted analogue **81c/31c** even enriched the *trans*-isomer with a diastereomeric excess of 0.45 after 5 recrystallisations. As a result, separation of diastereomers by fractional crystallisation was not successful in mixtures of all four isomers.

Again, the separation problem was broken down into two problems. A first step would be the separation of the *trans*-enantiomers. Then, each enantiomer would be epimerised and separation of the diastereomers would be easier with only two species present. The tests were carried out with racemic isopilocarpine (**15**). Fractional crystallisation with the enantiomers of tartaric acid did not lead to enantiomeric enrichment, but the fractional crystallisation with the enantiomers of *para*-O,O'-toluoyltartrate was successful. Both enantiomers were completely separated after 5–10 recrystallisations. The result of the recrystallisations was analysed by HPLC on the chiral Lux<sup>®</sup> cellulose-1 column (Figure 37). Comparison of the recrystallised samples with a reference of (+)-isopilocarpine (**15**) obtained from commercial (+)-pilocarpine (**2**) identified the isomer in crystal with (+)-O,O'-*para*-toluoyltartrate as (+)-isopilocarpine (**2**). As the starting mixture of isopilocarpine isomers contained 8% of the *cis*-enantiomers, these impurities could be traced in the chromatograms. After the fractional crystallisations, each *trans*-enantiomer was accompanied by its C3-epimer, but not by the other *cis*-enantiomer.

The successful separation of isopilocarpine enantiomers (**15**) was applied to the analogues with methyl (**81a**) or propyl (**81c**) residues. The crystals were analysed after 5, 10 and 15 recrystallisations. Unlike the tests with isopilocarpine enantiomers (**15**), the methyl substituted analogue **81a** did not show any enrichment of one or the other enantiomer. The propyl analogue **81c** was separated quite inefficiently so that enantiomeric purity was not reached after 15 recrystallisations. With only few milligrams of the crystals left, this inefficient approach was abandoned, because the low yields of such a long recrystallisation sequence would not provide enough material for a second fractional crystallisation after epimerisation of the pure *trans*-enantiomers.

The diastereomerically pure analogues of pilocarpine could not be obtained by separation of a racemic mixture. For this reason, a synthetic approach to synthesise the analogues in a strongly *cis*-enriched product mixture was adopted.

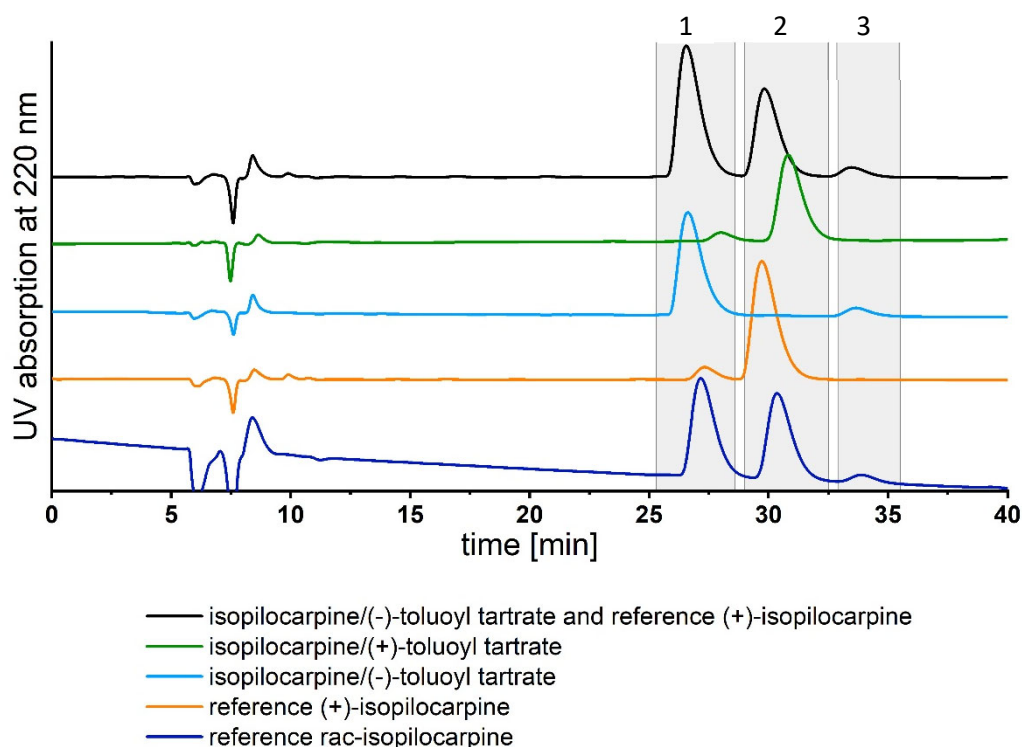


**Figure 37:** HPLC analysis of the fractional crystallisation of racemic isopilocarpine (**15**) with the enantiomers of *para*-O,*O'*-toluoyltartaric acid on a Lux® cellulose-1 column (4.6x250 mm, 40/60/0.1 *n*-hexane:isoprpopanol:diethylamine, 0.5 mL/min). The vertical markings approximate the retention times of (1) (-)-isopilocarpine and coeluting (+)-pilocarpine; (2) (+)-isopilocarpine, and (3) (-)-pilocarpine.

## 4.2 Diastereoselective Synthesis of Pilocarpine Analogues

### 4.2.1 Tested Diastereoselective Synthesis of Pilocarpine Analogue **31c** by Heterogenous Hydrogenation of an Exocyclic Double Bond

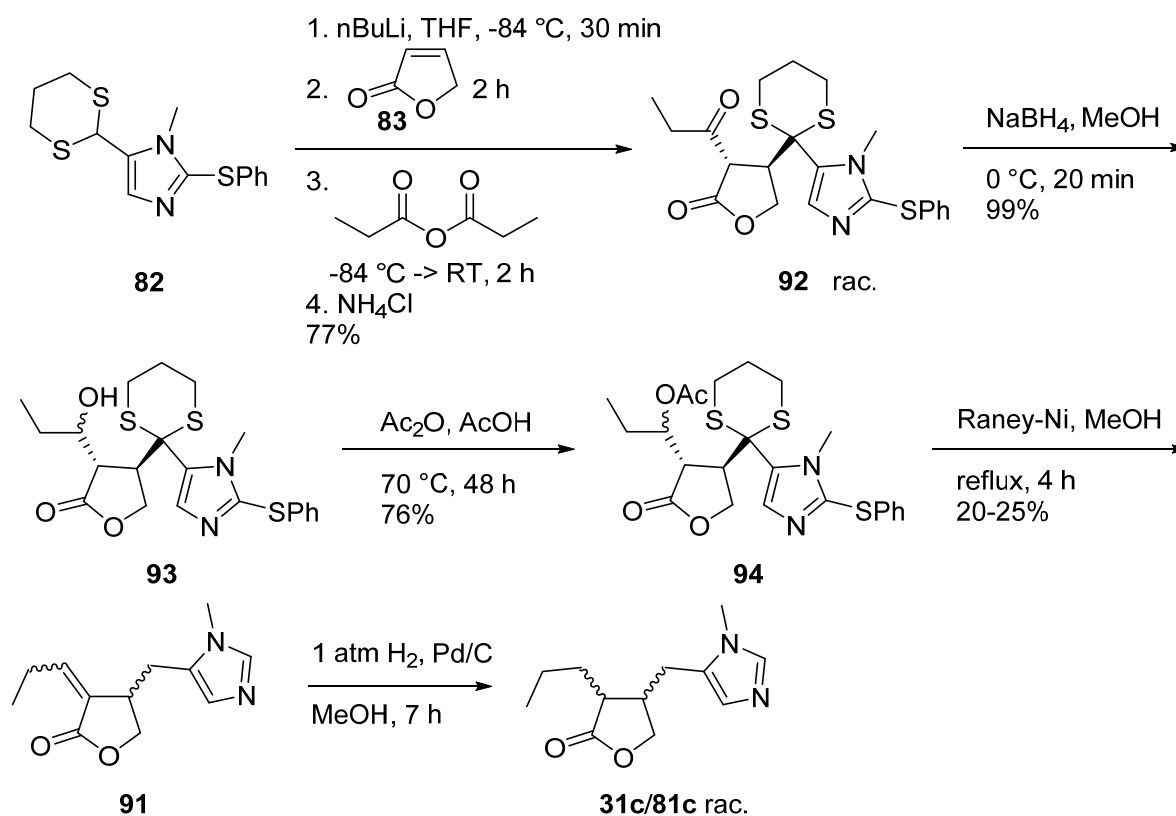
The first synthetic tentative to produce strongly *cis*-enriched diastereomeric mixtures of the pilocarpine propyl analogue relied on the heterogenous hydrogenation of the exocyclic double bond of **91** (Scheme 23), profiting from diastereoselectivity induced by the adjacent stereocenter.<sup>[131, 142-144]</sup> In a heterogenous hydrogenation, the reaction takes place at the surface of the catalyst, i.e. under sterically hindered conditions. Hydrogenation of compound **91** would occur from the least sterically hindered side of the double bond. This would be the side of the lactone which is not occupied by the substituent at position 4, leading to the *cis*-substituted product **31c**.

The synthesis of **91** relied on the previously studied Michael-addition-alkylation reaction. As proposed by Link and Bernauer<sup>[131]</sup> and similar to Böhne's synthesis<sup>[142]</sup>, the acylated lactone **92** was generated first. This was achieved similarly to the Michael-addition-alkylation reaction (Chapter 4.1.3). The iodoalkane was replaced by propionic anhydride to acylate the lactone at position 3. This led to **92** in good yields of 77%. A reaction with propionic aldehyde was equally successful to directly provide compound **93**. The acylation was chosen due to easier purification by column chromatography.

The reduction of the ketone of **92** with sodium borohydride in dry methanol was a spot-to-spot conversion within 20 minutes at 0 °C. Acidic workup followed by extractions at a pH of 9 provided the product **93** in quantitative yields and sufficient purity to use the crude product for the next step.

Compound **93** was heated in a mixture of acetic acid and acetic anhydride at 70 °C for 2 d to achieve complete acetylation of the alcohol. Link and Bernauer<sup>[131]</sup> propose longer heating to 130 °C to directly eliminate the acetyl group. This was not successful, so the acetylated intermediate was isolated by extractions and purified by column chromatography to yield 76% of **94**.

The acetylated product **94** was deprotected with Raney nickel in the same way as the alkylated analogues **84a–d**. Elimination of the acetyl group happened during refluxing in methanol with Raney nickel. Similar to the earlier syntheses, yields of 20–25% were obtained.



**Scheme 23:** Synthetic route to the pilocarpine analogue **31c** with the heterogeneous hydrogenation of an exocyclic double bond as the key step to attempted control of the diastereomeric ratio.

The exocyclic double bond of **91** was easily hydrogenated under different published conditions (Table 15).<sup>[131, 142, 144]</sup> However, the selectivity of the reaction did not correspond to the expectation and the published *cis/trans* ratios. Published ratios were in favour of the *cis* product with ratios of 60:40, whereas the experiment yielded nearly 1:1 product mixtures of **31c** and **81c**. To conclude, the heterogeneous hydrogenation of an exocyclic double bond exploiting stereoinduction of the adjacent stereocentre was not a suitable approach to improve the *cis/trans* ratios of the pilocarpine analogues.

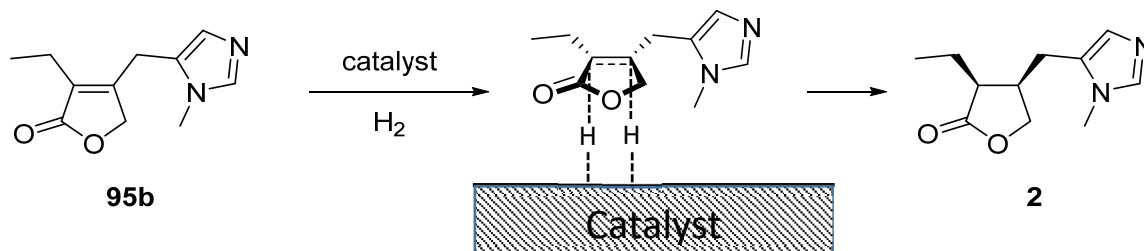


**Table 15:** Overview over different hydrogenation conditions and obtained product ratio. A sample of **99** (2 mg) was dissolved in dry methanol (2 mL). The catalyst was added and the mixture was vigorously stirred at the indicated conditions. The catalyst was removed by filtration and the filtrate was evaporated. The *cis/trans* ratios were determined by <sup>1</sup>H NMR spectroscopy of the product.

Catalyst	Temperature	H <sub>2</sub> -pressure	Time	<i>Cis/trans</i> ratio of the product ( <b>31c/81c</b> )
10% Pd/C <sup>[142]</sup>	RT	1 atm	7 h	43:57 (Lit <sup>[142]</sup> : 59:41)
10% Pd/C, pyridine <sup>[144]</sup>	RT	1 atm	4 h	45:55 (Lit <sup>[144]</sup> : 60:40)
PtO <sub>2</sub> <sup>[131]</sup>	RT	30 atm	4 h	48:52 (no literature value)

#### 4.2.2 Diastereospecific Synthesis of Racemic Pilocarpine Analogues by Hydrogenation of an Endocyclic Double Bond

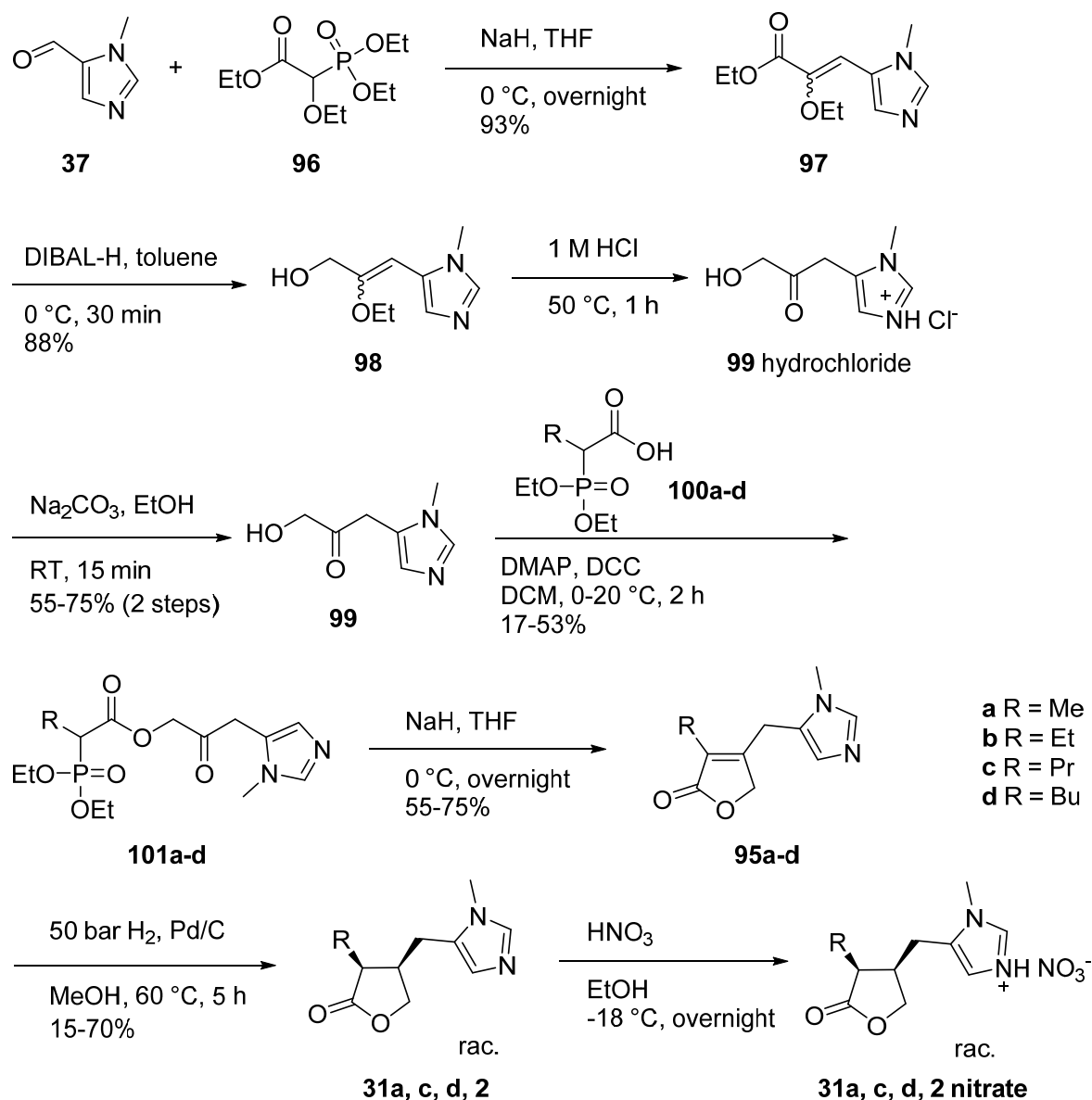
Having learned that diastereoselectivity induced by the substituent at lactone C-4 is not sufficient to overcome thermodynamic differences between the *cis*- and the *trans*-diastereomers, a diastereospecific approach was chosen to generate the *cis*-products. Catalytic heterogeneous hydrogenation is a stereospecific reaction. The reaction takes place at the catalyst surface where both hydrogen atoms are delivered to the same side of the double bond.<sup>[145]</sup> If a double bond links both stereocenters of pilocarpine or its analogues, both stereocenters can be created at once (Scheme 24). The specificity of the reaction should lead to high diastereomeric excesses of the *cis*-products.



**Scheme 24:** Supposed mechanism of the *syn*-hydrogenation of **95b** on a heterogeneous catalyst.

This approach has been applied to the synthesis of racemic pilocarpine (**2**). Reimann<sup>[146]</sup> used a *syn*-hydrogenation as the final step, Csuk and Woeste<sup>[147]</sup> and DeGraw<sup>[148]</sup> *syn*-hydrogenated intermediates in their syntheses of pilocarpine. The patent from Reimann was chosen as a basis for the synthesis of the racemic pilocarpine analogues **31a**, **b** and **d** (Scheme 25). The synthesis relies on two HWE reactions and one esterification as bond forming steps to construct the pilocarpine scaffold. The varying alkyl group is introduced at a late stage of the synthesis with only three downstream steps remaining.

This synthesis aiming for racemic pilocarpine analogues **31a**, **b** and **d**, racemic pilocarpine (**2**) needed to be provided as reference compound. Racemic pilocarpine (**2**) was synthesised in the same way as the analogues **31a**, **b** and **d**.

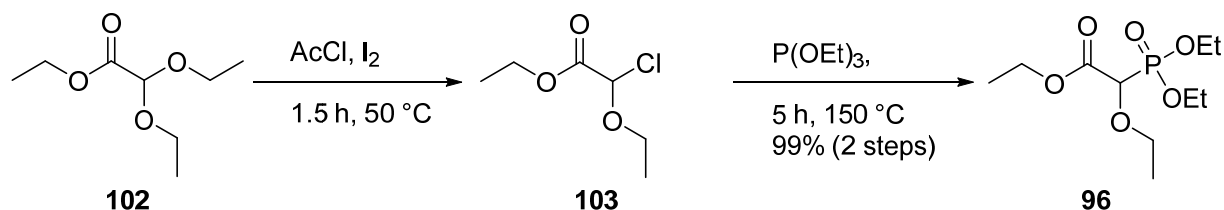


**Scheme 25:** Synthetic route to the pilocarpine analogues **2** and **31a, c, d** based on the procedures from Reimann.

### Synthesis of the required phosphonates **96** and **100**

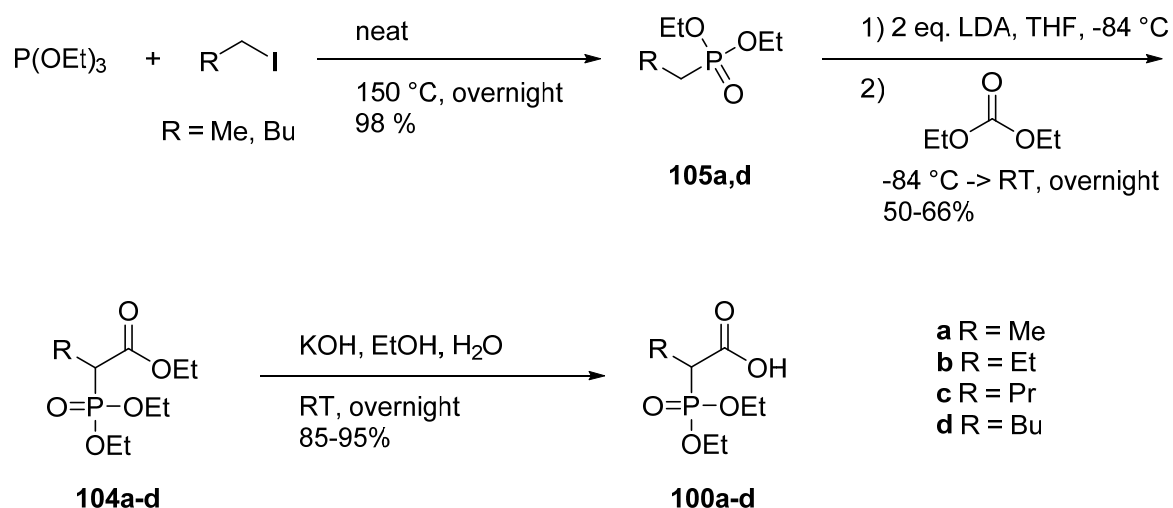
The imidazole carboxaldehyde (**37**) as starting molecule was available as it was used earlier (Chapter 3.2.1). The phosphonate **96** required for the first HWE reaction was synthesised starting from ethyl 2,2-diethoxyacetate (**102**) (Scheme 26). Deussen et al.<sup>[149]</sup> prepared **96** in a telescoped two step reaction at pilot scale by chlorination of ethyl diethoxyacetate (**102**) followed by a Michaelis-Arbuzov reaction. Ethyl 2,2-diethoxyacetate (**102**) was chlorinated with 1.20 equivalents of acetyl chloride and a catalytic amount of iodine in the absence of solvent. The reaction was complete after stirring at 50 °C for 1.5 h. Toluene was added and all volatile components such as acetyl chloride, iodine and ethyl acetate were removed together with the toluene by vacuum distillation to leave ethyl 2-chloro-2-ethoxyacetate (**103**). Triethylphosphite was added to the chloride and heated to 150 °C for 5 h to form the corresponding phosphonate **96** which was isolated by removal of all volatile components in a

vacuum distillation. The high yield of 99% over both steps shows that conversion was complete and losses minimal.



Scheme 26: Synthesis of the phosphonate **96**.<sup>[149]</sup>

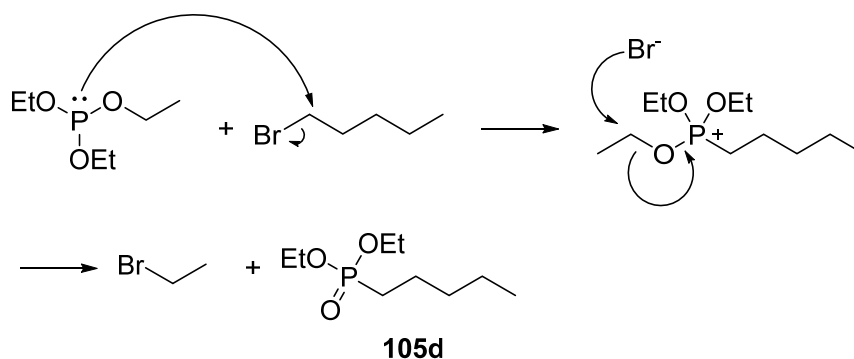
The second HWE reaction leads to cyclisation of the lactone. The phosphonate is introduced by esterification of **99** with the required diethylphosphono acid **100a–d**. The diethylphosphono acids **100a** (R = Me) and **100d** (R = Bu) were synthesised in three steps<sup>[150]</sup> (Scheme 27) whereas the corresponding esters of **100b** and **100c**, **104b** (R = Et) and **104c** (R = Pr) respectively, were commercially available.



Scheme 27: Preparation of the diethylphosphono acids **100a–d**.

The synthesis of **100a** and **d** starts with a Michaelis-Arbuzov reaction of triethylphosphite with an alkyl iodide or alkyl bromide.<sup>[150a]</sup> Both starting materials were heated to 150 °C overnight in a closed tube and the volatile components were removed by vacuum distillation. When using iodoethane, pure phosphonate **105a** was obtained in nearly quantitative yields. The reaction with bromopentane produced phosphonate **105d** and the ethyl phosphonate **105a** as byproduct. This can be explained by the mechanism of the Michaelis-Arbuzov reaction.<sup>[151]</sup> When the phosphite substitutes the bromide of 1-bromopentane, the displaced bromide reacts with an ethoxy group in an  $S_N2$  reaction to liberate the phosphonate product and bromoethane (Scheme 28). The bromoethane can undergo a Michaelis-Arbuzov reaction itself to form the ethyl phosphonate **105a**. If necessary to avoid the byproduct, the iodoethane can be removed by distillation during the reaction.<sup>[152]</sup> In the case of the

pentylphosphonate **105d** this was not necessary, because a separation was possible after the subsequent synthetic step.



**Scheme 28:** Mechanism of the Michaelis-Arbuzov reaction of triethylphosphite with 1-bromopentane.<sup>[151]</sup>

For the carboxylation, the respective alkyl phosphonates **105a** and **d** were dissolved in dry THF and deprotonated with LDA at  $-84\text{ }^{\circ}\text{C}$ . Addition of diethyl carbonate led to the phosphonate esters **104a** and **d**.<sup>[150b]</sup> After warming to RT overnight, the reaction was quenched with dilute hydrochloric acid and the phosphonate esters were extracted with ethyl acetate. The resulting yellow oil was purified by flash chromatography to provide 50–66% yield of the desired products. Product **104d** was separated from the methyl substituted byproduct **104a** carried through from the previous step.

Hydrolysis of the phosphonate esters **104a–d** with KOH in a mixture of water and ethanol provided the corresponding acids **100a–d** in very good yields.<sup>[150c]</sup> No purification other than extractions at basic and acidic pH were needed in this step.

### Intermolecular HWE reaction and transformation to the latest common intermediate **99**

With ethyl 2-(diethoxyphosphoryl)-2-ethoxyacetate (**96**) and 1-methyl-1*H*-imidazole-5-carbaldehyde (**37**) in hand, the first HWE reaction in the synthetic route was possible (Scheme 25).<sup>[146]</sup> A small excess of the phosphonate **96** was added to a suspension of sodium hydride in dry THF at  $0\text{ }^{\circ}\text{C}$ . Then, a solution of the aldehyde **37** in dry THF was added slowly and the reaction was stirred overnight to achieve complete conversion of **37**. Conversion was monitored by TLC which was stained with dinitrophenylhydrazine to distinguish the aldehyde from the product spot with the same  $R_f$  values. An acidic workup and extractions allowed the removal of excess **96** and paraffin oil while the product **97** and the dialkyl phosphate byproduct remained in the aqueous layer. The product **97** was extracted from the aqueous layer after adjustment of the pH to 9. The slightly yellow oil obtained as reaction product was of sufficient purity for further reactions. It was composed of a mixture of *E*- and *Z*-isomers with a ratio of 80:20 supposedly in favour of the *E*-configured product. The attribution of the  $^1\text{H}$  NMR signal sets to one or the other diastereomer relies on considerations of anisotropy effects of the

carbonyl function. Protons in a position perpendicular to the carbonyl bond are object to increased shielding and the proton of the *Z*-isomer is thus expected to have a lower chemical shift than the corresponding proton of the *E*-isomer of **97**.<sup>[153]</sup> The configuration of the double bond does not play any role in the chosen synthetic route due to later transformation of the enoether to the ketone.

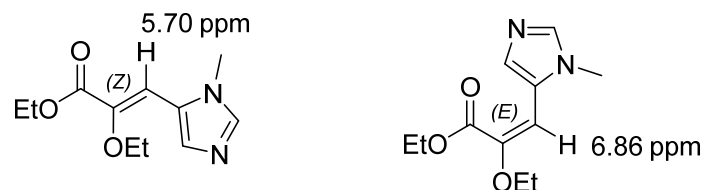


**Figure 38:** Representation of the *Z*- and *E*-isomers of **97** and annotation of the most different signals in <sup>1</sup>H NMR measured in CDCl<sub>3</sub>.

In the following step, the ester function of **97** was reduced to an alcohol by addition of diisobutylaluminium hydride to a solution of the ester in dry toluene at 0 °C.<sup>[146]</sup> The reaction took place within 20 minutes and was quenched with methanol and water to oxidise the aluminium complex to aluminium oxide. In most cases the aluminium oxide particles were too small to be retained on a filter. In these cases, the complete mixture was evaporated to dryness and the resulting powder was added onto a small silica column as dry loading. The product was eluted with methanol to provide the product **98** in very good yields close to 90%.

For the hydrolysis of the enol ether, compound **98** was stirred in 1 M hydrochloric acid at 50 °C for 2 h.<sup>[146]</sup> Evaporation of the diluted hydrochloric acid led to the desired ketone **99** as a hydrochloride salt. The hydrochloride salt needed to be transformed to the free base. As **99** proved to be highly soluble in water, a preliminary test to extract the compound from an aqueous mixture failed. Consequently, deprotonation of the hydrochloride salt of **99** required nonaqueous conditions to avoid long evaporation of aqueous mixtures during which decomposition might occur. A separation from the salts formed during deprotonation would thus be difficult. Reimann<sup>[146]</sup> proposed a deprotonation in methanolic solution by addition of sodium methoxide as the base would circumvent the extraction problem and the compound could be separated from inorganic salt by column chromatography.<sup>[146]</sup> For the target pH value, Reimann<sup>[146]</sup> stated that the pH of 6.5 should not be exceeded. This procedure led to low yields of 20–54%.

Estimated pK<sub>a</sub> values of **99** are 6.58 and 12.94.<sup>[153]</sup> This might explain the low yields as only half the molecules are deprotonated at pH = pK<sub>a</sub>. Consequently, a target pH value of 9 was chosen. Theoretically, this leads to a more than 100-fold excess of the deprotonated imidazole without deprotonation of the alcohol. Indeed, yields were increased to up to 70% when the target pH was set to 9. However, the yields were not well repeatable so that some reactions would generate only 15% of the product. Several observations showed reasons for these erratic yields:

- Samples of **99** dissolved in water or ethanol with added Na<sub>2</sub>CO<sub>3</sub> formed a polar decomposition product visible on TLC after 2 d at RT. This shows that the free base is not stable in basic solution.
- During column chromatography two fractions were collected. One corresponded to the product and a bigger, more polar second fraction, possibly a degradation product, could not be identified.
- The head of the column stayed brown showing potential degradation products.
- Solubility of the crude product in dichloromethane was poor. This might be due to HCl as impurity in commercial dichloromethane.

From these observations a need to avoid silica column chromatography and the need to use acid-free dichloromethane when dissolving the product was concluded. Additionally, the product should not be kept in solution for a long time.

As an alternative nonaqueous deprotonation, addition of Na<sub>2</sub>CO<sub>3</sub> to an ethanolic solution of the hydrochloride salt was attempted. With Na<sub>2</sub>CO<sub>3</sub> being less strong than sodium methanolate, the use of excess carbonate would not lead to potential deprotonation of the alcohol. Conversion to the free base was monitored by TLC. When conversion was complete, the suspension was filtered and evaporated. As ethanol dissolves small amounts of sodium chloride and Na<sub>2</sub>CO<sub>3</sub>, the residue was suspended in acid-free dichloromethane and filtered again, to remove the residual salts. Evaporation of the solvent left the free base. When this deprotonation method was carried out within few hours, good yields of 60–80% were achieved reliably. However, when the solution was kept on residual salts for 2 d, a decrease in yield was observed due to decomposition as mentioned above.

With the synthesis of ketone **99**, the common synthetic pathway for all desired analogues of pilocarpine was completed. The overall yield starting from imidazole **37** was between 45 and 61%.

### Diversification and Access to the Target Compounds

The following esterification step was the point of diversification of the synthesis towards the differently substituted target molecules (Scheme 25).

The last common intermediate **99** was esterified in a Steglich esterification with phosphono acids **100a–d** carrying the different alkyl groups R = Me to Bu respectively. Alcohol **99** and a small excess of the respective acid **100a–d** were dissolved in dry dichloromethane and catalytic amounts of 4-dimethylaminopyridine (DMAP) were added. The coupling agent *N,N'*-dicyclohexylcarbodiimide (DCC) was added in one portion at 0 °C. The reaction was complete after 2 h at RT. The byproduct dicyclohexylurea was removed by filtration and the product was isolated by extractions followed by column chromatography on silica with yields of 17–53%. The low yields can be explained by losses due

to product instability during column chromatography. However, this purification could not be avoided, because the consecutive cyclisation reaction only proceeded with pure starting material.

The resulting phosphono ester **101a–d** (Scheme 25) can then undergo an intramolecular HWE reaction to form the desired five-membered lactone. Reimann proposed two different protocols.<sup>[146]</sup> Both reactions are carried out using absolute toluene as solvent and sodium hydride combined with 15-crown-5 or potassium carbonate with 18-crown-6 for the deprotonation. Test reactions with these conditions revealed major difficulties in the separation of the excess crown ether from the desired product. Additionally, the proposed purification by flash chromatography on silica gel was not suitable due to decomposition of the product on the stationary phase. These problems were solved carrying out the reaction under standard Wittig conditions using sodium hydride in dry THF. A solution of the starting material **101a–d** in freshly dried THF was added to a suspension of sodium hydride in freshly dried THF at 0 °C. The reaction was complete after 24 h and the same workup as for the first HWE reaction could be applied. This provided the desired products **95a–d** in yields of 55–75%.

The newly formed double bond of **95a–d** was reduced by catalytic hydrogenation in dry methanol at 50 °C and 50 bar hydrogen for 5 h. 10% Palladium on activated charcoal was used in high catalyst loadings of more than 10 mol%. In case the reaction was not complete after 5 h, fresh catalyst was added, and the hydrogenation was repeated. The catalyst was removed by filtration through cotton followed by filtration through a PVDF syringe filter. After solvent removal, the product was dissolved in a small amount of ethanol and two drops of concentrated nitric acid were added to transform the target compound into their nitrate salts. The nitrate salts of compounds **2** and **31a, c** (R = Me, Et, and Pr) crystallised overnight. They were isolated after three recrystallisations in ethanol with a yield between 20 and 70%. <sup>1</sup>H NMR analysis revealed that the salts consisted of the desired racemic compound **2** and **31a, c** and less than 20% of their diastereomers. The recrystallisations reduced the relative amount of the *trans*-diastereomers in the product crystals (Table 16), so that the target compounds were obtained in purities exceeding 85%. The nitrate salt of **31d** did not crystallise and could therefore not be purified.

**Table 16:** Impact of the recrystallisations of the nitrate salts of **2** and **31a, c** on the relative amount of *trans*-diastereomers included in the product determined by <sup>1</sup>H NMR.

R	#	Before crystallisation	After three recrystallisations as nitrates
Me	<b>31a</b>	7%	2%
Et	<b>2</b>	20%	15%
Pr	<b>31</b>	13%	8%

## Enantiomeric Separation of the Target Compounds

The aim of the synthesis was to provide enantiomerically pure analogues of pilocarpine. The analytical separation of the free bases of enantiomers was tested on the analytical chiral Lux<sup>®</sup> cellulose-4 column with the methyl (**31a**) and propyl (**31c**) analogues. For the preparative resolution of the racemic mixture, the respective nitrate salts were dissolved in isopropanol and solid sodium carbonate was added until the apparent pH was above 8 and deprotonation of the salts was complete. The inorganic salts were removed by filtration and centrifugation. The remaining solution of the deprotonated compounds was evaporated and dissolved in 0.5 mL isopropanol. This mixture was separated by preparative chromatography on the analytical Lux<sup>®</sup> cellulose-4 column.

In the case of the methyl analogue (**31a**), this procedure provided both enantiomers as pure products with single peaks in the chromatographic analysis (Figure 39) and less than 5% of *trans*-isomers in the <sup>1</sup>H NMR spectra. In the case of the propyl analogue (**31c**), epimerisation to the *trans*-isomers (**81c**) occurred during the liberation of the free base from the nitrate salt. The chromatographic separation provided three product fractions analysed by chiral HPLC (Figure 40) and <sup>1</sup>H NMR: one *cis*-enantiomer in 1:3 mixture with one of the *trans*-enantiomers, one pure *trans*-enantiomer and one pure *cis*-enantiomer.

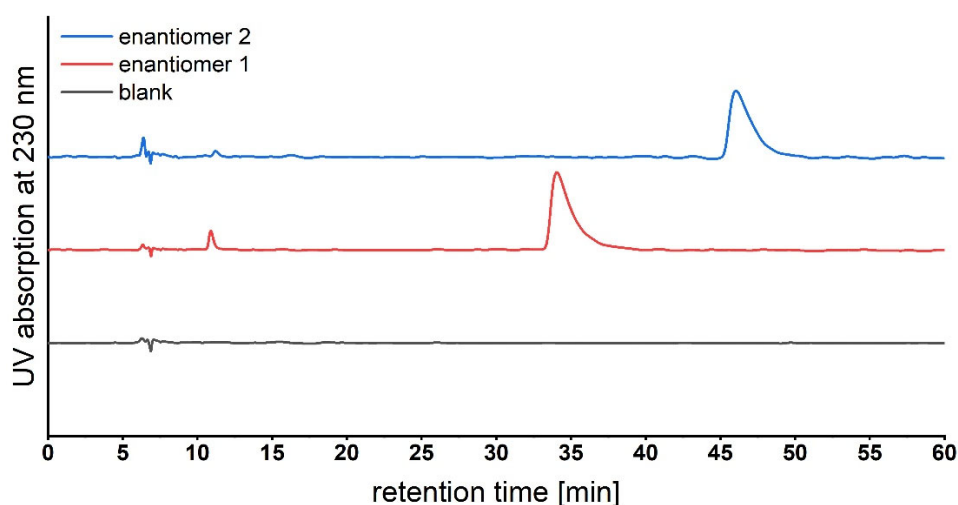


**Figure 39:** Chromatographic analysis of the two fractions obtained after chiral resolution of the methyl analogues (Lux<sup>®</sup> cellulose-4 column, 20:80:0.1 *n*-hexane/isopropanol/diethyl amine).

The enantiomers were identified in comparison to the chromatographic behaviour of (+)-pilocarpine (**2**). (+)-Pilocarpine was less retained by the cellulose-4 phase than its enantiomer. By analogy, the first peak of each chromatogram of the racemic mixtures supposedly corresponds to the desired enantiomer (Figure 41). Unfortunately, the first peak of the propyl analogues (**31c**) was the peak in which the desired enantiomer coeluted with a *trans*-diastereomer (**81c**). Nevertheless, the



enantiomer 1 of the methyl analogue (**31a**) was obtained pure and will undergo pharmacological testing.

The risk of epimerisation could have been avoided. The racemic mixture obtained from the hydrogenation step could have been directly separated without the additional crystallisation step.

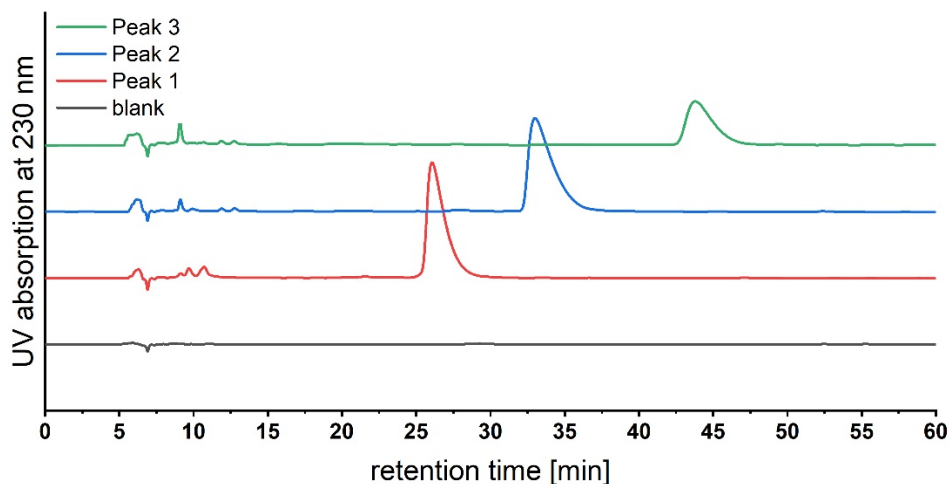


**Figure 40:** Chromatographic analysis of the three fractions obtained after chiral resolution of the methyl analogues (Lux<sup>®</sup> cellulose-4 column, 100:0.1 isopropanol/diethyl amine). Peak 1 consists of a mixture of one *cis*- and one *trans*-enantiomer, peak 2 is the other *trans*-enantiomer and peak 3 the other *cis*-enantiomer.

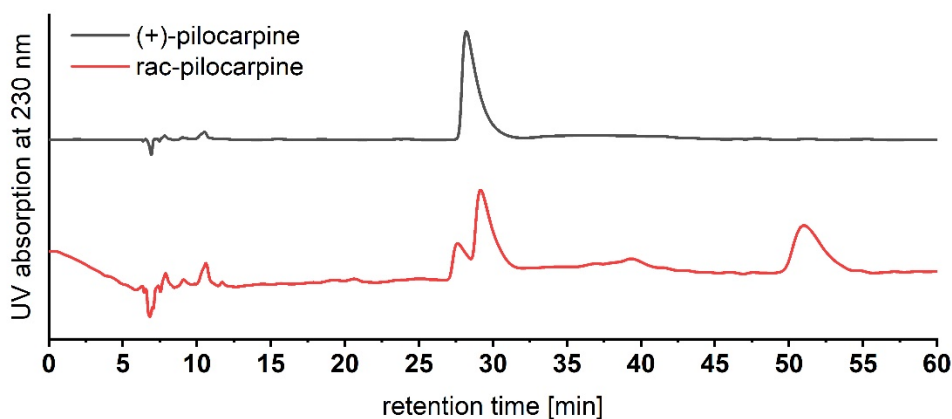


**Figure 41:** Chromatograms of (+)-pilocarpine and its racemic mixture on a Lux<sup>®</sup> cellulose-4 column (10:90:0.1 *n*-hexane/isopropanol/diethyl amine). The racemic mixture contained 15% of *trans*-diastereomers as determined by <sup>1</sup>H NMR, one of which elutes in front of (+)-pilocarpine. (–)-Pilocarpine has a higher retention time (51 min) than (+)-pilocarpine (29 min).

As a result of this and the previous synthetic route, a series of racemic pilocarpine analogues in which the ethyl substituent at the lactone C-3 is replaced by H (**16**), Me (**31a**), or Pr (**31c**) was synthesised. For this reason, racemic pilocarpine (**2**) was also provided by the same synthetic route as the methyl and propyl analogues. The chiral resolution of those compounds with chromatographic methods was shown to be possible and was successfully demonstrated with the methyl analogue (**31a**).

## 5 Summary

Muscarinic acetylcholine receptors (mAChRs) are involved in signal transmission at the synapses of the parasympathetic nervous system. The five subtypes of mAChRs regulate various body functions such as heart function, gland secretion, memory, and learning. For the development of drugs with the least side-effects possible, the molecular causes of subtype selectivity and signalling bias are under investigation. In this context, the study of dualsteric ligands binding simultaneously to the orthosteric and the allosteric binding sites of the receptor is of high interest.

To date, dualsteric ligands were synthesised as hybrids of full agonists or superagonists being the orthosteric element, linked to known subtype selective allosteric fragments. In this work, the existing library was expanded to hybrid ligands based on the partial agonist pilocarpine. A suitable linker attachment point to pilocarpine was investigated.

For this aim, pilocarpine (**2**), isopilocarpine (**15**), pilosinine (**16**) and desmethyl pilosinine (**35**) were synthesised as orthosteric ligands and orthosteric fragments for the construction of the hybrid molecules (Figure 42). Pilocarpine was liberated from the commercial hydrochloride or nitrate salt and isopilocarpine was generated by epimerisation of pilocarpine. Pilosinine was synthesised in a Michael addition reaction of a dithiane carrying the imidazole moiety **82** onto the lactone precursor furan-2(5*H*)-one (**83**) followed by complete deprotection (Figure 43a).<sup>[133]</sup> The desmethyl pilosinine (**35**) was obtained in a newly developed synthetic route based on a Horner-Wadsworth-Emmons (HWE) reaction to build the methylene bridge between the imidazole aldehyde and the precursor of the lactone moiety **57** (Figure 43b). All four orthosters were converted to the respective dualsteric compounds with a naphmethonium fragment as allosteric moiety.

The four orthosteric fragments and the four hybrid molecules with a linker length of six methylene units were tested for their dose dependent G protein recruitment at the receptor subtypes M<sub>1-5</sub> using a mini-G nanoBRET assay. The study of the orthosteric ligands revealed that pilocarpine has the highest ability of all four orthosters to induce activity at all receptor subtypes. A change of the *cis*- to a *trans*-configuration of the lactone substituents or a complete removal of the ethyl substituent provoked a significant reduction of activity. Removal of the methyl substituent of the imidazole moiety led to improved receptor activation.

## Summary

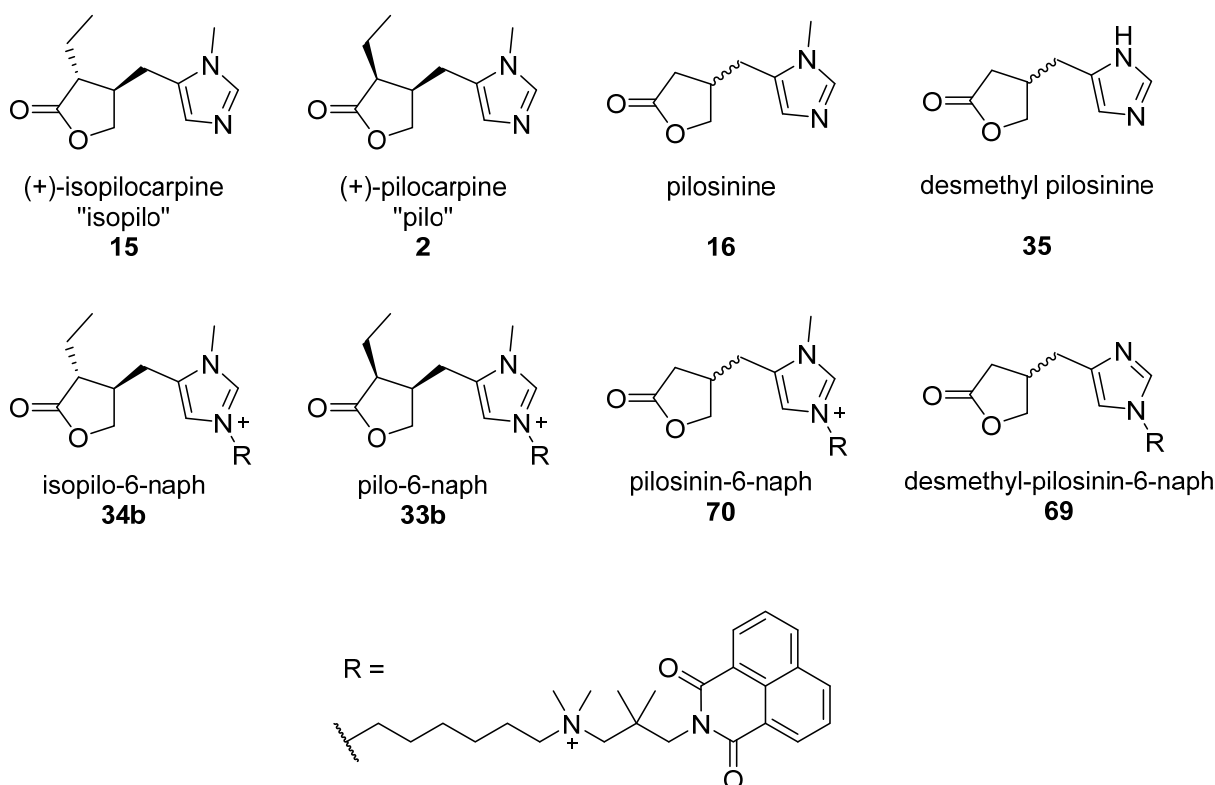


**Figure 42:** The studied orthosteric fragments and dualsteric hybrid molecules.

The efficacies of the hybrid ligands show that the linker attachment at the imidazole moiety of pilocarpine and its analogues does not abolish activity and hybrid formation of isopilocarpine even improved receptor activation. Thus, the linker attachment point seems a valid choice, but linker length might not be optimum. In contrast to the orthosters, the *trans*-substitution of the lactone was advantageous for receptor activation of the hybrid ligands. The hybrid without a methyl substituent at the imidazole (**69**) had an increased efficacy. Additionally, the naphmethonium fragment lowered the maximum effect of pilocarpine, whereas the activity of isopilocarpine was increased. The intensity of both effects was influenced by the subtype selectivity produced by naphmethonium leading, in the case of the pilocarpine hybrid, to less decreased responses or, in the case of the isopilocarpine hybrid, to more increased responses at the M<sub>2</sub> and M<sub>4</sub> receptors. The results generally lead to the assumption that the allosteric moiety strongly influences the binding poses of the hybrid ligands so that the orthosteric fragments do not interact with the binding site in the same way as the orthosters alone.

## Summary

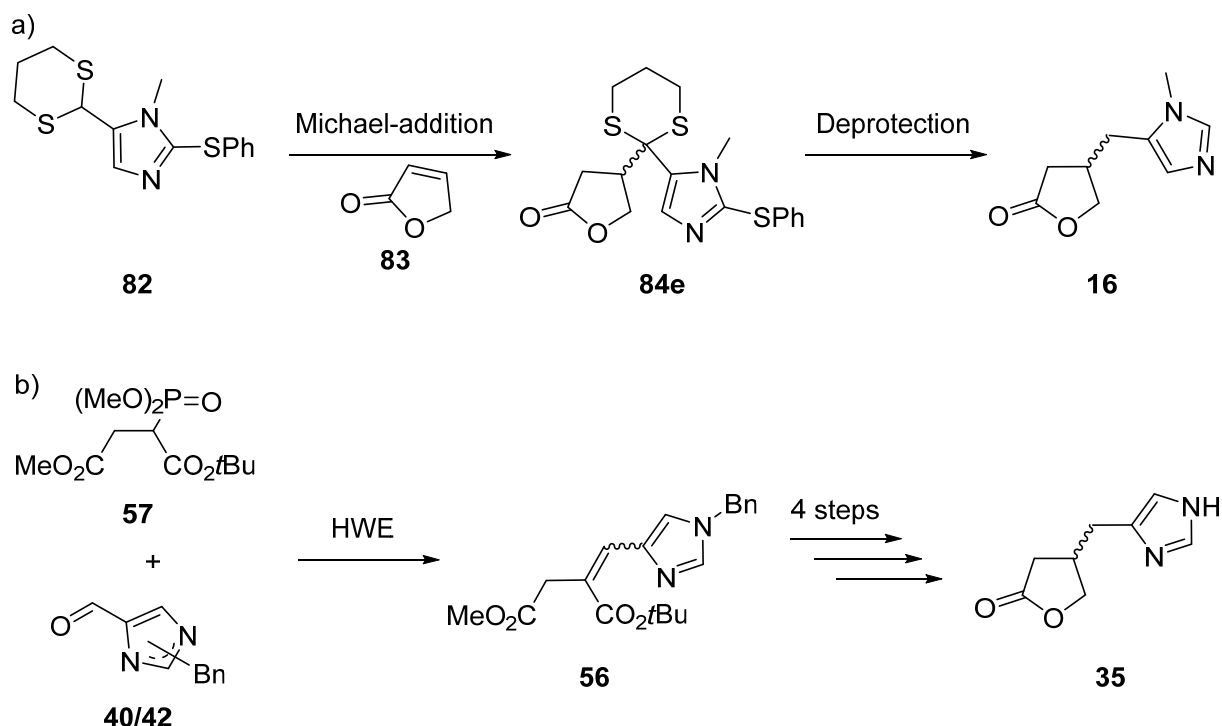


**Figure 43:** Key steps of the synthetic routes to a) racemic pilosinine and b) racemic desmethyl pilosinine.

A second project was based on molecular dynamics simulations of the binding pose of pilocarpine,<sup>[73]</sup> leading to the hypothesis that the partial agonism of pilocarpine results from an equilibrium between an agonistic and an antagonistic binding pose at the orthosteric binding site of the receptor. The ratio of occupancy of both binding poses determines the observed efficacy of pilocarpine. The orthosteric binding site provides more space for the ethyl substituent in the supposed antagonistic pose than in the agonistic binding pose. This hypothesis was tested by the synthesis and pharmacological evaluation of pilocarpine analogues with alkyl substituents of different sizes at the lactone (**16**, **31a**, **c**, **d**) (Figure 44). The analogues with larger alkyl residues are expected to shift the equilibrium towards the antagonistic binding pose, the analogues with smaller residues should have the inverse effect.

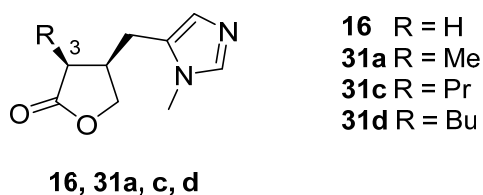


**Figure 44:** Structure of the pilocarpine analogues to challenge the hypothesis of the molecular reasons for pilocarpine's partial agonism.

The synthesis of the pilocarpine analogues was first attempted as a mixture of stereoisomers which were supposed to be separated at the end of the synthetic route. The racemic mixture of the thermodynamically more stable *trans*-isomers of the target compounds was prepared in a one-pot Michael-addition–alkylation reaction of a dithiane imidazole onto furan-2(5*H*)-one similarly to the synthesis of pilosinine (Figure 45). The resulting enolate was quenched by an iodoalkane to achieve

## Summary

alkylation of the lactone and subsequent complete deprotection yielded the racemic *trans*-analogues of pilocarpine.<sup>[133]</sup> After unsuccessful attempts of chiral resolution, the mixture of *trans*-isomers was converted to a mixture of all four possible diastereomers in a kinetic epimerisation reaction.<sup>[95]</sup> A separation of the stereoisomers was not possible in this project so only the racemic molecule **16** (pilosinine, R = H) was obtained from this synthetic route.

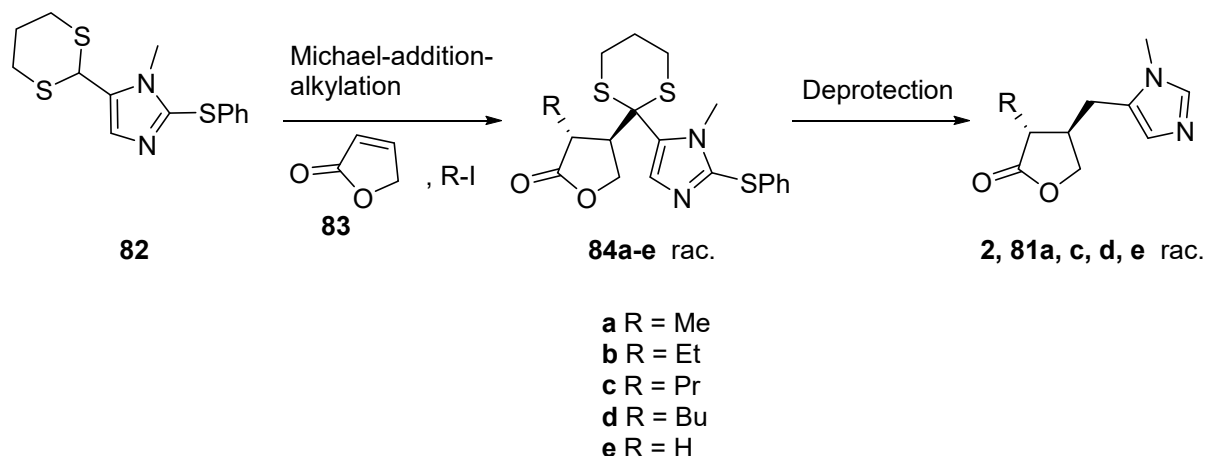


**Figure 45:** Key step of the synthesis of the racemic *trans*-analogues of pilocarpine.

For the selective synthesis of the *cis*-isomers following a patent from Reimann,<sup>[146]</sup> both stereocenters of the target molecules were produced in the last synthetic step by a *syn*-hydrogenation of the  $\alpha,\beta$ -unsaturated precursor (Figure 46). The racemic pilocarpine analogues, except the butyl derivative (**31d**), were purified by crystallisation as their nitrate salts. This provided the racemic mixtures with less than 8% of the *trans*-isomers as impurity. The racemic pilocarpine (**2**), itself, was obtained with 15% *trans*-impurity and was used as reference compound. Additionally, the possibility of chiral resolution by chromatographic methods was demonstrated in the case of the methyl derivative (**31a**). The pharmacological testing of the desired enantiomer of **31a** is in progress.

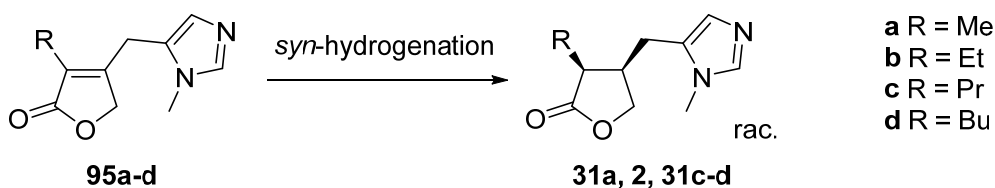


**Figure 46:** *Syn*-Hydrogenation of the  $\alpha,\beta$ -unsaturated precursor for the generation of the *cis*-substitution pattern at the lactone moiety.

## 6 Zusammenfassung

Muskarinische Acetylcholinrezeptoren (mAChRs) sind in den Synapsen des parasympathischen Nervensystems an der Signalübertragung beteiligt. Die fünf Subtypen der mAChRs regulieren verschiedenste Körperfunktionen, wie z.B. die Herzfunktion, die Sekretbildung, das Gedächtnis und Lernprozesse. Zur Entwicklung möglichst nebenwirkungsarmer Wirkstoffe werden die Ursachen von Subtypen- und Signalwegselektivität auf molekularer Ebene erforscht. Ein wichtiger Ansatz hierfür ist die Verwendung von dualsteren Hybridliganden, die gleichzeitig an die orthostere und die allosterische Bindungsstelle des Rezeptors binden.

Bisher wurden Vollagonisten und Superagonisten als orthostere Fragmente in Kombination mit bekannten subtypenselektiven allosteren Fragmenten zum Aufbau von Hybridliganden verwendet. In dieser Arbeit wurde die vorhandene Bibliothek um den Partialagonisten Pilocarpin erweitert. Dazu sollte eine geeignete Verknüpfungsstelle von Pilocarpin mit dem Linker gefunden werden.

Hierzu wurden Pilocarpin (**2**), Isopilocarpin (**15**), Pilosinin (**16**) und Desmethylpilosinin (**35**) als orthostere Liganden und orthostere Fragmente für den Aufbau der Hybridliganden verwendet (Abbildung 47). Pilocarpin wurde aus dem kommerziell erhältlichen Hydrochlorid oder Nitratsalz freigesetzt und Isopilocarpin durch Epimerisierung von Pilocarpin erhalten. Pilosinin wurde in einer Michael-Additions-Reaktion eines Imidazoldithians **82** an Furan-2(5*H*)-on (**83**) gefolgt von vollständiger Entschützung mit Raney-Nickel hergestellt (Abbildung 48a).<sup>[133]</sup> Das Desmethylpilosinin (**35**) entstand in einer im Zuge dieser Arbeit neu entwickelten Synthese basierend auf einer Horner-Wadsworth-Emmons-Reaktion (HWE-Reaktion) zum Aufbau der Methylenbrücke zwischen Imidazol und Laktone (Abbildung 48b). Alle vier Orthostere wurden zu den entsprechenden dualsteren Molekülen mit einem Naphmethoniumfragment als allosterische Einheit umgesetzt.

Die vier orthosteren Liganden und die vier Hybridmoleküle mit einer Linkerlänge von sechs CH<sub>2</sub>-Gruppen wurden in einem mini-G nanoBRET Assay zur Bestimmung der dosisabhängigen G-Protein-Rekrutierung an den Rezeptorsubtypen M<sub>1</sub> bis M<sub>5</sub> getestet. Bei der Untersuchung der orthosteren Liganden zeigte sich, dass Pilocarpin von allen Orthosteren alle Rezeptorsubtypen am besten aktivieren konnte. Eine Änderung der *cis*- zu einer *trans*-Konfiguration der Laktone substituente oder ein Entfernen der Ethylgruppe hatte signifikante Aktivitätsverluste zur Folge. Ein Entfernen des Methylsubstituenten des Imidazolrings führte zu einer verbesserten Rezeptoraktivierung.

## Zusammenfassung

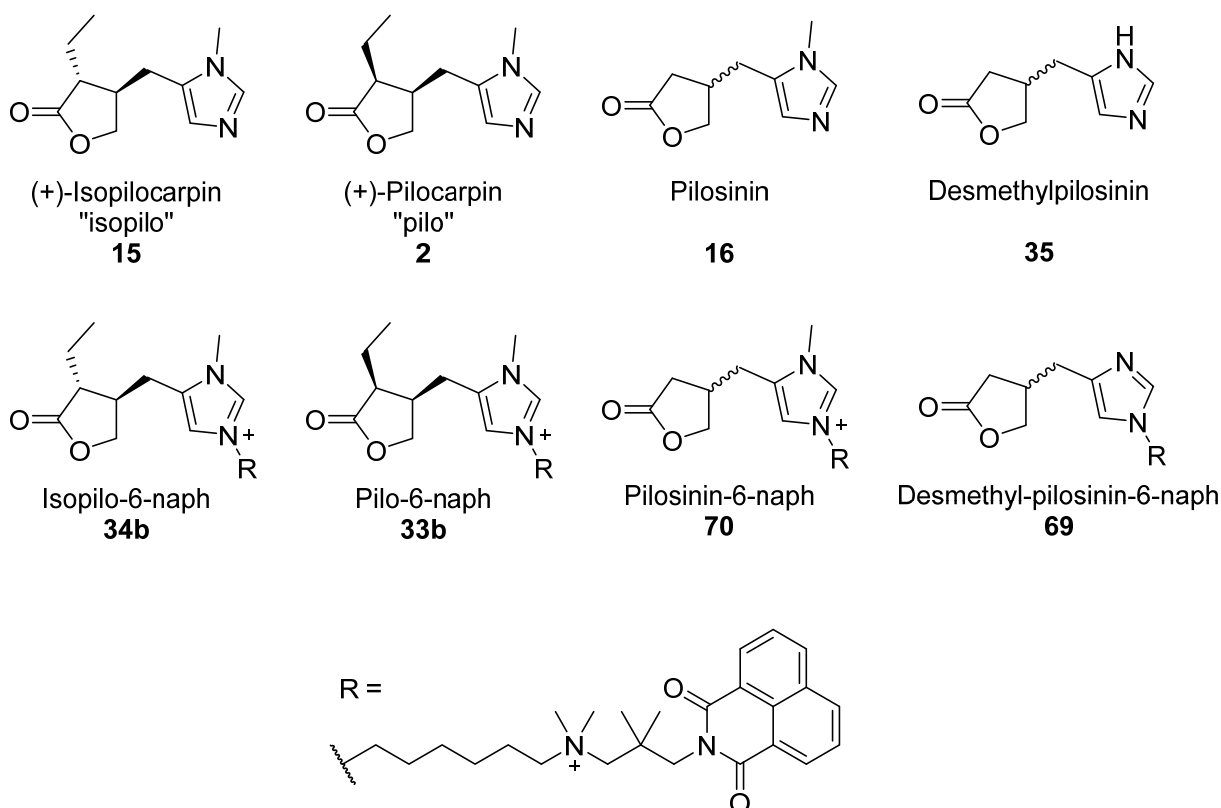
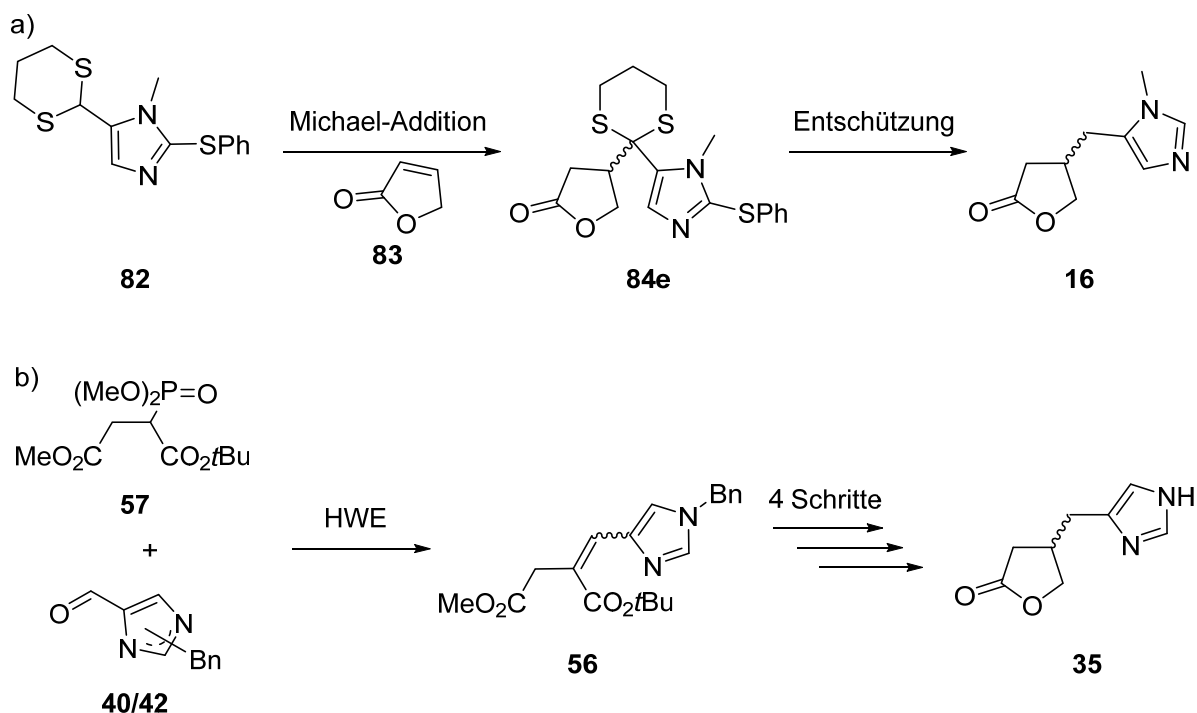


Abbildung 47: Die getesteten orthosteren Fragmente und dualsteren Hybridmoleküle.

Die Aktivität der Hybridliganden belegt, dass eine Verknüpfung des Linkers mit dem Imidazol nicht zu einem kompletten Aktivitätsverlust führt und eine Hybridbildung mit Isopilocarpin die Aktivität sogar verbessert. Deshalb erscheint die Verknüpfungsstelle des Linkers sinnvoll gewählt zu sein, aber die Linkerlänge entsprach möglicherweise noch nicht dem Optimum. Bei den Hybridliganden war im Gegensatz zu den Orthosteren eine *trans*-Substitution des Lactonrings für die Rezeptoraktivierung von Vorteil. Zudem resultiert ein Verzicht auf den Methylsubstituenten des Imidazols in einer Steigerung des maximalen Effekts. Außerdem zeigte sich eine Verringerung der Aktivität von Pilocarpin durch die Verknüpfung mit dem Naphmethoniumfragment, jedoch eine Aktivitätssteigerung im Zusammenspiel des Allosters mit Isopilocarpin. Beide Effekte wurden in ihrer Intensität durch die Subtypenselektivität von Naphmethonium geprägt. So war die Aktivität des Pilocarpinhybrids an den Rezeptoren M<sub>2</sub> und M<sub>4</sub> weniger reduziert als an den übrigen Rezeptorsubtypen sowie die Aktivitätssteigerung der Isopilocarpinhybride an M<sub>2</sub> und M<sub>4</sub> am stärksten ausgeprägt. Insgesamt ergibt sich die Vermutung, dass das allosterische Fragment die Bindungspose der Hybridliganden maßgeblich beeinflusst, sodass die Orthostere in einer veränderten Weise mit der orthosteren Bindungsstelle wechselwirken.

## Zusammenfassung



**Abbildung 48:** Schlüsselschritte der Syntheserouten zu a) racemischem Pilosinin und b) racemischem Desmethylpilosinin.

Ein zweites Projekt basierte auf molekulardynamischen Computersimulationen zur Bindungspose von Pilocarpin.<sup>[73]</sup> Die Ergebnisse lassen vermuten, dass der Partialagonismus von Pilocarpin dadurch erklärt werden kann, dass Pilocarpin in einem Gleichgewicht zwischen einer agonistischen und einer antagonistischen Bindungspose an der orthosteren Bindungsstelle des Rezeptors gebunden ist. Das Verhältnis zwischen beiden Bindungsposen bestimmt den beobachteten Maximizeffekt. Da dem Ethylrest des Pilocarpins in der vermuteten antagonistischen Bindungspose mehr Raum zur Verfügung steht als in der agonistischen Bindungspose, sollte diese Hypothese experimentell durch Synthese und pharmakologische Untersuchung von Pilocarpinanaloga mit veränderter Raumfüllung des Alkylsubstituenten am Lakton (**16**, **31a**, **c**, **d**) überprüft werden (Abbildung 49). Die Erwartung war, dass die Analoga mit größerem Alkylrest das Gleichgewicht zwischen den Bindungsposen zu Gunsten der antagonistischen Pose verschieben. Die kleineren Reste sollten das Gegenteil bewirken.

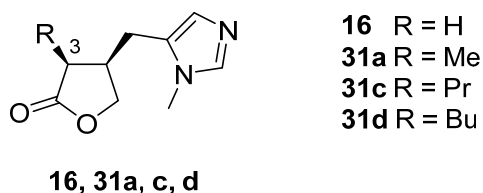


**Abbildung 49:** Struktur der Pilocarpinanaloga, anhand derer die Hypothese zur Ursache von Pilocarpins Partialagonismus überprüft werden sollte.

Die Synthese der Pilocarpinanaloga sollte zunächst als Gemisch der Stereoisomere erfolgen, um diese am Ende der Syntheseroute voneinander zu trennen. Die thermodynamisch stabileren *trans*-Isomere der Pilocarpinanaloga wurden in einer Eintopf-Michael-Addition-Alkylierungs-Reaktion analog zur



## Zusammenfassung

Synthese von Desmethylpilosinin hergestellt (Abbildung 50).<sup>[133]</sup> Nach vergeblichen Versuchen der Racematspaltung wurden die racemischen Mischungen der *trans*-Isomere einer kinetischen Epimerisierungsreaktion<sup>[95]</sup> unterzogen, um die gewünschten *cis*-Isomere herzustellen. Dadurch wurde jeweils ein Gemisch aller vier möglichen Stereoisomere erhalten. Eine Auftrennung war in diesem Projekt nicht möglich. Aus diesem Grund konnte nur das Analogon **16** (Pilosinin, R = H) als Racemat aus dieser Syntheseroute erhalten werden.

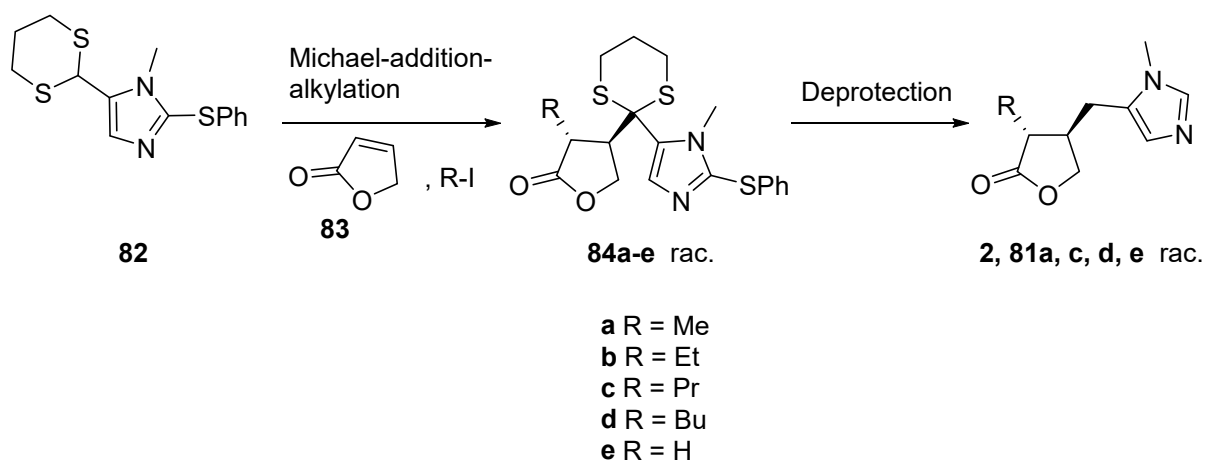


**Abbildung 50:** Schlüsselschritt der Synthese der racemischen *trans*-Analoga von Pilocarpin.

Zur selektiven Synthese der *cis*-Isomere wurden, nach einem Patent von Reimann,<sup>[146]</sup> beide Stereozentren der Zielmoleküle im letzten Reaktionsschritt durch die heterogenkatalytische *syn*-Hydrierung der  $\alpha,\beta$ -ungesättigten Vorstufe erzeugt (Abbildung 51). Die racemischen Pilocarpinanaloga mit Ausnahme des Butylderivats (**31d**) konnten anschließend durch Kristallisation als Nitratsalz aufgereinigt werden und wurden als Racemate mit einer Verunreinigung durch die *trans*-Isomere von nicht mehr als 8% erhalten. Das racemische Pilocarpin (**2**) wurde mit einem Anteil von 15% der *trans*-Isomere zur Verwendung als Referenzsubstanz hergestellt. Zudem wurde die Möglichkeit einer Racematspaltung durch chromatographische Methoden anhand des Methylderivats (**31a**) demonstriert. Die pharmakologische Testung des gewünschten Enantiomers von **31a** ist in Arbeit.

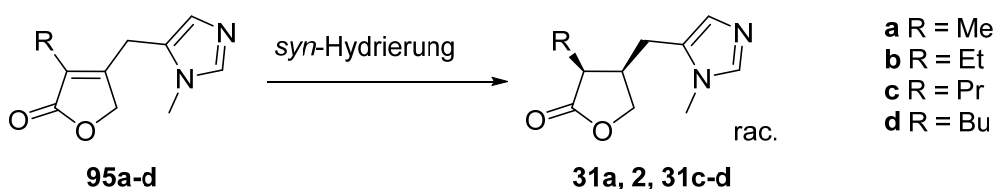


**Abbildung 51:** *Syn*-Hydrierung des  $\alpha,\beta$ -ungesättigten Vorläufermoleküls zur Erzeugung eines *cis*-Substitutionsmusters am Laktonring.

## 7 Experimental

### 7.1 General Methods and Techniques

#### 7.1.1 Chemicals

All starting materials and reagents were used as supplied from commercial sources (Merck, Darmstadt, Germany; abcr, Karlsruhe, Germany; tci, Eschborn, Germany). All solvents used in synthesis except acetonitrile were dried prior to use following standard drying procedures. Water was fully desalted. Argon supplied by Linde (Munich, Germany) was used as inert atmosphere.

Solvents used for reversed-phase analytical or preparative HPLC were HPLC-grade and were purchased from Merck (Darmstadt, Germany). Water was purified by a Reference A+ Milli-Q<sup>®</sup> system using a Quantum<sup>®</sup> TEX column by Merck, Darmstadt, Germany.

Solvents used for normal phase HPLC were either HPLC grade purchased from Merck (Darmstadt, Germany) (2-propanol) or purified by distillation (n-hexane).

#### 7.1.2 Thin Layer Chromatography (TLC)

TLC was performed on glass plates coated with silica G-25 UV254 purchased from Macherey-Nagel (Düren, Germany). The composition of eluents is indicated as volume ratio (v:v). Plates were visualised using UV light (254 or 366 nm), *p*-anisaldehyde, Dragendorff's reagent, Gibbs reagent, acidic 4-nitrophenylhydrazine solution or ethanolic basic KMnO<sub>4</sub>.

#### 7.1.3 Flash Column Chromatography

Flash column chromatography was performed using interchim PuriFlash 430 with interchim PuriFlash normal phase columns (Montluçon, France) filled with 50 µm (IR-50SI from 4 to 80 g) or 30 µm (PF-30SIHP-JP from 12 to 25 g) standard silica. For reversed phase purifications CHROMABOND columns C18-ec (4.3 to 26 g) were used (Macherey-Nagel, Düren, Germany). Interchim Flash-ELSD (Montluçon, France) was used as detector for substances without a chromophore, substances with a chromophore were detected by UV absorption. Solvents were not distilled prior to use. The solvent composition is reported as volume ratio (v:v).

#### 7.1.4 Purification by Preparative HPLC

Purification by preparative HPLC with achiral columns was carried out on an Agilent System (Agilent Technologies, Waldbronn, Germany) of the 1100 series consisting of two preparative pumps (PrepPump G1361 A), an automatic liquid sampler (PrepALS G2260 A), a multi-wavelength detector

## Experimental

(MWD G1365 B) and a fraction collector (PrepFC G1364 B). The AgilentChemStation Software (Release B.01.03) was used for control of the system and analysis of the chromatograms.

All achiral purification methods were run on a Gemini® 5 µm NX-C18 110 Å, 250 x 10 mm (Phenomenex, Aschaffenburg, Germany) column with a flow rate of 4.0 mL/min. The wavelengths 220 and 254 nm were used to detect the products and impurities.

### Method I:

Eluent:	water (A), methanol (B)	
Gradient:	0–2 min	5% B
	2–7 min	5 to 50% B
	7–10 min	50% B
	10–15 min	50 to 95% B
	15–21 min	95% B
	21–23 min	95 to 5% B
	23–26 min	5% B

### Method II:

Eluent:	water (A), methanol (B)	
Gradient:	0–22 min	5 to 35% B
	22–24 min	35 to 95% B
	24–26 min	95% B
	26–28 min	95 to 5% B
	28–30 min	5% B

### Method III:

Eluent:	water (A), methanol (B)	
Gradient:	0–16 min	10 to 40% B
	16–18 min	40 to 95% B
	18–21 min	95% B
	21–23 min	95 to 10% B
	23–27 min	10% B

### Method IV:

Eluent:	water + 0.1% formic acid (A), methanol + 0.1% formic acid(B)	
Gradient:	0–10 min	5 to 50% B
	10–12 min	50% B
	12–14 min	50 to 5% B
	14–17 min	5% B

### Method V:

Eluent:	water (A), methanol (B)	
Gradient:	0–17 min	5 to 95% B
	17–20 min	95% B
	20–22 min	95 to 5% B
	22–25 min	5% B

### Method VI:

Eluent:	water (A), methanol (B)	
Gradient:	0–15 min	20 to 60% B
	15–17 min	60 to 20% B
	17–21 min	20% B

## 7.1.5 LC–MS Analysis

LC–MS analysis was performed using a Shimadzu LC-MS-2020 mass spectrometer (Shimadzu Deutschland GmbH, Duisburg, Germany) containing a degassing unit (DGU-20A3R), a liquid chromatograph (LC20AB), a UV/VIS detector (SPD-20A) and a LC/MSD ion trap (Agilent Technologies,

## Experimental

Waldbronn, Germany). As stationary phase a Synergie 4U fusion-RP (150 × 4.6 mm) column (Phenomenex, Aschaffenburg, Germany) and as mobile phase a gradient of MeOH/water with 0.1% of formic acid were used.

Eluent: water + 0.1% formic acid (A), MeOH + 0.1% formic acid (B)

Flow rate: 1.0 mL/min

Gradient:	0–13 min	5 to 90% B
	13–18 min	90% B
	18–19 min	90 to 5% B
	19–23 min	5% B

UV-Detection: 254 nm unless otherwise stated

### 7.1.6 NMR Spectroscopy

<sup>1</sup>H, <sup>13</sup>C and 2D NMR spectra were recorded on a Bruker AVANCE 400 FT-NMR spectrometer (Rheinstetten, Germany) at 27 °C. <sup>1</sup>H NMR spectra were measured at 400.13 MHz, <sup>13</sup>C at 100.61 MHz. Solvents used for NMR were CDCl<sub>3</sub>, CD<sub>3</sub>OD, D<sub>2</sub>O or DMSO-d<sub>6</sub>. Chemical shifts  $\delta$  are reported in ppm with tetramethylsilane as standard at  $\delta = 0$  ppm. Spectra were calibrated to the residual solvent signals (<sup>1</sup>H NMR: CDCl<sub>3</sub> at 7.26 ppm, CD<sub>3</sub>OD at 3.31 ppm, D<sub>2</sub>O at 4.79 ppm, DMSO at 2.50 ppm; <sup>13</sup>C NMR: CDCl<sub>3</sub> at 77.16 ppm, CD<sub>3</sub>OD at 49.00 ppm, DMSO at 39.52 ppm).

Multiplicity of NMR signals are reported as s (singlet), br. s (broad singlet), d (doublet), dd (doublet of doublets), t (triplet) and q (quartet) with the chemical shift in the centre of the multiplet. Multiplets without defined pattern are reported as m (multiplet) with a range of chemical shifts.

### 7.1.7 FT-IR Spectroscopy

IR spectra were recorded on a JASCO FT/IR-6100 instrument (Gross-Umstadt, Germany) with an ATR crystal. The absorbed wavelength is reported in wave numbers  $\tilde{\nu}$  in cm<sup>-1</sup>. The range of the measurement is between 4000 and 600 cm<sup>-1</sup>.

### 7.1.8 Purity Determination

#### Purity Determination by HPLC

HPLC purity was measured on an Agilent System (Agilent Technologies, Böblingen, Germany) of the 1100/1200 series consisting of a binary pump (Bin Pump G1312 A), an automatic liquid sampler (ALS G1329 A) and a VWD detector (VWD G1314 A). The Agilent ChemStation Software (Release B.01.03) was used for control of the system and analysis of the chromatograms.

## Experimental

HPLC purity on a chiral column was measured on an Agilent System (Agilent Technologies, Böblingen, Germany) of the 1100 series consisting of a quaternary pump (QuatPump G1311 A) equipped with pump seals for normal phase use, an automatic liquid sampler (ALS G1329 A) and a VWD detector (VWD G1314 A). The Agilent ChemStation Software (Release B.01.03) was used for control of the system and analysis of the chromatograms.

When salts were analysed, 1.5 mg of the salt and 3 mg of potassium carbonate were sonicated in 500  $\mu$ L of HPLC-grade 2-propanol (for normal phase analysis) or methanol (for reversed phase analysis). The mixture was centrifuged, and the supernatant was passed through a syringe filter before injection onto the HPLC column.

Peaks in the UV chromatogram were integrated. Purity was determined by normalisation as the ratio of the peak area of interest to the sum of all peak areas.

Achiral method A:

HPLC column: Gemini<sup>®</sup> 5  $\mu$ m NX-C18 110 Å, 250 x 4.6 mm (Phenomenex, Aschaffenburg, Germany)

Flow rate: 1.0 mL/min

Eluent: water + 0.1% formic acid (A), methanol + 0.1% formic acid (B)

Gradient:	0–10 min	5 to 50% B
	10–17 min	50 to 95% B
	17–19 min	95% B
	19–21 min	95 to 5% B
	21–25 min	5% B

UV-Detection: 254 nm

Achiral method B:

HPLC column: Gemini<sup>®</sup> 5  $\mu$ m NX-C18 110 Å, 250 x 4.6 mm (Phenomenex, Aschaffenburg, Germany)

Flow rate: 1.0 mL/min

Eluent: water (A), methanol (B)

Gradient:	0–18 min	5 to 95% B
	18–20 min	95% B
	20–22 min	95 to 5% B
	22–25 min	5% B

UV-Detection: 220 nm

Chiral method A:

HPLC column: Lux<sup>®</sup> i-Amylose-1, 5  $\mu$ m, 250 x 4.6 mm (Phenomenex, Aschaffenburg, Germany)

Flow rate: 0.5 mL/min

## Experimental

Eluent: 80:20:0.1 *n*-hexane/2-propanol/diethylamine

UV-Detection: 220 nm

Chiral method B:

HPLC column: Lux® i-Cellulose-1, 5 µm, 250 x 4.6 mm (Phenomenex, Aschaffenburg, Germany)

Flow rate: 0.5 mL/min

Eluent: 40:60:0.1 *n*-hexane/2-propanol/diethylamine

UV-Detection: 220 nm

Chiral method C:

HPLC column: Lux® Cellulose-4, 5 µm, 250 x 4.6 mm (Phenomenex, Aschaffenburg, Germany)

Flow rate: 0.5 mL/min

Eluent: 20:80:0.1 *n*-hexane/2-propanol/diethylamine

UV-Detection: 230 nm

Chiral method D:

HPLC column: Lux® Cellulose-4, 5 µm, 250 x 4.6 mm (Phenomenex, Aschaffenburg, Germany)

Flow rate: 0.5 mL/min

Eluent: 100:0.1 2-propanol/diethylamine

UV-Detection: 230 nm

### Purity Determination by LC–MS

The LC-MS analysis was performed as mentioned above. Peaks in the UV chromatogram were integrated. Purity was determined by normalisation as the ratio of the peak area of interest to the sum of all peak areas.

### Purity Determination by Quantitative NMR (qNMR)

#### qNMR with Internal Standard

A precise amount of sample and of an adequate internal standard were weighed, mixed and dissolved in deuterated solvent, and the <sup>1</sup>H NMR spectrum of the solution was recorded with 16 scans, a D1 time of 50 s and without rotation. The signals of the standard and the sample were manually integrated. The purity (% w/w) was obtained by the following calculation:

$$\text{purity [\%]} = \frac{m_s}{m_p} \times \frac{I_p/n_p}{I_s/n_s} \times \frac{M_p}{M_s} \times 100\%$$

With the subscripts *p* for the sample and *s* for the standard. *I* describes the respective Integrals, *n* the number of protons represented by this integral, *m* the mass weighed and *M* the molecular weight of the substance.

## Experimental

qNMR results are reported with mention of the internal standard substance and the solvent.

### qNMR with External Standard in a Coaxial Insert

Each pair of NMR tube and coaxial insert was calibrated: The coaxial insert was filled with a solution of 3,4,5-trichloropyridine in CDCl<sub>3</sub>, the NMR tube was filled with a solution of 1,2,4,5-tetrachloro-3-nitrobenzene. Both concentrations were precisely known. For the calculation of the geometric factor  $F$  of each pair of NMR tube and coaxial insert, the <sup>1</sup>H NMR spectrum (16 scans, D1=50 s, without rotation) was recorded. All signals were integrated and  $F$  was determined using the following formula:<sup>[154]</sup>

$$\frac{c_{insert}}{c_{tube}} = F \times \frac{I_{insert}/n_{insert}}{I_{tube}/n_{tube}}$$

With  $c$  being the known concentration of the standard solution,  $I$  being the integral and  $n$  being the number of protons represented by the integral.

A precise amount of sample and of an adequate external standard were weighed separately. Each was dissolved in a precisely known amount of the same deuterated solvent. The sample solution was filled into the NMR tube, the standard solution was filled into the coaxial insert. After measurement of the <sup>1</sup>H NMR spectrum (16 scans, D1=50 s, without rotation) and manual integration of the signals, the purity (% w/w) of the sample was obtained by the following calculation:

$$purity [\%] = \frac{m_s}{m_p} \times \frac{I_p/n_p}{I_s/n_s} \times \frac{V_p}{V_s} \times \frac{M_p}{M_s} \times \frac{100\%}{F}$$

With the subscripts  $p$  for the sample and  $s$  for the standard.  $I$  describes the respective integrals,  $n$  the number of protons represented by this integral,  $m$  the mass weighed,  $M$  the molecular weight of the substance,  $V$  the volume of the solution and  $F$  the geometric factor.

qNMR results are reported with mention of the internal standard substance and the solvent.

### 7.1.9 Melting Point Determination

Melting points were measured with an MPM-H2 melting point meter from Coesfeld GmbH & Co. KG (Dortmund, Germany). The temperature ranges from 20 °C to 360 °C.

### 7.1.10 Determination of Specific Optical Rotation

Optical rotation of chiral compounds was measured using a MCP 200 polarimeter from Anton Paar (Graz, Austria). The measurement of the rotation  $\alpha$  was taken at a temperature of 25 °C and a wavelength of 589 nm. The length of the cuvette was 1.00 dm. The specific rotation was calculated as

$[\alpha]_D^{25} = \alpha / (l \times c)$  respectively, with  $\alpha$  the measured rotation in degrees,  $l$  the path length of the light in dm and  $c$  the concentration of the solution in g/mL.

### 7.1.11 Vacuum Pumps

The Schlenk line was powered by a PC 2004 VARIO by Vacuubrand (Wertheim, Germany). Vacuum distillation between 5 and 1000 mbar was performed with a Vacuubrand rotary vane pump RD-8 (Wertheim, Germany). Pressures below 5 mbar were obtained with a Vacuubrand chemistry-hybrid-pump RC 5 (Wertheim, Germany).

### 7.1.12 Degasification of Solvents

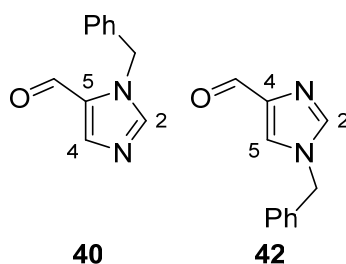
If not mentioned otherwise, solvents were not degassed prior to use. Solvents were degassed by the freeze-pump-thaw method. After freezing the solvent in liquid nitrogen, the flask is evacuated for 10 min, before thawing the solvent in the closed flask. This cycle was repeated three times.

### 7.1.13 Cooling Baths

A cooling bath with  $-78\text{ }^\circ\text{C}$  was prepared by addition of dry ice to acetone.  $-84\text{ }^\circ\text{C}$  were reached by cooling of ethyl acetate to its melting point by addition of liquid nitrogen.

## 7.2 Synthesis of the Aldehyde Precursors

### 7.2.1 Synthesis of a Regioisomeric Mixture of 1-Benzyl-1*H*-imidazole-4/5-carbaldehyde (**40/42**)<sup>[83]</sup>



1*H*-Imidazol-5-carboxaldehyde (5.00g, 52.0 mmol) was dissolved in DMF and  $\text{Na}_2\text{CO}_3$  (11.0 g, 104 mmol) was added. Benzyl bromide (9.19 g, 53.7 mmol, 6.18 mL) was slowly added and the mixture was heated to  $100\text{ }^\circ\text{C}$  for 2 d. The suspension was cooled down, water was added, and the mixture was extracted five times with ethyl acetate. The combined organic layers were dried over  $\text{MgSO}_4$ , filtered and the solvent was removed under reduced pressure. The product was obtained as a brown oil as a 39:61 mixture of the regioisomers **40** and **42**, respectively (8.41 g, 45.2 mmol, 87%).



## Experimental

Formula: C<sub>11</sub>H<sub>10</sub>N<sub>2</sub>O;

MW: 186.21 g/mol;

R<sub>f</sub> (95:5 dichloromethane/dichloromethane) = 0.6 and 0.4;

IR (ATR, cm<sup>-1</sup>): 3110, 3032, 2821, 1667, 1605, 1536, 1495, 1454, 1400, 1346, 1122, 768, 708, 653.

NMR signals of the 1,4-substituted regioisomer **42**:

<sup>1</sup>H NMR (CDCl<sub>3</sub>, 400 MHz): δ (ppm) = 9.87 (s, 1H, **CHO**), 7.62–7.61 (m, 1H, **5-H**), 7.61–7.60 (m, 1H, **2-H**), 7.42–7.31 (m, 3H, **Ph**), 7.23–7.19 (m, 2H, **Ph**), 5.16 (s, 2H, **-CH<sub>2</sub>-**);

<sup>13</sup>C NMR (CDCl<sub>3</sub>, 101 MHz): δ (ppm) = 186.1 (CH, **CHO**), 142.6 (C<sub>q</sub>, **C-4**), 138.9 (CH, **C-5**), 134.7 (C<sub>q</sub>, **Ph**), 128.9 (CH, **Ph**), 128.3 (CH, **Ph**), 127.6 (CH, **Ph**), 124.8 (CH, **C-2**), 51.5 (CH<sub>2</sub>, **-CH<sub>2</sub>-**).

NMR signals of the 1,5-substituted regioisomer **40**:

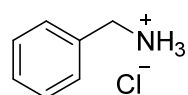
<sup>1</sup>H NMR (CDCl<sub>3</sub>, 400 MHz): δ (ppm) = 9.77 (d, *J* = 1.0 Hz, 1 H, **CHO**), 7.83–7.82 (m, 1 H, **4-H**), 7.70 (s, 1 H, **2-H**), 7.42–7.31 (m, 3 H, **Ph**), 7.23–7.19 (m, 2 H, **Ph**), 5.52 (s, 2 H, **-CH<sub>2</sub>-**);

<sup>13</sup>C NMR (CDCl<sub>3</sub>, 101 MHz): δ (ppm) = 179.2 (CH, **CHO**), 143.8 (CH, **C-4**), 143.7 (CH, **C-2**), 135.6 (C<sub>q</sub>, **Ph**), 131.0 (C<sub>q</sub>, **C-5**), 129.2 (CH, **Ph**), 128.8 (CH, **Ph**), 127.7 (CH, **Ph**), 50.2 (CH<sub>2</sub>, **-CH<sub>2</sub>-**).

The spectral data correspond to literature data.<sup>[155]</sup>

### 7.2.2 Synthesis of 1-Benzyl-1*H*-imidazole-5-carbaldehyde (**40**)

#### Conversion of Benzylamine to the Hydrochloride<sup>[155]</sup>



Benzylamine (9.81 g, 10.0 ml, 91.5 mmol) was dissolved in diethylether (50 mL). Concentrated hydrochloric acid was slowly added at 0 °C until the apparent pH of the mixture was below 4. The resulting white precipitate was isolated by filtration and washed with diethylether. The product was obtained as white crystals (13.86 g, 96.5 mmol, 95%).

Formula: C<sub>7</sub>H<sub>10</sub>ClN;

MW: 143.61 g/mol;

R<sub>f</sub> (95:5 dichloromethane/MeOH) = 0;

Melting point: 260–262 °C (diethylether) (Lit.:<sup>[156]</sup> 264–265 °C, MtBE);

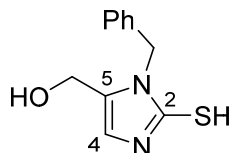
<sup>1</sup>H NMR (D<sub>2</sub>O, 400 MHz): δ (ppm) = 7.54–7.48 (m, 5H, **Ph**), 4.22 (s, 2H, **-CH<sub>2</sub>-**);

## Experimental

IR (ATR,  $\text{cm}^{-1}$ ): 2958 (br), 2877, 1595, 1466, 1455, 1380, 1111, 1058, 880, 744, 692.

The spectral data correspond to literature data.<sup>[157]</sup>

### Marckwald Synthesis of (1-Benzyl-2-Mercapto-1*H*-imidazol-5-yl)methanol<sup>[158]</sup>



Benzylamine hydrochloride (11.40 g, 79.38 mmol) was suspended in a mixture of acetonitrile (75 mL) and water (4.0 mL). Dihydroxyacetone (8.58 g, 95.26 mmol), potassium thiocyanate (11.57 g, 119.07 mmol) and glacial acetic acid (10.49 g, 10.0 mL, 174.63 mmol) were added. The mixture was stirred at 60 °C overnight. The resulting brown suspension was filtered and the filter cake was washed with cold water and dichloromethane. After drying the filter cake in vacuo, the product was obtained as a white powder (17.19 g, 17.19 mmol, 98%).

Formula:  $\text{C}_{11}\text{H}_{12}\text{N}_2\text{OS}$ ;

MW: 220.29 g/mol;

$R_f$  (95:5 dichloromethane/MeOH) = 0.2;

Melting point: 242–243 °C (acetonitrile/water) (Lit.<sup>[99b]</sup> 203–206 °C, solvent not reported);

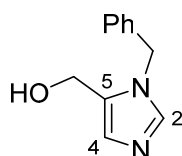
$^1\text{H}$  NMR (DMSO- $d_6$ , 400 MHz):  $\delta$  (ppm) = 12.15 (s, 1H, **SH**), 7.36–7.21 (m, 5H, **Ph**), 6.85 (d,  $J = 2.5$  Hz, 1H, **4-H**), 5.32 (s, 2H, **N-CH<sub>2</sub>-**), 4.14 (s, 2H, **-CH<sub>2</sub>-OH**);

$^{13}\text{C}$  NMR (DMSO- $d_6$ , 101 MHz):  $\delta$  (ppm) = 162.6 ( $\text{C}_q$ , **C-2**), 137.1 ( $\text{C}_q$ , **C-5**), 130.3 ( $\text{C}_q$ , **Ph**), 128.4 (CH, **Ph**), 127.2 (CH, **Ph**), 126.8 (CH, **Ph**), 112.8 (CH, **C-4**), 53.3 ( $\text{CH}_2$ , **-CH<sub>2</sub>-OH**), 46.3 ( $\text{CH}_2$ , **N-CH<sub>2</sub>-**);

IR (ATR,  $\text{cm}^{-1}$ ): 3110 (br), 2924, 1619, 1481, 1441, 1378, 1291, 1256, 1173, 1001, 741, 709, 637.

The spectral data correspond to literature data.<sup>[158]</sup>

### Synthesis of (1-Benzyl-1*H*-imidazol-5-yl)methanol<sup>[99a]</sup>



(1-Benzyl-2-mercapto-1*H*-imidazol-5-yl)methanol (460 mg, 2.09 mmol) was suspended in a mixture of water (4 mL) and acetic acid (1 mL). Hydrogen peroxide (35% aqueous solution, 14.6 mmol, 1.28 mL) was added slowly. The solution was stirred at RT for 3.5 h, then 8 mL of a 20% solution of sodium sulfite

## Experimental

was added slowly. The reaction was neutralised with aqueous ammonia and was extracted with ethyl acetate. The combined organic layers were dried over Na<sub>2</sub>SO<sub>4</sub> and the solvent was removed under reduced pressure. The product was obtained as a slightly yellow crystalline solid (376 mg, 2.00 mmol, 96%).

Formula: C<sub>11</sub>H<sub>12</sub>N<sub>2</sub>O;

MW: 188.23 g/mol;

R<sub>f</sub> (95:5 dichloromethane/MeOH) = 0.3;

Melting Point: 141–142 °C (ethyl acetate) (Lit.:<sup>[155]</sup> 135–136 °C);

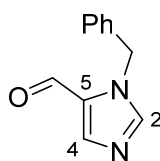
<sup>1</sup>H NMR (DMSO-d<sub>6</sub>, 400 MHz): δ (ppm) = 7.67 (s, 1H, **2-H**), 7.37–7.725 (m, 3H, **Ph**), 7.19–7.14 (m, 2H, **Ph**), 6.82 (s, 1H, **4-H**), 5.23 (s, 2H, N-CH<sub>2</sub>-), 4.31 (s, 2H, -CH<sub>2</sub>-OH);

<sup>13</sup>C NMR (DMSO-d<sub>6</sub>, 101 MHz): δ (ppm) = 138.4 (CH, C-**2**), 137.6 (C<sub>q</sub>, C-**5**), 131.6 (C<sub>q</sub>, **Ph**), 128.6 (CH, **Ph**), 127.5 (CH, C-**4**), 127.4 (CH, **Ph**), 127.0 (CH, **Ph**), 52.8 (CH<sub>2</sub>, -CH<sub>2</sub>-OH), 47.5 (CH<sub>2</sub>, N-CH<sub>2</sub>-);

IR (ATR, cm<sup>-1</sup>): 3954 (br), 2831, 1666, 1572, 1504, 1491, 1437, 1255, 1107, 1020, 741, 701, 616.

The spectral data correspond to literature data.<sup>[155]</sup>

### Synthesis of 1-Benzyl-1*H*-imidazole-5-Carbaldehyde (**40**)<sup>[155]</sup>



**40**

(1-Benzyl-1*H*-imidazol-5-yl)methanol (2.00 g, 10.6 mmol) was dissolved in 1,4-dioxane (110 mL) and activated MnO<sub>2</sub> (4.62 g, 53.1 mmol) was added. The mixture was refluxed overnight, then filtered through a pad of celite. The solvent of the filtrate was removed under reduced pressure to yield the product **40** as a slightly yellow oily solid (1.81 g, 9.73 mmol, 92%).

Formula: C<sub>11</sub>H<sub>10</sub>N<sub>2</sub>O;

MW: 186.21 g/mol;

R<sub>f</sub> (95:5 dichloromethane/MeOH) = 0.6;

<sup>1</sup>H NMR (CDCl<sub>3</sub>, 400 MHz): δ (ppm) = 9.77 (s, 1H, **CHO**), 7.83 (s, 1H, **4-H**), 7.69 (s, 1H, **2-H**), 7.37–7.28 (m, 3H, **Ph**), 7.22–7.19 (m, 2H, **Ph**), 5.52 (s, 2H, -CH<sub>2</sub>-);

## Experimental

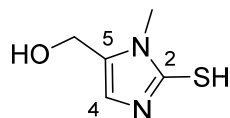
$^{13}\text{C}$  NMR ( $\text{CDCl}_3$ , 101 MHz):  $\delta$  (ppm) = 179.2 (CH, **CHO**), 143.8 (CH, **C-4**), 143.7 (CH, **C-2**), 135.6 ( $\text{C}_q$ , **Ph**), 131.0 ( $\text{C}_q$ , **C-5**), 129.2 (CH, **Ph**), 128.8 (CH, **Ph**), 127.7 (CH, **Ph**), 50.2 ( $\text{CH}_2$ , **-CH<sub>2</sub>-**);

IR (ATR,  $\text{cm}^{-1}$ ): 3100, 2921, 2823, 1668, 1537, 1496, 1481, 1455, 1427, 1337, 761, 727, 692, 650.

The spectral data correspond to literature data.<sup>[155]</sup>

### 7.2.3 Synthesis of 1-Methyl-1*H*-imidazole-5-carbaldehyde (**37**)

#### Marckwald Synthesis of (2-Mercapto-1-Methyl-1*H*-Imidazol-5-yl)methanol (**75**)



**75**

Methylammonium chloride (9.29 g, 138 mmol), dihydroxyacetone (9.53 g, 106 mmol) and potassium thiocyanate (15.4 g, 159 mmol) were suspended in a mixture of *n*-butanol (75 mL) and glacial acetic acid (12.7 g, 212 mmol, 12.1 mL). After stirring for 3 d at RT and the solid was isolated by filtration. The filter cake was washed with diethylether (44 mL). Drying of the filter cake in vacuo yielded the product **75** as a white solid (10.57 g, 73.3 mmol, 69%).

Formula:  $\text{C}_5\text{H}_8\text{N}_2\text{OS}$ ;

MW: 144.19 g/mol;

$R_f$  (95:5 dichloromethane/MeOH) = 0.2;

Melting Point: 228–229 °C (diethyl ether) (Lit.:<sup>[82]</sup> 203–206 °C, solvent not reported);

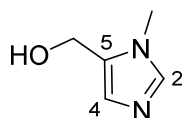
$^1\text{H}$  NMR ( $\text{DMSO-d}_6$ , 400 MHz):  $\delta$  (ppm) = 11.88 (br. s, 1H, **SH**), 6.78 (s, 1H, **4-H**), 5.21 (br. s, 1H, **OH**), 4.32 (s, 2H, **-CH<sub>2</sub>-OH**), 3.44 (s, 3H, **N-CH<sub>3</sub>**);

$^{13}\text{C}$  NMR ( $\text{DMSO-d}_6$ , 101 MHz):  $\delta$  (ppm) = 161.7 ( $\text{C}_q$ , **C-2**), 130.5 ( $\text{C}_q$ , **C-5**), 112.2 (CH, **C-4**), 53.0 ( $\text{CH}_2$ , **-CH<sub>2</sub>-OH**), 30.6 ( $\text{CH}_3$ , **N-CH<sub>3</sub>**);

IR (ATR,  $\text{cm}^{-1}$ ): 3105 (br), 2927, 1620, 1480, 1445, 1294, 1255, 1010, 805, 657, 626.

The spectral data correspond to literature data.<sup>[82]</sup>

#### Synthesis of (1-Methyl-1*H*-Imidazol-5-yl)methanol (**77**)<sup>[99a]</sup>



**77**

## Experimental

(2-Mercapto-1-methyl-1*H*-imidazol-5-yl)methanol (**75**) (3.33 g, 23.1 mmol) was dissolved in 20% (v/v) glacial acetic acid (60 mL). A 35% solution of hydrogen peroxide (162 mmol, 14.2 mL) was added dropwise, then the reaction was stirred overnight at RT. At 0 °C, sodium sulfite (21.4 g) and water (85 mL) were added portionwise. After additional stirring for 1 h at RT, the pH of the solution was adjusted to pH>8 by addition of aqueous ammonia. The solution was continuously extracted with ethyl acetate for 30 h. The layers were separated and the organic layer was dried over Na<sub>2</sub>SO<sub>4</sub>. The solvent was evaporated under reduced pressure to yield the product as a slightly yellow oil (2.42 g, 21.6 mmol, 94%).

Formula: C<sub>5</sub>H<sub>8</sub>N<sub>2</sub>O;

MW: 112.13 g/mol;

R<sub>f</sub> (95:5 dichloromethane/MeOH) = 0.1;

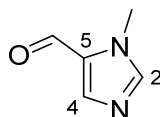
<sup>1</sup>H NMR (CDCl<sub>3</sub>, 400 MHz): δ (ppm) = 7.43 (s, 1H, **2-H**), 6.92 (s, 1H, **4-H**), 4.62 (s, 2H, **-CH<sub>2</sub>-OH**), 3.71 (s, 3H, **N-CH<sub>3</sub>**);

<sup>13</sup>C NMR (CDCl<sub>3</sub>, 101 MHz): δ (ppm) = 139.1 (CH, **C-2**), 131.5 (C<sub>q</sub>, **C-5**), 128.3 (CH, **C-4**), 54.3 (CH<sub>2</sub>, **-CH<sub>2</sub>-OH**), 31.8 (CH<sub>3</sub>, **N-CH<sub>3</sub>**);

IR (ATR, cm<sup>-1</sup>): 3169 (br), 3114, 2936, 2859, 1511, 1244, 1209, 1013, 834, 753, 664, 618.

The spectral data correspond to literature data.<sup>[82]</sup>

### Synthesis of 1-Methyl-1*H*-Imidazole-5-Carbaldehyde (**37**)<sup>[82]</sup>



**37**

(1-Methyl-1*H*-imidazol-5-yl)methanol (2.42 g, 21.6 mmol) was dissolved in 1,4-dioxane (100 mL) and activated MnO<sub>2</sub> (9.38 g, 108 mmol) was added. After refluxing for 4 h, the mixture was filtered through a pad of celite. The filtrate was evaporated under reduced pressure to yield the product as a slightly brown oil (1.82 g, 16.5 mmol, 77%).

Formula: C<sub>5</sub>H<sub>7</sub>N<sub>2</sub>O;

MW: 110.12 g/mol;

R<sub>f</sub> (95:5 dichloromethane/MeOH) = 0.4;

<sup>1</sup>H NMR (CDCl<sub>3</sub>, 400 MHz): δ (ppm) = 9.76 (s, 1H, **CHO**), 7.78 (br. s, 1H, **2-H**), 7.63 (br. s, 1H, **4-H**), 3.94 (s, 3H, **-CH<sub>3</sub>**);

## Experimental

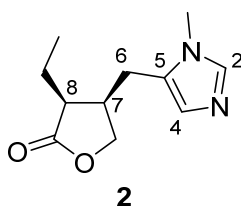
$^{13}\text{C}$  NMR ( $\text{CDCl}_3$ , 101 MHz):  $\delta$  (ppm) = 179.6 (CH, **CHO**), 144.2 (CH, C-**4**), 143.2 (CH, C-**2**), 131.7 ( $\text{C}_q$ , C-**5**), 34.3 ( $\text{CH}_3$ , -**CH**<sub>3</sub>);

IR (ATR,  $\text{cm}^{-1}$ ): 3087, 2826, 1657, 1434, 1335, 772, 654.

The spectral data correspond to literature data.<sup>[82]</sup>

## 7.3 Synthesis of Pilocarpine Analogues as Orthosteric Moieties and References

### 7.3.1 Generation of Pilocarpine as a free base (**2**)<sup>[81]</sup>



Pilocarpine nitrate (**2** nitrate) (520 mg, 1.92 mmol) was dissolved in saturated aqueous sodium hydrogencarbonate solution (10 mL). The solution was extracted five times with dichloromethane. The combined organic layers were dried over  $\text{MgSO}_4$  and evaporated under reduced pressure to yield the product as a colourless oil (321 mg, 1.54 mmol, 80%).

Formula:  $\text{C}_{11}\text{H}_{16}\text{N}_2\text{O}_2$ ;

MW: 208.26 g/mol;

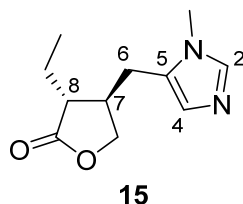
$R_f$  (95:5 dichloromethane/MeOH) = 0.3;

$^1\text{H}$  NMR ( $\text{CDCl}_3$ , 400 MHz):  $\delta$  (ppm) = 7.45 (s, 1H, **2-H**), 6.80 (s, 1H, **4-H**), 4.19 (dd,  $J = 9.4, 5.4$  Hz, 1H, -**CH**<sub>2</sub>-O-), 4.09 (dd,  $J = 9.4, 2.3$  Hz, 1H, -**CH**<sub>2</sub>-O-), 3.56 (s, 3H, N-**CH**<sub>3</sub>), 2.88–2.79 (m, 1H, **7-H**), 2.71–2.60 (m, 2H, **8-H**, **6-H**), 2.41 (dd,  $J = 15.5, 12.0$  Hz, 1H, **6-H**), 1.96–1.85 (m, 1H, -**CH**<sub>2</sub>-**CH**<sub>3</sub>), 1.63–1.51 (m, 1H, -**CH**<sub>2</sub>-**CH**<sub>3</sub>), 1.11 (t,  $J = 7.4$  Hz, 3H, -**CH**<sub>2</sub>-**CH**<sub>3</sub>);

$^{13}\text{C}$  NMR ( $\text{CDCl}_3$ , 101 MHz):  $\delta$  (ppm) = 178.0 ( $\text{C}_q$ , **C=O**), 138.4 (CH, C-**2**), 128.8 ( $\text{C}_q$ , C-**5**), 127.0 (CH, C-**4**), 70.0 ( $\text{CH}_2$ , -**CH**<sub>2</sub>-O-), 45.0 (CH, C-**8**), 37.4 (CH, C-**7**), 31.5 ( $\text{CH}_3$ , N-**CH**<sub>3</sub>), 21.5 ( $\text{CH}_2$ , C-**6**), 18.5 ( $\text{CH}_2$ , -**CH**<sub>2</sub>-**CH**<sub>3</sub>), 12.4 ( $\text{CH}_3$ , -**CH**<sub>2</sub>-**CH**<sub>3</sub>);

IR (ATR,  $\text{cm}^{-1}$ ): 2961, 1763, 1504, 1447, 1413, 1257, 1070, 1009, 789, 702, 685, 662.

The spectral data correspond to literature data.<sup>[81, 95]</sup>

7.3.2 Preparation of Isopilocarpine (**15**)Epimerisation of Pilocarpine<sup>[111a]</sup>

The free base of pilocarpine (**2**) (61.0 mg, 293  $\mu\text{mol}$ ) was dissolved in dry methanol (10 mL) and sodium methoxide (25% solution in MeOH, 73.7  $\mu\text{L}$ , 322  $\mu\text{mol}$ ) was added. The reaction was refluxed overnight, then quenched by addition of diluted hydrochloric acid. Saturated aqueous  $\text{NaHCO}_3$  solution was added until  $\text{pH} > 8$ , and the mixture was extracted five times with dichloromethane. The combined organic layers were dried over  $\text{MgSO}_4$  and evaporated under reduced pressure to yield the crude product. The product was purified by preparative HPLC (method I, Chapter 7.1.4) to obtain a colourless oil (28.3 mg, 136  $\mu\text{mol}$ , 46%).

Formula:  $\text{C}_{11}\text{H}_{16}\text{N}_2\text{O}_2$ ;

MW: 208.26 g/mol;

$R_f$  (95:5 dichloromethane/MeOH) = 0.3;

$^1\text{H}$  NMR ( $\text{CDCl}_3$ , 400 MHz):  $\delta$  (ppm) = 7.42 (s, 1H, **2-H**), 6.81 (s, 1H, **4-H**), 4.41 (dd,  $J = 9.3, 7.2$  Hz, 1H, **-CH<sub>2</sub>-O-**), 3.92 (dd,  $J = 9.3, 6.7$  Hz, 1H, **-CH<sub>2</sub>-O-**), 3.58 (s, 3H, **N-CH<sub>3</sub>**), 2.84 (dd,  $J = 15.2, 5.4$  Hz, 1H, **6-H**), 2.71–2.56 (m, 2H, **7-H, 6-H**), 2.32–2.26 (m, 1H, **8-H**), 1.84–1.67 (m, 2H, **-CH<sub>2</sub>-CH<sub>3</sub>**), 1.04 (t,  $J = 7.4$  Hz, 3H, **-CH<sub>2</sub>-CH<sub>3</sub>**);

$^{13}\text{C}$  NMR ( $\text{CDCl}_3$ , 101 MHz):  $\delta$  (ppm) = 178.4 ( $\text{C}_q$ , **C=O**), 138.5 (CH, **C-2**), 128.3 ( $\text{C}_q$ , **C-5**), 127.3 ( $\text{C}_q$ , **C-4**), 71.2 ( $\text{CH}_2$ , **-CH<sub>2</sub>-O-**), 46.7 (CH, **C-8**), 39.3 (CH, **C-7**), 31.5 ( $\text{CH}_3$ , **N-CH<sub>3</sub>**), 27.6 ( $\text{CH}_2$ , **C-6**), 22.6 ( $\text{CH}_2$ , **-CH<sub>2</sub>-CH<sub>3</sub>**), 11.3 ( $\text{CH}_3$ , **-CH<sub>2</sub>-CH<sub>3</sub>**);

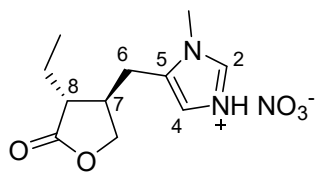
IR (ATR,  $\text{cm}^{-1}$ ): 2967, 1750, 1573, 1508, 1459, 1379, 1227, 1174, 1011, 737, 706, 664, 625.

The spectral data correspond to literature data.<sup>[81, 95]</sup>

qNMR purity ( $\text{CDCl}_3$ , external standard: 3,4,5-trichloropyridine): 86%; major impurity: 6% pilocarpine.

## Experimental

### Preparation of Isopilocarpine Nitrate<sup>[143]</sup>



**15** nitrate

Isopilocarpine (**15**) (580 mg, 2.78  $\mu$ mol) was dissolved in few methanol as possible. Nitric acid (0.13 mL, 2.92 mmol) was added. The product precipitated as a colourless solid by addition of diethyl ether. The suspension was kept at RT for 30 min, then cooled to  $-20^{\circ}\text{C}$  overnight. The solid was filtered and washed with cold methanol. The solid was recrystallised in ethanol to yield colourless needles (597 mg, 2.20  $\mu$ mol, 79%).

Formula:  $\text{C}_{11}\text{H}_{17}\text{N}_3\text{O}_5$ ;

MW: 271.27 g/mol;

$R_f$  (95:5 dichloromethane/MeOH) = 0;

Melting point: decomposition at  $153\text{--}156^{\circ}\text{C}$ ;

$^1\text{H}$  NMR ( $\text{D}_2\text{O}$ , 400 MHz):  $\delta$  (ppm) = 8.66 (s, 1H, **2-H**), 7.36 (s, 1H, **4-H**), 4.58 (dd,  $J = 9.2, 7.6$  Hz, 1H, **-CH<sub>2</sub>-O-**), 4.13 (dd,  $J = 9.2, 7.2$  Hz, 1H, **-CH<sub>2</sub>-O-**), 3.87 (s, 3H, **N-CH<sub>3</sub>**), 3.09 (dd,  $J = 15.8, 6.2$  Hz, 1H, **6-H**), 3.03–2.84 (m, 2H, **7-H**, **6-H**), 2.65–2.59 (m, 1H, **8-H**), 1.78–1.70 (m, 2H, **-CH<sub>2</sub>-CH<sub>3</sub>**), 0.98 (t,  $J = 7.5$  Hz, 3H, **-CH<sub>2</sub>-CH<sub>3</sub>**);

$^{13}\text{C}$  NMR ( $\text{D}_2\text{O}$ , 101 MHz):  $\delta$  (ppm) = 182.7 ( $\text{C}_q$ , **C=O**), 135.3 (CH, **C-2**), 132.1 ( $\text{C}_q$ , **C-5**), 116.9 ( $\text{C}_q$ , **C-4**), 72.0 ( $\text{CH}_2$ , **-CH<sub>2</sub>-O-**), 46.3 (CH, **C-7**), 37.3 (CH, **C-8**), 33.1 ( $\text{CH}_3$ , **N-CH<sub>3</sub>**), 25.6 ( $\text{CH}_2$ , **C-6**), 21.5 ( $\text{CH}_2$ , **-CH<sub>2</sub>-CH<sub>3</sub>**), 9.95 ( $\text{CH}_3$ , **-CH<sub>2</sub>-CH<sub>3</sub>**);

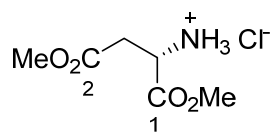
IR (ATR,  $\text{cm}^{-1}$ ): 3106, 3064, 2905, 1776, 1608, 1556, 1476, 1383, 1313, 1169, 757, 715, 634, 620;

HPLC purity (chiral method A): 96%. The remaining 4% of impurity is pilocarpine;

qNMR purity ( $\text{D}_2\text{O}$ , internal standard: maleic acid): 89%.



## 7.3.3 Attempted Stereospecific Synthesis of Pilocarpine and Pilosinine

Synthesis of Dimethyl *L*-Aspartate Hydrochloride (**46**)<sup>[90]</sup>**46**

Thionyl chloride (1.97 g, 16.5 mmol, 1.20 mL) was added dropwise to a suspension of *L*-aspartic acid (**44**) (1.00 g, 7.51 mmol) in dry methanol (6 mL) at 0 °C. The ice bath was removed, and the solution was allowed to stir at RT for 19 h and was then concentrated in vacuo. The residual oil was triturated with diethyl ether and the resulting white crystalline solid was filtered, washed with cold diethyl ether, and dried to give 1.28 g (7.51 mmol, 87%) of dimethyl *L*-aspartate hydrochloride.

Formula: C<sub>6</sub>H<sub>12</sub>ClNO<sub>4</sub>;

MW: 197.62 g/mol;

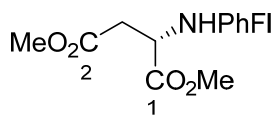
Melting point: 111–113 °C (diethyl ether) (Lit.:<sup>[90]</sup> 114–115 °C, diethyl ether);

<sup>1</sup>H NMR (D<sub>2</sub>O, 400 MHz): δ (ppm) = 4.53 (t, 1H, *J* = 5.3 Hz, -CH-), 3.89 (s, 3H, C<sup>1</sup>O<sub>2</sub>Me), 3.80 (s, 3H, C<sup>2</sup>O<sub>2</sub>Me), 3.27–3.15 (m, 2H, -CH<sub>2</sub>-);

<sup>13</sup>C NMR (D<sub>2</sub>O, 101 MHz): δ (ppm) = 171.6 (C<sub>q</sub>, CO<sub>2</sub>Me), 169.4 (C<sub>q</sub>, CO<sub>2</sub>Me), 53.9 (CH<sub>3</sub>, C<sup>1</sup>O<sub>2</sub>Me), 52.9 (CH<sub>3</sub>, C<sup>2</sup>O<sub>2</sub>Me), 49.2 (CH, -CH-), 33.6 (CH<sub>2</sub>, -CH<sub>2</sub>-);

IR (ATR, cm<sup>-1</sup>): 2859 (br), 1764, 1733, 1594, 1554, 1527, 1204, 1179, 1162, 990, 845, 762.

The spectral data correspond to literature data.<sup>[90]</sup>

Synthesis of Dimethyl *L*-*N*-(9-Phenyl-9*H*-Fluoren-9-yl)-Aspartate (**48**)<sup>[90]</sup>**48**

To a stirred suspension of dimethyl *L*-aspartate hydrochloride (**46**) (1.00 g, 5.06 mmol) in dry acetonitrile (8 mL) were added anhydrous lead nitrate (1.42 g, 4.30 mmol, 0.85 eq.) and anhydrous potassium phosphate (2.15 g, 10.12 mmol), followed by 9-bromo-9-phenylfluorene (2.03 g, 6.33 mmol) in dry CH<sub>3</sub>CN (40 mL) at RT. The suspension was stirred for 16 h. Then, the reaction mixture was filtered through celite and the inorganic residue was washed with CHCl<sub>3</sub>. The combined filtrates were evaporated, and the residue was partitioned between 5% aqueous citric acid (20 mL) and Et<sub>2</sub>O (40 mL). The organic layer was dried over MgSO<sub>4</sub>, the solvents were evaporated, and the thick yellow

## Experimental

residue was purified by column chromatography (silica, hexane/EtOAc 8:1) to leave dimethyl *L-N*-(9-phenylfluoren-9-yl)-aspartate (1.62 g, 4.04 mmol, 80%).

Formula: C<sub>25</sub>H<sub>23</sub>NO<sub>4</sub>;

MW: 401.45 g/mol;

R<sub>f</sub> (80:10 cyclohexane/ethyl acetate) = 0.2;

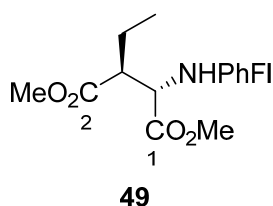
<sup>1</sup>H NMR (CDCl<sub>3</sub>, 400 MHz): δ (ppm) = 7.71–7.66 (m, 2H, **PhFI**), 7.40–7.16 (m, 11H, **PhFI**), 3.66 (s, 3H, C<sup>1</sup>O<sub>2</sub>Me), 3.36 (s, 3H, C<sup>2</sup>O<sub>2</sub>Me), 3.03 (dd, *J* = 6.7, 5.5 Hz, 1H, **CH**), 2.53 (dd, *J* = 6.7, 15.1 Hz, 1H, **CH<sub>2</sub>**), 2.37 (dd, *J* = 5.5, 15.1 Hz, 1H, **CH<sub>2</sub>**);

<sup>13</sup>C NMR (CDCl<sub>3</sub>, 101 MHz): δ (ppm) = 174.8 (C<sub>q</sub>, CO<sub>2</sub>Me), 171.1 (C<sub>q</sub>, CO<sub>2</sub>Me), 148.7, 148.5, 144.5, 141.4, 140.1 (5C<sub>q</sub>, **PhFI**), 128.6, 128.6, 128.4, 127.9, 127.7, 127.4, 126.2, 126.1, 125.7, 120.2, 120.0 (11CH, **PhFI**), 73.0 (C<sub>q</sub>, **PhFI**), 53.0 (CH, **CH**), 52.1 (CH<sub>3</sub>, CO<sub>2</sub>Me), 51.9 (CH<sub>3</sub>, CO<sub>2</sub>Me), 39.9 (CH<sub>2</sub>, **CH<sub>2</sub>**);

IR (ATR, cm<sup>-1</sup>): 3000 (br), 2951, 1734, 1436, 1369, 1163, 753, 733, 698.

The spectral data correspond to literature data.<sup>[90]</sup>

### Synthesis of Dimethyl (2*S*,3*S*)-Ethyl-((9-Phenyl-9*H*-fluoren-9-yl)amino)succinate (**49**)<sup>[82]</sup>



At –84 °C, lithium bis(trimethylsilyl)amide (1.0 M in THF, 874 mg, 5.22 mmol, 5.22 mL) was added to a stirred solution of dimethyl *L-N*-(9-phenyl-9*H*-fluoren-9-yl)-aspartate (**48**) (1.91 g, 4.75 mmol) in dry THF (80 mL). The yellow solution was stirred for 45 min at –84 °C. Then, ethyl trifluoromethanesulfonate (930 mg, 5.22 mmol, 642 μL) was added in one portion and the reaction mixture was stirred for 10 min at –84 °C before it was allowed to warm up to RT. The reaction mixture was quenched with 1 M aqueous phosphoric acid and was extracted three times with diethyl ether. The combined organic layers were washed with saturated aqueous sodium chloride and dried over MgSO<sub>4</sub>. The solvent was evaporated, and the residue was crystallised from methanol to provide **49** (457 mg, 1.06 mmol, 22%) as colourless crystals. The mother liquor was evaporated, and the residue was separated by column chromatography (silica, cyclohexane/ethyl acetate 95:5). This provided a diastereomeric mixture of the product (398 mg, 0.93 mmol, 20%) as a yellow oil and starting material **48** (526 mg, 1.42 mmol, 30%) was recovered.

Formula: C<sub>27</sub>H<sub>27</sub>NO<sub>4</sub>;

## Experimental

MW: 429.52 g/mol;

R<sub>f</sub> (80:10 cyclohexane/ethyl acetate) = 0.2;

Melting point: 134–136 °C (MeOH) (Lit.:<sup>[82]</sup> 138–139 °C, MeOH);

Specific optical rotation:  $[\alpha]_D^{25} = -284^\circ$  (4.84 mg/mL CHCl<sub>3</sub>) (Lit.<sup>[82]</sup>:  $-302^\circ$ , CHCl<sub>3</sub>);

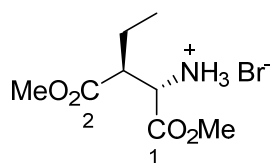
<sup>1</sup>H NMR (CDCl<sub>3</sub>, 400 MHz):  $\delta$  (ppm) = 7.70–7.65 (m, 2H, **PhFI**), 7.43–7.18 (m, 11H, **PhFI**), 3.54 (s, 3H, C<sup>1</sup>O<sub>2</sub>**Me**), 3.28 (s, 3H, C<sup>2</sup>O<sub>2</sub>**Me**), 2.82 (d,  $J = 6.3$  Hz, 1H, -NH-**CH**-), 2.46 (m, 1H, -**CH**-Et), 1.76–1.55 (m, 2H, **CH**<sub>2</sub>), 0.73 (t,  $J = 7.2$  Hz, 3H, -CH<sub>2</sub>-**CH**<sub>3</sub>);

<sup>13</sup>C NMR (CDCl<sub>3</sub>, 101 MHz):  $\delta$  (ppm) = 174.8 (C<sub>q</sub>, **CO**<sub>2</sub>**Me**), 173.5 (C<sub>q</sub>, **CO**<sub>2</sub>**Me**), 147.8, 147.3, 144.5, 141.4, 140.2 (5C<sub>q</sub>, **PhFI**), 128.6, 128.6, 128.5, 128.0, 127.5, 127.4, 126.6, 126.2, 125.9, 120.1, 120.1 (11CH, **PhFI**), 73.0 (C<sub>q</sub>, **PhFI**), 57.0 (CH, -**CH**-NH-), 52.4 (CH, -**CH**-Et), 51.8 (CH<sub>3</sub>, **CO**<sub>2</sub>**Me**), 51.8 (CH<sub>3</sub>, **CO**<sub>2</sub>**Me**), 21.2 (CH<sub>2</sub>, **CH**<sub>2</sub>), 12.0 (CH<sub>3</sub>, -CH<sub>2</sub>-**CH**<sub>3</sub>);

IR (ATR, cm<sup>-1</sup>): 3049, 2949, 2873, 1735, 1440, 1261, 1164, 1119, 988, 737, 702.

The spectral data correspond to literature data.<sup>[82]</sup>

### Synthesis of Dimethyl (2*S*,3*S*)-2-Amino-3-Ethylsuccinate Hydrobromide(**50**)<sup>[82]</sup>



**49** (587 mg, 1.37 mmol) was suspended in methanol (8 mL). The mixture was degassed by bubbling argon through the suspension for 10 min. A 2:1 (v:v) mixture of acetic acid and 48% aqueous hydrobromic acid (0.8 mL) was added, followed by 40 mg of 10% palladium on activated charcoal. The mixture was hydrogenated at 4 bar and RT for 2.5 h. The reaction mixture was filtered over cotton and the solvents were removed. The residue was suspended in water and the remaining solid removed by filtration over cotton. The solvent of the filtrate was removed under reduced pressure to yield an orange–brown oil (325 mg, 1.20 mmol, 88%).

Formula: C<sub>8</sub>H<sub>16</sub>BrNO<sub>4</sub>;

MW: 270.12 g/mol;

R<sub>f</sub> (80:10 cyclohexane/ethyl acetate) = 0;

<sup>1</sup>H NMR (D<sub>2</sub>O, 400 MHz):  $\delta$  (ppm) = 4.50 (d,  $J = 4.4$  Hz, 1H, -**CH**-NH<sub>3</sub><sup>+</sup>), 3.89 (s, 3H, C<sup>1</sup>O<sub>2</sub>**Me**), 3.81 (s, 3H, C<sup>2</sup>O<sub>2</sub>**Me**), 3.14–3.08 (m, 1H, -**CH**-Et), 1.93–1.70 (m, 2H, **CH**<sub>2</sub>), 1.02 (t,  $J = 7.3$  Hz, 3H, -CH<sub>2</sub>-**CH**<sub>3</sub>);

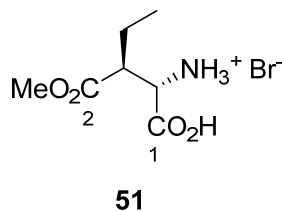
## Experimental

$^{13}\text{C}$  NMR ( $\text{D}_2\text{O}$ , 101 MHz):  $\delta$  (ppm) = 174.7 ( $\text{C}_q$ ,  $\text{C}^2\text{O}_2\text{Me}$ ), 169.7 ( $\text{C}_q$ ,  $\text{C}^1\text{O}_2\text{Me}$ ), 54.5 ( $\text{CH}_3$ ,  $\text{C}^1\text{O}_2\text{Me}$ ), 53.7 ( $\text{CH}$ ,  $-\text{CH}-\text{NH}_3^+$ ), 53.6 ( $\text{CH}_3$ ,  $\text{C}^2\text{O}_2\text{Me}$ ), 47.7 ( $\text{CH}$ ,  $\text{CH}-\text{Et}$ ), 22.1 ( $\text{CH}_2$ ,  $-\text{CH}_2-\text{CH}_3$ ), 11.7 ( $\text{CH}_3$ ,  $\text{CH}_2-\text{CH}_3$ );

IR (ATR,  $\text{cm}^{-1}$ ): 3368 (br), 2957, 1723, 1719, 1617, 1498, 1439, 1245, 1087, 1001, 685.

The spectral data correspond to literature data.<sup>[82]</sup>

### Synthesis of (2S,3S)-2-amino-3-(methoxycarbonyl)pentanoic acid Hydrobromide (51)<sup>[82]</sup>



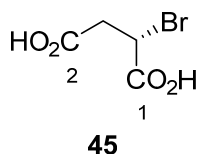
**50** (243 mg, 1.07 mmol) was dissolved in a mixture of water (5 mL) and methanol (5 mL). Basic copper carbonate (1.43 g, 6.45 mmol) was added and the suspension was stirred at RT for 7 days.  $\text{H}_2\text{S}$  was generated by addition of dilute aqueous HCl to an aqueous solution of  $\text{Na}_2\text{S}$  and bubbled through the reaction mixture until the supernatant was colourless. The mixture was filtered and washed with water/MeOH 1:2. Evaporation of the solvent left an orange–brown oil which consisted of mainly the desired product (3 mg, 17.1  $\mu\text{mol}$ , 16%).

Formula:  $\text{C}_7\text{H}_{13}\text{NO}_4$ ;

MW: 175.18 g/mol;

$^1\text{H}$  NMR ( $\text{D}_2\text{O}$ , 400 MHz):  $\delta$  (ppm) = 3.76 (s, 3H,  $\text{CO}_2\text{Me}$ ), 3.63 (d,  $J = 6.0$  Hz, 1H,  $\text{CH}-\text{NH}_2$ ), 2.75 (ddd,  $J = 10.2, 6.0, 4.3$  Hz, 1H,  $\text{CH}-\text{Et}$ ), 1.77–1.51 (m, 2H,  $\text{CH}_2-\text{CH}_3$ ), 0.93 (t,  $J = 7.4$  Hz, 3H,  $\text{CH}_3$ ).

### Synthesis of (S)-2-Bromo-Succinate (45)<sup>[84]</sup>



*L*-Aspartic acid (2.15 g, 16.2 mmol) was dissolved in a mixture of water (35 mL) and sulfuric acid (5.3 mL). KBr (7.84 g, 65.9 mmol) was added. The reaction mixture was cooled to  $-10^\circ\text{C}$  and sodium nitrite (1.82 g, 26.4 mmol) was added slowly. The mixture was stirred for 5 h while warming to RT in the ice bath. The reaction mixture was extracted three times with ethyl acetate and the combined organic layers were dried over  $\text{MgSO}_4$ . The solvents were removed under reduced pressure to provide the product as a white solid residue (2.59 g, 13.2 mmol, 81%).

## Experimental

Formula: C<sub>4</sub>H<sub>5</sub>BrO<sub>4</sub>;

MW: 196.98 g/mol;

R<sub>f</sub> (50:50 cyclohexane/ethyl acetate) = 0.4;

Melting point: decomposition at 158–160 °C (Lit.:<sup>[159]</sup> 157–158 °C);

Specific optical rotation:  $[\alpha]_D^{25} = -39.9^\circ$  (61.3 mg/mL H<sub>2</sub>O) (Lit.:<sup>[85]</sup>  $-39.6^\circ$  (184 mg/mL H<sub>2</sub>O));

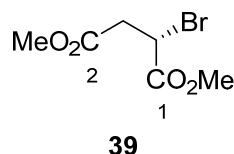
<sup>1</sup>H NMR (CD<sub>3</sub>OD, 400 MHz):  $\delta$  (ppm) = 4.55 (1H, dd,  $J = 6.2, 8.7$  Hz, -CH-Br), 3.18 (1H, dd,  $J = 8.7, 17.2$  Hz, CH<sub>2</sub>), 2.94 (1H, dd,  $J = 6.2, 17.2$  Hz, CH<sub>2</sub>);

<sup>13</sup>C NMR (CD<sub>3</sub>OD, 101 MHz):  $\delta$  (ppm) = 173.2 (C<sub>q</sub>, C<sup>2</sup>O<sub>2</sub>H), 172.3 (C<sub>q</sub>, C<sup>1</sup>O<sub>2</sub>H), 40.8 (CH, -CH-Br), 40.2 (CH<sub>2</sub>, CH<sub>2</sub>);

IR (ATR, cm<sup>-1</sup>): 2904, 1696, 1403, 1282, 1184, 932, 648.

The spectral data correspond to literature data.<sup>[84]</sup>

### Synthesis of (S)-Dimethyl 2-Bromosuccinate (**39**)<sup>[90]</sup>



(S)-2-Bromosuccinic acid (**45**) (2.80 g, 14.2 mmol) was dissolved in methanol (30 mL). Thionyl chloride (5.07 g, 42.6 mmol, 3.10 mL) was added at 0 °C and the reaction mixture was stirred at RT for 6 h. Water was added and most of the organic solvent was removed under reduced pressure. The remaining aqueous solution was extracted with ethyl acetate. The combined organic layers were washed with a solution of NaHCO<sub>3</sub>. After drying the organic layer over Na<sub>2</sub>SO<sub>4</sub>, the solvent was evaporated under reduced pressure to leave the product as a colourless oil (2.73 g, 12.1 mmol, 85%).

Formula: C<sub>6</sub>H<sub>9</sub>BrO<sub>4</sub>;

MW: 225.04 g/mol;

R<sub>f</sub> (30:10 cyclohexane/ethyl acetate) = 0.3;

Specific optical rotation:  $[\alpha]_D^{25} = -65.2^\circ$  (402 mg/mL CHCl<sub>3</sub>) (Lit.:<sup>[85]</sup>  $-65.6^\circ$ , solvent not reported);

<sup>1</sup>H NMR (CDCl<sub>3</sub>, 400 MHz):  $\delta$  (ppm) = 4.58 (1H, dd,  $J = 6.2, 8.8$  Hz, CH), 3.81 (3H, s, C<sup>1</sup>O<sub>2</sub>Me), 3.72 (3H, s, C<sup>2</sup>O<sub>2</sub>Me), 3.29 (1H, dd,  $J = 8.8, 17.2$  Hz, CH<sub>2</sub>), 3.00 (1H, dd,  $J = 6.2, 17.2$  Hz, CH<sub>2</sub>);

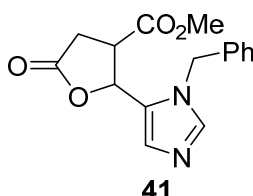
## Experimental

$^{13}\text{C}$  NMR ( $\text{CDCl}_3$ , 101 MHz):  $\delta$  (ppm) = 170.2 ( $\text{C}_q$ ,  $\text{C}^2\text{O}_2\text{Me}$ ), 169.7 ( $\text{C}_q$ ,  $\text{C}^1\text{O}_2\text{Me}$ ), 53.4 ( $\text{CH}_3$ ,  $\text{C}^1\text{O}_2\text{Me}$ ), 52.3 ( $\text{CH}_3$ ,  $\text{C}^2\text{O}_2\text{Me}$ ), 39.7 ( $\text{CH}_2$ ,  $\text{CH}_2$ ), 37.9 ( $\text{CH}$ ,  $\text{CH}$ );

IR (ATR,  $\text{cm}^{-1}$ ): 2956, 1732, 1437, 1158, 999, 621.

The spectral data correspond to literature data.<sup>[160]</sup>

### Lactone Formation by a Reformatsky Reaction<sup>[82]</sup>



Silver acetate (20 mg) was dissolved in acetic acid (40 mL). At reflux, coarse zinc powder (20.1 g) was added. Then the mixture was immediately cooled to 0 °C. The liquid was decanted, and the residue was washed several times with predried diethylether. The zinc/silver couple was dried in vacuo.<sup>[89]</sup>

The zinc/silver couple (21.8 mg, 333  $\mu\text{mol}$ ) and copper(I)-bromide (4.4 mg, 31.1  $\mu\text{mol}$ , 0.10 eq.) were mixed in dry THF or diethylether (1 mL). At RT, dimethylaluminium chloride (1M in hexanes, 267  $\mu\text{mol}$ , 267  $\mu\text{L}$ ) was added and the mixture was stirred for 20 min. The suspension was cooled to -8 °C and a solution of both aldehyde (**40/42**) (41.4 mg, 222  $\mu\text{mol}$ ) and 2-bromodimethylsuccinate (**39**) (50.0 mg, 222  $\mu\text{mol}$ ) in dry THF (1 mL) was added slowly. After stirring for 2 h, the mixture was warmed to RT and stirred overnight. The reaction was stopped by addition of a 1:1 mixture of methanol/water at -8 °C. The mixture was acidified with dilute HCl and extracted with ethyl acetate. The aqueous layer was adjusted to pH 10 with  $\text{Na}_2\text{CO}_3$  and extracted with chloroform. The combined organic layers were dried over  $\text{Na}_2\text{SO}_4$  and the solvent was evaporated to yield a yellow oil (42 mg, 63%) as the crude product. LC-MS analysis revealed that the crude product consisted mainly of the desired product ( $m/z = 301.15$ ) and the ringopened intermediate ( $m/z = 333.00$ ).

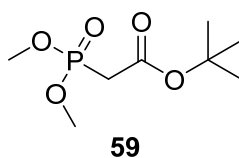
Formula:  $\text{C}_{16}\text{H}_{16}\text{N}_2\text{O}_4$ ;

MW: 300.31 g/mol;

LC-MS [ $m/z$ ]: 301.15 [ $\text{M}+\text{H}$ ]<sup>+</sup>.

### 7.3.4 Synthesis of the Racemic Simplified Analogue of Pilosinine (**35**)

#### Synthesis of *tert*-Butyl 2-(Dimethoxyphosphoryl)acetate (**59**)<sup>[97]</sup>



## Experimental

In a pressure tube under argon atmosphere, trimethylphosphite (3.18 g, 25.6 mmol, 3.03 mL) was added to *tert*-butyl bromoacetate (5.00 g, 25.6 mmol, 3.79 mL). The mixture was heated to 100 °C overnight. The reaction mixture was distilled at 14 mbar until complete removal of all compounds with a boiling point up to 62 °C. The colourless liquid residue of the distillation is the desired compound **59** (3.58 g, 15.97 mmol, 62%).

Formula: C<sub>8</sub>H<sub>17</sub>O<sub>5</sub>P;

MW: 224.19 g/mol;

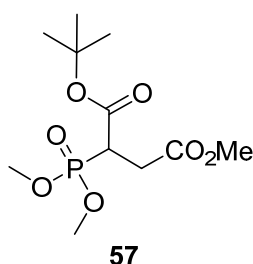
Boiling Point: > 60 °C at 14 mbar (Lit.:<sup>[161]</sup> 53 °C at 7 mbar);

<sup>1</sup>H NMR (CDCl<sub>3</sub>, 400 MHz): δ (ppm) = 3.81 (d, <sup>3</sup>J(<sup>1</sup>H, <sup>31</sup>P) = 11.2 Hz, 6H, OCH<sub>3</sub>), 2.90 (d, <sup>2</sup>J(<sup>1</sup>H, <sup>31</sup>P) = 21.4 Hz, 2H, CH<sub>2</sub>), 1.47 (s, 9H, C(CH<sub>3</sub>)<sub>3</sub>);

<sup>13</sup>C NMR (CDCl<sub>3</sub>, 101 MHz): δ (ppm) = 164.4 (C<sub>q</sub>, d, <sup>2</sup>J(<sup>13</sup>C, <sup>31</sup>P) = 6.0 Hz, C=O), 81.9 (C<sub>q</sub>, s, C(CH<sub>3</sub>)<sub>3</sub>), 52.9 (CH<sub>3</sub>, d, <sup>2</sup>J(<sup>13</sup>C, <sup>31</sup>P) = 6.3 Hz, OCH<sub>3</sub>), 34.3 (CH<sub>2</sub>, d, <sup>1</sup>J(<sup>13</sup>C, <sup>31</sup>P) = 134.2 Hz, CH<sub>2</sub>), 27.7 (CH<sub>3</sub>, C(CH<sub>3</sub>)<sub>3</sub>);

IR (ATR, cm<sup>-1</sup>): 2979, 1722, 1369, 1286, 1254, 1165, 1114, 1022, 807.

### Synthesis of 1-(*tert*-Butyl) 4-Methyl 2-(Dimethoxyphosphoryl)succinate (**57**)<sup>[98]</sup>



Sodium hydride (487 mg, 20.3 mmol) was suspended in dry THF (3 mL). At 0 °C, *tert*-butyl 2-(dimethoxyphosphoryl)-acetate (**59**) (1.30 g, 5.80 mmol) was added dropwise. After stirring for 2 h at 0 °C, methyl 2-bromoacetate (887 mg, 5.80 mmol, 538 μL) was added slowly and the reaction was stirred at RT for 3 h. Water was added, and the mixture was extracted three times with ethyl acetate. The combined organic layers were washed with brine and dried over Na<sub>2</sub>SO<sub>4</sub>. After removal of the solvent under reduced pressure, product **57** was obtained as a colourless liquid (1.29 g, 4.36 mmol, 75%). The product was used without further purification.

Formula: C<sub>11</sub>H<sub>21</sub>O<sub>7</sub>P;

MW: 296.26 g/mol;

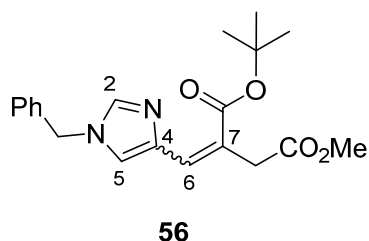
<sup>1</sup>H NMR (CDCl<sub>3</sub>, 400 MHz): δ (ppm) = 3.79 (m, 6H, OCH<sub>3</sub>), 3.67 (s, 3H, CO<sub>2</sub>Me), 3.38 (ddd, *J* = 11.3, 3.7 Hz, <sup>2</sup>J(<sup>1</sup>H, <sup>13</sup>P) = 24.2 Hz, 1H, CH), 2.99 (ddd, *J* = 17.4, 11.3 Hz, <sup>3</sup>J(<sup>1</sup>H, <sup>13</sup>P) = 7.9 Hz, 1H, CH<sub>2</sub>), 2.74 (ddd, *J* = 17.4, 3.7 Hz, <sup>3</sup>J(<sup>1</sup>H, <sup>13</sup>P) = 9.4 Hz, 1H, CH<sub>2</sub>), 1.45 (s, 9H, C(CH<sub>3</sub>)<sub>3</sub>);

## Experimental

$^{13}\text{C}$  NMR ( $\text{CDCl}_3$ , 101 MHz):  $\delta$  (ppm) = 171.6 ( $\text{C}_q$ , d,  $^3J(^{13}\text{C}, ^{31}\text{P}) = 19.3$  Hz,  $\text{CO}_2\text{Me}$ ), 167.0 ( $\text{C}_q$ , d,  $^2J(^{13}\text{C}, ^{31}\text{P}) = 5.5$  Hz,  $\text{CO}_2t\text{Bu}$ ), 82.5 ( $\text{C}_q$ ,  $\text{C}(\text{CH}_3)_3$ ), 53.5 ( $\text{CH}_3$ , d,  $^2J(^{13}\text{C}, ^{31}\text{P}) = 1.1$  Hz,  $\text{OCH}_3$ ), 53.4 ( $\text{CH}_3$ , d,  $^2J(^{13}\text{C}, ^{31}\text{P}) = 1.8$  Hz,  $\text{OCH}_3$ ), 52.2 ( $\text{CH}_3$ ,  $\text{CO}_2\text{Me}$ ), 41.6 ( $\text{CH}$ , d,  $^1J(^{13}\text{C}, ^{31}\text{P}) = 131.7$  Hz,  $\text{CH}$ ), 31.2 ( $\text{CH}_2$ , d,  $^2J(^{13}\text{C}, ^{31}\text{P}) = 2.4$  Hz,  $\text{CH}_2$ ), 2.79 (3 $\text{CH}_3$ ,  $\text{C}(\text{CH}_3)_3$ );

IR (ATR,  $\text{cm}^{-1}$ ): 2921, 2852, 1734, 1478, 1376, 1258, 1028, 797.

### Synthesis of 1-(*tert*-Butyl) 4-Methyl 2-((1-Benzyl-1*H*-Imidazol-4-yl)-methylene)-succinate (**56**)<sup>[101]</sup>



1-(*tert*-Butyl) 4-methyl 2-(dimethoxyphosphoryl)succinate (**57**) (4.60 g, 15.5 mmol) was dissolved in dry acetonitrile (100 mL). LiCl (688 mg, 16.2 mmol) and 1,8-diazabicyclo[5.4.0]undec-7-en (2.47 g, 16.2 mmol, 2.42 mL) were added at RT. A regioisomeric mixture of 1-benzyl-1*H*-imidazole-4/5-carbaldehyde (**40/42**) (2.52 g, 13.5 mmol) was added as a solution in dry acetonitrile (15 mL). The reaction was stirred overnight at RT. Water was added and the mixture was extracted three times with diethyl ether. The combined organic layers were washed with brine and dried over  $\text{MgSO}_4$ . The solvent was removed under reduced pressure to leave the crude as an inhomogeneous brown and colourless oil. **56** (1,4-substitution at the imidazole) was isolated by column chromatography (silica gel, 70:30  $\rightarrow$  20:80 cyclohexane/ethyl acetate) as a slightly yellow oil (2.08 g, 7.27 mmol, 54%).

Formula:  $\text{C}_{20}\text{H}_{24}\text{N}_2\text{O}_4$ ;

MW: 356.42 g/mol;

$R_f$  (50:50 cyclohexane/ethyl acetate) = 0.4;

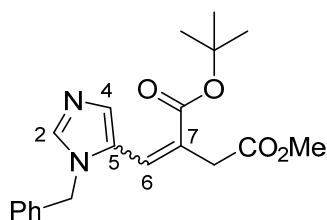
$^1\text{H}$  NMR ( $\text{CDCl}_3$ , 400 MHz):  $\delta$  (ppm) = 7.56 (s, 1H, **2-H**), 7.52 (s, 1H, **6-H**), 7.28–7.41 (m, 3H, **Ph**), 7.13–7.24 (m, 2H, **Ph**), 7.08 (s, 1H, **5-H**), 5.10 (s, 2H,  $-\text{CH}_2-\text{Ph}$ ), 4.09 (s, 2H,  $-\text{CH}_2-\text{CO}_2\text{Me}$ ), 3.64 (s, 3H,  $\text{CO}_2\text{Me}$ ), 1.49 (s, 9H,  $\text{C}(\text{CH}_3)_3$ );

$^{13}\text{C}$  NMR ( $\text{CDCl}_3$ , 101 MHz):  $\delta$  (ppm) = 172.4 ( $\text{C}_q$ ,  $\text{CO}_2t\text{Bu}$ ), 167.2 ( $\text{C}_q$ ,  $\text{CO}_2\text{Me}$ ), 139.0 ( $\text{C}_q$ , C-**4**), 138.3 (CH, C-**2**), 135.6 ( $\text{C}_q$ , **Ph**), 131.2 (CH, C-**6**), 129.2, 128.6, 127.5 (CH, **Ph**), 124.0 ( $\text{C}_q$ , C-**7**), 123.2 (CH, C-**5**), 80.6 ( $\text{C}_q$ ,  $\text{C}(\text{CH}_3)_3$ ), 51.8 ( $\text{CH}_3$ ,  $\text{CO}_2\text{Me}$ ), 51.1 ( $\text{CH}_2$ ,  $-\text{CH}_2-\text{Ph}$ ), 33.6 ( $\text{CH}_2$ ,  $-\text{CH}_2-\text{CO}_2\text{Me}$ ), 28.2 ( $\text{CH}_3$ ,  $\text{C}(\text{CH}_3)_3$ );

IR (ATR,  $\text{cm}^{-1}$ ): 3116, 2976, 1732, 1690, 1641, 1530, 1496, 1455, 1274, 1141, 777, 714, 696.



Synthesis of 1-(*tert*-Butyl 4-Methyl 2-((1-Benzyl-1*H*-Imidazol-5-yl)methylene)-succinate)<sup>[101]</sup>



With pure 1-benzyl-5-imidazolcarboxaldehyde (164 mg, 881  $\mu$ mol) as starting material for the previous reaction, the related product was obtained.

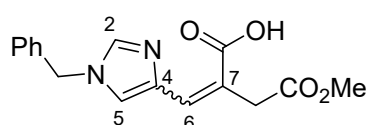
R<sub>f</sub> (95:5 dichloromethane/MeOH) = 0.6;

<sup>1</sup>H NMR (CDCl<sub>3</sub>, 400 MHz):  $\delta$  (ppm) = 7.68 (s, 1H, **2-H**), 7.44 (s, 1H, **6-H**), 7.39–7.29 (m, 4H, **4-H, Ph**), 7.17–7.09 (m, 2H, **Ph**), 5.17 (s, 2H, **-CH<sub>2</sub>-Ph**), 3.70 (s, 3H, **CO<sub>2</sub>Me**), 3.55 (s, 2H, **-CH<sub>2</sub>-CO<sub>2</sub>Me**), 1.46 (s, 9H, **C(CH<sub>3</sub>)<sub>3</sub>**);

<sup>13</sup>C NMR (CDCl<sub>3</sub>, 101 MHz):  $\delta$  (ppm) = 171.0 (C<sub>q</sub>, **CO<sub>2</sub>Me**), 165.9 (C<sub>q</sub>, **CO<sub>2</sub>tBu**), 139.9 (CH, **C-2**), 135.3 (C<sub>q</sub>, **Ph**), 132.3 (CH, **C-4**), 129.3, 128.6 (CH, **Ph**), 127.7 (C<sub>q</sub>, **C-5**), 127.2 (CH, **Ph**), 126.8 (C<sub>q</sub>, **C-7**), 125.5 (CH, **C-6**), 81.5 (C<sub>q</sub>, **C(CH<sub>3</sub>)<sub>3</sub>**), 52.3 (CH<sub>3</sub>, **CO<sub>2</sub>Me**), 49.4 (CH<sub>2</sub>, **-CH<sub>2</sub>-Ph**), 34.3 (CH<sub>2</sub>, **-CH<sub>2</sub>-CO<sub>2</sub>Me**), 28.2 (CH<sub>3</sub>, **C(CH<sub>3</sub>)<sub>3</sub>**).

IR (ATR, cm<sup>-1</sup>): 3106, 2977, 1736, 1697, 1635, 1496, 1476, 1455, 1436, 1278, 1150, 1096, 763, 708, 660.

Synthesis of 2-((1-Benzyl-1*H*-Imidazol-4-yl)methylene)-4-Methoxy-4-Oxobutanoic Acid (**61**)<sup>[102]</sup>



**61**

The *tert*-butyl ester **56** (121 mg, 340  $\mu$ mol) was dissolved in toluene (1.5 mL). 85% aqueous phosphoric acid (180  $\mu$ L) was added, and the reaction was stirred at RT overnight. Water and ethyl acetate were added until the precipitate was dissolved. The layers were separated and the aqueous layer was extracted three times with ethyl acetate. The combined organic layers were dried over MgSO<sub>4</sub> and the solvent was removed under reduced pressure. The product was obtained as an off-white solid (77.1 mg, 256  $\mu$ mol, 75%).

Formula: C<sub>16</sub>H<sub>16</sub>N<sub>2</sub>O<sub>4</sub>;

MW: 300.31 g/mol;

## Experimental

Melting point: decomposition at 143–145 °C;

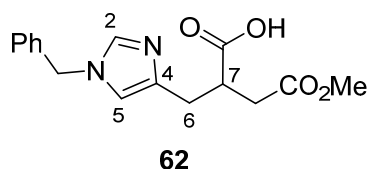
R<sub>f</sub> (30:10 ethyl acetate/cyclohexane) = 0.2;

<sup>1</sup>H NMR (CDCl<sub>3</sub>, 400 MHz): δ (ppm) = 9.70 (br. s, COOH), 7.70 (s, 1H, **2-H**), 7.77 (s, 1H, **6-H**), 7.30–7.40 (m, 3H, **Ph**), 7.14–7.21 (m, 3H, **Ph**, **5-H**), 5.11 (s, 2H, -CH<sub>2</sub>-Ph), 3.99 (s, 2H, -CH<sub>2</sub>-CO<sub>2</sub>Me), 3.65 (s, 3H, **Me**);

<sup>13</sup>C NMR (CDCl<sub>3</sub>, 101 MHz): δ (ppm) = 172.4 (C<sub>q</sub>, CO<sub>2</sub>H), 172.1 (C<sub>q</sub>, CO<sub>2</sub>Me), 138.6 (CH, C-**2**), 138.1 (C<sub>q</sub>, C-**4**), 135.3 (C<sub>q</sub>, **Ph**), 133.7 (CH, C-**6**), 129.3, 128.8, 127.7 (CH, **Ph**), 123.4 (CH, C-**5**), 122.4 (C<sub>q</sub>, C-**7**), 52.2 (CH<sub>3</sub>, **Me**), 51.4 (CH<sub>2</sub>, -CH<sub>2</sub>-Ph), 33.4 (CH<sub>2</sub>, -CH<sub>2</sub>-CO<sub>2</sub>Me);

IR (ATR, cm<sup>-1</sup>): 3116, 2952, 1726, 1651, 1545, 1496, 1436, 1392, 1170, 1011, 782, 706, 693, 627, 614.

### Synthesis of Methyl 2-((1-Benzyl-1*H*-imidazol-5-yl)methyl)succinate (**62**)



The α,β-unsaturated acid **61** (116 mg, 388 mmol) was dissolved in dry methanol (8 mL). 10% Palladium on activated charcoal (15 mg) was added and the mixture was hydrogenated at RT and atmospheric pressure for 1 h. The mixture was filtered over cotton and the solvent was removed in vacuo. The product was obtained as a slightly yellow oil (116 mg, 384 mmol, 99%).

Formel: C<sub>16</sub>H<sub>18</sub>N<sub>2</sub>O<sub>4</sub>;

MW: 302.33 g/mol;

R<sub>f</sub> (10:30 cyclohexane/ethyl acetate) = 0.2;

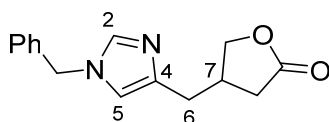
<sup>1</sup>H NMR (CDCl<sub>3</sub>, 400 MHz): δ (ppm) = 7.63 (br. s, 1H, **2-H**), 7.36–7.33 (m, 3H, **Ph**), 7.17–7.14 (m, 2H, **Ph**), 7.05 (br. s, 1H, CO<sub>2</sub>H), 6.69 (br. s, 1H, **5-H**), 5.04 (s, 2H, -CH<sub>2</sub>-Ph), 3.65 (s, 3H, **Me**), 3.20–3.11 (m, 1H, **7-H**), 2.97–2.86 (m, 2H, **6-H**), 2.82 (dd, *J* = 16.6, 7.2 Hz, 1H, -CH<sub>2</sub>-CO<sub>2</sub>Me), 2.42 (dd, *J* = 16.6, 7.2 Hz, 1H, -CH<sub>2</sub>-CO<sub>2</sub>Me);

<sup>13</sup>C NMR (CDCl<sub>3</sub>, 101 MHz): δ (ppm) = 176.3 (C<sub>q</sub>, CO<sub>2</sub>H), 173.0 (C<sub>q</sub>, CO<sub>2</sub>Me), 138.7 (C<sub>q</sub>, C-**4**), 136.4 (CH, C-**2**), 135.5 (C<sub>q</sub>, **Ph**), 129.4, 128.8, 127.8 (CH, **Ph**), 117.0 (CH, C-**5**), 51.9 (CH<sub>3</sub>, CO<sub>2</sub>Me), 51.5 (CH<sub>2</sub>, -CH<sub>2</sub>-Ph), 41.9 (CH, C-**7**), 35.8 (CH<sub>2</sub>, -CH<sub>2</sub>-CO<sub>2</sub>Me), 28.9 (CH<sub>2</sub>, C-**6**);

IR (ATR, cm<sup>-1</sup>): 3147, 2951, 1728, 1560, 1498, 1436, 1408, 1157, 773, 726, 643.

## Experimental

### Synthesis of 4-((1-Benzyl-1*H*-imidazol-4-yl)methyl)dihydrofuran-2(3*H*)-one (**63**)<sup>[162]</sup>



**63**

The acid **62** (300 mg, 992  $\mu\text{mol}$ ) was dissolved in dry THF (3 mL). Catecholborane (381 mg, 3.18 mmol, 340  $\mu\text{L}$ ) was added at RT before stirring at 60 °C for 2 d. After cooling down, methanol was added and the mixture was stirred for 30 min. All volatiles were removed under reduced pressure and the residue was separated on a short silica gel column (0%  $\rightarrow$  100% ethyl acetate in cyclohexane, then flushing with isopropanol). The product was obtained as a brown oil (248 mg, 969  $\mu\text{mol}$ , 97%).

Formula:  $\text{C}_{15}\text{H}_{16}\text{N}_2\text{O}_2$ ;

MW: 256.31 g/mol;

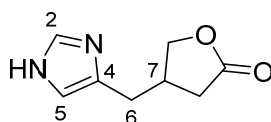
$R_f$  (95:5 dichloromethane/MeOH) = 0.3;

$^1\text{H}$  NMR ( $\text{CDCl}_3$ , 400 MHz):  $\delta$  (ppm) = 7.46 (s, 1H, **2-H**), 7.37–7.29 (m, 3H, **Ph**), 7.15–7.12 (m, 2H, **Ph**), 6.65 (s, 1H, **5-H**), 5.04 (s, 2H, **-CH<sub>2</sub>-Ph**), 4.38 (dd,  $J = 7.2, 9.1$  Hz, 1H, **-CH<sub>2</sub>-O-**), 4.08 (dd,  $J = 6.2, 9.1$  Hz, 1H, **-CH<sub>2</sub>-O-**), 3.01–2.88 (m, 1H, **7-H**), 2.68 (d,  $J = 7.3$ , 2H, **6-H**), 2.60 (dd,  $J = 8.4, 17.6$  Hz, 1H, **-CH<sub>2</sub>-COO-**), 2.29 (dd,  $J = 7.0, 17.6$  Hz, 1H, **-CH<sub>2</sub>-COO-**);

$^{13}\text{C}$  NMR ( $\text{CDCl}_3$ , 101 MHz):  $\delta$  (ppm) = 177.3 ( $\text{C}_q$ , **C=O**), 139.6 ( $\text{C}_q$ , **C-4**), 137.3 (CH, **C-2**), 136.0 ( $\text{C}_q$ , **Ph**), 129.1, 128.4, 127.4 (CH, **Ph**), 116.6 (CH, **C-5**), 73.0 ( $\text{CH}_2$ , **-CH<sub>2</sub>-O-**), 50.9 ( $\text{CH}_2$ , **-CH<sub>2</sub>-Ph**), 35.5 (CH, **C-7**), 34.2 ( $\text{CH}_2$ , **-CH<sub>2</sub>-COO-**), 31.5 ( $\text{CH}_2$ , **C-6**);

IR (ATR,  $\text{cm}^{-1}$ ): 3095, 2924, 1763, 1685, 1605, 1583, 1558, 1498, 1454, 1168, 1011, 762, 716, 396, 669, 613.

### Synthesis of *N*-Desmethyl-Pilosinine (4-((1*H*-Imidazol-4-yl)methyl)dihydrofuran-2(3*H*)-one) (**35**)<sup>[108]</sup>



**35**

The benzylated desmethyl pilosinine **63** (100 mg, 390  $\mu\text{mol}$ ) was dissolved in a mixture of methanol (2.5 mL), water (2.5 mL) and glacial acetic acid (0.1 mL). After addition of 10% palladium on activated charcoal (100 mg, 10% w/w), the mixture was hydrogenated at RT and 10 bar of hydrogen for 3 d. The volatiles were removed under reduced pressure. The residue was reslurried in methanol and filtered

## Experimental

over cotton. The product was purified by filtration through a short column of basic alumina (activity II–III, elution with 10% methanol/dichloromethane). The product was obtained as a slightly brown oil in 76% yield (49.3 mg, 296  $\mu\text{mol}$ ).

Formula:  $\text{C}_8\text{H}_{10}\text{N}_2\text{O}_2$ ;

MW: 166.18 g/mol;

$R_f$  (90:10 dichloromethane/MeOH) = 0.4;

$^1\text{H}$  NMR ( $\text{CDCl}_3$ , 400 MHz):  $\delta$  (ppm) = 9.32 (br. s, 2H, **NH**), 7.66 (s, 1H, **2-H**), 6.83 (s, 1H, **5-H**), 4.39 (dd,  $J = 7.1, 9.2$  Hz, 1H, **-CH<sub>2</sub>-O-**), 4.09 (dd,  $J = 5.7, 9.2$  Hz, 1H, **-CH<sub>2</sub>-O-**), 3.00–2.88 (m, 1H, **7-H**), 2.77 (d,  $J = 7.2$ , 2H, **6-H**), 2.64 (dd,  $J = 8.4, 17.6$  Hz, 1H, **-CH<sub>2</sub>-COO-**), 2.31 (dd,  $J = 6.5, 17.6$  Hz, 1H, **-CH<sub>2</sub>-COO-**);

$^{13}\text{C}$  NMR ( $\text{CDCl}_3$ , 101 MHz):  $\delta$  (ppm) = 179.8 ( $\text{C}_q$ , **C=O**), 136.4 ( $\text{C}_q$ , **C-4**), 136.4 (CH, **C-2**), 117.3 (CH, **C-5**), 74.4 ( $\text{CH}_2$ , **-CH<sub>2</sub>-O-**), 36.9 (CH, **C-7**), 34.9 ( $\text{CH}_2$ , **-CH<sub>2</sub>-COO-**), 31.0 ( $\text{CH}_2$ , **C-6**);

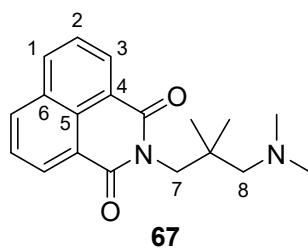
IR (ATR,  $\text{cm}^{-1}$ ): 3124 (br), 2910, 1759, 1565, 1478, 1439, 1291, 1173, 1010, 830, 662, 623, 611;

qNMR purity ( $\text{CD}_3\text{OD}$ , internal standard: 1,2,4,5-tetrachloro-3-nitrobenzene): 95%.

## 7.4 Synthesis of the Hybrid Ligands

### 7.4.1 Synthesis of the Allosteric Moiety with Linker (**64**)

*N*-[3-(*N*', *N*'-Dimethylamino)-2-Dimethyl-Propyl]-Naphthalimide (**67**)<sup>[125b]</sup>



1,8-Naphthalic anhydride (**65**) (2.00 g, 10.1 mmol) and *N*<sup>1</sup>,*N*<sup>1</sup>,2,2-tetramethylpropane-1,3-diamine (**66**) (1.31 g, 10.1 mmol, 1.61 mL) were dissolved in toluene (125 mL). The solution was heated to reflux for 24 h using a Dean-Stark trap. The solvent was removed at reduced pressure and the brownish residue was washed three times with ethanol. The product was obtained as a beige solid (2.41 g, 7.75 mmol, 77%).

Formula:  $\text{C}_{19}\text{H}_{22}\text{N}_2\text{O}_2$ ;

MW: 310.39 g/mol;

$R_f$  (50:50 cyclohexane/ethyl acetate): 0.5;

## Experimental

Melting point: 110–111 °C (toluene) (Lit<sup>[125b]</sup>: 112–114 °C);

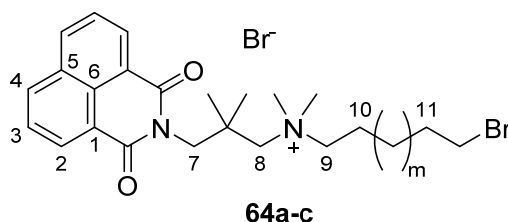
<sup>1</sup>H NMR (CDCl<sub>3</sub>, 400 MHz):  $\delta$  (ppm) = 8.60 (dd,  $J$  = 7.3, 1.0 Hz, 2H, **3-H**), 8.21 (dd,  $J$  = 8.3, 1.0 Hz, 2H, **1-H**), 7.76 (dd,  $J$  = 8.3, 7.3 Hz, 2H, **2-H**), 4.22 (s, 2H, **7-H**), 2.41 (br. s, 7H, **-CH<sub>2</sub>-NMe<sub>2</sub>**, **-CH<sub>2</sub>-NMe<sub>2</sub>**), 2.30 (s, 1H, **-CH<sub>2</sub>-NMe<sub>2</sub>**), 1.02 (s, 6H, C(**CH<sub>3</sub>**)<sub>2</sub>);

<sup>13</sup>C NMR (CDCl<sub>3</sub>, 101 MHz):  $\delta$  (ppm) = 165.1 (C<sub>q</sub>, **C=O**), 133.9 (CH, C-**1**), 131.7 (C<sub>q</sub>, C-**6**), 131.5 (CH, C-**3**), 128.2 (C<sub>q</sub>, C-**5**), 127.1 (CH, C-**2**), 123.0 (C<sub>q</sub>, C-**4**), 70.1 (CH<sub>2</sub>, **-CH<sub>2</sub>-NMe<sub>2</sub>**), 48.9 (CH<sub>3</sub>, **NMe<sub>2</sub>**), 47.8 (CH<sub>2</sub>, C-**7**), 39.1 (C<sub>q</sub>, C(**CH<sub>3</sub>**)<sub>2</sub>), 25.0 (CH<sub>3</sub>, C(**CH<sub>3</sub>**)<sub>2</sub>);

IR (ATR, cm<sup>-1</sup>): 3087, 2960, 2763, 1700, 1670, 1660, 1589, 1363, 1330, 1229, 1036, 846, 779.

The spectral data correspond to literature data.<sup>[125b]</sup>

### General Procedure for the Attachment of the Linker<sup>[163]</sup>



In a microwave tube *N*-[3-(*N,N'*-dimethylamino)-2-dimethyl-propyl]-naphthalimide **67** (1.00 eq.) was suspended in dibromoalkane (20.0 eq.). Acetonitrile (2 mL) was added. After heating to 80 °C (heating rate 30 °C/min; 800 W) for 8 h, the solvent was removed under reduced pressure and the product was precipitated by addition of diethyl ether. After filtration, the residue was boiled in diethyl ether for 10 min and filtered again. The residue was washed with diethyl ether. If necessary, the product was further purified by column chromatography (alumina, activity II–III, 95:5 dichloromethane/MeOH). The product was obtained as a colourless solid.

**Table 17:** General data of the compounds **64a–c**.

#	m	Formula	MW [g/mol]	Yield [%]	Melting point [°C]
<b>64a</b>	0	C <sub>23</sub> H <sub>30</sub> Br <sub>2</sub> N <sub>2</sub> O <sub>2</sub>	526.31	67	202.3–204.8 (Lit <sup>[164]</sup> : 178–181)
<b>64b</b>	2	C <sub>25</sub> H <sub>34</sub> Br <sub>2</sub> N <sub>2</sub> O <sub>2</sub>	554.37	75	177.1–178.4 (Lit <sup>[163]</sup> : 178–180)
<b>64c</b>	4	C <sub>27</sub> H <sub>38</sub> Br <sub>2</sub> N <sub>2</sub> O <sub>2</sub>	582.42	56	140.5–141.6 (Lit <sup>[164]</sup> : 149–153)

**Table 18:** IR data of the compounds **64a–c**.

#	IR data [cm <sup>-1</sup> ]
<b>64a</b>	3350, 2958, 1704, 1658, 1587, 1335, 1233, 1205, 1097, 1030, 875, 848, 781, 741, 660
<b>64b</b>	3489, 2943, 1702, 1657, 1589, 1339, 1236, 1200, 1089, 1033, 878, 846, 782, 731, 681
<b>64c</b>	3400, 2925, 1702, 1655, 1588, 1339, 1236, 1204, 1088, 1038, 886, 846, 781, 746, 671

Table 19: <sup>1</sup>H NMR data of the compounds **64a–c** measured in CDCl<sub>3</sub> for m = 4 and in DMSO-d<sub>6</sub> for m = 0 and 2.

#	2-H	3-H	4-H	7-H	8-H	C(CH <sub>3</sub> ) <sub>2</sub>
<b>64a</b>	8.53–8.45 (m, 4H)	7.88 (t, J = 7.8 Hz, 2H)	8.53–8.45 (m, 4H)	4.13 (s, 2H)	3.53–3.42 (m, 4H)	1.25 (s, 6H)
<b>64b</b>	8.54–8.48 (m, 4H)	7.92–7.88 (m, 2H)	8.54–8.48 (m, 4H)	4.13 (s, 2H)	3.45 (s, 2H)	1.25 (s, 6H)
<b>64c</b>	8.55 (d, J = 7.2 Hz, 2H)	7.76 (t, J = 7.8 Hz, 2H)	8.25 (d, J = 8.2 Hz, 2H)	4.33 (s, 2H)	3.67 (s, 2H)	1.50–1.23 (m, 14H)

Table 20: <sup>1</sup>H NMR data of the compounds **64a–c** measured in CDCl<sub>3</sub> for m = 4 and in DMSO-d<sub>6</sub> for m = 0 and 2 (continued).

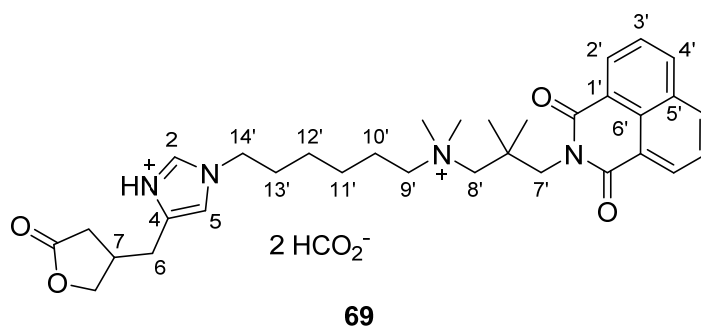
#	N(CH <sub>3</sub> ) <sub>2</sub>	9-H	10-H	m-H	11-H	CH <sub>2</sub> -Br
<b>64a</b>	3.18 (s, 6H)	3.53–3.42 (m, 4H)	1.93–1.81 (m, 2H)	-	1.81–1.70 (m, 2H)	3.69 (t, J = 6.3 Hz, 2H)
<b>64b</b>	3.15 (s, 6H)	3.38–3.33 (m, 2H)	1.80–1.71 (m, 2H)	1.48–1.40 (m, 2H); 1.33–1.26 (m, 2H)	1.87–1.80 (m, 2H)	3.55 (t, J = 6.5 Hz, 2H)
<b>64c</b>	3.60 (s, 6H)	3.86–3.75 (m, 2H)	1.88–1.75 (m, 4H)	1.50–1.23 (m, 14H)	1.88–1.75 (m, 4H)	3.37 (t, J = 6.8 Hz, 2H)

Table 21: <sup>13</sup>C NMR data of the compounds **64a–c** measured in CDCl<sub>3</sub> for m = 4 and in DMSO-d<sub>6</sub> for m = 0 and 2.

#	C-1	C-2	C-3	C-4	C-5	C-6	C=O	C-7	C(CH <sub>3</sub> ) <sub>2</sub>
<b>64a</b>	122.2	134.9	127.2	130.9	131.3	127.4	164.6	49.0	39.2
<b>64b</b>	122.3	134.3	128.0	130.9	131.3	127.3	164.7	49.1	39.2
<b>64c</b>	122.1	134.7	127.3	132.0	131.7	128.2	165.3	48.4	39.4

Table 22: <sup>13</sup>C NMR data of the compounds **64a–c** measured in CDCl<sub>3</sub> for m = 4 and in DMSO-d<sub>6</sub> for m = 0 and 2 (continued).

#	C-8	C(CH <sub>3</sub> ) <sub>2</sub>	N(CH <sub>3</sub> ) <sub>2</sub>	C-9	C-10	C-m	C-11	CH <sub>2</sub> -Br
<b>64a</b>	71.6	25.5	52.0	66.6	19.8	-	28.9	44.6
<b>64b</b>	71.5	25.5	51.9	67.5	21.9	27.0, 24.8	31.8	35.0
<b>64c</b>	72.1	26.7	53.1	68.3	32.7	26.2, 28.0, 28.5, 29.1	23.3	34.1

7.4.2 Synthesis of *rac*-*N*-Desmethyl-Pilosinine-6-Naph (69)

4-((1*H*-Imidazol-4-yl)methyl)dihydrofuran-2(3*H*)-one (**35**) (72.5 mg, 436  $\mu$ mol) and **64b** (266 mg, 480  $\mu$ mol) were dissolved in DMF (6 mL). Potassium iodide (14.5 mg, 87.3  $\mu$ mol, 0.20 eq.) and potassium carbonate (66.3 mg, 480  $\mu$ mol) were added and the mixture was heated to 60 °C by microwave irradiation in a pressure tube for 10 h. The solvent was evaporated under reduced pressure and the product was isolated by reversed-phase flash-chromatography (water/methanol/0.1% formic acid). This yielded 55.5 mg (85.4  $\mu$ mol, 20%) of a slightly yellow oil.

Formula: C<sub>35</sub>H<sub>46</sub>N<sub>4</sub>O<sub>8</sub>;

MW: 650.33 g/mol;

R<sub>f</sub> (3:2 methanol/0.2 M ammonium nitrate): 0.4;

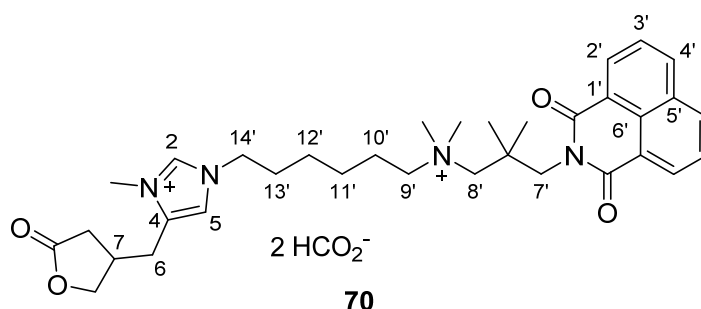
<sup>1</sup>H NMR (CDCl<sub>3</sub>, 400 MHz):  $\delta$  (ppm) = 9.00 (br. s, 1H, N-H), 8.51 (d, 2H, *J* = 7.2 Hz, **2'**-H), 8.39 (br. s, 2H, HCO<sub>2</sub><sup>-</sup>), 8.21 (d, *J* = 8.2 Hz, 2H, **4'**-H), 7.73 (dd, 2H, *J* = 7.2, 8.2 Hz, **3'**-H), 7.49 (s, 1H, **2**-H), 6.77 (s, 1H, **4**-H), 4.33 (dd, 1H, *J* = 9.1, 7.4 Hz, -CH<sub>2</sub>-O-), 4.27 (s, 2H, **7'**-H), 4.07 (dd, 1H, *J* = 9.1, 5.6 Hz, -CH<sub>2</sub>-O-), 3.89 (t, 2H, *J* = 6.7 Hz, **14'**-H), 3.66–3.56 (m, 2H, **9'**-H), 3.51 (s, 2H, **8'**-H), 3.39 (s, 6H, N(CH<sub>3</sub>)<sub>2</sub>), 2.96–2.83 (m, 1H, **7**-H), 2.67 (d, 2H, *J* = 6.8 Hz, **6**-H), 2.55 (dd, 1H, *J* = 17.6, 8.5 Hz, -CH<sub>2</sub>-COO-), 2.26 (dd, 1H, *J* = 17.6, 6.6 Hz, -CH<sub>2</sub>-COO-), 1.90–1.68 (m, 4H, **13'**-H, **10'**-H), 1.49–1.20 (m, 10H, **12'**-H, **11'**-H, C(CH<sub>3</sub>)<sub>2</sub>);

<sup>13</sup>C NMR (CDCl<sub>3</sub>, 101 MHz):  $\delta$  (ppm) = 177.5 (C<sub>q</sub>, -COO-), 166.4 (C<sub>q</sub>, HCO<sub>2</sub><sup>-</sup>), 165.3 (C<sub>q</sub>, -CON-), 138.2 (C<sub>q</sub>, C-4), 136.8 (CH, C-2), 134.7 (CH, C-4'), 131.9 (CH, C-2'), 131.6 (C<sub>q</sub>, C-5'), 128.1 (C<sub>q</sub>, C-6'), 127.2 (CH, C-3'), 122.1 (C<sub>q</sub>, C-1'), 116.7 (CH, C-5), 73.0 (CH<sub>2</sub>, -CH<sub>2</sub>-O-), 72.6 (CH<sub>2</sub>, C-8'), 68.5 (CH<sub>2</sub>, C-9'), 52.8 (CH<sub>3</sub>, N(CH<sub>3</sub>)<sub>2</sub>), 48.4 (CH<sub>2</sub>, C-7'), 47.0 (CH<sub>2</sub>, C-14'), 39.3 (C<sub>q</sub>, C(CH<sub>3</sub>)<sub>2</sub>), 35.2 (CH, C-7), 34.1 (CH<sub>2</sub>, -CH<sub>2</sub>-COO-), 31.0 (CH<sub>2</sub>, C-6), 30.5 (CH<sub>2</sub>, C-10'), 26.5 (CH<sub>3</sub>, C(CH<sub>3</sub>)<sub>2</sub>), 25.8 (CH<sub>2</sub>, C-11'), 25.6 (CH<sub>2</sub>, C-12'), 22.8 (CH<sub>2</sub>, C-13');

IR (ATR, cm<sup>-1</sup>): 3386 (br), 2939, 1766, 1700, 1656, 1626, 1587, 1438, 1337, 1235, 1171, 1091, 1011, 847, 781, 643;

HPLC purity (achiral method A): 86%.

## 7.4.3 Synthesis of Pilosinine-6-Naph (70)



*rac*-Pilosinine (*rac*-4-((1-methyl-1*H*-imidazol-5-yl)methyl)dihydrofuran-2(3*H*)-one) (**16**) (63.0 mg, 350  $\mu$ mol) and **64b** (213 mg, 385  $\mu$ mol) were dissolved in MeCN (9 mL). Potassium iodide (5.80 mg, 35.0  $\mu$ mol) and potassium carbonate (53.2 mg, 385  $\mu$ mol) were added and the mixture was stirred at 60 °C in a sealed tube for 1 week. The mixture was filtered and the solvent was evaporated under reduced pressure. The product was purified by reversed-phase flash-chromatography (water/methanol/0.1% formic acid). This yielded 30.0 mg (45.1  $\mu$ mol, 13%) of a slightly yellow oil.

Formula: C<sub>36</sub>H<sub>48</sub>N<sub>4</sub>O<sub>8</sub>;

MW: 664.80 g/mol;

R<sub>f</sub> (3:2 methanol/0.2 M ammonium nitrate): 0.4;

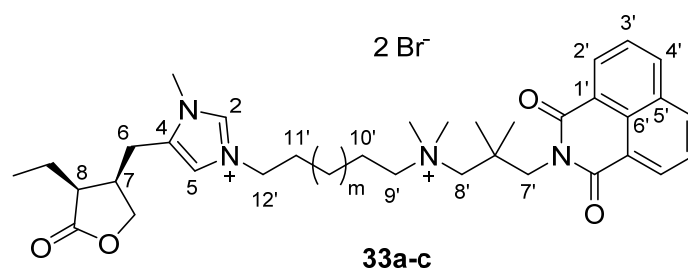
<sup>1</sup>H NMR (CDCl<sub>3</sub>, 400 MHz):  $\delta$  (ppm) = 8.97 (s, 1H, **2**-H), 8.57 (d, 2H, *J* = 7.2 Hz, **2'**-H), 8.42–8.22 (m, 4H, **4'**-H, 2 HCO<sub>2</sub><sup>-</sup>), 7.84 (t, 2H, *J* = 7.8 Hz, **3'**-H), 7.59 (s, 1H, **5**-H), 4.58–4.48 (m, 1H, -CH<sub>2</sub>-O-), 4.32 (s, 2H, **7'**-H), 4.21 (t, 2H, *J* = 7.1 Hz, **14'**-H), 4.10 (dd, 1H, *J* = 8.9, 6.4 Hz, -CH<sub>2</sub>-O-), 3.85 (s, 3H, N-CH<sub>3</sub>), 3.58–3.45 (m, 4H, **8'**-H, **9'**-H), 3.30 (s, 6H, N(CH<sub>3</sub>)<sub>2</sub>), 3.08–2.85 (m, 3H, **7**-H, **6**-H), 2.79 (dd, 1H, *J* = 17.5, 8.3 Hz, -CH<sub>2</sub>-COO-), 2.38 (dd, 1H, *J* = 17.5, 7.0 Hz, -CH<sub>2</sub>-COO-), 2.02–1.82 (m, 4H, **13'**-H, **10'**-H), 1.55–1.41 (m, 4H, **11'**-H, **12'**-H), 1.34 (s, 6H, C(CH<sub>3</sub>)<sub>2</sub>);

<sup>13</sup>C NMR (CDCl<sub>3</sub>, 101 MHz):  $\delta$  (ppm) = 178.8 (C<sub>q</sub>, -COO-), 167.1 (C<sub>q</sub>, 2 HCO<sub>2</sub><sup>-</sup>), 166.7 (C<sub>q</sub>, -CON-), 137.9 (C<sub>q</sub>, C-**2**), 135.8 (CH, C-**4'**), 135.0 (CH, C-**4**), 133.2 (CH, C-**5'**), 132.6 (C<sub>q</sub>, C-**2'**), 129.3 (C<sub>q</sub>, C-**6'**), 128.3 (CH, C-**3'**), 123.6 (C<sub>q</sub>, C-**1'**), 120.9 (CH, C-**5**), 74.1 (CH<sub>2</sub>, -CH<sub>2</sub>-O-), 73.8 (CH<sub>2</sub>, C-**8'**), 69.6 (CH<sub>2</sub>, C-**9'**), 53.3 (CH<sub>3</sub>, N(CH<sub>3</sub>)<sub>2</sub>), 50.6 (CH<sub>2</sub>, C-**14'**), 49.9 (CH<sub>2</sub>, C-**7'**), 40.5 (C<sub>q</sub>, C(CH<sub>3</sub>)<sub>2</sub>), 34.7 (CH<sub>2</sub>, -CH<sub>2</sub>-COO-), 34.6 (CH, N-CH<sub>3</sub>), 34.1 (CH, C-**7**), 30.7 (CH<sub>2</sub>, C-**10'**), 27.5 (CH<sub>2</sub>, C-**6**), 26.8 (CH<sub>2</sub>, C-**11'**), 26.7 (CH<sub>2</sub>, C-**12'**), 26.5 (CH, C(CH<sub>3</sub>)<sub>2</sub>), 23.7 (CH<sub>2</sub>, C-**13'**);

IR (ATR, cm<sup>-1</sup>): 3395 (br), 2951, 1766, 1699, 1655, 1586, 1438, 1338, 1235, 1173, 1090, 1014, 849, 781, 634;

LC–MS purity: 90%.



7.4.4 General Procedure for the Synthesis of the Pilo-n-Naph Hybrids (**33a–c**)

Pilocarpine (**2**) (1.00 eq.) and **64a–c** (1.20 eq.), respectively, were suspended with potassium carbonate (1.20 eq.) and potassium iodide (1.00 eq.) in dry acetonitrile. The mixture was stirred at 60 °C for several days until TLC (methanol/0.2M ammonium nitrate 3:2, UV and Dragendorff stain detection) showed complete conversion of pilocarpine and a fluorescent product spot at  $R_f=0.4–0.5$ . After filtration the solvent was evaporated. The residue was purified by column chromatography ( $\text{Al}_2\text{O}_3$ , act. II-III, 5–20% MeOH/DCM) and again by preparative HPLC (method II for  $m=0$  and 2; method III for  $m=4$ , Chapter 7.1.4).

**Table 23:** General data of the pilo-n-naph hybrid compounds **33a–c**.

#	m	Formula	MW [g/mol]	Reaction time	Yield [%]	LC–MS purity [%]	LC–MS [m/z]
<b>Pilo-4-naph</b> <b>33a</b>	0	$\text{C}_{34}\text{H}_{45}\text{Br}_2\text{N}_4\text{O}_4$	734.58	9 d	7	93	287
<b>Pilo-6-naph</b> <b>33b</b>	2	$\text{C}_{36}\text{H}_{49}\text{Br}_2\text{N}_4\text{O}_4$	762.63	14 d	18	88	301
<b>Pilo-8-naph</b> <b>33c</b>	4	$\text{C}_{38}\text{H}_{53}\text{Br}_2\text{N}_4\text{O}_4$	790.68	13 d	18	99*	315

\* measured at  $\lambda=215$  nm.

**Table 24:** General data of the pilo-n-naph hybrid compounds **33a–c**.

#	m	IR data [ $\text{cm}^{-1}$ ]
<b>Pilo-4-naph</b> <b>33a</b>	0	3416 (br), 2962, 1760, 1699, 1656, 1587, 1437, 1338, 1235, 1173, 1015, 848, 781, 625, 604
<b>Pilo-6-naph</b> <b>33b</b>	2	3399 (br), 2927, 1764, 1700, 1657, 1588, 1438, 1338, 1235, 1171, 1027, 849, 782, 625, 613
<b>Pilo-8-naph</b> <b>33c</b>	4	3384 (br), 2927, 1764, 1701, 1656, 1587, 1438, 1339, 1236, 1177, 1021, 849, 783, 622, 613

Table 25: <sup>1</sup>H NMR data of the pilo-n-naph hybrids **33a-c** measured in acetonitrile-d<sub>3</sub> for n = 4 and 8, and in CD<sub>3</sub>OD for n = 6.

#	N-CH <sub>3</sub>	2-H	5-H	6-H	7-H	8-H	-CH <sub>2</sub> -CH <sub>3</sub>	
<b>Pilo-4-naph</b>	<b>33a</b>	3.78 (s, 3H)	9.95 (s, 1H)	7.64 (s, 1H)	2.80–2.70 (m, 2H),	3.06–2.96 (m, 1H)	2.80–2.70 (m, 2H)	1.90–1.64 (m, 3H)
<b>Pilo-6-naph</b>	<b>33b</b>	3.85 (s, 3H)	7.49 (s, 1H)	7.62 (s, 1H)	2.55 (dd, J = 16.1, 11.6 Hz, 1H),	3.10–3.01 (m, 1H)	(t, J = 7.4 Hz, 3H)	1.62–1.49 (m, 1H),
<b>Pilo-8-naph</b>	<b>33c</b>	3.77 (s, 3H)	9.76 (s, 1H)	7.53 (s, 1H)	2.90 (dd, J = 16.2, 4.34 Hz, 1H),	(m, 1H)	1.11 (t, J = 7.4 Hz, 3H)	1.86–1.76 (m, 1H),
					2.63 (dd, J = 16.2, 11.4 Hz, 1H)	3.02–2.92 (m, 1H)	1.05 (t, J = 7.4 Hz, 3H)	1.67–1.57 (m, 1H)
					2.80–2.68 (m, 2H),	(m, 2H)	1.05 (t, J = 7.4 Hz, 3H)	1.90–1.69 (m, 5H),
					2.53 (dd, J = 16.2, 11.5 Hz, 1H)	(m, 1H)		1.61–1.48 (m, 1H)

Table 26: <sup>1</sup>H NMR data of the pilo-n-naph hybrids **33a-c** measured in acetonitrile-d<sub>3</sub> for n = 4 and 8, and in CD<sub>3</sub>OD for n = 6 (continued).

#	-CH <sub>2</sub> -O-	12'-H	11'-H	m-H	10'-H	9'-H
<b>Pilo-4-naph</b>	<b>33a</b>	4.27 (dd, J = 9.5, 5.7 Hz, 1H),	4.32 (t, J = 7.3 Hz, 2H)	2.00–1.91 (m, 2H)	1.90–1.64 (m, 3H)	3.77–3.67 (m, 2H)
		4.04 (dd, J = 9.5, 2.9 Hz, 1H)				
<b>Pilo-6-naph</b>	<b>33b</b>	4.36–4.31 (m, 3H),	4.22 (t, J = 7.3 Hz, 2H)	2.03–1.86 (m, 4H)	2.03–1.86 (m, 4H)	3.54–3.49 (m, 2H)
		4.10 (dd, J = 9.5, 3.2 Hz, 1H)		(m, 4H)		
<b>Pilo-8-naph</b>	<b>33c</b>	4.28–4.22 (m, 3H),	4.16 (t, J = 7.2 Hz, 2H)	1.90–1.69 (m, 5H)	1.90–1.69 (m, 5H)	3.56–3.48 (m, 4H)
		4.00 (dd, J = 9.4, 3.1 Hz, 1H)		(m, 14H)		

Table 27: <sup>1</sup>H NMR data of the pilo-n-naph hybrids **33a-c** measured in acetonitrile-d<sub>3</sub> for n = 4 and 8, and in CD<sub>3</sub>OD for n = 6 (continued).

#	N(CH <sub>3</sub> ) <sub>2</sub>	8'-H	C(CH <sub>3</sub> ) <sub>2</sub>	7'-H	2'-H	3'-H	4'-H	
<b>Pilo-4-naph</b>	<b>33a</b>	3.28 (s, 6H)	3.56 (s, 2H)	1.28 (s, 6H)	4.23 (s, 2H)	8.53 (d, J = 7.3 Hz, 2H)	7.83 (dd, J = 7.3, 8.4 Hz, 2H)	8.37 (d, J = 8.4 Hz, 2H)
<b>Pilo-6-naph</b>	<b>33b</b>	3.30 (s, 6H)	3.56 (s, 2H)	1.34 (s, 6H)	4.36–4.31 (m, 3H)	8.59 (dd, J = 7.3, 1.0 Hz, 2H)	7.85 (dd, J = 7.3, 8.4 Hz, 2H)	8.40 (dd, J = 8.4, 1.0 Hz, 2H)
<b>Pilo-8-naph</b>	<b>33c</b>	3.25 (s, 6H)	3.56–3.48 (m, 4H)	1.49–1.24 (m, 14H)	4.28–4.22 (m, 3H)	8.53 (d, J = 7.3 Hz, 2H)	7.82 (dd, J = 7.3, 8.3 Hz, 2H)	8.36 (d, J = 8.3 Hz, 2H)

## Experimental

**Table 28:** <sup>13</sup>C NMR data of the pilo-n-naph hybrids **33a–c** measured in acetonitrile-d<sub>3</sub> for n = 4 and 8, and in CD<sub>3</sub>OD for n = 6.

	#	N-CH <sub>3</sub>	C-2	C-4	C-5	C-6	C-7	C-8	-CH <sub>2</sub> -CH <sub>3</sub>	-CH <sub>2</sub> -CH <sub>3</sub>
<b>Pilo-4-naph</b>	<b>33a</b>	34.4	138.7	134.3	120.6	22.1	37.0	45.0	12.4	19.1
<b>Pilo-6-naph</b>	<b>33b</b>	34.2	137.5*	135.0	121.0	22.2	37.6	45.6	12.5	19.4
<b>Pilo-8-naph</b>	<b>33c</b>	34.3	138.2	134.1	120.6	22.0	37.0	45.0	12.4	19.1

\* determined from HMBC spectrum

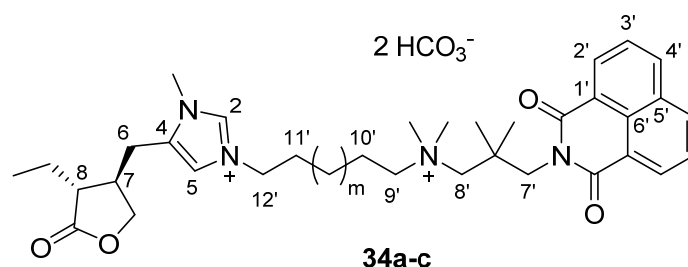
**Table 29:** <sup>13</sup>C NMR data of the pilo-n-naph hybrids **33a–c** measured in acetonitrile-d<sub>3</sub> for n = 4 and 8, and in CD<sub>3</sub>OD for n = 6 (continued).

	#	-COO-	-CH <sub>2</sub> -O-	C-12'	C-11'	C-10'	C-9'	N(CH <sub>3</sub> ) <sub>2</sub>	C-8'	C(CH <sub>3</sub> ) <sub>2</sub>
<b>Pilo-4-naph</b>	<b>33a</b>	179.0	70.6	48.9	27.0	20.0	68.0	53.4	73.5	40.4
<b>Pilo-6-naph</b>	<b>33b</b>	180.2	71.2	50.6	23.7	30.7	69.6	53.3	74.1	40.5
<b>Pilo-8-naph</b>	<b>33c</b>	179.0	70.5	50.1	30.1	23.2	69.4	53.3	73.1	40.4

**Table 30:** <sup>13</sup>C NMR data of the pilo-n-naph hybrids **33a–c** measured in acetonitrile-d<sub>3</sub> for n = 4 and 8, and in CD<sub>3</sub>OD for n = 6 (continued).

	#	C(CH <sub>3</sub> ) <sub>2</sub>	C-7'	-CON-	C-1'	C-2'	C-3'	C-4'	C-5'	C-6'	C-m
<b>Pilo-4-naph</b>	<b>33a</b>	26.4, 26.3	49.7	166.3	123.7	132.1	128.2	135.4	132.6	129.0	-
<b>Pilo-6-naph</b>	<b>33b</b>	26.6	49.9	166.8	123.6	132.6	128.3	135.8	133.2	129.4	26.7, 26.7
<b>Pilo-8-naph</b>	<b>33c</b>	26.4	49.9	166.2	123.7	132.1	128.2	135.3	132.6	128.9	29.0, 28.8, 26.5, 26.2

### 7.4.5 General Procedure for the Synthesis of the Isopilo-n-Naph Hybrids (**34a–c**)



In a closed microwave reactor isopilocarpine (**15**) (1.00 eq.), **64a–c** (1.10 eq.), potassium carbonate (1.10 eq.) and potassium iodide (1.00 eq.) were suspended in acetonitrile (9mL/50mg of **15**). The mixture was heated by microwave irradiation to 80 °C for 72 h. The mixture was filtered through cotton and the solvent of the filtrate was evaporated. The residue was chromatographed on a reversed-phase flash-column (water/methanol/0.1% formic acid, 0–55% methanol) followed by preparative HPLC (method IV, Chapter 7.1.4) to yield the hybrid molecules.

Table 31: General data of the isopilo-n-naph hybrid compounds **34a-c** formate salts.

#	m	Formula	MW [g/mol]	Yield [%]	LC-MS purity [%]	LC-MS [m/z]	IR data [cm <sup>-1</sup> ]
<b>Isopilo-4-naph</b>	<b>34a</b>	0	C <sub>36</sub> H <sub>48</sub> N <sub>4</sub> O <sub>8</sub>	29	94	287	3423 (br), 2967, 1763, 1701, 1654, 1550, 1437, 1338, 1234, 1170, 1014, 848, 781, 625
<b>Isopilo-6-naph</b>	<b>34b</b>	2	C <sub>38</sub> H <sub>52</sub> N <sub>4</sub> O <sub>8</sub>	14	93	301	3362 (br), 2935, 1762, 1700, 1656, 1586, 1439, 1338, 1235, 1170, 1014, 849, 782, 624
<b>Isopilo-8-naph</b>	<b>34c</b>	4	C <sub>40</sub> H <sub>56</sub> N <sub>4</sub> O <sub>8</sub>	51	99	315	3393 (br), 2932, 1764, 1701, 1656, 1587, 1438, 1337, 1235, 1171, 1013, 849, 782, 623

Table 32: <sup>1</sup>H NMR data of the isopilo-n-naph hybrids **34a-c** measured in CD<sub>3</sub>OD.

#	N-CH <sub>3</sub>	2-H	5-H	6-H	7-H	8-H	-CH <sub>2</sub> -CH <sub>3</sub>	
<b>Isopilo-4-naph</b>	<b>34a</b>	3.88 (s, 3H)	9.05 (s, 1H)	7.71 (s, 1H)	3.08 (dd, J = 15.9, 4.8 Hz, 1H),	2.87-2.74 (m, 1H)	2.51-2.43 (m, 1H)	1.03 (t, J = 7.4 Hz, 3H)
<b>Isopilo-6-naph</b>	<b>34b</b>	3.85 (s, 3H)	8.95 (s, 1H)	7.58 (s, 1H)	3.07-3.01 (m, 1H),	2.80-2.70 (m, 1H)	2.44 (dt, J = 8.3, 6.1 Hz, 1H)	1.02 (t, J = 7.5 Hz, 3H)
<b>Isopilo-8-naph</b>	<b>34c</b>	3.85 (s, 3H)	8.95 (s, 1H)	7.57 (s, 1H)	3.08-2.97 (m, 1H),	2.81-2.67 (m, 1H)	2.48-2.39 (m, 1H)	1.02 (t, J = 7.5 Hz, 3H)

Table 33: <sup>1</sup>H NMR data of the isopilo-n-naph hybrids **34a-c** measured in CD<sub>3</sub>OD (continued).

#	-CH <sub>2</sub> -O-	12'-H	11'-H	m-H	10'-H	9'-H
<b>Isopilo-4-naph</b>	<b>34a</b>	4.55 (t, J = 8.28 Hz, 1H), 4.10 (t, J = 8.3 Hz, 1H)	4.37-4.29 (s, 4H)	2.00 (br. s, 4H)	2.00 (br. s, 4H)	3.65-3.55 (m, 4H)
<b>Isopilo-6-naph</b>	<b>34b</b>	4.46 (dd, J = 9.1, 7.6 Hz, 1H), 3.97 (dd, J = 9.1, 7.5 Hz, 1H)	4.20 (t, J = 7.4 Hz, 2H)	1.95-1.87 (m, 4H)	1.47 (br. s, 4H)	3.50-3.45 (m, 2H)
<b>Isopilo-8-naph</b>	<b>34c</b>	4.49-4.43 (m, 1H), 3.99- 3.92 (m, 1H)	4.18 (t, J = 7.3 Hz, 2H)	1.95-1.80 (m, 4H)	1.49-1.31 (m, 14H)	3.49-3.42 (m, 2H)

Table 34: <sup>1</sup>H NMR data of the isopilo-n-naph hybrids **34a–c** measured in CD<sub>3</sub>OD (continued).

#	N(CH <sub>3</sub> ) <sub>2</sub>	8'-H	C(CH <sub>3</sub> ) <sub>2</sub>	7'-H	2'-H	3'-H	4'-H	HCO <sub>2</sub> '
<b>Isopilo-4-naph 34a</b>	3.35 (s, 6H)	3.65–3.55 (m, 4H)	1.32 (s, 6H)	4.37–4.29 (s, 4H)	8.51 (d, J = 7.2 Hz, 2H)	7.80 (dd, J = 7.2, 8.4 Hz, 2H)	8.35–8.31 (m, 4H)	8.35–8.31 (m, 4H)
<b>Isopilo-6-naph 34b</b>	3.28 (s, 6H)	3.54 (s, 2H)	1.34 (s, 6H)	4.34 (s, 2H)	8.61 (dd, J = 7.2, 1.0 Hz, 2H)	7.87 (dd, J = 7.2, 8.4 Hz, 2H)	8.42 (dd, J = 8.4, 1.0 Hz, 2H)	8.24 (s, 2H)
<b>Isopilo-8-naph 34c</b>	3.27 (s, 6H)	3.53 (m, 2H)	1.49–1.31 (m, 14H)	4.33 (s, 2H)	8.60 (d, J = 7.3 Hz, 2H)	7.86 (dd, J = 7.3, 8.3 Hz, 2H)	8.41 (d, J = 8.3, 2H)	8.34 (s, 2H)

Table 35: <sup>13</sup>C NMR data of the isopilo-n-naph hybrids **34a–c** measured in CD<sub>3</sub>OD.

#	N-CH <sub>3</sub>	C-2	C-4	C-5	C-6	C-7	C-8	-CH <sub>2</sub> -CH <sub>3</sub>	-CH <sub>2</sub> -CH <sub>3</sub>	-COO-	-CH <sub>2</sub> -O-	C-12'	C-11'	C-10'	C-9'
<b>Isopilo-4-naph 34a</b>	34.5	138.2	134.8	121.0	27.3	39.1	47.3	11.3	23.0	180.6	72.2	50.0	27.8	21.3	68.7
<b>Isopilo-6-naph 34b</b>	34.1	137.8*	134.6	120.9	27.1	39.1	47.3	11.2	23.0	180.6	72.0	50.5	30.8	23.4	69.6
<b>Isopilo-8-naph 34c</b>	34.1	138.0	134.7	121.0	27.2	39.1	47.3	11.2	23.1	180.4	71.9	50.8	31.0	23.9	69.8

\* determined from HMBC spectrum

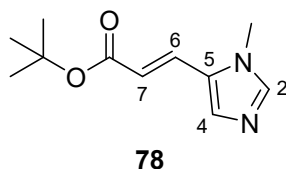
Table 36: <sup>13</sup>C NMR data of the isopilo-n-naph hybrids **34a–c** measured in CD<sub>3</sub>OD (continued).

#	N(CH <sub>3</sub> ) <sub>2</sub>	C-8'	C(CH <sub>3</sub> ) <sub>2</sub>	C-7'	-CON-	C-1'	C-2'	C-3'	C-4'	C-5'	C-6'	C-m	HCO <sub>2</sub> '
<b>Isopilo-4-naph 34a</b>	53.5	74.4	40.6	26.6	49.9	166.6	133.1	132.6	128.3	135.7	123.4	129.2	167.6
<b>Isopilo-6-naph 34b</b>	53.3	74.1	40.5	26.5	49.9	166.8	133.2	132.6	128.3	135.8	123.5	129.3	168.1
<b>Isopilo-8-naph 34c</b>	53.2	74.0	40.5	26.5	50.0	166.8	133.2	132.6	128.3	135.8	123.6	129.3	167.5

## 7.5 Synthesis of Pilocarpine Analogues for the Study of Pilocarpine's Binding Mode in mAChRs

### 7.5.1 Attempted Nonstereospecific Synthesis by Radical Ring Closure

#### Synthesis of *tert*-Butyl (*E*)-3-(1-Methyl-1*H*-imidazol-5-yl)acrylate (**78**)



At 0 °C, *tert*-butyl 2-(dimethoxyphosphoryl)acetate (**59**) (3.71 g, 16.5 mmol) (Chapter 7.3.4) was added to a suspension of sodium hydride (60% suspension in oil, 1.19 g, 29.8 mmol) in dry THF (80 mL). The mixture was stirred at 0 °C for 2 h, then a solution of the aldehyde (1.82 g, 16.5 mmol) in dry THF (40 mL) was added dropwise. The ice bath was removed and the reaction was stirred at RT overnight. Water was added and the reaction was extracted three times with diethyl ether. The combined organic layers were washed with brine. The layers were separated, the organic layer was dried over MgSO<sub>4</sub>, and evaporated. The biphasic oil was dissolved in a mixture of acetonitrile and *n*-hexane. The layers were separated, and the acetonitrile layer was evaporated to yield the product **78** as a yellow oil (2.03 g, 9.75 mmol, 59%).

Formula: C<sub>11</sub>H<sub>16</sub>N<sub>2</sub>O<sub>2</sub>;

MW: 208.26 g/mol;

R<sub>f</sub> (95:5 dichloromethane/MeOH) = 0.4;

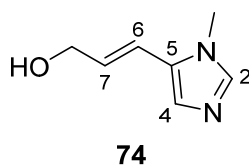
<sup>1</sup>H NMR (CDCl<sub>3</sub>, 400 MHz): δ (ppm) = 7.54 (s, 1H, **2-H**), 7.45–7.40 (m, 2H, **7-H**, **4-H**), 6.21 (d, 1H, *J* = 16.0 Hz, **6-H**), 3.71 (s, 3H, N-**CH**<sub>3</sub>), 1.52 (s, 9H, C(**CH**<sub>3</sub>)<sub>3</sub>);

<sup>13</sup>C NMR (CDCl<sub>3</sub>, 101 MHz): δ (ppm) = 166.4 (C<sub>q</sub>, **C=O**), 140.7 (CH, C-**2**), 131.8 (CH, C-**4**), 129.0 (C<sub>q</sub>, C-**5**), 128.6 (CH, C-**7**), 118.7 (CH, C-**6**), 80.9 (C<sub>q</sub>, C(**CH**<sub>3</sub>)<sub>3</sub>), 32.5 (CH<sub>3</sub>, N-**CH**<sub>3</sub>), 28.3 (CH<sub>3</sub>, C(**CH**<sub>3</sub>)<sub>3</sub>);

IR (ATR, cm<sup>-1</sup>): 2974, 2932, 1697, 1629, 1536, 1497, 1475, 1450, 1385, 1364, 1146, 1119, 972, 655, 646.

The spectral data correspond to literature data.<sup>[165]</sup>

#### Synthesis of (*E*)-3-(1-Methyl-1*H*-imidazol-5-yl)prop-2-en-1-ol (**74**)<sup>[81]</sup>



## Experimental

The *tert*-butylester **78** (1.76 g, 8.45 mmol) was dissolved in dry dichloromethane (60 mL) and a solution of diisobutylaluminium hydride (1 M in dichloromethane, 2.76 g, 19.4 mmol, 19.4 mL) was added dropwise. The reaction was complete after 90 min and was quenched at 0 °C by addition of water (0.78 mL), followed by 15% aqueous NaOH (0.78 mL), and water (1.94 mL). After warming to RT, the mixture was left in the fridge overnight. The solvents were evaporated to dryness and the solid residue was refluxed in ethanol and filtrated while warm. The filter cake was washed with ethanol before evaporating the combined filtrates. The crude product was purified by column chromatography (24 g silica, 3–5% MeOH/dichloromethane) to yield the product **74** as a yellow oil (865 mg, 6.26 mmol, 74%).

Formula: C<sub>7</sub>H<sub>10</sub>N<sub>2</sub>O;

MW: 138.17 g/mol;

R<sub>f</sub> (95:5 dichloromethane/MeOH) = 0.08;

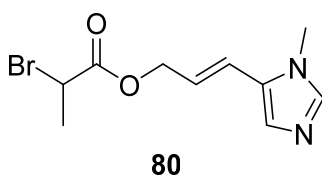
<sup>1</sup>H NMR (CDCl<sub>3</sub>, 400 MHz): δ (ppm) = 7.37 (s, 1H, **2-H**), 7.13 (s, 1H, **4-H**), 6.44 (d, *J* = 15.9 Hz, 1H, **6-H**), 6.21 (dt, *J* = 15.9, 5.3 Hz, 1H, **7-H**), 4.31 (dd, *J* = 5.3, 1.2 Hz, 2H, **-CH<sub>2</sub>-OH**), 3.61 (s, 2H, **N-CH<sub>3</sub>**), 2.36 (br. s, 1H, **OH**);

<sup>13</sup>C NMR (CDCl<sub>3</sub>, 101 MHz): δ (ppm) = 138.5 (CH, **C-2**), 130.6 (C<sub>q</sub>, **C-5**), 127.3 (CH, **C-4**), 129.9 (CH, **C-7**), 116.5 (CH, **C-6**), 63.3 (CH<sub>2</sub>, **-CH<sub>2</sub>-OH**), 32.0 (CH<sub>3</sub>, **N-CH<sub>3</sub>**);

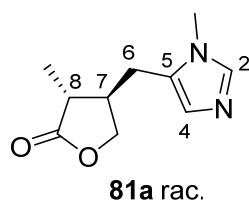
IR (ATR, cm<sup>-1</sup>): 3184 (br), 3120, 3004, 2856, 1671, 1652, 1609, 1500, 1451, 1414, 1024, 695.

The spectral data correspond to literature data.<sup>[81]</sup>

### Synthesis of (*E*)-3-(1-Methyl-1*H*-imidazol-5-yl)allyl 2-Bromopropanoate (**80**)<sup>[81]</sup>



The allyl alcohol **74** (123 mg, 890 μmol) was dissolved in dry chloroform (6 mL). At 0 °C, 2-bromopropanoyl bromide (192 mg, 890 μmol) as a solution in dry chloroform (1.9 mL) was added over 5 min. The reaction was stirred at 0 °C for 1 h, then for 1 h at RT. Saturated aqueous NaHCO<sub>3</sub> solution was added until pH>8. The aqueous mixture was extracted five times with dichloromethane. The combined organic layers were dried over MgSO<sub>4</sub>. The filtrate was completely evaporated at RT in vacuo. The product was immediately wetted with dry degassed acetonitrile (30 mL) to be used as a solution in the next reaction. The product is stable in solution but degrades when dry. As the TLC showed a spot-to-spot conversion, no further analysis was carried out.

Lactone Formation by Radical Cyclisation<sup>[81]</sup>

Azobisisobutyronitrile (0.2M in toluene, 99.5  $\mu\text{mol}$ , 498  $\mu\text{L}$ ) and tributyltin hydride (305 mg, 1.04 mmol, 282  $\mu\text{L}$ ) were added to a solution of allyl ester **80** (271.8 mg, 995  $\mu\text{mol}$ ) in degassed dry acetonitrile (30 mL). This emulsion was added through a syringe pump to a vessel with refluxing degassed dry acetonitrile (30 mL) over 5 h, followed by reflux for 19 h. The TLC showed the starting material and a new spot. The mixture was extracted two times with petroleum ether (40–65 °C). The petroleum ether fractions were discarded. The acetonitrile layers were evaporated to provide a yellow oil. Column chromatography (silica, 3–10% MeOH/dichloromethane) yielded 4 mg of the product (20.6  $\mu\text{mol}$ , 2%).

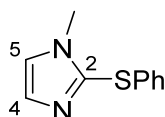
Formula:  $\text{C}_{10}\text{H}_{14}\text{N}_2\text{O}_2$ ;

MW: 194.23 g/mol;

$R_f$  (95:5 dichloromethane/MeOH) = 0.3;

$^1\text{H}$  NMR ( $\text{CDCl}_3$ , 400 MHz):  $\delta$  (ppm) = 7.92 (s, 1H, **2-H**), 6.82 (s, 1H, **4-H**), 4.43 (dd,  $J = 9.2, 7.4$  Hz, 1H, **-CH<sub>2</sub>-O-**), 3.91–3.84 (m, 1H, **-CH<sub>2</sub>-O-**), 3.58 (s, 3H, **N-CH<sub>3</sub>**), 2.90–2.83 (m, 1H, **7-H**), 2.74–2.63 (m, 1H, **8-H**), 2.52–2.41 (m, 1H, **6-H**), 2.37–2.29 (m, 1H, **6-H**), 1.26 (d,  $J = 7.1$  Hz, 3H, **-CH-CH<sub>3</sub>**).

The spectral data correspond to the data obtained for the same molecule on p.129.

7.5.2 Nonstereospecific Synthesis by Conjugate Addition to 3(2*H*)-FuranoneSynthesis of 1-Methyl-2-(Phenylthio)-1*H*-Imidazole (**89**)<sup>[137]</sup>

**89**

At  $-84$  °C, *n*-butyllithium (5 M in hexanes, 9.34 mL) was added to a solution of 1-methyl imidazole (3.76 g, 45.8 mmol, 3.65 mL) in dry THF (100 mL). After stirring for 30 min, the phenyl disulfide, prepared from thiophenol according to Kirihara et al.<sup>[136]</sup>, (10.0 g, 45.8 mmol) was added in one portion. After stirring for further 60 min at  $-84$  °C, the solid was completely dissolved and the reaction was warmed to RT. The reaction was quenched with methanol. A 2 M solution of hydrochloric acid was added until the aqueous layer was acidic. The mixture was extracted three times with cyclohexane.



## Experimental

Then, Na<sub>2</sub>CO<sub>3</sub> was added to the aqueous layer until pH>8 was reached. The mixture was extracted three times with dichloromethane. The combined dichloromethane layers were dried over MgSO<sub>4</sub> and evaporated under reduced pressure. The residue was purified by column chromatography (silica, 1:1 cyclohexane/ethyl acetate) to yield the product **89** as a slightly yellow oil (5.23 g, 27.5 mmol, 60%).

Formula: C<sub>10</sub>H<sub>10</sub>N<sub>2</sub>S;

MW: 190.26 g/mol;

R<sub>f</sub> (95:5 dichloromethane/MeOH) = 0.5;

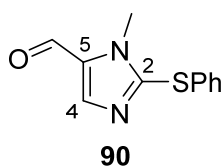
<sup>1</sup>H NMR (CDCl<sub>3</sub>, 400 MHz): δ (ppm) = 7.27–7.23 (m, 2H, **Ph**), 7.18–7.13 (m, 4H, **Ph**, **4-H**), 7.06 (br. s, 1H, **5-H**), 3.63 (s, 3H, N-**CH**<sub>3</sub>);

<sup>13</sup>C NMR (CDCl<sub>3</sub>, 101 MHz): δ (ppm) = 138.2 (C<sub>q</sub>, C-**2**), 135.1 (C<sub>q</sub>, C<sub>q</sub>-**Ph**), 130.3 (CH, C-**4**), 129.4, 128.1, 126.7 (CH, **Ph**), 123.9 (CH, C-**5**), 34.0 (CH<sub>3</sub>, N-**CH**<sub>3</sub>);

IR (ATR, cm<sup>-1</sup>): 3060, 2944, 1615, 1580, 1476, 1454, 1439, 1373, 739, 699, 685.

The spectral data correspond to literature data.<sup>[137]</sup>

### Synthesis of 1-Methyl-2-(Phenylthio)-1*H*-imidazole-5-Carbaldehyde (**90**)<sup>[138]</sup>



At –84 °C, *n*-butyllithium (5 M in hexanes, 4.65 mL) was added to a solution of **89** (2.21 g, 11.6 mmol) in dry THF (40 mL). After stirring for 15 min, dry DMF (4.25 g, 58.2 mmol, 4.48 mL) was added in one portion. After stirring for further 60 min at –84 °C, the reaction was warmed to RT and quenched with saturated aqueous NH<sub>4</sub>Cl solution. The mixture was extracted three times with ethyl acetate. The combined organic layers were dried over MgSO<sub>4</sub> and evaporated to provide the desired product **90** as a slightly yellow oil (2.23 g, 10.2 mmol, 88%).

Formula: C<sub>11</sub>H<sub>10</sub>N<sub>2</sub>OS;

MW: 218.27 g/mol;

R<sub>f</sub> (95:5 dichloromethane/MeOH) = 0.8;

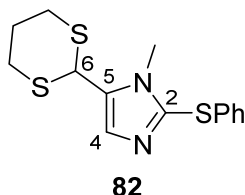
<sup>1</sup>H NMR (CDCl<sub>3</sub>, 400 MHz): δ (ppm) = 9.67 (s, 1H, **CHO**), 7.78 (s, 1H, **4-H**), 7.45–7.31 (m, 5H, **Ph**), 3.92 (s, 3H, N-**CH**<sub>3</sub>);

## Experimental

$^{13}\text{C}$  NMR ( $\text{CDCl}_3$ , 101 MHz):  $\delta$  (ppm) = 178.7 (CH, **CHO**), 150.1 ( $\text{C}_q$ , **C-2**), 143.7 (CH, **C-4**), 134.3 ( $\text{C}_q$ , **C-Ph**), 133.4 ( $\text{C}_q$ , **C-5**), 131.8, 129.8, 128.7 (CH, **Ph**), 33.6 ( $\text{CH}_3$ , **N-CH<sub>3</sub>**);

IR (ATR,  $\text{cm}^{-1}$ ): 3058, 2956, 2795, 2730, 1664, 1577, 1519, 1460, 1437, 1377, 1324, 751, 684.

### Synthesis of 5-(1,3-Dithian-2-yl)-1-Methyl-2-(Phenylthio)-1*H*-imidazole (**82**)<sup>[134]</sup>



The aldehyde **90** (6.00 g, 27.5 mmol) was dissolved in toluene (250 mL). *p*-Toluenesulfonic acid (6.27 g, 33.0 mmol) and 1,3-dimercaptopropane (2.97 g, 27.5 mmol, 2.75 mL) were added, and the mixture was refluxed with a Dean-Stark trap overnight. A 4 M solution of NaOH (30 mL) was added and the layers were separated. The organic layer was dried over  $\text{MgSO}_4$  and the solvent was evaporated. The product was recrystallised from ethyl acetate by addition of *n*-hexane to afford a white crystalline solid (5.70 g, 18.5 mmol, 67%).

Formula:  $\text{C}_{14}\text{H}_{16}\text{N}_2\text{S}_3$ ;

MW: 308.48 g/mol;

$R_f$  (95:5 dichloromethane/MeOH) = 0.9;

Melting point: 122–124 °C (*n*-hexane/ethyl acetate) (Lit<sup>[133]</sup>: 124 °C, solvent not reported);

$^1\text{H}$  NMR ( $\text{CDCl}_3$ , 400 MHz):  $\delta$  (ppm) = 7.30–7.23 (m, 3H, **Ph**, **4-H**), 7.20–7.14 (m, 3H, **Ph**), 5.18 (s, 1H, **6-H**), 3.70 (s, 2H, **N-CH<sub>3</sub>**), 3.06–2.90 (m, 4H, **-CH<sub>2</sub>-S-**), 2.20–2.13 (m, 1H, **-CH<sub>2</sub>-CH<sub>2</sub>-CH<sub>2</sub>-**), 2.01–1.90 (m, 1H, **-CH<sub>2</sub>-CH<sub>2</sub>-CH<sub>2</sub>-**);

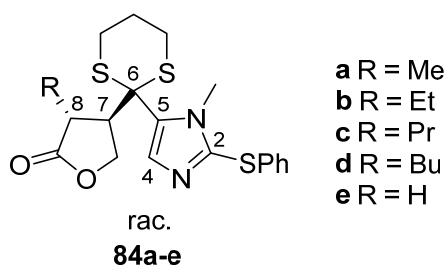
$^{13}\text{C}$  NMR ( $\text{CDCl}_3$ , 101 MHz):  $\delta$  (ppm) = 139.6 ( $\text{C}_q$ , **C-2**), 134.5 ( $\text{C}_q$ , **Ph**), 132.4 ( $\text{C}_q$ , **C-5**), 129.7 (CH, **C-4**), 129.4, 128.4, 126.9 (CH, **Ph**), 40.8 (CH, **C-6**), 32.1 ( $\text{CH}_3$ , **N-CH<sub>3</sub>**), 31.4 ( $\text{CH}_2$ , **-CH<sub>2</sub>-S-**), 25.0 ( $\text{CH}_2$ , **-CH<sub>2</sub>-CH<sub>2</sub>-CH<sub>2</sub>-**);

IR (ATR,  $\text{cm}^{-1}$ ): 3102, 3071, 2901, 2824, 1648, 1578, 1478, 1448, 1371, 771, 738, 697, 686.

The spectral data correspond to literature data.<sup>[133]</sup>

## Experimental

### General Procedure for the One-Pot Michael-Addition-Alkylation Reaction<sup>[133]</sup>



At  $-84\text{ }^{\circ}\text{C}$ , *n*-butyllithium (2.5 M in hexanes, 1.30 eq.) was added to a solution of **82** (1.00 eq.) in dry THF (30 mL/1 g of dithiane). After stirring for 30 min, furan-2(5*H*)-one (1.10 eq.) was added in one portion. After stirring for further 2 h at  $-84\text{ }^{\circ}\text{C}$ , the respective iodoalkane (1.20 eq.) was added and the reaction was left to slowly reach RT. After quenching with saturated aqueous  $\text{NH}_4\text{Cl}$  solution, the mixture was extracted three times with ethyl acetate. The combined organic layers were dried over  $\text{MgSO}_4$  and evaporated. The crude was purified by column chromatography (silica, 70:30 cyclohexane/ethyl acetate) to achieve the desired product.

**Table 37:** General data of the fully protected *trans*-isomers **84a–e** of the analogues of pilocarpine.

R	#	Formula	MW [g/mol]	Aspect	Yield [%]	Melting point [ $^{\circ}\text{C}$ ] (from cyclohexane/ethyl acetate)
H	<b>84e</b>	$\text{C}_{18}\text{H}_{20}\text{N}_2\text{O}_2\text{S}_3$	392.55	yellow oil	89	-
Me	<b>84a</b>	$\text{C}_{19}\text{H}_{22}\text{N}_2\text{O}_2\text{S}_3$	406.48	white solid	95	149
Et	<b>84b</b>	$\text{C}_{20}\text{H}_{24}\text{N}_2\text{O}_2\text{S}_3$	420.60	white solid	62 (Lit <sup>[133]</sup> : 76)	137–138 (Lit <sup>[133]</sup> : 135 from $\text{Et}_2\text{O}$ )
Pr	<b>84c</b>	$\text{C}_{21}\text{H}_{26}\text{N}_2\text{O}_2\text{S}_3$	434.63	white solid	68	129–131
Bu	<b>84d</b>	$\text{C}_{22}\text{H}_{28}\text{N}_2\text{O}_2\text{S}_3$	448.66	white solid	53	116–117

**Table 38:** IR data of the fully protected *trans*-isomers **84a–e** of the analogues of pilocarpine.

R	#	IR data [ $\text{cm}^{-1}$ ]
H	<b>84e</b>	3056, 2949, 2905, 1770, 1580, 1514, 1477, 1439, 1169, 1020, 739, 699, 687
Me	<b>84a</b>	3067, 2944, 2893, 1756, 1582, 1520, 1473, 1440, 1176, 1023, 741, 698, 688
Et	<b>84b</b>	3060, 2962, 2906, 1755, 1582, 1509, 1463, 1439, 1181, 1037, 740, 700, 686
Pr	<b>84c</b>	3071, 2950, 2911, 1752, 1582, 1507, 1476, 1438, 1181, 1040, 734, 701, 685
Bu	<b>84d</b>	3067, 2948, 2914, 1751, 1582, 1517, 1477, 1437, 1177, 1039, 733, 700, 687

Table 39: <sup>1</sup>H NMR data of the fully protected *trans*-isomers **84a-e** of the analogues of pilocarpine measured in CDCl<sub>3</sub>.

R	#	N-CH <sub>3</sub>	4-H	-CH <sub>2</sub> S-	-CH <sub>2</sub> -CH <sub>2</sub> -CH <sub>2</sub> -	7-H	8-H	-CH <sub>2</sub> -O-	R-H	Ph-H
H	<b>84e</b>	3.84 (s, 3H)	7.52 (s, 1H)	3.05-2.71 (m, 6H)	2.14-2.00 (m, 1H), 1.97-1.82 (m, 1H)	3.25-3.16 (m, 1H),	3.05-2.71 (m, 6H)	4.57-4.49 (m, 1H), 4.21-4.13 (m, 1H)	-	7.33-7.11 (m, 5H)
Me	<b>84a</b>	3.85 (s, 3H)	7.52 (s, 1H)	3.14-2.63 (m, 6H)	2.14-2.00 (m, 1H), 1.97-1.82 (m, 1H)	3.14-2.63 (m, 6H)	3.14-2.63 (m, 6H)	4.71-4.52 (m, 1H), 4.34-4.21 (m, 1H)	0.9 (d, J = 5.6 Hz, 3H)	7.29-7.19 (m, 5H)
Et	<b>84b</b>	3.84 (s, 3H)	7.53 (s, 1H)	3.02-2.68 (m, 6H)	2.08-2.02 (m, 1H), 1.93-1.82 (m, 1H)	3.02-2.68 (m, 6H)	3.02-2.68 (m, 6H)	4.70-4.55 (m, 1H), 4.26-4.16 (m, 1H)	1.52-1.24 (m, 2H), 0.77 (t, J = 7.2 Hz, 3H)	7.30-7.18 (m, 5H)
Pr	<b>84c</b>	3.84 (s, 3H)	7.54 (s, 1H)	3.10-2.64 (m, 6H)	2.11-1.99 (m, 1H), 1.96-1.80 (m, 1H)	3.10-2.64 (m, 6H)	3.10-2.64 (m, 6H)	4.80-4.77 (m, 1H), 4.31-4.10 (m, 1H)	1.45-1.18 (m, 4H), 0.79 (t, J = 7.1 Hz, 3H)	7.37-7.18 (m, 5H)
Bu	<b>84d</b>	3.84 (s, 3H)	7.53 (s, 1H)	3.05-2.68 (m, 6H)	2.07-2.03 (m, 1H), 1.94-1.83 (m, 1H)	3.05-2.68 (m, 6H)	3.05-2.68 (m, 6H)	4.72-4.54 (m, 1H), 4.28-4.11 (m, 1H)	1.51-1.18 (m, 6H), 0.82 (t, 3H, J = 6.6 Hz)	7.30-7.19 (m, 5H)

Table 40: <sup>13</sup>C NMR data of the fully protected *trans*-isomers **84a-e** of the analogues of pilocarpine measured in CDCl<sub>3</sub>.

R	#	N-CH <sub>3</sub>	C-2	C-4	C-5	C-6	-CH <sub>2</sub> S-	-CH <sub>2</sub> -CH <sub>2</sub> -	C-7	C-8
H	<b>84e</b>	34.4	143.0	135.4	131.8	53.6	27.8, 27.7	24.5	43.9	30.1
Me	<b>84a</b>	34.3	142.9	135.8	132.0	53.2	28.1, 27.4	24.6	51.2	35.6
Et	<b>84b</b>	34.4	142.8	135.7	131.8	54.5	27.7, 27.5	24.5	47.5	41.9
Pr	<b>84c</b>	34.5	142.9	135.9	131.9	54.7	27.7, 27.6	24.5	48.4	40.8
Bu	<b>84d</b>	34.5	142.8	135.8	131.7	54.6	27.7, 27.5	24.5	48.3	440.9

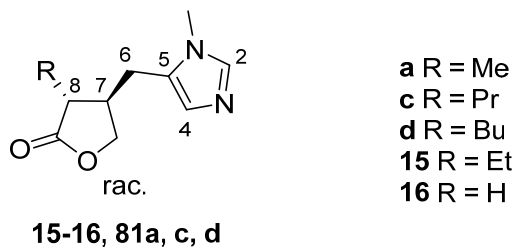
Table 41: <sup>13</sup>C NMR data of the fully protected *trans*-isomers **84a-e** of the analogues of pilocarpine measured in CDCl<sub>3</sub> (continued).

R	#	C=O	-CH <sub>2</sub> -O-	R	Ph
H	<b>84e</b>	175.4	68.2	-	133.9 (C <sub>q</sub> ), 129.6, 128.7, 127.3
Me	<b>84a</b>	178.4	66.9	16.3	133.8 (C <sub>q</sub> ), 129.5, 129.0, 127.4
Et	<b>84b</b>	178.0	67.1	23.9, 10.4	133.8 (C <sub>q</sub> ), 129.5, 128.9, 127.3
Pr	<b>84c</b>	178.2	67.1	33.3, 19.6, 13.6	133.8 (C <sub>q</sub> ), 129.6, 128.9, 127.4
Bu	<b>84d</b>	178.2	67.1	30.8, 28.3, 22.5, 14.0	133.8 (C <sub>q</sub> ), 129.6, 128.9, 127.3

### Preparation of Raney Nickel<sup>[166]</sup>

Sodium hydroxide (38 g) were dissolved in water (150 mL). While cooling with an ice bath, nickel-aluminium-alloy (38 g) was added in small portions to the solution of sodium hydroxide. The suspension was left to reach RT, then it was heated to 70 °C for 1 h. Back at RT, the suspension was decanted and washed with distilled water by repeated decantation until the pH was neutral. Ten further washings were applied. The suspension in water was stored in the fridge. The amount needed for the deprotection reactions was washed three times with methanol and three times with dry methanol immediately before use.

### General Procedure for the Deprotection of the Fully Protected *trans*-Isomers of the Analogues of Pilocarpine<sup>[133]</sup>



The respective fully protected precursor molecule **84a–e** (1.00 eq.) was dissolved in methanol (24 mL/500 mg) and a suspension of freshly prepared Raney nickel in methanol (4 mL) was added. The mixture was refluxed for 4 h whilst stirring vigorously. As the TLC (95:5 dichloromethane/MeOH, UV) showed various spots, more Raney nickel (2 mL) was added, and the mixture was refluxed further. This was repeated until the TLC did not show any spots under the UV lamp and only one new spot could be revealed by Dragendorff's reagent. The mixture was filtered through a double filter paper. The filtrate was evaporated and the residue was suspended in dichloromethane and filtered again. Then, the filtrate was evaporated to yield the product as a colourless oil. The product was purified by preparative HPLC (method V, Chapter 7.1.4).

The product **16** (R = H) was 95% pure by HPLC analysis (achiral method B, Chapter 7.1.8).

Table 42: General data of the deprotected *trans*-isomers of the analogues of pilocarpine **81a**, **c**, **d** and **15–16**.

R	#	Formula	MW [g/mol]	aspect	Yield [%]	IR data [cm <sup>-1</sup> ]	de
H	16	C <sub>9</sub> H <sub>12</sub> N <sub>2</sub> O <sub>2</sub>	180.21	colourless oil	23	3121, 2913, 1765, 1660, 1508, 1441, 1174, 1013, 754, 663	-
Me	81a	C <sub>10</sub> H <sub>14</sub> N <sub>2</sub> O <sub>2</sub>	194.23	colourless oil	20	3118, 2905, 1760, 1641, 1505, 1455, 1179, 1007, 759, 662	81
Et	15	C <sub>11</sub> H <sub>16</sub> N <sub>2</sub> O <sub>2</sub>	208.26	colourless oil	25	3119, 2911, 1760, 1647, 1505, 1458, 1174, 1011, 754, 663	78
Pr	81c	C <sub>12</sub> H <sub>18</sub> N <sub>2</sub> O <sub>2</sub>	222.29	colourless oil	27	3112, 2911, 1752, 1582, 1507, 1476, 1181, 1015, 734, 669	79
Bu	81d	C <sub>13</sub> H <sub>20</sub> N <sub>2</sub> O <sub>2</sub>	236.32	colourless oil	24	3107, 2928, 1762, 1557, 1505, 1466, 1162, 1014, 731, 663	77

Table 43: <sup>1</sup>H NMR data of the deprotected *trans*-isomers of the analogues of pilocarpine **81a**, **c**, **d** and **15–16** measured in CDCl<sub>3</sub>.

R	#	N-CH <sub>3</sub>	2-H	4-H	6-H	7-H	-CH <sub>2</sub> O-	R-H	8-H
H	16	3.56 (s, 3H)	7.42 (s, 1H)	6.80 (s, 1H)	2.78–2.71 (m, 3H),	2.95–2.83 (m, 1H)	4.45 (dd, J = 9.3, 7.0 Hz, 1H),	-	2.78–2.71 (m, 3H)
Me	81a	3.53 (s, 3H)	7.37 (s, 1H)	6.75 (s, 1H)	2.83 (dd, J = 17.6, 6.1 Hz, 1H),	2.47–2.37 (m, 1H)	4.06 (dd, J = 9.3, 5.4 Hz, 1H),	1.20 (d, J = 7.1 Hz, 3H)	2.29 (dq, J = 9.6, 7.1 Hz, 1H)
Et	15	3.60 (s, 3H)	7.57 (s, 1H)	6.84 (s, 1H)	2.63 (dd, J = 15.5, 9.0 Hz, 1H),	2.74–2.45 (m, 2H)	4.41 (dd, J = 9.3, 7.2 Hz, 1H),	1.83–1.65 (m, 2H),	2.29 (ddd, J = 3x6.6 Hz, 1H)
Pr	81c	3.60 (s, 3H)	7.59 (s, 1H)	6.83 (s, 1H)	2.85 (dd, J = 15.3, 5.5 Hz, 1H),	2.77–2.51 (m, 2H)	3.92 (dd, J = 9.3, 6.7 Hz, 1H),	1.80–1.35 (m, 4H),	2.32 (ddd, J = 3x6.7 Hz, 1H)
Bu	81d	3.59 (s, 3H)	7.49 (s, 1H)	6.82 (s, 1H)	2.84 (dd, J = 15.4, 5.6 Hz, 1H),	2.63–2.54 (m, 1H)	4.40 (dd, J = 9.4, 7.2 Hz, 1H),	0.95 (t, J = 7.2 Hz, 3H)	2.32 (ddd, J = 3x6.7 Hz, 1H)
					2.77–2.51 (m, 2H)		3.92 (dd, J = 9.4, 6.5 Hz, 1H),	1.81–1.57 (m, 2H),	
					2.84 (dd, J = 15.3, 5.5 Hz, 1H),		4.41 (dd, J = 9.3, 7.2 Hz, 1H),	1.53–1.27 (m, 4H),	
					2.67 (dd, J = 15.3, 9.4 Hz, 1H)		3.92 (dd, J = 9.4, 6.5 Hz, 1H)	0.91 (t, J = 7.1 Hz, 3H)	

Table 44: <sup>13</sup>C NMR data of the deprotected *trans*-isomers of the analogues of pilocarpine **81a**, **c**, **d** and **15–16** measured in CDCl<sub>3</sub>.

R	#	N-CH <sub>3</sub>	C-2	C-4	C-5	C-6	C-7	-CH <sub>2</sub> O-	C-R	C-8	C=O
H	16	31.5	138.6	127.3	128.5	27.8	34.6	72.7	-	176.3	34.5
Me	81a	31.4	138.3	127.1	128.1	26.3	40.3	71.0	14.1	179.1	42.4
Et	15	31.7	138.3	126.5	128.6	27.6	39.2	71.1	22.6, 11.2	178.3	46.7
Pr	81c	31.7	138.2	126.4	128.6	27.6	39.8	71.1	31.8, 20.3, 14.1	178.6	45.3
Bu	81d	31.6	138.3	126.9	128.5	27.6	39.8	71.2	29.4, 29.1, 22.7, 14.0	178.6	45.5

## General procedure for Fractional Crystallisation

The racemic pilocarpine analogue to crystallise (1.00 eq.) and one enantiomer of the specified chiral acid (0.50 eq.) were dissolved at reflux in as few ethanol as possible. After cooling to RT and storage at  $-20\text{ }^{\circ}\text{C}$  overnight, the crystals were recovered by filtration. The mother liquor was concentrated in vacuo and the other enantiomer of the chiral acid (0.50 eq.) was added. This mixture was crystallised in the same way as the first crystallisation and the crystals were recovered by filtration. Both fractions of crystals were recrystallised from ethanol several times to observe enrichment of one or the other enantiomer of the basic compound. The crystals were analysed by HPLC using chiral method A or B (Chapter 7.1.8).

### Fractional Crystallisation of *rac*-Isopilocarpine (*rac*-15)

*rac*-Isopilocarpine (**15**) was crystallised with D- or L-tartaric acid according to the general procedure for fractional crystallisation and recrystallised once. The resulting crystals were analysed with chiral method A (Figure 52). No enrichment of one or the other enantiomer was observed (Table 45).

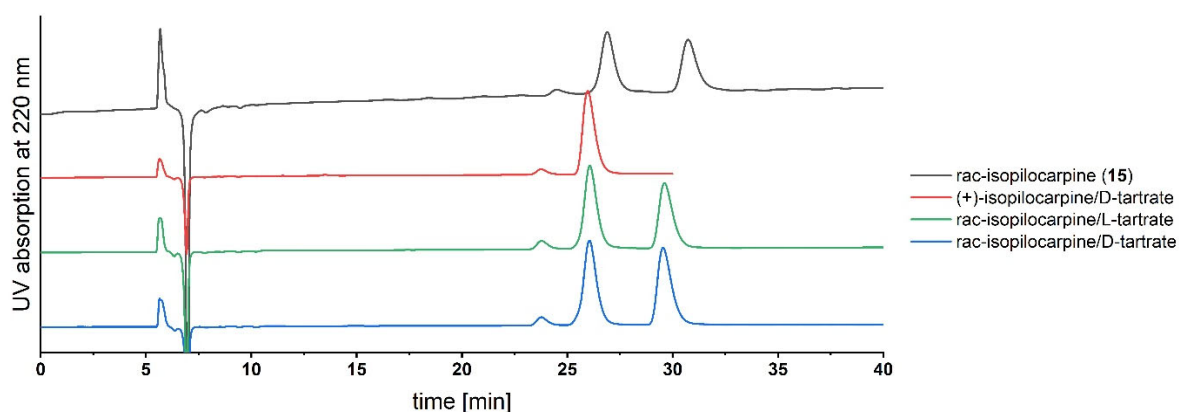


**Figure 52:** Chromatograms (chiral method A) of racemic isopilocarpine (*rac*-15), (+)-isopilocarpine D-tartrate ((+)-isopilocarpine/D-tartrate) and the crystals resulting from the attempted fractional crystallisation of *rac*-isopilocarpine with D- or L-tartrate (*rac*-isopilocarpine/D-tartrate and *rac*-isopilocarpine/L-tartrate, respectively).

**Table 45:** Analysis of the enantiomeric composition of the isopilocarpine tartrate crystals.

Sample	Peak area of (+)-isopilocarpine	Peak area of (–)-isopilocarpine	Enantiomeric ratio
<i>rac</i> -15 L-tartrate	7299	6154	54:46
<i>rac</i> -15 D-tartrate	8420	8224	50:50

*rac*-Isopilocarpine (**15**) was crystallised with D- or L-O,*O'*-*p*-toluoyltartaric acid according to the general procedure for fractional crystallisation and recrystallised once. The resulting crystals were analysed with chiral method B (Chapter 7.1.8). Separation of the enantiomers was achieved after 5–10 recrystallisations (Figure 37). The crystals contained 8% of their C3-epimers.

### Fractional Crystallisation of the *trans*-Analogues of Pilocarpine

The *trans*-analogues of pilocarpine **81a** and **81c** were recrystallised with the enantiomers of *O,O'*-*p*-toluoyltartaric acid. The crystals were analysed every five recrystallisations. Almost no enrichment was observed with the methyl analogue **81a** (Figure 53). The propyl analogue **81c** was not separated after 15 crystallisations although strong enrichment was achieved (Figure 54).

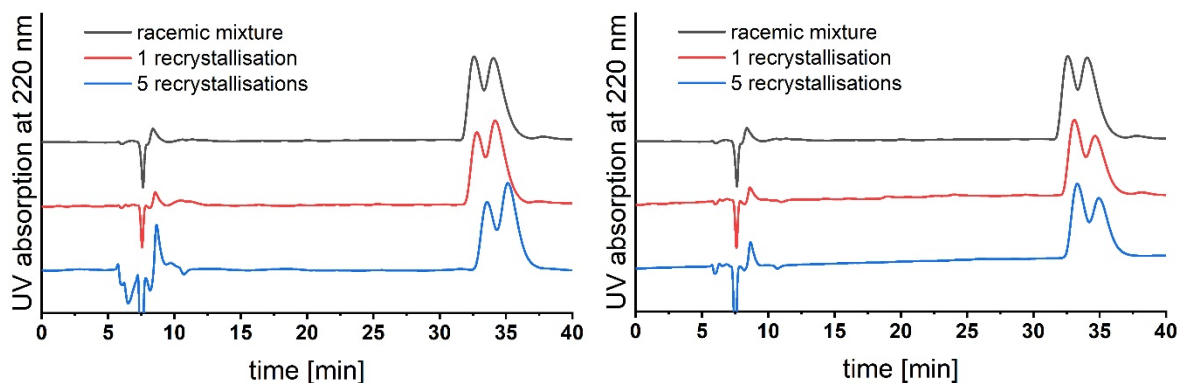


**Figure 53:** Chromatograms (chiral method B) of the crystals resulting from the attempted fractional crystallisation of the methyl analogue of isopilocarpine (**81a**) with *D*- or *L*-tartrate (left and right, respectively).

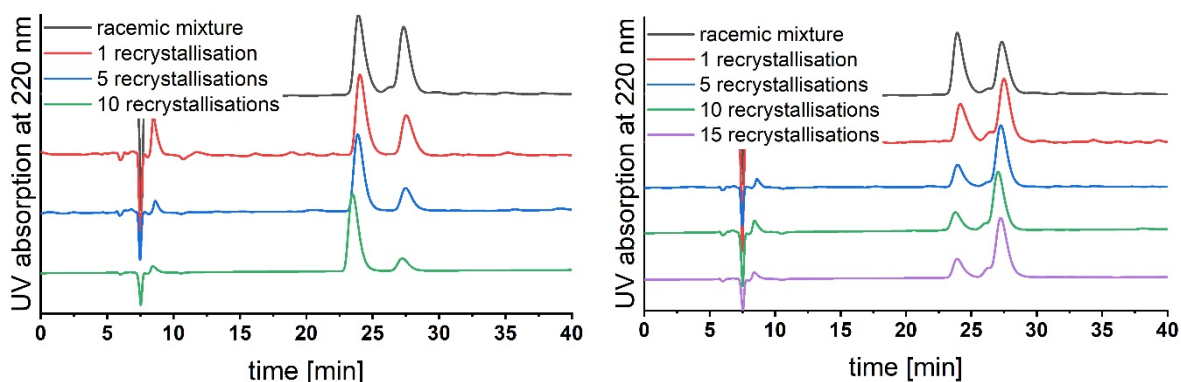
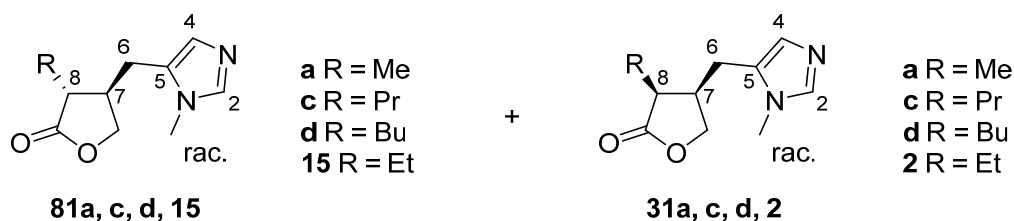


**Figure 54:** Chromatograms (chiral method B) of the crystals resulting from the attempted fractional crystallisation of the propyl analogue of isopilocarpine (**81c**) with *D*- or *L*-tartrate (left and right, respectively).

### General Procedure for the Epimerisation of the Enantiomeric Mixture of the *trans*-isomers<sup>[95]</sup>



A solution of lithium diisopropylamide (3.00 eq.) was added to dry THF (10 mL/mmol) at  $-84\text{ }^{\circ}\text{C}$ . A solution of the respective enantiomeric mixture of the deprotected *trans*-isomers of the analogues of pilocarpine **81a, c, d, 15** (1.00 eq.) in dry THF (15 mL/mmol) was slowly added and the mixture was



## Experimental

stirred at  $-84\text{ }^{\circ}\text{C}$  for 2 h before quenching the reaction by a one-shot addition of a solution of 2,6-di-*tert*-butyl-4-methylphenol (9.00 eq.) in dry THF (7 mL/mmol). The reaction was slowly warmed to RT and dilute HCl was added until the apparent pH was below 4. The aqueous phase was extracted with chloroform, then the pH of the aqueous layer was adjusted to 8 by addition of  $\text{Na}_2\text{CO}_3$ . The aqueous layer was extracted with chloroform. The combined organic layers from the latter extractions were dried over  $\text{MgSO}_4$  and the solvents were removed under reduced pressure. The compound was purified by preparative HPLC (method V, Chapter 7.1.4). The diastereomeric composition was determined by comparison of the proton integrals of the lactone  $\text{CH}_2$ -group in the  $^1\text{H}$  NMR spectrum.

**Table 46:** General data of the diastereomeric mixtures of the analogues of pilocarpine.

R	#	Formula	MW [g/mol]	aspect	yield [%]	de [%] of the <i>cis</i> -diastereomers
Me	<b>81a/31a</b>	$\text{C}_{10}\text{H}_{14}\text{N}_2\text{O}_2$	194.23	colourless oil	14	-53 to +30
Et	<b>15/2</b>	$\text{C}_{11}\text{H}_{16}\text{N}_2\text{O}_2$	208.26	colourless oil	18	+22
Pr	<b>81c/31c</b>	$\text{C}_{12}\text{H}_{18}\text{N}_2\text{O}_2$	222.29	colourless oil	16	-30 to +3
Bu	<b>81d/31d</b>	$\text{C}_{13}\text{H}_{20}\text{N}_2\text{O}_2$	236.32	colourless oil	20	-34 to +8

**Table 47:** IR data of the diastereomeric mixtures of the analogues of pilocarpine.

R	#	IR data [ $\text{cm}^{-1}$ ]
Me	<b>81a/31a</b>	3108, 2910, 1763, 1558, 1505, 1455, 1178, 1010, 722, 664
Et	<b>15/2</b>	3118, 2905, 1765, 1558, 1505, 1460, 1174, 1019, 748, 664
Pr	<b>81c/31c</b>	3114, 2872, 1761, 1559, 1505, 1466, 1164, 1015, 735, 663
Bu	<b>81d/31d</b>	3119, 2859, 1763, 1556, 1504, 1466, 1162, 1016, 758, 663

**Table 48:**  $^1\text{H}$  NMR data of the *cis*-isomers of the analogues of pilocarpine **2**, **31a**, **c** and **d** measured in  $\text{CDCl}_3$ . The spectra show the signals of the *cis*- and the *trans*-isomers, the signals of the *trans*-isomers being reported in the previous step.

R	#	N- $\text{CH}_3$	2-H	4-H	6-H	7-H
Me	<b>31a</b>	3.55 (s, 3H)	7.42 (s, 1H)	6.78 (s, 1H)	2.89–2.79 (m, 2H); 2.76–2.63 (m, 1H)	2.89–2.79 (m, 2H)
Et	<b>2</b>	3.55 (s, 3H)	7.44 (s, 1H)	6.79 (s, 1H)	2.71–2.50 (m, 2H); 2.39 (dd, $J = 15.4, 12.0$ Hz, 1H)	2.88–2.75 (m, 1H)
Pr	<b>31c</b>	3.53 (s, 3H)	7.37 (s, 1H)	6.74 (s, 1H)	2.71–2.48 (m, 2H); 2.40–2.33 (m, 1H)	2.82–2.73 (m, 1H)
Bu	<b>31d</b>	3.53 (s, 3H)	7.37 (s, 1H)	6.73 (s, 1H)	2.67–2.59 (m, 2H); 2.36 (dd, $J = 15.5, 12.0$ Hz, 1H)	2.81–2.73 (m, 1H)

## Experimental

**Table 49:**  $^1\text{H}$  NMR data of the *cis*-isomers of the analogues of pilocarpine **2**, **31a**, **c** and **d** measured in  $\text{CDCl}_3$ . The spectra show the signals of the *cis*- and the *trans*-isomers, the signals of the *trans*-isomers being reported in the previous step (continued).

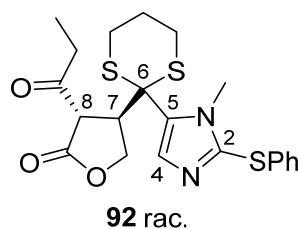
R	#	$-\text{CH}_2-\text{O}-$	R-H	8-H
Me	<b>31a</b>	4.25 (dd, $J = 9.4, 5.4$ Hz, 1H); 4.05 (dd, $J = 9.4, 2.9$ Hz, 1H)	1.27–1.23 (m, 6H)	2.51 - 2.38 (m, 1H)
Et	<b>2</b>	4.17 (dd, $J = 9.4, 5.5$ Hz, 1H); 4.06 (dd, $J = 9.4, 2.2$ Hz, 1H)	1.94–1.81 (m, 1H); 1.62–1.49 (m, 1H); 1.09 (t, $J = 7.4$ Hz)	2.71–2.50 (m, 2H)
Pr	<b>31c</b>	4.15 (dd, $J = 9.4, 5.3$ Hz, 1H); 4.05 (dd, $J = 9.4, 2.2$ Hz, 1H)	1.79–1.43 (m, 4H); 0.97–0.88 (m, 3H)	2.71–2.48 (m, 2H)
Bu	<b>31d</b>	4.13 (dd, $J = 9.4, 5.4$ Hz, 1H); 4.03 (dd, $J = 9.4, 2.2$ Hz, 1H)	1.84–1.76 (m, 1H); 1.70–1.23 (m, 5H); 0.90–0.83 (m, 3H)	2.67–2.59 (m, 1H)

**Table 50:**  $^{13}\text{C}$  NMR data of the *cis*-isomers of the analogues of pilocarpine **2**, **31a**, **c** and **d** measured in  $\text{CDCl}_3$ . The spectra show the signals of the *cis*- and the *trans*-isomers, the signals of the *trans*-isomers being reported in the previous step.

R	#	N- $\text{CH}_3$	C-2	C-4	C-5	C-6	C-7	$-\text{CH}_2-\text{O}-$	C-R	C=O	C-8
Me	<b>31a</b>	31.5	138.3	126.8	128.6	22.1	37.9	70.2	10.2	179.0	38.1
Et	<b>2</b>	31.5	138.4	126.9	128.5	21.4	37.3	69.9	18.4, 12.3	178.0	44.9
Pr	<b>31c</b>	31.4	138.2	127.1	128.6	21.5	37.5	69.9	27.0, 20.8, 13.9	178.6	43.0
Bu	<b>31d</b>	31.3	138.2	126.8	128.3	21.4	37.4	69.8	24.6, 29.7, 22.5, 13.8	178.6	43.2

### 7.5.3 Attempted Stereospecific Synthesis by Hydrogenation of an Exocyclic Double Bond

#### Synthesis of *rac*-(3*S*,4*R*)-4-(2-(1-Methyl-2-(Phenylthio)-1*H*-imidazol-5-yl)-1,3-Dithian-2-yl)-3-Propionylidihydrofuran-2(3*H*)-one (**92**)



A solution of *n*-butyllithium (2.5 M in hexanes, 4.51 mmol, 1.80 mL) was slowly added to a solution of **82** (1.07 g, 3.47 mmol) in dry THF (24 mL) at  $-84^\circ\text{C}$ . After stirring for 45 min, furan-2(5*H*)-one (328 mg, 3.81 mmol, 276  $\mu\text{L}$ ) was added in one portion. After stirring for further 2 h at  $-84^\circ\text{C}$ , propionic anhydride (474 mg, 3.64 mmol, 465  $\mu\text{L}$ ) was added and the reaction was left to slowly reach RT. After quenching with saturated aqueous  $\text{NH}_4\text{Cl}$  solution, the mixture was extracted three times with ethyl acetate. The combined organic layers were dried over  $\text{MgSO}_4$  and evaporated. The crude product was purified by column chromatography (silica, 70:30 cyclohexane/ethyl acetate) to provide the desired product as a white solid (1.19 g, 2.65 mmol, 77%).

Formula:  $\text{C}_{21}\text{H}_{24}\text{N}_2\text{O}_3\text{S}_3$ ;

## Experimental

MW: 448.61 g/mol;

R<sub>f</sub> (2:1 cyclohexane/EtOAc) = 0.4;

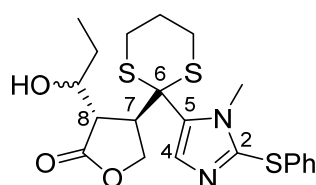
Melting point: 140–142 °C (cyclohexane/ethyl acetate);

<sup>1</sup>H NMR (CDCl<sub>3</sub>, 400 MHz): δ (ppm) = 7.45 (s, 1H, **4-H**), 7.34–7.25 (m, 5H, **Ph-H**), 4.73–4.58 (m, 1H, -CH<sub>2</sub>-O-), 4.40–4.28 (m, 1H, -CH<sub>2</sub>-O-), 4.03–3.91 (m, 4H, N-CH<sub>3</sub>, **7-H**), 3.07–2.88 (m, 2H, -CH<sub>2</sub>-CH<sub>3</sub>), 2.86–2.68 (m, 4H, -CH<sub>2</sub>-S-), 2.47–2.24 (m, 1H, **8-H**), 2.11–1.00 (m, 1H, -CH<sub>2</sub>-CH<sub>2</sub>-CH<sub>2</sub>-), 1.95–1.81 (m, 1H, -CH<sub>2</sub>-CH<sub>2</sub>-CH<sub>2</sub>-), 0.99–0.83 (m, 3H, -CH<sub>2</sub>-CH<sub>3</sub>);

<sup>13</sup>C NMR (CDCl<sub>3</sub>, 101 MHz): δ (ppm) = 202.0 (C<sub>q</sub>, C=O<sub>ketone</sub>), 170.9 (C<sub>q</sub>, C=O<sub>lactone</sub>), 143.3 (C<sub>q</sub>, C-**2**), 134.1 (C<sub>q</sub>, **Ph**), 133.2 (CH, C-**4**), 131.6 (C<sub>q</sub>, C-**5**), 129.5, 129.2, 127.4 (CH, **Ph**), 67.3 (CH<sub>2</sub>, -CH<sub>2</sub>-O-), 54.4 (C<sub>q</sub>, C-**6**), 53.0 (CH, C-**8**), 44.4 (CH, C-**7**), 36.4 (CH<sub>2</sub>, -CH<sub>2</sub>-CH<sub>3</sub>), 34.4 (CH<sub>3</sub>, N-CH<sub>3</sub>), 27.7 (CH<sub>2</sub>, -CH<sub>2</sub>-S-), 27.5 (CH<sub>2</sub>, -CH<sub>2</sub>-S-), 24.3 (CH<sub>2</sub>, -CH<sub>2</sub>-CH<sub>2</sub>-CH<sub>2</sub>-), 7.49 (CH<sub>3</sub>, -CH<sub>2</sub>-CH<sub>3</sub>);

IR (ATR, cm<sup>-1</sup>): 2975, 2902, 1760, 1717, 1582, 1517, 1476, 1457, 1438, 1379, 1174, 1024, 739, 687, 675.

### Synthesis of *rac*-(3*S*,4*R*)-3-(1-Hydroxypropyl)-4-(2-(1-Methyl-2-(Phenylthio)-1*H*-Imidazol-5-yl)-1,3-Dithian-2-yl)dihydrofuran-2(3*H*)-one (**93**)



NaBH<sub>4</sub> (37.1 mg, 981 μmol) was added to a solution of **92** (1.76 g, 3.93 mmol) in dry methanol (40 mL) at 0 °C. The reaction was complete after 20 min. Dilute HCl was added to quench the excess of NaBH<sub>4</sub>. Na<sub>2</sub>CO<sub>3</sub> was added to adjust the pH to 8. The mixture was extracted with chloroform. The combined organic layers were dried over MgSO<sub>4</sub> and the solvents were evaporated to yield the product as a white solid (1.93 g, 4.26 mmol, 99%).

Formula: C<sub>21</sub>H<sub>26</sub>N<sub>2</sub>O<sub>3</sub>S<sub>3</sub>;

MW: 450.63 g/mol;

R<sub>f</sub> (2:1 cyclohexane/EtOAc) = 0.3;

Melting point: 174–175 °C (chloroform);

<sup>1</sup>H NMR (CDCl<sub>3</sub>, 400 MHz): δ (ppm) = 7.62 (s, 1H, **4-H**), 7.47–7.27 (m, 5H, **Ph**), 4.88–4.57 (m, 1H, -CH<sub>2</sub>-O-), 4.40–4.20 (m, 1H, -CH<sub>2</sub>-O-), 3.95 (s, 3H, N-CH<sub>3</sub>), 3.86–3.71 (m, 1H, **8-H**), 3.20–3.14 (m, 1H,

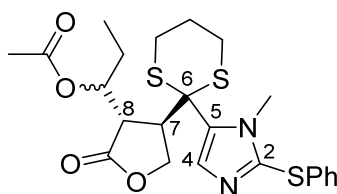
## Experimental

7-H), 3.04–2.65 (m, 5H, -CH<sub>2</sub>-S-, -CH-OH), 2.44 (br. s, 1H, OH), 2.08–2.02 (m, 1H, -CH<sub>2</sub>-CH<sub>2</sub>-CH<sub>2</sub>-), 1.92–1.81 (m, 1H, -CH<sub>2</sub>-CH<sub>2</sub>-CH<sub>2</sub>-), 1.29–1.20 (m, 2H, -CH<sub>2</sub>-CH<sub>3</sub>), 0.96 - 0.65 (m, 3H, -CH<sub>2</sub>-CH<sub>3</sub>);

<sup>13</sup>C NMR (CDCl<sub>3</sub>, 101 MHz): δ (ppm) = 177.6 (C<sub>q</sub>, C=O<sub>lactone</sub>), 143.0 (C<sub>q</sub>, C-2), 132.9 (C<sub>q</sub>, C-5), 132.5 (CH, C-4), 130.3 (C<sub>q</sub>, Ph), 129.9, 129.8, 128.2 (CH, Ph), 73.6 (CH, C-8), 68.6 (CH<sub>2</sub>, -CH<sub>2</sub>-O-), 55.1 (C<sub>q</sub>, C-6), 48.3 (CH, -CH-OH), 44.8 (CH, C-7), 35.1 (CH<sub>3</sub>, N-CH<sub>3</sub>), 28.2 (CH<sub>2</sub>, -CH<sub>2</sub>-CH<sub>3</sub>), 27.6 (CH<sub>2</sub>, -CH<sub>2</sub>-S-), 27.4 (CH<sub>2</sub>, -CH<sub>2</sub>-S-) 24.1 (CH<sub>2</sub>, -CH<sub>2</sub>-CH<sub>2</sub>-CH<sub>2</sub>-), 10.3 (CH<sub>3</sub>, -CH<sub>2</sub>-CH<sub>3</sub>);

IR (ATR, cm<sup>-1</sup>): 3192 (br), 2960, 2930, 2908, 1766, 1582, 1522, 1479, 1439, 1386, 1182, 1025, 736, 701, 687.

### Synthesis of *rac*-1-((3*S*,4*R*)-4-(2-(1-Methyl-2-(Phenylthio)-1*H*-imidazol-5-yl)-1,3-Dithian-2-yl)-2-Oxotetrahydrofuran-3-yl)propyl Acetate (**94**)<sup>[131]</sup>



**94** *rac*.

The alcohol **93** (1.24 g, 2.75 mmol) was heated in a mixture of acetic acid (15 mL) and acetic anhydride (10 mL) to 70 °C for 48 h. After evaporation to dryness, water (4 mL) was added and the pH was adjusted to 8 by addition of Na<sub>2</sub>CO<sub>3</sub>. The aqueous mixture was extracted with chloroform. The combined organic layers were dried over MgSO<sub>4</sub> and the solvent was evaporated. The product was isolated by column chromatography (silica, 1:1 cyclohexane/ethyl acetate) as a colourless oil (1.04 g, 2.11 mmol, 76%).

Formula: C<sub>23</sub>H<sub>28</sub>N<sub>2</sub>O<sub>4</sub>S<sub>3</sub>;

MW: 492.67 g/mol;

R<sub>f</sub> (50:50 cyclohexane/EtOAc) = 0.6;

<sup>1</sup>H NMR (CDCl<sub>3</sub>, 400 MHz): δ (ppm) = 7.61 (s, 1H, 4-H), 7.36–7.26 (m, 5H, Ph), 5.20–5.09 (m, 1H, -CH-OAc), 4.75–4.51 (m, 1H; -CH<sub>2</sub>-O-), 4.23–4.14 (m, 1H, -CH<sub>2</sub>-O-), 3.87 (s, 3H, N-CH<sub>3</sub>), 3.25–3.09 (m, 1H, 8-H), 3.02–2.96 (m, 1H, 7-H), 2.95–2.65 (m, 4H, -CH<sub>2</sub>-S-), 2.11–2.00 (m, 4H, -CH<sub>2</sub>-CH<sub>2</sub>-CH<sub>2</sub>-, -CH<sub>3</sub>-COO-), 1.94–1.78 (m, 1H, -CH<sub>2</sub>-CH<sub>2</sub>-CH<sub>2</sub>-), 1.63–1.20 (m, 2H, -CH<sub>2</sub>-CH<sub>3</sub>), 0.90–0.64 (m, 3H, -CH<sub>2</sub>-CH<sub>3</sub>);

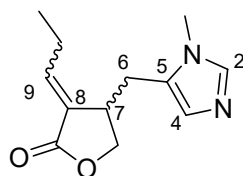
<sup>13</sup>C NMR (CDCl<sub>3</sub>, 101 MHz): δ (ppm) = 176.0 (C<sub>q</sub>, C=O<sub>lactone</sub>), 169.9 (C<sub>q</sub>, C=O<sub>acetate</sub>), 143.4 (C<sub>q</sub>, C-2), 135.1 (CH, C-4), 132.9 (C<sub>q</sub>, Ph), 131.6 (C<sub>q</sub>, C-5), 130.2, 129.8, 128.2 (CH, Ph), 75.2 (CH, -CH-OAc), 68.4

## Experimental

(CH<sub>2</sub>, -CH<sub>2</sub>-O-), 55.8 (C<sub>q</sub>, C-**6**), 46.2 (CH, C-**8**), 45.4 (CH, C-**7**), 34.8 (CH<sub>3</sub>, N-CH<sub>3</sub>), 27.7 (CH<sub>2</sub>, -CH<sub>2</sub>-S-), 25.9 (CH<sub>2</sub>, -CH<sub>2</sub>-CH<sub>3</sub>), 24.1 (CH<sub>2</sub>, -CH<sub>2</sub>-CH<sub>2</sub>-CH<sub>2</sub>-), 21.1 (CH<sub>3</sub>, CH<sub>3</sub>-COO-), 9.81 (CH<sub>3</sub>, -CH<sub>2</sub>-CH<sub>3</sub>);

IR (ATR, cm<sup>-1</sup>): 3054, 2967, 2916, 1769, 1736, 1581, 1477, 1439, 1371, 1222, 1180, 1014, 736, 700, 687.

### Synthesis of 4-((1-Methyl-1*H*-Imidazol-5-yl)methyl)-3-Propylidenedihydrofuran-2(3*H*)-one (**91**)



**91**

The acetate **94** (1.04 g, 2.11 mmol) was dissolved in dry methanol and freshly prepared Raney nickel in dry methanol was added. The reaction mixture was refluxed for 4 h. As the reduction was not complete, more Raney nickel was added, and reflux was continued. The reaction was complete when only one spot appeared on TLC (silica, 95:5 dichloromethane/MeOH, Dragendorff stain). The hot suspension was filtered through a double filter paper. The filtrate was evaporated, the residue dissolved in dilute HCl. The pH was adjusted to 8 with Na<sub>2</sub>CO<sub>3</sub> and the mixture was extracted with chloroform. The combined organic layers were dried over MgSO<sub>4</sub> and evaporated to leave the product (diastereomeric mixture *Z/E* = 85:15) as a slightly brown oil (95.0 mg, 431 μmol, 20%).

Formula: C<sub>12</sub>H<sub>16</sub>N<sub>2</sub>O<sub>2</sub>;

MW: 220.27 g/mol;

R<sub>f</sub> (95:5 dichloromethane/MeOH) = 0.3;

IR (ATR, cm<sup>-1</sup>): 2966, 2929, 1750, 1674, 1556, 1505, 1485, 1442, 1377, 1207, 1022, 693, 665;

NMR signals of the *Z*-enantiomers:

<sup>1</sup>H NMR (CDCl<sub>3</sub>, 400 MHz): δ (ppm) = 7.68 (s, 1H, **2**-H), 6.87 (s, 1H, **4**-H), 6.82–6.77 (m, 1H, **9**-H), 4.33 (dd, *J* = 9.4, 6.8 Hz, 1H, -CH<sub>2</sub>-O-), 4.17 (dd, *J* = 9.4, 1.3 Hz, 1H, -CH<sub>2</sub>-O-), 3.60 (s, 3H, N-CH<sub>3</sub>), 3.42–3.33 (m, 1H, **7**-H), 2.95–2.62 (m, 2H, **6**-H), 2.18–1.98 (m, 2H, =CH-CH<sub>2</sub>-CH<sub>3</sub>), 1.13–0.93 (m, 3H, =CH-CH<sub>2</sub>-CH<sub>3</sub>);

<sup>13</sup>C NMR (CDCl<sub>3</sub>, 101 MHz): δ (ppm) = 170.8 (C<sub>q</sub>, C=O), 147.0 (CH, C-**9**), 138.2 (CH, C-**2**), 128.2 (C<sub>q</sub>, C-**5**), 127.1 (C<sub>q</sub>, C-**8**), 126.5 (CH, C-**4**), 70.2 (CH<sub>2</sub>, -CH<sub>2</sub>-O-), 36.5 (CH, C-**7**), 31.4 (CH<sub>3</sub>, N-CH<sub>3</sub>), 28.3 CH<sub>2</sub>, C-**6**), 22.9 (CH<sub>2</sub>, =C-CH<sub>2</sub>-CH<sub>3</sub>), 13.0 (CH<sub>3</sub>, =C-CH<sub>2</sub>-CH<sub>3</sub>);

## Experimental

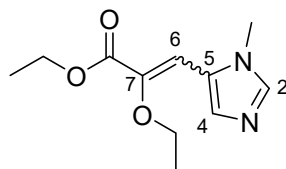
NMR signals of the *E*-enantiomers:

$^1\text{H}$  NMR ( $\text{CDCl}_3$ , 400 MHz):  $\delta$  (ppm) = 7.68 (s, 1H, **2-H**), 6.87 (s, 1H, **4-H**), 6.10–6.04 (m, 1H, **9-H**), 4.44–4.37 (m, 1H,  $-\text{CH}_2\text{-O-}$ ), 4.07–4.01 (m, 1H,  $-\text{CH}_2\text{-O-}$ ), 3.66 (s, 3H, **N-CH<sub>3</sub>**), 3.42–3.33 (m, 1H, **7-H**), 2.95–2.62 (m, 2H, **6-H**), 2.18–1.98 (m, 2H,  $=\text{CH-CH}_2\text{-CH}_3$ ), 1.13–0.93 (m, 3H,  $=\text{CH-CH}_2\text{-CH}_3$ );

$^{13}\text{C}$  NMR ( $\text{CDCl}_3$ , 101 MHz):  $\delta$  (ppm) = 169.6 ( $\text{C}_q$ , **C=O**), 144.1 (CH, **C-9**), 138.2 (CH, **C-2**), 128.2 ( $\text{C}_q$ , **C-5**), 127.1 ( $\text{C}_q$ , **C-8**), 126.5 (CH, **C-4**), 70.2 ( $\text{CH}_2$ ,  $-\text{CH}_2\text{-O-}$ ), 36.5 (H, **C-7**), 31.4 ( $\text{CH}_3$ , **N-CH<sub>3</sub>**), 28.3 ( $\text{CH}_2$ , **C-6**), 21.0 ( $\text{CH}_2$ ,  $=\text{C-CH}_2\text{-CH}_3$ ), 10.4 ( $\text{CH}_3$ ,  $=\text{C-CH}_2\text{-CH}_3$ ).

### 7.5.4 Stereospecific Synthesis by Hydrogenation of an Endocyclic Double Bond

#### Synthesis of Ethyl 2-Ethoxy-3-(1-Methyl-1*H*-imidazol-5-yl)acrylate (**97**)<sup>[146]</sup>



**97**

Ethyl 2-(diethoxyphosphoryl)-2-ethoxyacetate (**102**) (2.01 g, 7.49 mmol), prepared according to a procedure from Deussen et al.,<sup>[149]</sup> was added dropwise to a suspension of NaH (60% in mineral oil, 300 mg, 7.49 mmol) in dry THF (11 mL) at 0 °C. After stirring for 60 min at 0 °C, a solution of 1-methyl-1*H*-imidazole-5-carbaldehyde (360 mg, 4.99 mmol) in dry THF (3 mL) was added. The reaction was stirred overnight at RT. Dilute aqueous HCl was added and the mixture was extracted with diethyl ether. The aqueous layer was adjusted to a pH above 8 by addition of  $\text{Na}_2\text{CO}_3$  and was extracted with ethyl acetate. The combined ethyl acetate layers were dried over  $\text{Na}_2\text{SO}_4$  and the solvent was evaporated to yield the product as a slightly yellow oil (1.02 g, 4.54 mmol, 91%) which is composed of the *E*- and *Z*-isomers.

Formula:  $\text{C}_{11}\text{H}_{16}\text{N}_2\text{O}_3$ ;

MW: 224.26 g/mol;

$R_f$  (95:5 dichloromethane/MeOH) = 0.3;

IR (ATR,  $\text{cm}^{-1}$ ): 3106, 2979, 2939, 2903, 1707, 1632, 1531, 1493, 1467, 1370, 1245, 1096, 1034, 764, 670, 657.

## Experimental

Major isomer (79%):

$^1\text{H}$  NMR ( $\text{CDCl}_3$ , 400 MHz):  $\delta$  (ppm) = 7.78 (s, 1H, **2-H**), 7.48 (s, 1H, **4-H**), 6.86 (s, 1H, **6-H**), 4.30 (q,  $J = 7.1$  Hz, 2H,  $-\text{COO}-\text{CH}_2-$ ), 4.06 (q,  $J = 7.1$  Hz, 2H,  $-\text{O}-\text{CH}_2-$ ), 3.66 (s, 3H, **N-CH<sub>3</sub>**), 1.43–1.31 (m, 6H,  $-\text{COO}-\text{CH}_2-\text{CH}_3$ ,  $-\text{O}-\text{CH}_2-\text{CH}_3$ );

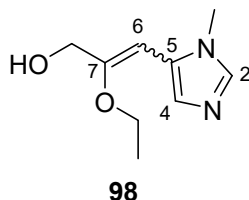
$^{13}\text{C}$  NMR ( $\text{CDCl}_3$ , 101 MHz):  $\delta$  (ppm) = 164.2 ( $\text{C}_q$ , **C=O**), 143.6 ( $\text{C}_q$ , **C-7**), 139.2 (CH, **C-4**), 134.2 (CH, **C-2**), 126.7 ( $\text{C}_q$ , **C-5**), 109.8 (CH, **C-6**), 67.5 ( $\text{CH}_2$ ,  $-\text{O}-\text{CH}_2-$ ), 61.3 ( $\text{CH}_2$ ,  $-\text{COO}-\text{CH}_2-$ ), 31.8 ( $\text{CH}_3$ , **N-CH<sub>3</sub>**), 15.8 ( $\text{CH}_3$ ,  $-\text{O}-\text{CH}_2-\text{CH}_3$ ), 14.5 ( $\text{CH}_3$ ,  $-\text{COO}-\text{CH}_2-\text{CH}_3$ ).

Minor isomer (21%):

$^1\text{H}$  NMR ( $\text{CDCl}_3$ , 400 MHz):  $\delta$  (ppm) = 7.43 (s, 1H, **2-H**), 7.05 (s, 1H, **4-H**), 5.70 (s, 1H, **6-H**), 4.18 (q,  $J = 7.1$  Hz, 2H,  $-\text{COO}-\text{CH}_2-$ ), 3.94 (q,  $J = 7.0$  Hz, 2H,  $-\text{O}-\text{CH}_2-$ ), 3.55 (s, 3H, **N-CH<sub>3</sub>**), 1.43–1.31 (m, 3H,  $-\text{O}-\text{CH}_2-\text{CH}_3$ ), 1.20 (t,  $J = 7.1$  Hz, 3H,  $-\text{COO}-\text{CH}_2-\text{CH}_3$ );

$^{13}\text{C}$  NMR ( $\text{CDCl}_3$ , 101 MHz):  $\delta$  (ppm) = 163.6 ( $\text{C}_q$ , **C=O**), 149.5 ( $\text{C}_q$ , **C-7**), 138.0 (CH, **C-2**), 129.6 (CH, **C-4**), 126.0 ( $\text{C}_q$ , **C-5**), 96.0 (CH, **C-6**), 65.2 ( $\text{CH}_2$ ,  $-\text{O}-\text{CH}_2-$ ), 61.4 ( $\text{CH}_2$ ,  $-\text{COO}-\text{CH}_2-$ ), 31.7 ( $\text{CH}_3$ , **N-CH<sub>3</sub>**), 15.4 ( $\text{CH}_3$ ,  $-\text{O}-\text{CH}_2-\text{CH}_3$ ), 14.0 ( $\text{CH}_3$ ,  $-\text{COO}-\text{CH}_2-\text{CH}_3$ ).

### 2-Ethoxy-3-(1-methyl-1*H*-imidazol-5-yl)prop-2-en-1-ol (**98**)<sup>[146]</sup>



Diisobutylaluminium hydride (1 M in toluene, 44.2 mmol, 44.2 mL) was added dropwise to a solution of **97** (4.51 g, 20.11  $\mu\text{mol}$ ) in dry toluene (120 mL) at 0 °C. After stirring at 0 °C for 5 min, the reaction was stirred at RT for 30 min. Methanol (120 mL) and water (30 mL) were added slowly at 0 °C. The mixture was evaporated to dryness and the residue was added as a solid depot onto a short silica column. The product was eluted with methanol. Evaporation of the solvent left the product as a slightly yellow oil (3.24 g, 17.8  $\mu\text{mol}$ , 88%).

Formula:  $\text{C}_9\text{H}_{14}\text{N}_2\text{O}_2$ ;

MW: 182.22 g/mol;

$R_f$  (95:5 dichloromethane/MeOH) = 0.1 (tailing);

IR (ATR,  $\text{cm}^{-1}$ ): 3096 (br), 2975, 2907, 2848, 1646, 1505, 1442, 1331, 1112, 1032, 711, 649.

## Experimental

Major isomer (80%):

$^1\text{H}$  NMR ( $\text{CDCl}_3$ , 400 MHz):  $\delta$  (ppm) = 7.43 (s, 1H, **4-H**), 7.35 (s, 1H, **2-H**), 5.46 (s, 1H, **6-H**), 4.31 (s, 2H, **-CH<sub>2</sub>-OH**), 4.11 (q,  $J = 7.0$  Hz, 2H, **-O-CH<sub>2</sub>-**), 3.55 (s, 3H, **N-CH<sub>3</sub>**), 2.54 (br. s, 1H, **OH**), 1.36 (t,  $J = 7.0$  Hz, 3H, **-O-CH<sub>2</sub>-CH<sub>3</sub>**);

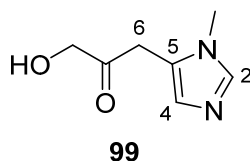
$^{13}\text{C}$  NMR ( $\text{CDCl}_3$ , 101 MHz):  $\delta$  (ppm) = 154.6 ( $\text{C}_q$ , **C-7**), 136.8 (CH, **C-2**), 129.3 (CH, **C-4**), 127.9 ( $\text{C}_q$ , **C-5**), 94.6 (CH, **C-6**), 64.0 ( $\text{CH}_2$ , **-O-CH<sub>2</sub>-**), 62.0 ( $\text{CH}_2$ , **-CH<sub>2</sub>-OH**), 31.6 ( $\text{CH}_3$ , **N-CH<sub>3</sub>**), 15.7 ( $\text{CH}_3$ , **-O-CH<sub>2</sub>-CH<sub>3</sub>**).

Minor isomer (20%):

$^1\text{H}$  NMR ( $\text{CDCl}_3$ , 400 MHz):  $\delta$  (ppm) = 7.42 (s, 1H, **2-H**), 6.83 (s, 1H, **4-H**), 5.22 (s, 1H, **6-H**), 4.25 (s, 2H, **-CH<sub>2</sub>-OH**), 3.92 (q,  $J = 7.0$  Hz, 2H, **-O-CH<sub>2</sub>-**), 3.52 (s, 3H, **N-CH<sub>3</sub>**), 2.54 (br. s, 1H, **OH**), 1.40 (t,  $J = 7.0$  Hz, 3H, **-O-CH<sub>2</sub>-CH<sub>3</sub>**);

$^{13}\text{C}$  NMR ( $\text{CDCl}_3$ , 101 MHz):  $\delta$  (ppm) = 153.0 ( $\text{C}_q$ , **C-7**), 137.8 (CH, **C-2**), 127.9 (CH, **C-4**), 127.4 ( $\text{C}_q$ , **C-5**), 87.5 (CH, **C-6**), 63.7 ( $\text{CH}_2$ , **-O-CH<sub>2</sub>-**), 60.4 ( $\text{CH}_2$ , **-CH<sub>2</sub>-OH**), 31.6 ( $\text{CH}_3$ , **N-CH<sub>3</sub>**), 15.7 ( $\text{CH}_3$ , **-O-CH<sub>2</sub>-CH<sub>3</sub>**).

### Synthesis of 1-Hydroxy-3-(1-Methyl-1H-imidazol-5-yl)propan-2-one (**99**)<sup>[146]</sup>



The enol ether **98** (512 mg, 2.81 mmol) was dissolved in 1 N HCl (6 mL) and was stirred at 30–35 °C for 1 h. The solvent was evaporated and the residue dried at 4 mbar and 45 °C. The residue was dissolved in ethanol (10 mL) and  $\text{Na}_2\text{CO}_3$  (1.79 g, 16.9 mmol) was added. After stirring for 15 min at RT, the suspension was filtered, and the filtrate was evaporated to dryness. The residue was dissolved in dichloromethane and filtered. The filtrate was evaporated to dryness to yield the product as a yellow oil (283 mg, 1.84 mmol, 65%).

Formula:  $\text{C}_7\text{H}_{10}\text{N}_2\text{O}_2$ ;

MW: 154.17 g/mol;

$R_f$  (95:5 dichloromethane/MeOH) = 0.2;

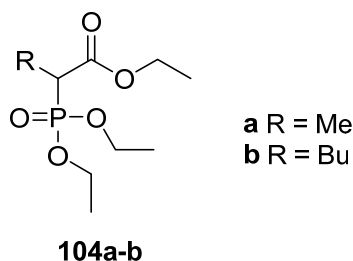
$^1\text{H}$  NMR ( $\text{CDCl}_3$ , 400 MHz):  $\delta$  (ppm) = 7.41 (s, 1H, **2-H**), 6.87 (s, 1H, **4-H**), 4.31 (s, 2H, **-CH<sub>2</sub>-OH**), 3.73 (s, 2H, **6-H**), 3.55 (s, 3H, **N-CH<sub>3</sub>**);

$^{13}\text{C}$  NMR ( $\text{CDCl}_3$ , 101 MHz):  $\delta$  (ppm) = 206.2 ( $\text{C}_q$ , **C=O**), 139.0 (CH, **C-2**), 129.0 (CH, **C-4**), 123.7 ( $\text{C}_q$ , **C-5**), 67.7 ( $\text{CH}_2$ , **-CH<sub>2</sub>-OH**), 34.3 ( $\text{CH}_2$ , **C-6**), 31.8 ( $\text{CH}_3$ , **N-CH<sub>3</sub>**);

IR (ATR,  $\text{cm}^{-1}$ ): 3112 (br), 2885, 2831, 1725, 1599, 1508, 1450, 1106, 1034, 706, 661.



## General Procedure for the Synthesis of Ethyl 2-(Diethoxyphosphoryl)alkanoates

**(104a, d)**<sup>[150b]</sup>

The respective diethyl alkylphosphonate (1.00 eq.), prepared following a procedure from Frlan et al.,<sup>[150a]</sup> was dissolved in dry THF (5 mL/1 mmol). Lithium diisopropylamide (1.63 M in THF/heptane/ethylbenzene, 2.00 eq.) was added to the solution at  $-84\text{ }^{\circ}\text{C}$ . After stirring for 30 min at  $-84\text{ }^{\circ}\text{C}$ , diethyl carbonate (1.00 eq.) was added. The reaction was stirred overnight while warming up to RT. Diluted aqueous HCl was added and the layers were separated. The aqueous layer was extracted with ethyl acetate. The combined organic layers were dried over  $\text{Na}_2\text{SO}_4$  and the solvents removed under reduced pressure. Purification by flash chromatography (silica, 50:50 cyclohexane/ethyl acetate) yielded the product as a colourless liquid.

**Table 51:** General data of the phosphonate esters **104a** and **d**.

R	#	Formula	MW [g/mol]	Yield [%]	IR data [ $\text{cm}^{-1}$ ]
Me	<b>104a</b>	$\text{C}_9\text{H}_{19}\text{O}_5\text{P}$	238.22	66	2984, 2942, 2908, 1731, 1476, 1457, 1392, 1368, 1245, 1162, 1046, 1014
Bu	<b>104d</b>	$\text{C}_{12}\text{H}_{25}\text{O}_5\text{P}$	280.30	50	2981, 2960, 2873, 1734, 1467, 1445, 1392, 1368, 1254, 1159, 1051, 1022

**Table 52:**  $^1\text{H}$  NMR data of the phosphonate esters **104a** and **d**.

R	#	-COO-CH <sub>2</sub> -CH <sub>3</sub>	-COO-CH <sub>2</sub> -	-CH-
Me	<b>104a</b>	1.36–1.24 (m, 9H)	4.32–4.09 (m, 6H)	3.00 (dq, $^2J(^1\text{H}, ^{31}\text{P}) = 23.3\text{ Hz}$ , $J = 7.3\text{ Hz}$ , 1H)
Bu	<b>104d</b>	1.35–1.25 (m, 13H)	4.24–4.08 (m, 6H)	2.91 (ddd, $^2J(^1\text{H}, ^{31}\text{P}) = 22.5\text{ Hz}$ , $J = 11.1\text{ Hz}$ , $J = 3.8\text{ Hz}$ , 1H)

**Table 53:**  $^1\text{H}$  NMR data of the phosphonate esters **104a** and **d** (continued).

R	#	P-O-CH <sub>2</sub> -	P-O-CH <sub>2</sub> -CH <sub>3</sub>	R
Me	<b>104a</b>	4.32–4.09 (m, 6H)	1.36–1.24 (m, 9H)	1.42 (dd, $^3J(^1\text{H}, ^{31}\text{P}) = 18.0\text{ Hz}$ , $J = 7.3\text{ Hz}$ , 3H)
Bu	<b>104d</b>	4.24–4.08 (m, 6H)	1.35–1.25 (m, 13H)	2.10–1.77 (m, 2H); 1.35–1.25 (m, 13H), 0.90–0.85 (m, 3H)

## Experimental

**Table 54:**  $^{13}\text{C}$  NMR data of the phosphonate esters **104a** and **d**.

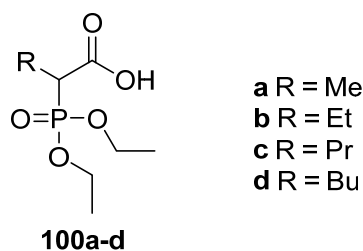
R	#	-COO-CH <sub>2</sub> -CH <sub>3</sub>	-COO-CH <sub>2</sub> -	C=O	-CH-
Me	<b>104a</b>	14.2	61.5	169.8 (d, $^2J(^{13}\text{C}, ^{31}\text{P}) = 4.7$ Hz)	39.5 (d, $^1J(^{13}\text{C}, ^{31}\text{P}) = 133.6$ Hz)
Bu	<b>104d</b>	14.3	61.4	169.5 (d, $^2J(^{13}\text{C}, ^{31}\text{P}) = 4.8$ Hz)	46.0 (d, $^1J(^{13}\text{C}, ^{31}\text{P}) = 131.1$ Hz)

**Table 55:**  $^{13}\text{C}$  NMR data of the phosphonate esters **104a** and **d** (continued).

R	#	P-O-CH <sub>2</sub> -	P-O-CH <sub>2</sub> -CH <sub>3</sub>	R
Me	<b>104a</b>	62.8 (d, $^2J(^{13}\text{C}, ^{31}\text{P}) = 6.6$ Hz)	16.5 (d, $^3J(^{13}\text{C}, ^{31}\text{P}) = 5.9$ Hz), 16.5 (d, $^3J(^{13}\text{C}, ^{31}\text{P}) = 6.1$ Hz)	11.8 (d, $^2J(^{13}\text{C}, ^{31}\text{P}) = 6.3$ Hz)
Bu	<b>104d</b>	62.8 (t, $^2J(^{13}\text{C}, ^{31}\text{P}) = 7.0$ Hz)	16.5 (d, $^3J(^{13}\text{C}, ^{31}\text{P}) = 5.9$ Hz), 16.5 (d, $^3J(^{13}\text{C}, ^{31}\text{P}) = 6.1$ Hz)	26.8 (d, $^2J(^{13}\text{C}, ^{31}\text{P}) = 5.0$ Hz); 30.7 (d, $J(^{13}\text{C}, ^{31}\text{P}) = 14.9$ Hz); 22.3; 16.9

The spectral data correspond to literature data.<sup>[167]</sup>

### General Procedure for the Synthesis of 2-(Diethoxyphosphoryl)alkanoic Acid **100a–d**<sup>[150c]</sup>



Ethyl 2-(diethoxyphosphoryl)alkanoate **103a–d**, respectively, (3.38 mmol, 1.00 eq.) and KOH (1.50 eq.) were stirred in a mixture ethanol (6 mL) and water (6 mL) overnight at RT. The solvents were evaporated, and the oily residue was dissolved in water and washed twice with diethyl ether. After addition of dilute HCl until a pH below 4 was reached, the mixture was extracted with chloroform to yield the product as a slightly yellow oil.

**Table 56:** General data of the phosphonate acids **100a–d**.

R	#	Formula	MW [g/mol]	Yield [%]	IR data [cm <sup>-1</sup> ]
Me	<b>100a</b>	C <sub>7</sub> H <sub>15</sub> O <sub>5</sub> P	210.17	95	2984 (br), 2943, 2912, 1732, 1478, 1458, 1393, 1370, 1245, 1044, 1014, 962
Et	<b>100b</b>	C <sub>8</sub> H <sub>17</sub> O <sub>5</sub> P	224.08	95	2976 (br), 2933, 2910, 1727, 1478, 1459, 1392, 1369, 1263, 1046, 1013, 962
Pr	<b>100c</b>	C <sub>9</sub> H <sub>19</sub> O <sub>5</sub> P	238.22	96	2962 (br), 2933, 2912, 1724, 1465, 1444, 1393, 1291, 1045, 1014, 962
Bu	<b>100d</b>	C <sub>10</sub> H <sub>21</sub> O <sub>5</sub> P	252.25	87	2958 (br), 2931, 2873, 1726, 1457, 1444, 1393, 1369, 1283, 1047, 1015, 961

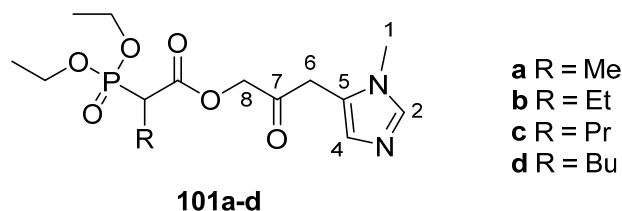
Table 57: <sup>1</sup>H NMR data of the phosphonate acids **100a-d**.

R	#	-CH-	P-O-CH <sub>2</sub> -	P-O-CH <sub>2</sub> -CH <sub>3</sub>	OH	R
Me	<b>100a</b>	3.05 (dq, <sup>2</sup> J( <sup>1</sup> H, <sup>31</sup> P) = 23.9 Hz, J = 7.2 Hz, 1H)	4.23-4.14 (m, 4H)	1.33 (t, J = 7.1 Hz, 6H)	9.02 (br. s)	1.42 (dd, <sup>3</sup> J( <sup>1</sup> H, <sup>31</sup> P) = 18.0 Hz, J = 7.2 Hz, 3H)
Et	<b>100b</b>	2.88 (ddd, <sup>2</sup> J( <sup>1</sup> H, <sup>31</sup> P) = 22.5 Hz, J = 10.6, 4.1 Hz, 1H)	4.28-4.12 (m, 4H)	1.33 (td, J = 7.1 Hz, <sup>4</sup> J( <sup>1</sup> H, <sup>31</sup> P) = 2.1 Hz, 6H)	9.00 (br. s)	2.05-1.79 (m, 2H), 1.01 (t, J = 7.4 Hz, 3H)
Pr	<b>100c</b>	2.97 (ddd, <sup>2</sup> J( <sup>1</sup> H, <sup>31</sup> P) = 22.7 Hz, J = 10.9, 3.7 Hz, 1H)	4.28-4.06 (m, 4H)	1.57-1.26 (m, 8H)	8.11 (br. s)	2.05-1.89 (m, 2H); 1.57-1.26 (m, 8H); 0.92 (t, J = 7.3 Hz, 3H)
Bu	<b>100d</b>	2.95 (ddd, <sup>2</sup> J( <sup>1</sup> H, <sup>31</sup> P) = 22.7 Hz, J = 11.0, 3.7 Hz, 1H)	4.25-4.11 (m, 4H)	1.46-1.31 (m, 10 H)	8.65 (br. s)	2.09-1.77 (m, 2H); 1.46-1.31 (m, 10 H); 0.90-0.86 (m, 3H)

Table 58: <sup>13</sup>C NMR data of the phosphonate acids **100a-d**.

R	#	C=O	-CH-	P-O-CH <sub>2</sub> -	P-O-CH <sub>2</sub> -CH <sub>3</sub>	R
Me	<b>100a</b>	171.8 (d, <sup>2</sup> J( <sup>13</sup> C, <sup>31</sup> P) = 3.7 Hz)	39.4 (d, <sup>1</sup> J( <sup>13</sup> C, <sup>31</sup> P) = 133.1 Hz)	63.5 (d, <sup>2</sup> J( <sup>13</sup> C, <sup>31</sup> P) = 6.6 Hz)	16.5 (s), 16.4 (s)	11.7 (d, <sup>2</sup> J( <sup>13</sup> C, <sup>31</sup> P) = 6.5 Hz)
Et	<b>100b</b>	171.2 (d, <sup>2</sup> J( <sup>13</sup> C, <sup>31</sup> P) = 3.8 Hz)	47.5 (d, <sup>1</sup> J( <sup>13</sup> C, <sup>31</sup> P) = 130.6 Hz)	63.7 (d, <sup>2</sup> J( <sup>13</sup> C, <sup>31</sup> P) = 6.5 Hz), 63.0 (d, <sup>2</sup> J( <sup>13</sup> C, <sup>31</sup> P) = 6.9 Hz)	16.5 (s), 16.4 (s)	20.8 (d, <sup>2</sup> J( <sup>13</sup> C, <sup>31</sup> P) = 5.5 Hz); 13.0 (d, <sup>3</sup> J( <sup>13</sup> C, <sup>31</sup> P) = 15.6 Hz)
Pr	<b>100c</b>	171.2 (d, <sup>2</sup> J( <sup>13</sup> C, <sup>31</sup> P) = 3.9 Hz)	45.6 (d, <sup>1</sup> J( <sup>13</sup> C, <sup>31</sup> P) = 130.4 Hz)	63.8 (d, <sup>2</sup> J( <sup>13</sup> C, <sup>31</sup> P) = 6.4 Hz), 63.0 (d, <sup>2</sup> J( <sup>13</sup> C, <sup>31</sup> P) = 6.8 Hz)	16.5 (d, <sup>3</sup> J( <sup>1</sup> H, <sup>31</sup> P) = 1.9 Hz), 16.4 (d, <sup>3</sup> J( <sup>1</sup> H, <sup>31</sup> P) = 1.9 Hz)	29.2 (d, <sup>2</sup> J( <sup>13</sup> C, <sup>31</sup> P) = 5.5 Hz); 21.7 (d, <sup>3</sup> J( <sup>13</sup> C, <sup>31</sup> P) = 15.0 Hz); 13.7 (s)
Bu	<b>100d</b>	171.4 (s)	45.9 (d, <sup>1</sup> J( <sup>13</sup> C, <sup>31</sup> P) = 130.4 Hz)	63.7 (d, <sup>2</sup> J( <sup>13</sup> C, <sup>31</sup> P) = 6.4 Hz), 63.0 (d, <sup>2</sup> J( <sup>13</sup> C, <sup>31</sup> P) = 6.8 Hz)	16.5 (d, <sup>3</sup> J( <sup>1</sup> H, <sup>31</sup> P) = 1.3 Hz), 16.4 (d, <sup>3</sup> J( <sup>1</sup> H, <sup>31</sup> P) = 1.3 Hz)	26.9 (d, <sup>2</sup> J( <sup>13</sup> C, <sup>31</sup> P) = 5.5 Hz); 30.5 (d, <sup>3</sup> J( <sup>13</sup> C, <sup>31</sup> P) = 14.6 Hz); 22.4 (s); 13.9 (s)

The spectral data correspond to literature data.<sup>[150c, 168]</sup>

General Procedure for the Synthesis of Phosphonate Esters **101a–d**<sup>[146]</sup>

The 2-(diethoxyphosphoryl)alkanoic acid **100a–d**, respectively, (389  $\mu\text{mol}$ , 1.00 eq.) was dissolved in dry dichloromethane (2 mL/400  $\mu\text{mol}$ ) and added to a mixture of alcohol **99** (1.00 eq.) and DMAP (0.20 eq.). The resulting solution was cooled to 0 °C before addition of DCC (1.20 eq.). The mixture was stirred overnight. Then, the reaction was filtered and the filtrate was extracted four times with saturated aqueous  $\text{NaHCO}_3$  solution. The organic layer was dried over  $\text{Na}_2\text{SO}_4$  and the solvents were evaporated under reduced pressure. The residue was purified by column chromatography (silica, 3–10% MeOH/dichloromethane) to yield the product as a yellow to orange oil.

**Table 59:** General data of the phosphonate esters **101a–d**.

R	#	Formula	MW [g/mol]	Yield [%]	IR data [ $\text{cm}^{-1}$ ]
Me	<b>101a</b>	$\text{C}_{14}\text{H}_{23}\text{N}_2\text{O}_6\text{P}$	346.32	17	3126, 2983, 2928, 2919, 1733 (br), 1613, 1505, 1455, 1388, 1227, 1160, 1041, 1016, 752, 705
Et	<b>101b</b>	$\text{C}_{15}\text{H}_{25}\text{N}_2\text{O}_6\text{P}$	360.35	23	3125, 2982, 2934, 2882, 1731 (br), 1646, 1509, 1458, 1390, 1238, 1161, 1039, 1014, 759, 699
Pr	<b>101c</b>	$\text{C}_{16}\text{H}_{27}\text{N}_2\text{O}_6\text{P}$	374.37	54	3125, 2961, 2937, 2872, 1732 (br), 1651, 1506, 1456, 1390, 1238, 1160, 1044, 1016, 760, 703
Bu	<b>101d</b>	$\text{C}_{17}\text{H}_{29}\text{N}_2\text{O}_6\text{P}$	388.40	21	3129, 2958, 2930, 2871, 1733 (br), 1600, 1505, 1456, 1370, 1227, 1161, 1045, 1017, 750, 704

Table 60: <sup>1</sup>H NMR data of the phosphonate esters **101a–d** measured in CDCl<sub>3</sub>.

R	#	N-CH <sub>3</sub>	2-H	4-H	6-H	8-H	P-CH-	R	P-O-CH <sub>2</sub> -	P-O-CH <sub>2</sub> -CH <sub>3</sub>
Me	<b>101a</b>	3.67 (s, 1H)	8.14 (s, 1H)	7.14 (s, 1H)	3.67 (s, 2H)	4.70 (s, 2H)	3.16 (dq, <sup>2</sup> J( <sup>1</sup> H, <sup>31</sup> P) = 23.5 Hz, J = 7.3 Hz, 1H)	1.49 (dd, <sup>3</sup> J( <sup>1</sup> H, <sup>31</sup> P) = 17.7 Hz, J = 7.3 Hz, 3H)	4.21–4.12 (m, 4H)	1.34 (td, J = 7.1 Hz, <sup>3</sup> J( <sup>1</sup> H, <sup>31</sup> P) = 1.1 Hz, 6H)
Et	<b>101b</b>	3.53 (s, 1H)	7.44 (s, 1H)	6.93 (s, 1H)	3.78 (s, 2H)	4.79 (d, J = 16.7 Hz, 1H), 4.70 (d, J = 16.7 Hz, 1H)	2.97 (ddd, <sup>2</sup> J( <sup>1</sup> H, <sup>31</sup> P) = 22.4 Hz, J = 10.6, 4.2 Hz, 1H)	2.06–1.90 (m, 2H), 1.05 (t, J = 7.4 Hz, 3H)	4.20–4.10 (m, 4H)	1.31 (t, J = 7.1 Hz, 6H)
Pr	<b>101c</b>	3.57 (s, 1H)	7.67 (s, 1H)	7.00 (s, 1H)	3.83 (s, 2H)	4.78 (d, J = 16.7 Hz, 1H), 4.72 (J = 16.7 Hz, 1H)	3.08 (ddd, <sup>2</sup> J( <sup>1</sup> H, <sup>31</sup> P) = 22.7 Hz, J = 11.1, 3.7 Hz, 1H)	2.08–1.77 (m, 2H), 1.58–1.18 (m, 2H), 0.94 (t, J = 7.3 Hz, 3H)	4.24–4.02 (m, 4H)	1.58–1.18 (m, 6H)
Bu	<b>101d</b>	3.55 (s, 1H)	7.52 (s, 1H)	6.96 (s, 1H)	3.80 (s, 2H)	4.77 (d, J = 16.7 Hz, 1H), 4.71 (J = 16.7 Hz, 1H)	3.05 (ddd, <sup>2</sup> J( <sup>1</sup> H, <sup>31</sup> P) = 22.7 Hz, J = 11.0, 3.8 Hz, 1H)	2.08–1.77 (m, 2H), 1.52–1.22 (m, 10H), 0.94–0.86 (m, 3H)	4.21–4.09 (m, 4H)	1.52–1.22 (m, 10H)

Table 61: <sup>13</sup>C NMR data of the phosphonate esters **101a–d** measured in CDCl<sub>3</sub>.

R	#	P-CH-	R	P-O-CH <sub>2</sub> -	P-O-CH <sub>2</sub> -CH <sub>3</sub>
Me	<b>101a</b>	39.3 (d, <sup>1</sup> J( <sup>13</sup> C, <sup>31</sup> P) = 133.9 Hz)	12.0 (d, <sup>2</sup> J( <sup>13</sup> C, <sup>31</sup> P) = 6.4 Hz)	63.1 (d, <sup>2</sup> J( <sup>13</sup> C, <sup>31</sup> P) = 6.6 Hz), 63.0 (d, <sup>2</sup> J( <sup>13</sup> C, <sup>31</sup> P) = 6.8 Hz)	16.6 (d, <sup>3</sup> J( <sup>13</sup> C, <sup>31</sup> P) = 1.0 Hz), 16.5 (d, <sup>3</sup> J( <sup>13</sup> C, <sup>31</sup> P) = 1.1 Hz)
Et	<b>101b</b>	47.3 (d, <sup>1</sup> J( <sup>13</sup> C, <sup>31</sup> P) = 131.7 Hz)	21.0 (d, <sup>2</sup> J( <sup>13</sup> C, <sup>31</sup> P) = 5.1 Hz), 13.1 (d, <sup>3</sup> J( <sup>13</sup> C, <sup>31</sup> P) = 15.4 Hz)	63.1 (d, <sup>2</sup> J( <sup>13</sup> C, <sup>31</sup> P) = 6.5 Hz), 62.9 (d, <sup>2</sup> J( <sup>13</sup> C, <sup>31</sup> P) = 6.8 Hz)	16.5 (d, <sup>3</sup> J( <sup>13</sup> C, <sup>31</sup> P) = 2.0 Hz), 16.5 (d, <sup>3</sup> J( <sup>13</sup> C, <sup>31</sup> P) = 2.1 Hz)
Pr	<b>101c</b>	45.4 (d, <sup>1</sup> J( <sup>13</sup> C, <sup>31</sup> P) = 131.6 Hz)	29.3 (s), 21.6 (d, <sup>3</sup> J( <sup>13</sup> C, <sup>31</sup> P) = 15.1 Hz), 13.7 (s)	63.2 (d, <sup>2</sup> J( <sup>13</sup> C, <sup>31</sup> P) = 6.4 Hz), 63.0 (d, <sup>2</sup> J( <sup>13</sup> C, <sup>31</sup> P) = 6.8 Hz)	16.5 (br. s), 16.5 (br. s)
Bu	<b>101d</b>	45.6 (d, <sup>1</sup> J( <sup>13</sup> C, <sup>31</sup> P) = 131.3 Hz)	27.1 (d, <sup>2</sup> J( <sup>13</sup> C, <sup>31</sup> P) = 5.1 Hz), 30.5 (d, <sup>3</sup> J( <sup>13</sup> C, <sup>31</sup> P) = 14.3 Hz), 22.3 (s), 13.9 (s)	63.1 (d, <sup>2</sup> J( <sup>13</sup> C, <sup>31</sup> P) = 6.5 Hz), 62.9 (d, <sup>2</sup> J( <sup>13</sup> C, <sup>31</sup> P) = 6.8 Hz)	16.6 (d, <sup>3</sup> J( <sup>13</sup> C, <sup>31</sup> P) = 1.7 Hz), 16.5 (d, <sup>3</sup> J( <sup>13</sup> C, <sup>31</sup> P) = 1.9 Hz)

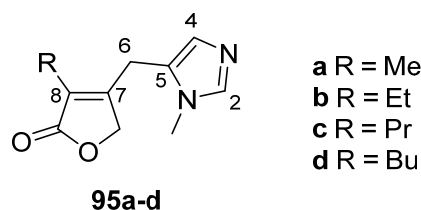
## Experimental

**Table 62:**  $^{13}\text{C}$  NMR data of the phosphonate esters **101a–d** measured in  $\text{CDCl}_3$  (continued).

R	#	N-CH <sub>3</sub>	C-2	C-4	C-5	C-6	C-7	C-8	C=O <sub>ester</sub>
Me	<b>101a</b>	32.2	138.5	127.6	124.0	34.9	199.4	63.3	169.5 (d, $^2J(^{13}\text{C}, ^{31}\text{P}) = 4.4$ Hz)
Et	<b>101b</b>	31.7	139.2	129.4	123.4	35.1	199.4	68.1	169.0 (d, $^2J(^{13}\text{C}, ^{31}\text{P}) = 4.5$ Hz)
Pr	<b>101c</b>	32.0	138.7	127.8	123.9	34.9	199.3	68.2	169.2*
Bu	<b>101d</b>	31.9	139.0	128.8	123.6	35.1	199.4	68.2	169.2 (d, $^2J(^{13}\text{C}, ^{31}\text{P}) = 4.6$ Hz)

\* determined from HMBC spectrum

### General Procedure for the Cyclisation of Phosphonate Esters **95a–d**<sup>[146]</sup>



A solution of the respective phosphonate ester **103a–d** (1 mmol, 1.00 eq.) in dry THF (5 mL) was added to a suspension of sodium hydride (60%, 1.00 eq.) in freshly distilled dry THF (20 mL) at 0 °C. The reaction was stirred overnight at RT. When the reaction control by TLC (silica, 90:10 dichloromethane/methanol,  $\text{KMnO}_4$ ) indicated incomplete conversion, more sodium hydride was added until completion. After addition of diluted aqueous HCl until an acidic pH was reached the mixture was extracted with diethyl ether.  $\text{Na}_2\text{CO}_3$  was added to the aqueous phase to reach pH 8–9. The aqueous phase was extracted with chloroform. The combined organic layers were dried over  $\text{Na}_2\text{SO}_4$  and the solvent was evaporated under reduced pressure to yield the product as a yellow to brown oil, which was used in the next step without purification.

The sample of **95b** for potential pharmacological testing was purified by preparative HPLC using method VI (Chapter 7.1.4). Its purity was 98% by HPLC (achiral method B).

**Table 63:** General data of the cyclisation products **95a–d**.

R	#	Formula	MW [g/mol]	Yield [%]	IR data [ $\text{cm}^{-1}$ ]
Me	<b>95a</b>	$\text{C}_{10}\text{H}_{12}\text{N}_2\text{O}_2$	192.22	68	3119, 2954, 2924, 1736, 1678, 1507, 1447, 1080, 1027, 755, 692
Et	<b>95b</b>	$\text{C}_{11}\text{H}_{14}\text{N}_2\text{O}_2$	206.25	65	3112, 2959, 2877, 1737, 1671, 1507, 1455, 1106, 1029, 772, 699
Pr	<b>95c</b>	$\text{C}_{12}\text{H}_{16}\text{N}_2\text{O}_2$	220.27	75	3116, 2959, 2871, 1739, 1671, 1504, 1451, 1078, 1033, 768, 707
Bu	<b>95d</b>	$\text{C}_{13}\text{H}_{18}\text{N}_2\text{O}_2$	234.30	56	3114, 2956, 2870, 1739, 1671, 1505, 1453, 1079, 1032, 751, 730

## Experimental

**Table 64:**  $^1\text{H}$  NMR data of the cyclisation products **95a–d** in  $\text{CDCl}_3$ .

R	#	N-CH <sub>3</sub>	2-H	4-H	6-H	-CH <sub>2</sub> -O-
Me	<b>95a</b>	3.53 (s, 3H)	7.46 (s, 1H)	6.84 (s, 1H)	3.71 (s, 2H)	4.56 (s, 2H)
Et	<b>95b</b>	3.54 (s, 3H)	7.44 (s, 1H)	6.84 (s, 1H)	3.73 (s, 2H)	4.55 (s, 2H)
Pr	<b>95c</b>	3.56 (s, 3H)	7.53 (s, 1H)	6.85 (s, 1H)	3.73 (s, 2H)	4.56 (s, 2H)
Bu	<b>95c</b>	3.53 (s, 3H)	7.45 (s, 1H)	6.82 (s, 1H)	3.71 (s, 2H)	4.53 (s, 2H)

**Table 65:**  $^1\text{H}$  NMR data of the cyclisation products **95a–d** in  $\text{CDCl}_3$  (continued).

R	#	R
Me	<b>95a</b>	1.87 (s, 3H)
Et	<b>95b</b>	2.35 (q, J = 7.6 Hz, 2H), 1.14 (t, J = 7.6 Hz, 3H)
Pr	<b>95c</b>	2.29 (t, J = 7.7 Hz, 2H), 1.62–1.51 (m, 2H), 0.94 (t, J = 7.4 Hz, 3H)
Bu	<b>95c</b>	2.29 (t, J = 7.6 Hz, 2H), 1.53–1.45 (m, 2H), 1.40–1.28 (m, 2H), 0.90 (t, J = 7.3 Hz)

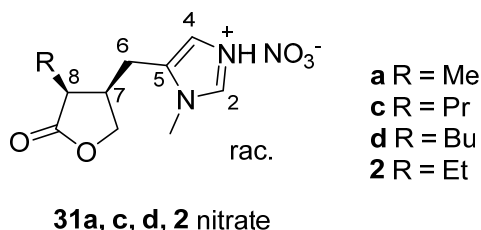
**Table 66:**  $^{13}\text{C}$  NMR data of the cyclisation products **95a–d** in  $\text{CDCl}_3$ .

R	#	N-CH <sub>3</sub>	C-2	C-4	C-5	C-6
Me	<b>95a</b>	31.5	138.9	128.2	125.9	22.5
Et	<b>95b</b>	31.3	138.7	127.7	126.0	21.9
Pr	<b>95c</b>	31.5	138.9	128.0	126.1	22.3
Bu	<b>95d</b>	31.5	138.8	128.1	126.0	22.3

**Table 67:**  $^{13}\text{C}$  NMR data of the cyclisation products **95a–d** in  $\text{CDCl}_3$  (continued).

R	#	C-7	-CH <sub>2</sub> -O-	C=O	C-8	R
Me	<b>95a</b>	155.3	71.4	174.8	124.8	8.8
Et	<b>95b</b>	155.0	71.0	174.2	129.9	17.0, 12.5
Pr	<b>95c</b>	155.6	71.2	174.4	128.9	25.8, 21.4, 14.1
Bu	<b>95d</b>	155.3	71.2	174.4	129.2	23.6, 30.2, 22.8, 13.9

### General Procedure for the Reduction of the Endocyclic Double Bond and Crystallisation of the Target Compounds



10% Palladium on activated charcoal (10 wt.-%) was added to a solution of the unsaturated precursor **95a–d** (485  $\mu\text{mol}$ , 1.00 eq.), respectively, in dry methanol (6 mL). The mixture was hydrogenated with 50 bar hydrogen atmosphere at a temperature of 50  $^{\circ}\text{C}$  (microwave irradiation) for 5 h. The reaction mixture was filtered through cotton and was washed with several portions of methanol. The filtrate

## Experimental

was evaporated and analysed by NMR. If complete conversion was not achieved, the reaction was repeated under the same conditions until complete conversion was achieved. The product was dissolved in methanol and filtered through a PVDF syringe filter (0.45  $\mu\text{m}$ ) to remove residual charcoal and catalyst. After evaporation of the solvent, the product was dissolved in a small amount of ethanol. Two drops of concentrated nitric acid were added. The mixture was kept at  $-18\text{ }^{\circ}\text{C}$  overnight and white needles of the methyl, ethyl and propyl analogues as nitrate salts crystallised. The crystals were recrystallised three times in ethanol.

In the case of the butyl analogue **31d**, crystallisation was not achieved and the compound could not be purified. **31d** was analysed as the free base crude product directly after reduction:

Formula:  $\text{C}_{13}\text{H}_{20}\text{N}_2\text{O}_2$ ;

MW: 236.32 g/mol;

*Trans*-impurity: 14%;

$^1\text{H}$  NMR ( $\text{CD}_3\text{OD}$ , 400 MHz):  $\delta$  (ppm) = 7.57 (s, 1H, **2-H**), 6.79 (s, 1H, **4-H**), 4.25 (dd,  $J = 9.2, 5.6$  Hz, 1H, **-CH<sub>2</sub>-O-**), 4.08 (dd,  $J = 9.2, 2.7$  Hz, **-CH<sub>2</sub>-O-**), 3.63 (s, 3H, **N-CH<sub>3</sub>**), 2.97–2.87 (m, 1H, **7-H**), 2.85–2.74 (m, 2H, **6-H, 8-H**), 2.58 (dd,  $J = 15.5, 11.5$  Hz, 1H, **6-H**), 1.82–1.14 (m, 6H, **R-H**), 0.96 (t,  $J = 7.1$  Hz, 3H, **R-H**);

$^{13}\text{C}$  NMR ( $\text{CD}_3\text{OD}$ , 101 MHz):  $\delta$  (ppm) = 180.9 ( $\text{C}_q$ , **C=O**), 139.5 (CH, **C-2**), 131.0 ( $\text{C}_q$ , **C-5**), 127.0 (CH, **C-4**), 71.5 ( $\text{CH}_2$ , **-CH<sub>2</sub>-O-**), 44.3 (CH, **C-8**), 38.6 (CH, **C-7**), 31.7 ( $\text{CH}_3$ , **N-CH<sub>3</sub>**), 30.9 ( $\text{CH}_2$ , **R**), 25.7 ( $\text{CH}_2$ , **R**), 23.6 ( $\text{CH}_2$ , **R**), 22.3 ( $\text{CH}_2$ , **C-6**), 14.2 ( $\text{CH}_3$ , **R**).

**Table 68:** General data of the nitrate salts of **31a, c** and **2**.

R	#	Formula	MW [g/mol]	Yield [%]	Purity [%] *	trans-Impurity [%]
Me	<b>31a</b> nitrate	$\text{C}_{10}\text{H}_{15}\text{N}_3\text{O}_5$	257.25	69	98	2
Et	<b>2</b> nitrate	$\text{C}_{11}\text{H}_{17}\text{N}_3\text{O}_5$	271.27	17	85	15
Pr	<b>31c</b> nitrate	$\text{C}_{12}\text{H}_{19}\text{N}_3\text{O}_5$	285.30	20	90	10

\* by qNMR in  $\text{CD}_3\text{OD}$ , external standard: maleic acid

**Table 69:** IR data of the nitrate salts of **31a, c** and **2**.

R	#	IR data [ $\text{cm}^{-1}$ ]
Me	<b>31a</b> nitrate	3113, 2900, 2804, 1760, 1607, 1556, 1458, 1232, 1175, 1011, 719, 689
Et	<b>2</b> nitrate	3122, 2884, 2805, 1764, 1610, 1556, 1456, 1232, 1175, 1009, 718, 677
Pr	<b>31c</b> nitrate	3111, 2863, 2791, 1770, 1605, 1557, 1457, 1210, 1166, 1020, 718, 654

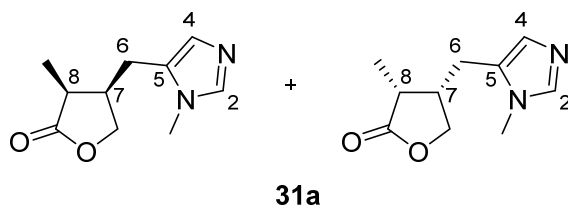


Table 70: <sup>1</sup>H NMR data of the nitrate salts of **31a**, **c** and **2** in CD<sub>3</sub>OD.

R #	N-CH <sub>3</sub>	2-H	4-H	6-H	7-H	-CH <sub>2</sub> -O-	8-H	R
<b>Me 31a</b> nitrate	3.87 (s, 3H)	8.85 (s, 1H)	7.46 (s, 1H)	2.69 (dd, J = 15.9, 9.9 Hz), 3.06-2.90 (m, 3H)	3.06-2.90 (m, 3H)	4.38 (dd, J = 9.3, 6.0 Hz, 1H), 4.09 (dd, J = 9.3, 4.2 Hz, 1H)	3.06-2.90 (m, 3H)	1.25 (d, J = 7.2 Hz, 3H)
<b>Et 2</b> nitrate	3.87 (s, 3H)	8.86 (s, 1H)	7.46 (s, 1H)	2.91 (dd, J = 16.0, 4.2 Hz, 1H), 2.65 (dd, J = 16.0, 11.5 Hz, 1H)	3.09-3.01 (m, 1H)	4.32 (dd, J = 9.4, 5.8 Hz, 1H), 4.09 (dd, J = 9.4, 3.3 Hz, 1H)	2.83-2.77 (m, 1H)	1.87-1.57 (m, 2H); 1.11 (t, J = 7.4 Hz, 3H)
<b>Pr 31c</b> nitrate	3.87 (s, 3H)	8.85 (s, 1H)	7.46 (s, 1H)	2.93-2.87 (m, 2H), 2.65 (dd, J = 15.8, 11.5 Hz, 1H)	3.08-3.00 (m, 1H)	4.31 (dd, J = 9.4, 5.7 Hz, 1H), 4.09 (dd, J = 9.4, 3.1 Hz, 1H)	2.93-2.87 (m, 2H)	1.76-1.46 (m, 4H); 1.01 (t, J = 7.1 Hz, 3H)

Table 71: <sup>13</sup>C NMR data of the nitrate salts of **31-3a**, **c** and **2** in CD<sub>3</sub>OD.

R #	N-CH <sub>3</sub>	C-2	C-4	C-5	C-6	C-7	-CH <sub>2</sub> -O-	C=O	C-8	R
<b>Me 31a</b> nitrate	33.8	137.1	118.1	134.5	22.5	38.1	71.4	181.6	38.7	10.4
<b>Et 2</b> nitrate	33.9	137.2	118.2	134.4	22.0	37.7	71.1	180.3	45.6	19.4, 12.4
<b>Pr 31c</b> nitrate	33.9	137.2	118.2	134.4	22.1	37.8	71.1	180.4	43.8	21.7, 28.1, 14.2

Separation of the Enantiomers of the Methylated *cis*-Analogues of Pilocarpine **31a**

The racemic mixture of the nitrate salt of **31a** (26 mg, 100  $\mu\text{mol}$ ) was dissolved in isopropanol (1.5 mL) and  $\text{Na}_2\text{SO}_4$  (85 mg, 600  $\mu\text{mol}$ ) was added. The mixture was sonicated for 2 min, the supernatant was pipetted into Eppendorf caps, and was centrifuged. The supernatant was filtered through a PVDF syringe filter. The solution was preparatively separated on a Lux<sup>®</sup> cellulose-4, 5  $\mu\text{m}$ , 4.6 x 200 mm column (20:80:0.1 *n*-hexane/isopropanol/diethylamine, 0.5 mL/min, 50 min). This yielded 3.59 mg and 3.47 mg of peak 1 and peak 2, respectively.

Purity of enantiomer 1: 89%, chiral HPLC (chiral method C) shows a purity of 94% which includes less than 5% of the coeluting *trans*-diastereomer seen in  $^1\text{H}$  NMR spectroscopy.

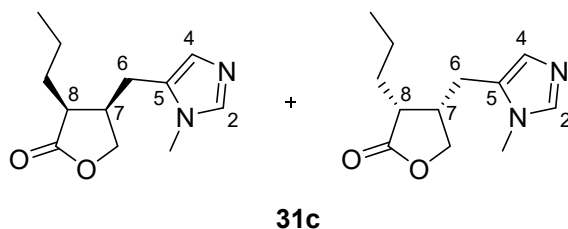
Purity of enantiomer 2: 98% (chiral method C);  $^1\text{H}$  NMR does not show the signals of *trans*-diastereomers.

$^1\text{H}$  NMR ( $\text{CD}_3\text{OD}$ , 400 MHz):  $\delta$  (ppm) = 7.61 (s, 1H, **2-H**), 6.81 (s, 1H, **4-H**), 4.31 (dd,  $J = 9.2, 5.7$  Hz, 1H, **-CH<sub>2</sub>-O-**), 4.08 (dd,  $J = 9.2, 3.7$  Hz, 1H, **-CH<sub>2</sub>-O-**), 3.64 (s, 3H, **N-CH<sub>3</sub>**), 3.00–2.90 (m, 2H, **7-H, 8-H**), 2.81 (dd,  $J = 15.6, 4.2$  Hz, 1H, **6-H**), 2.53 (dd,  $J = 15.6, 10.0$  Hz, 1H, **6-H**), 1.24 (d,  $J = 7.0$  Hz, 3H, **CH-CH<sub>3</sub>**);

$^{13}\text{C}$  NMR ( $\text{CD}_3\text{OD}$ , 101 MHz):  $\delta$  (ppm) = 182.1 ( $\text{C}_q$ , **C=O**), 139.4 (CH, **C-2**), 126.4 (CH, **C-4**), 71.7 ( $\text{CH}_2$ , **-CH<sub>2</sub>-O-**), 39.0 (CH, **C-8**), 38.9 (CH, **C-7**), 31.7 ( $\text{CH}_3$ , **N-CH<sub>3</sub>**), 22.7 ( $\text{CH}_2$ , **C-6**), 10.3 ( $\text{CH}_3$ , **CH-CH<sub>3</sub>**).

The  $^{13}\text{C}$  NMR signal of C-5 was not visible due to generally low intensities of detected peaks from this very dilute sample and assumed line broadening as a consequence of the quadrupolar moment of the neighbouring nitrogen atom.

## Attempted Separation of the Enantiomers of the Propylated *cis*-Analogues of Pilocarpine **31c**



The racemic mixture of the nitrate salt of **31c** (30 mg, 105  $\mu$ mol) was treated in the same way as the nitrate salt of **31a**. During the liberation of the free base, epimerisation occurred and three peaks were observed during the preparative separation on Lux<sup>®</sup> cellulose-4, 5  $\mu$ m, 4.6 x 200 mm (100:0.1 isopropanol/diethylamine, 0.5 mL/min, 50 min). All three peaks were collected to yield a mixture of the coeluting *cis*-enantiomer 1 and one *trans*-diastereomer (27:73; 4.93 mg), a pure *trans*-diastereomer (4.10 mg) and pure *cis*-enantiomer 2 (1.79 mg).

Purity of the *trans*-diastereomer: 94%; chiral HPLC (chiral method D) shows a purity of 96% which includes less than 2% of the coeluting *trans*-diastereomer seen in <sup>1</sup>H NMR spectroscopy.

Purity of *cis*-enantiomer 2: 89%; chiral HPLC (chiral method D) shows a purity of 91% which includes less than 2% of the coeluting *trans*-diastereomer seen in <sup>1</sup>H NMR spectroscopy.

NMR signals of the *cis*-enantiomers:

<sup>1</sup>H NMR (CD<sub>3</sub>OD, 400 MHz):  $\delta$  (ppm) = 7.64 (s, 1H, **2-H**), 6.83 (s, 1H, **4-H**), 4.25 (dd,  $J = 9.2, 5.6$  Hz, 1H, **-CH<sub>2</sub>-O-**), 4.07 (dd,  $J = 9.2, 2.7$  Hz, 1H, **-CH<sub>2</sub>-O-**), 3.64 (s, 3H, **N-CH<sub>3</sub>**), 2.98–2.73 (m, 3H, **7-H, 8-H, 6-H**), 2.49 (dd,  $J = 15.6, 11.3$  Hz, 1H, **6-H**), 1.80–1.42 (m, 4H, **-CH<sub>2</sub>-CH<sub>2</sub>-**), 1.01 (t,  $J = 7.1$  Hz, 3H, **CH<sub>2</sub>-CH<sub>3</sub>**);

<sup>13</sup>C NMR (CD<sub>3</sub>OD, 101 MHz):  $\delta$  (ppm) = 180.9 (C<sub>q</sub>, **C=O**), 71.4 (CH<sub>2</sub>, **-CH<sub>2</sub>-O-**), 44.1 (CH, **C-8**), 38.5 (CH, **C-7**), 31.8 (CH<sub>3</sub>, **N-CH<sub>3</sub>**), 28.2 (CH<sub>2</sub>, **-CH-CH<sub>2</sub>-CH<sub>2</sub>-**), 22.3 (CH<sub>2</sub>, **C-6**), 21.8 (CH<sub>2</sub>, **-CH<sub>2</sub>-CH<sub>2</sub>-CH<sub>3</sub>**), 14.2 (CH<sub>3</sub>, **CH-CH<sub>3</sub>**).

The <sup>13</sup>C NMR signal of C-2, C-4, and C-5 was not visible due to generally low intensities of detected peaks from this very dilute sample and assumed line broadening as a consequence of the quadrupolar moment of the neighbouring nitrogen atoms.

NMR signals of the *trans*-enantiomers:

<sup>1</sup>H NMR (CD<sub>3</sub>OD, 400 MHz):  $\delta$  (ppm) = 7.59 (s, 1H, **2-H**), 6.81 (s, 1H, **4-H**), 4.41 (dd,  $J = 9.1, 7.5$  Hz, 1H, **-CH<sub>2</sub>-O-**), 3.95 (dd,  $J = 9.1, 7.5$  Hz, 1H, **-CH<sub>2</sub>-O-**), 3.65 (s, 3H, **N-CH<sub>3</sub>**), 2.91 (dd,  $J = 15.4, 6.3$  Hz, 1H, **6-H**), 2.79 (dd,  $J = 15.4, 8.7$  Hz, 1H, **6-H**), 2.71–2.59 (m, 1H, **7-H**), 2.42 (dt,  $J = 8.2, 6.2$  Hz, 1H, **8-H**), 1.70–1.33 (m, 4H, **-CH<sub>2</sub>-CH<sub>2</sub>-CH<sub>3</sub>**), 0.92 (t,  $J = 7.2$  Hz, 3H, **-CH<sub>2</sub>-CH<sub>3</sub>**);

## Experimental

$^{13}\text{C}$  NMR ( $\text{CD}_3\text{OD}$ , 101 MHz):  $\delta$  (ppm) = 181.5 ( $\text{C}_q$ , **C=O**), 139.4 (CH, **C-2**), 126.8 (CH, **C-4**), 72.6 ( $\text{CH}_2$ , **-CH<sub>2</sub>-O-**), 46.1 (CH, **C-8**), 40.8 (CH, **C-7**), 32.5 ( $\text{CH}_3$ , **N-CH<sub>3</sub>**), 32.5 ( $\text{CH}_2$ , **-CH-CH<sub>2</sub>-CH<sub>2</sub>-**), 27.5 ( $\text{CH}_2$ , **C-6**), 20.9 ( $\text{CH}_2$ , **-CH<sub>2</sub>-CH<sub>2</sub>-CH<sub>3</sub>**), 14.3 ( $\text{CH}_3$ , **CH-CH<sub>3</sub>**).

The  $^{13}\text{C}$  NMR signal of **C-5** was not visible due to generally low intensities of detected peaks from this very dilute sample and assumed line broadening as a consequence of the quadrupolar moment of the neighbouring nitrogen atom.

## 7.6 Stability of Pilocarpine

### 7.6.1 Sample Preparation<sup>[112]</sup>

Pilocarpine (**2**) hydrochloride: 10 mg of commercial pilocarpine hydrochloride were dissolved in 10 mL of Millipore® water.

Hydrolysis products: 2 mL of the pilocarpine solution were mixed with 0.04 mL 35% ammonia and heated to 100 °C for 30 min.

HEPES buffer: 0.477 g HEPES, 0.407 g magnesium chloride hexahydrate and 1.168 g sodium chloride were dissolved in Milli-Q® water and adjusted to pH 7.4 with NaOH. The solution was adjusted to 200 mL.

Preparation of the stability sample: 10 mg of pilocarpine hydrochloride were dissolved in 10 mL of HEPES buffer.

### 7.6.2 HPLC Method

Column: Eurospher II 100-5 C18, Vertex Plu Column 125x4.6 mm, 16% carbon content, ca. 50% end-capped

Mobile phase: methanol/acetonitrile/aqueous tetrabutylammonium dihydrogen phosphate at pH 7.7 (ammonia) (0.679 g/L) 55:60:885

Flow rate: 1.2 mL/min

UV-Detection: 220 nm

Injection: 5  $\mu\text{L}$

Time of measurement: 40 min

### 7.6.3 Measurements

All reference samples were analysed once per HPLC, the stability sample was analysed 5 minutes after preparation and 24 h after preparation. The resulting chromatograms are shown in Figure 24, integrals can be found in Table 7 (Chapter 3.3).

## 8 References

- [1] a) S. Böhm, *Cholinerge Systeme*, in *Pharmakologie und Toxikologie: Von den molekularen Grundlagen zur Pharmakotherapie*, Springer, Berlin, Heidelberg, **2016**, pp. 123-127; b) M. P. Caulfield, N. J. M. Birdsall, *Pharmacol. Rev.* **1998**, *50*, 279-290.
- [2] S. Böhm, *Neurotransmission und Neuromodulation*, in *Pharmakologie und Toxikologie: Von den molekularen Grundlagen zur Pharmakotherapie*, Springer Berlin, Heidelberg, **2016**, pp. 105-115.
- [3] J. M. Berg, J. L. Tymoczko, G. J. Gatto jr., L. Stryer, *Signaltransduktionswege*, in *Stryer Biochemie*, Springer, Berlin, Heidelberg, **2018**, pp. 469-498.
- [4] V. Syrovatkina, K. O. Alegre, R. Dey, X.-Y. Huang, *J. Mol. Biol.* **2016**, *428*, 3850-3868.
- [5] M. Freissmuth, *Pharmakodynamik*, in *Pharmakologie und Toxikologie: Von den molekularen Grundlagen zur Pharmakotherapie*, Springer Berlin, Heidelberg, **2016**, pp. 41-54.
- [6] Boghog, *Idealized dose response curves of an agonist, partial agonist, neutral antagonist, and inverse agonist.*, <https://commons.wikimedia.org/w/index.php?curid=34657034>, **2014**, accessed 11.06.2021.
- [7] J. Wess, R. M. Eglen, D. Gautam, *Nat. Rev. Drug Discov.* **2007**, *6*, 721-733.
- [8] F. E. Köhler, *Köhler's Medizinal-Pflanzen*, [https://commons.wikimedia.org/wiki/File:Pilocarpus\\_pennatifolius\\_-\\_K%C3%B6hler%E2%80%93s\\_Medizinal-Pflanzen-238.jpg](https://commons.wikimedia.org/wiki/File:Pilocarpus_pennatifolius_-_K%C3%B6hler%E2%80%93s_Medizinal-Pflanzen-238.jpg), **1897**, accessed 06.04.2020.
- [9] K. Starke, *Pharmakologie cholinergischer Systeme*, in *Allgemeine und Spezielle Pharmakologie und Toxikologie* (Eds.: K. Aktories, U. Förstermann, F. Hofmann, K. Starke), Urban & Fischer Verlag, Philadelphia, Germany, **2017**, pp. 113-136.
- [10] A. Fisher, *Neurodegener. Dis.* **2008**, *5*, 237-240.
- [11] F. P. Bymaster, D. L. McKinzie, C. C. Felder, J. Wess, *Neurochem. Res.* **2003**, *28*, 437-442.
- [12] a) K. Haga, A. C. Kruse, H. Asada, T. Yurugi-Kobayashi, M. Shiroishi, C. Zhang, W. I. Weis, T. Okada, B. K. Kobilka, T. Haga, T. Kobayashi, *Nature* **2012**, *482*, 547-551; b) A. C. Kruse, J. Hu, A. C. Pan, D. H. Arlow, D. M. Rosenbaum, E. Rosemond, H. F. Green, T. Liu, P. S. Chae, R. O. Dror, D. E. Shaw, W. I. Weis, J. Wess, B. K. Kobilka, *Nature* **2012**, *482*, 552-556; c) D. M. Thal, B. Sun, D. Feng, V. Nawaratne, K. Leach, C. C. Felder, M. G. Bures, D. A. Evans, W. I. Weis, P. Bachhawat, T. S. Kobilka, P. M. Sexton, B. K. Kobilka, A. Christopoulos, *Nature* **2016**, *531*, 335-340; d) Z. Vuckovic, P. R. Gentry, A. E. Berizzi, K. Hirata, S. Varghese, G. Thompson, E. T. van

## References

- der Westhuizen, W. A. C. Burger, R. Rahmani, C. Valant, C. J. Langmead, C. W. Lindsley, J. B. Baell, A. B. Tobin, P. M. Sexton, A. Christopoulos, D. M. Thal, *Proc. Natl. Acad. Sci. USA* **2019**, *116*, 26001-26007.
- [13] A. C. Kruse, A. M. Ring, A. Manglik, J. Hu, K. Hu, K. Eitel, H. Hubner, E. Pardon, C. Valant, P. M. Sexton, A. Christopoulos, C. C. Felder, P. Gmeiner, J. Steyaert, W. I. Weis, K. C. Garcia, J. Wess, B. K. Kobilka, *Nature* **2013**, *504*, 101-106.
- [14] S. Maeda, Q. Qu, M. J. Robertson, G. Skiniotis, B. K. Kobilka, *Science* **2019**, *364*, 552-557.
- [15] J. A. Ballesteros, H. Weinstein, *Integrated methods for the construction of three-dimensional models and computational probing of structure-function relations in G protein-coupled receptors*, in *Methods in Neurosciences*, Vol. 25 (Ed.: S. C. Sealfon), Academic Press, **1995**, pp. 366-428.
- [16] K. Mohr, J. Schmitz, R. Schrage, C. Tränkle, U. Holzgrabe, *Angew. Chem. Int. Ed.* **2013**, *52*, 508-516.
- [17] D. Jäger, C. Schmalenbach, S. Prilla, J. Schrobang, A. Kebig, M. Sennwitz, E. Heller, C. Tränkle, U. Holzgrabe, H.-D. Höltje, K. Mohr, *J. Biol. Chem.* **2007**, *282*, 34968-34976.
- [18] a) W. A. C. Burger, P. M. Sexton, A. Christopoulos, D. M. Thal, *J. Gen. Physiol.* **2018**, *150*, 1360-1372; b) A. Bock, R. Schrage, K. Mohr, *Neuropharmacology* **2018**, *136*, 427-437.
- [19] T. P. Kenakin, *Br. J. Pharmacol.* **2012**, *165*, 1659-1669.
- [20] T. Kenakin, *Pharmacol. Rev.* **2019**, *71*, 267-315.
- [21] a) J. E. Davoren, C.-W. Lee, M. Garnsey, M. A. Brodney, J. Cordes, K. Dlugolenski, J. R. Edgerton, A. R. Harris, C. J. Helal, S. Jenkinson, G. W. Kauffman, T. P. Kenakin, J. T. Lazzaro, S. M. Lotarski, Y. Mao, D. M. Nason, C. Northcott, L. Nottebaum, S. V. O'Neil, B. Pettersen, M. Popiolek, V. Reinhart, R. Salomon-Ferrer, S. J. Steyn, D. Webb, L. Zhang, S. Grimwood, *J. Med. Chem.* **2016**, *59*, 6313-6328; b) J. E. Marlo, C. M. Niswender, E. L. Days, T. M. Bridges, Y. Xiang, A. L. Rodriguez, J. K. Shirey, A. E. Brady, T. Nalywajko, Q. Luo, C. A. Austin, M. B. Williams, K. Kim, R. Williams, D. Orton, H. A. Brown, C. W. Lindsley, C. D. Weaver, P. J. Conn, *Mol. Pharmacol.* **2009**, *75*, 577-588.
- [22] S. J. Bradley, C. Molloy, P. Valuskova, L. Dwomoh, M. Scarpa, M. Rossi, L. Finlayson, K. A. Svensson, E. Chernet, V. N. Barth, K. Gherbi, D. A. Sykes, C. A. Wilson, R. Mistry, P. M. Sexton, A. Christopoulos, A. J. Mogg, E. M. Rosethorne, S. Sakata, R. A. John Challiss, L. M. Broad, A. B. Tobin, *Nat. Chem. Biol.* **2020**, *16*, 240-249.
- [23] S. A. Hollingsworth, B. Kelly, C. Valant, J. A. Michaelis, O. Mastromihalis, G. Thompson, A. J. Venkatakrishnan, S. Hertig, P. J. Scammells, P. M. Sexton, C. C. Felder, A. Christopoulos, R. O. Dror, *Nat. Commun.* **2019**, *10*, 3289.
- [24] R. A. Leppik, R. C. Miller, M. Eck, J. L. Paquet, *Mol. Pharmacol.* **1994**, *45*, 983-990.

## References

- [25] a) R. Schwyzer, *Ann. N.Y. Acad. Sci.* **1977**, 297, 3-26; b) J. Antony, K. Kellershohn, M. Mohr-Andrä, A. Kebig, S. Prilla, M. Muth, E. Heller, T. Disingrini, C. Dallanoce, S. Bertoni, J. Schrobang, C. Tränkle, E. Kostenis, A. Christopoulos, H.-D. Höltje, E. Barocelli, M. DeAmici, U. Holzgrabe, K. Mohr, *FASEB J.* **2009**, 23, 442-450; c) K. Mohr, C. Tränkle, E. Kostenis, E. Barocelli, M. DeAmici, U. Holzgrabe, *Br. J. Pharmacol.* **2010**, 159, 997-1008.
- [26] R. Schrage, W. K. Seemann, J. Klöckner, C. Dallanoce, K. Racké, E. Kostenis, M. DeAmici, U. Holzgrabe, K. Mohr, *Br. J. Pharmacol.* **2013**, 169, 357-370.
- [27] T. Disingrini, M. Muth, C. Dallanoce, E. Barocelli, S. Bertoni, K. Kellershohn, K. Mohr, M. DeAmici, U. Holzgrabe, *J. Med. Chem.* **2006**, 49, 366-372.
- [28] a) A. Bock, M. Bermudez, F. Krebs, C. Matera, B. Chirinda, D. Sydow, C. Dallanoce, U. Holzgrabe, M. DeAmici, M. J. Lohse, G. Wolber, K. Mohr, *J. Biol. Chem.* **2016**, 16375-16389; b) A. Bock, B. Chirinda, F. Krebs, R. Messerer, J. Bätz, M. Muth, C. Dallanoce, D. Klingenthal, C. Tränkle, C. Hoffmann, M. DeAmici, U. Holzgrabe, E. Kostenis, K. Mohr, *Nat. Chem. Biol.* **2014**, 10, 18-20.
- [29] a) J. Schmitz, Ph.D. thesis, Julius-Maximilians-Universität Würzburg **2008**; b) A. Pegoli, X. She, D. Wifling, H. Hübner, G. Bernhardt, P. Gmeiner, M. Keller, *J. Med. Chem.* **2017**, 60, 3314-3334; c) A. Pegoli, D. Wifling, C. G. Gruber, X. She, H. Hübner, G. Bernhardt, P. Gmeiner, M. Keller, *J. Med. Chem.* **2019**, 62, 5358-5369; d) X. She, A. Pegoli, J. Mayr, H. Hübner, G. Bernhardt, P. Gmeiner, M. Keller, *ACS Omega* **2017**, 2, 6741-6754.
- [30] a) D. Volpato, M. Kauk, R. Messerer, M. Bermudez, G. Wolber, A. Bock, C. Hoffmann, U. Holzgrabe, *ACS Omega* **2020**, 5, 31706-31715; b) R. Messerer, M. Kauk, D. Volpato, M. C. Alonso Canizal, J. Klöckner, U. Zabel, S. Nuber, C. Hoffmann, U. Holzgrabe, *ACS Chem. Biol.* **2017**, 12, 833-843; c) A. Bonifazi, H. Yano, F. Del Bello, A. Farande, W. Quaglia, R. Petrelli, R. Matucci, M. Nesi, G. Vistoli, S. Ferré, A. Piergentili, *J. Med. Chem.* **2014**, 57, 9065-9077.
- [31] a) M. Bermudez, A. Bock, F. Krebs, U. Holzgrabe, K. Mohr, M. J. Lohse, G. Wolber, *ACS Chem. Biol.* **2017**, 12, 1743-1748; b) A. Bock, N. Merten, R. Schrage, C. Dallanoce, J. Bätz, J. Klöckner, J. Schmitz, C. Matera, K. Simon, A. Kebig, L. Peters, A. Müller, J. Schrobang-Ley, C. Tränkle, C. Hoffmann, M. DeAmici, U. Holzgrabe, E. Kostenis, K. Mohr, *Nat. Commun.* **2012**, 3, 1044.
- [32] J. Holze, M. Bermudez, E. M. Pfeil, M. Kauk, T. Bodefild, M. Irmen, C. Matera, C. Dallanoce, M. De Amici, U. Holzgrabe, G. M. König, C. Tränkle, G. Wolber, R. Schrage, K. Mohr, C. Hoffmann, E. Kostenis, A. Bock, *ACS Pharmacol Transl Sci* **2020**, 3, 859-867.
- [33] W. K. Seemann, D. Wenzel, R. Schrage, J. Etscheid, T. Bodefild, A. Bartol, M. Warnken, P. Sasse, J. Klöckner, U. Holzgrabe, M. DeAmici, E. Schlicker, K. Racké, E. Kostenis, R. Meyer, B. K. Fleischmann, K. Mohr, *J. Pharmacol. Exp. Ther.* **2017**, 360, 289-299.

## References

- [34] a) C. Matera, L. Flammini, M. Quadri, V. Vivo, V. Ballabeni, U. Holzgrabe, K. Mohr, M. DeAmici, E. Barocelli, S. Bertoni, C. Dallanoce, *Eur. J. Med. Chem.* **2014**, *75*, 222-232; b) C. Matera, L. Flammini, F. Riefolo, G. Domenichini, M. DeAmici, E. Barocelli, C. Dallanoce, S. Bertoni, *Eur. J. Pharmacol.* **2020**, *876*, 173061.
- [35] I. Cristofaro, Z. Spinello, C. Matera, M. Fiore, L. Conti, M. DeAmici, C. Dallanoce, A. M. Tata, *Neurochem. Int.* **2018**, *118*, 52-60.
- [36] a) L. Agnetta, M. Kauk, M. C. A. Canizal, R. Messerer, U. Holzgrabe, C. Hoffmann, M. Decker, *Angew. Chem. Int. Ed.* **2017**, *56*, 7282-7287; b) F. Riefolo, C. Matera, A. Garrido-Charles, A. M. J. Gomila, R. Sortino, L. Agnetta, E. Claro, R. Masgrau, U. Holzgrabe, M. Batlle, M. Decker, E. Guasch, P. Gorostiza, *J. Am. Chem. Soc.* **2019**, *141*, 7628-7636.
- [37] S. S. Hegde, M. T. Pulido-Rios, M. A. Luttmann, J. J. Foley, G. E. Hunsberger, T. Steinfeld, T. Lee, Y. Ji, M. M. Mammen, J. R. Jasper, *Pharmacol. Res. Perspect.* **2018**, *6*, e00400.
- [38] US Food and Drug Administration, *Drug Approval Package: Yupelri (revefenacin)*, [https://www.accessdata.fda.gov/drugsatfda\\_docs/nda/2018/210598Orig1s000TOC.cfm](https://www.accessdata.fda.gov/drugsatfda_docs/nda/2018/210598Orig1s000TOC.cfm), accessed 03.02.2022.
- [39] S. S. Hegde, A. D. Hughes, Y. Chen, T. Steinfeld, J. R. Jasper, T.-W. Lee, A. McNamara, W. J. Martin, M. T. Pulido-Rios, M. Mammen, *J. Pharmacol. Exp. Ther.* **2014**, *351*, 190-199.
- [40] B. Holmstedt, S. H. Wassén, R. E. Schultes, *J. Ethnopharmacol.* **1979**, *1*, 3-21.
- [41] R. Grewe, *Klin. Monatsbl. Augenheilkd.* **1986**, *188*, 167-169.
- [42] a) A. W. Gerrard, *Pharm. J.* **1875**, 865; b) M. E. Hardy, *Bull. Soc. Chim. Paris* **1875**, *24*, 497-500.
- [43] a) H. A. D. Jowett, *J. Chem. Soc. Trans.* **1900**, *77*, 473-498; b) A. Pinner, R. Schwarz, *Ber. Dtsch. Chem. Ges.* **1902**, *35*, 2441-2459.
- [44] R. K. Hill, S. Barcza, *Tetrahedron* **1966**, *22*, 2889-2893.
- [45] L. Maat, H. C. Beyerman, *The Imidazole Alkaloids*, in *The Alkaloids. Chemistry and Pharmacology*, Vol. 22 (Ed.: A. Brossi), Academic Press, New York, **1983**, pp. 282-334.
- [46] *Arzneimittel-Informationssystem (AMIce)*, Bundesinstitut für Arzneimittel und Medizinprodukte; <https://portal.dimdi.de/amguifree/termsfuse.xhtml>; search for "Stoffname"="Pilocarpin", accessed 30.06.2021.
- [47] a) G. Curia, D. Longo, G. Biagini, R. S. G. Jones, M. Avoli, *J. Neurosci. Methods* **2008**, *172*, 143-157; b) E. A. Cavalheiro, *Ital. J. Neurol. Sci.* **1995**, *16*, 33-37.
- [48] L. Berggren, *Acta Ophthalmol.* **1970**, *48*, 293-302.
- [49] W. Langenbeck, *J. prakt. Chem.* **1928**, *119*, 77-80.
- [50] a) H. Yoshida, K. Takeyasu, S. Uchida, *Trends Pharmacol. Sci.* **1979**, *1*, 34-36; b) P. D. Williams, W. E. Colbert, T. J. Shetler, J. A. Turk, *Gen. Pharmac.* **1992**, *23*, 177-185.



## References

- [51] K. W. Figueroa, M. T. Griffin, F. J. Ehlert, *J. Pharmacol. Exp. Ther.* **2009**, *328*, 331-342.
- [52] M. K. O. Grant, E. E. El-Fakahany, *J. Pharmacol. Exp. Ther.* **2005**, *315*, 313-319.
- [53] F. J. Ehlert, M. T. Griffin, G. W. Sawyer, R. Bailon, *J. Pharmacol. Exp. Ther.* **1999**, *289*, 981-992.
- [54] J. C. Foreman, T. Johansen, A. J. Gibb, *Textbook of Receptor Pharmacology*, CRC Press, Boca Roca, US, **2010**.
- [55] F. B. Hofmann, *Wirkungen von Pharmaka auf den Organismus: allgemeine Pharmakodynamik*, in *Allgemeine und Spezielle Pharmakologie und Toxikologie: Begründet Von W. Forth, D. Henschler, W. Rummel*, Urban & Fischer, Philadelphia, Germany, **2017**, p. 8f.
- [56] T. Kenakin, *FASEB J.* **2001**, *15*, 598-611.
- [57] R. Mistry, M. R. Dowling, R. A. J. Challiss, *Br. J. Pharmacol.* **2005**, *144*, 566-575.
- [58] A. N. Pronin, Q. Wang, V. Z. Slepak, *Mol. Pharmacol.* **2017**, *92*, 601-612.
- [59] R. T. Koda, F. J. Dea, K. Fung, C. Elison, J. A. Biles, *J. Pharm. Sci.* **1973**, *62*, 2021-2023.
- [60] a) P. Floersheim, E. Pombo-Villar, G. Shapiro, *Chimia* **1992**, *46*, 323-334; b) G. Shapiro, P. Floersheim, J. Boelsterli, R. Amstutz, G. Bolliger, H. Gammenthaler, G. Gmelin, P. Supavilai, M. Walkinshaw, *J. Med. Chem.* **1992**, *35*, 15-27.
- [61] R. F. Borne, H. Y. Aboul-Enein, I. W. Waters, J. Hicks, *J. Med. Chem.* **1973**, *16*, 245-247.
- [62] H. Y. Aboul-Enein, A. A. Al-Badr, *Meth. Find. Exptl. Clin. Pharmacol.* **1982**, *4*, 321-329.
- [63] H. Y. Aboul-Enein, S. E. Ibrahim, A. A. Al-Badr, M. Ismail, *Toxicol. Environ. Chem.* **1986**, *11*, 253-259.
- [64] A. Noordam, K. Waliszewski, C. Olieman, L. Maat, H. C. Beyerman, *J. Chromatogr. A* **1978**, *153*, 271-273.
- [65] P. Sauerberg, J. Chen, E. WoldeMussie, H. Rapoport, *J. Med. Chem.* **1989**, *32*, 1322-1326.
- [66] S. H. Hobbs, S. J. Johnson, S. R. Kesten, M. R. Pavia, R. E. Davis, R. D. Schwarz, L. L. Coughenour, S. L. Myers, D. T. Dudley, W. H. Moss, *Bioorg. Med. Chem. Lett.* **1991**, *1*, 147-150.
- [67] E. Brochmann-Hanssen, G. L. Jenkins, J. B. Data, *J. Am. Pharm. Assoc.* **1951**, *40*, 61-67.
- [68] A. Ben Bassat, D. Lavie, H. Edery, G. Porath, *J. Med. Chem.* **1971**, *14*, 1066-1069.
- [69] H. Y. Aboul-Enein, A. A. Al-Badr, M. S. Rashed, M. Ismail, *Toxicol. Environ. Chem.* **1986**, *11*, 183-190.
- [70] P. Druzgala, D. Winwood, M. Drewniak-Deyrup, S. Smith, N. Bodor, J. J. Kaminski, *Pharm. Res.* **1992**, *9*, 372-377.
- [71] a) A. Rinne, J. C. Mobarec, M. Mahaut-Smith, P. Kolb, M. Bünemann, *Sci. Signal.* **2015**, *8*, ra110-ra110; b) F. Heitz, J. A. Holzwarth, J.-P. Gies, R. M. Pruss, S. Trumpp-Kallmeyer, M. F. Hibert, C. Guenet, *Eur. J. Pharmacol.* **1999**, *380*, 183-195; c) G. Vistoli, A. Pedretti, S. Dei, S. Scapecchi, C. Marconi, M. N. Romanelli, *Bioorg. Med. Chem.* **2008**, *16*, 3049-3058; d) K.

## References

- Leach, A. E. Davey, C. C. Felder, P. M. Sexton, A. Christopoulos, *Mol. Pharmacol.* **2011**, *79*, 855-865.
- [72] H. Bourdon, S. Trumpp-Kallmeyer, H. Schreuder, J. Hoflack, M. Hibert, C.-G. Wermuth, *J. Comput. Aided Mol. Des.* **1997**, *11*, 317-332.
- [73] M. Bermudez, University of Münster, unpublished results.
- [74] J. Jakubík, L. Bačáková, E. E. El-Fakahany, S. Tuček, *Mol. Pharmacol.* **1997**, *52*, 172-179.
- [75] K. Zahn, N. Eckstein, C. Tränkle, W. Sadée, K. Mohr, *J. Pharmacol. Exp. Ther.* **2002**, *301*, 720-728.
- [76] C. Valant, C. C. Felder, P. M. Sexton, A. Christopoulos, *Mol. Pharmacol.* **2012**, *81*, 41-52.
- [77] A. E. Berizzi, P. R. Gentry, P. Rueda, S. Den Hoedt, P. M. Sexton, C. J. Langmead, A. Christopoulos, *Mol. Pharmacol.* **2016**, *90*, 427-436.
- [78] a) L. Agnetta, M. Bermudez, F. Riefolo, C. Matera, E. Claro, R. Messerer, T. Littmann, G. Wolber, U. Holzgrabe, M. Decker, *J. Med. Chem.* **2019**, *62*, 3009-3020; b) K. Mohr, C. Tränkle, U. Holzgrabe, *Recept. Channels* **2003**, *9*, 229-240.
- [79] M. V. Drake, J. J. O'Donnell, J. R. Polansky, *J. Pharm. Sci.* **1986**, *75*, 278-279.
- [80] C. Liao, M. C. Nicklaus, *J. Chem. Inf. Model.* **2009**, *49*, 2801-2812.
- [81] J. L. Belletire, N. O. Mahmoodi, *J. Nat. Prod.* **1992**, *55*, 194-206.
- [82] J. M. Dener, L. H. Zhang, H. Rapoport, *J. Org. Chem.* **1993**, *58*, 1159-1166.
- [83] D. D. Long, L. Jiang, D. R. Saito, D. P. Van (Theravance Inc.), WO2009029253 A1, **2009**.
- [84] B. J. Naysmith, M. A. Brimble, *Org. Lett.* **2013**, *15*, 2006-2009.
- [85] L. J. Andrews, J. E. Hardwicke, *J. Am. Chem. Soc.* **1952**, *74*, 3582-3586.
- [86] E. R. Samuels, I. Sevrioukova, *Tetrahedron Lett.* **2018**, *59*, 1140-1142.
- [87] A. Baba, M. Yasuda, Y. Nishimoto, *Zinc Enolates: The Reformatsky and Blaise Reaction*, in *Comprehensive Organic Synthesis, Vol. 2. Additions to C-X pi-bonds, Part 2*, 2nd ed. (Eds.: K. Mikami, P. Knochel, G. A. Molander), Elsevier Science, Amsterdam, Oxford, Waltham, **2014**.
- [88] a) H. E. Zimmerman, M. D. Traxler, *J. Am. Chem. Soc.* **1957**, *79*, 1920-1923; b) L. Fernández-Sánchez, J. A. Fernández-Salas, M. C. Maestro, J. L. García Ruano, *J. Org. Chem.* **2018**, *83*, 12903-12910.
- [89] G. Rousseau, J. M. Conia, *Tetrahedron Lett.* **1981**, *22*, 649-652.
- [90] P. Gmeiner, P. L. Feldman, M. Y. Chu-Moyer, H. Rapoport, *J. Org. Chem.* **1990**, *55*, 3068-3074.
- [91] E. J. Karppanen, A. M. P. Koskinen, *Molecules* **2010**, *15*, 6512.
- [92] J. M. Humphrey, R. J. Bridges, J. A. Hart, A. R. Chamberlin, *J. Org. Chem.* **1994**, *59*, 2467-2472.
- [93] J. P. Wolf, H. Rapoport, *J. Org. Chem.* **1989**, *54*, 3164-3173.
- [94] a) D. F. Bowersox, E. H. Swift, *Anal. Chem.* **1958**, *30*, 1288-1291; b) H. Barber, E. Grzeskowiak, *Anal. Chem.* **1949**, *21*, 192-192.

## References

- [95] R. S. Compagnone, H. Rapoport, *J. Org. Chem.* **1986**, *51*, 1713-1719.
- [96] P. G. M. Wuts, *Greene's Protective Groups in Organic Chemistry*, 5th ed., John Wiley & Sons, Hoboken, New Jersey, **2014**.
- [97] D. Hellwinkel, T. Kosack, *Liebigs Ann. Chem.* **1985**, *1985*, 226-238.
- [98] X. Wang, J. Lin, Y. Chen, W. Zhong, G. Zhao, H. Liu, S. Li, L. Wang, S. Li, *Bioorg. Med. Chem.* **2009**, *17*, 1898-1904.
- [99] a) T. Le Diguarher, J.-C. Ortuno, G. Dorey, D. Shanks, N. Guilbaud, A. Pierré, J.-L. Fauchère, J. A. Hickman, G. C. Tucker, P. J. Casara, *Bioorg. Med. Chem.* **2003**, *11*, 3193-3204; b) P. E. Maligres, M. S. Waters, S. A. Weissman, J. C. McWilliams, S. Lewis, J. Cowen, R. A. Reamer, R. P. Volante, P. J. Reider, D. Askin, *J. Heterocycl. Chem.* **2003**, *40*, 229-241.
- [100] M. Mettry, M. P. Moehlig, R. J. Hooley, *Org. Lett.* **2015**, *17*, 1497-1500.
- [101] M. A. Blanchette, W. Choy, J. T. Davis, A. P. Essensfeld, S. Masamune, W. R. Roush, T. Sakai, *Tetrahedron Lett.* **1984**, *25*, 2183-2186.
- [102] B. Li, M. Berliner, R. Buzon, C. K. F. Chiu, S. T. Colgan, T. Kaneko, N. Keene, W. Kissel, T. Le, K. R. Leeman, B. Marquez, R. Morris, L. Newell, S. Wunderwald, M. Witt, J. Weaver, Z. Zhang, Z. Zhang, *J. Org. Chem.* **2006**, *71*, 9045-9050.
- [103] a) N. M. Yoon, C. S. Pak, C. Brown Herbert, S. Krishnamurthy, T. P. Stocky, *J. Org. Chem.* **1973**, *38*, 2786-2792; b) H. C. Brown, Y. M. Choi, S. Narasimhan, *J. Org. Chem.* **1982**, *47*, 3153-3163; c) R. O. Hutchins, F. Cistone, *Org. Prep. Proced. Int.* **1981**, *13*, 225-240; d) G. W. Kabalka, *Org. Prep. Proced. Int.* **1977**, *9*, 131-147.
- [104] T. H. Graham, *Tetrahedron Lett.* **2015**, *56*, 2688-2690.
- [105] S. Ram, L. D. Spicer, *Tetrahedron Lett.* **1987**, *28*, 515-516.
- [106] I. T. Forbes, C. N. Johnson, M. Thompson, *J. Chem. Soc., Perkin Trans. 1* **1992**, 275-281.
- [107] R. Gigg, R. Conant, *J. Chem. Soc., Chem. Commun.* **1983**, 465-466.
- [108] E. C. Jorgensen, G. C. Windridge, T. C. Lee, *J. Med. Chem.* **1970**, *13*, 352-356.
- [109] J. Schmitz, D. van der Mey, M. Bermudez, J. Klöckner, R. Schrage, E. Kostenis, C. Tränkle, G. Wolber, K. Mohr, U. Holzgrabe, *J. Med. Chem.* **2014**, *57*, 6739-6750.
- [110] F. Winter, R. Kimmich, *Mol. Phys.* **1982**, *45*, 33-49.
- [111] a) M. A. Nunes, E. Brochmann-Hanssen, *J. Pharm. Sci.* **1974**, *63*, 716-721; b) H. Bundgaard, S. H. Hansen, *Int. J. Pharm.* **1982**, *10*, 281-289.
- [112] *Europäisches Arzneibuch (amtliche deutsche Ausgabe)*, 7th ed., Deutscher Apothekerverlag, Stuttgart, **2011**.
- [113] US National Library of Medicine, *ChemIDplus database*, <https://chem.nlm.nih.gov/chemidplus/name/pilocarpine>, accessed 20.12.2021.
- [114] S. A. I. Ltd., *SiriusT3Control*, Version 1.1.3.0, **2013**.

## References

- [115] B. Carpenter, C. G. Tate, *Protein Eng. Des. Sel.* **2016**, *29*, 583-594.
- [116] a) R. Nehmé, B. Carpenter, A. Singhal, A. Strege, P. C. Edwards, C. F. White, H. Du, R. Grisshammer, C. G. Tate, *PLOS ONE* **2017**, *12*, e0175642; b) Q. Wan, N. Okashah, A. Inoue, R. Nehmé, B. Carpenter, C. G. Tate, N. A. Lambert, *J. Biol. Chem.* **2018**, *293*, 7466-7473.
- [117] C. G. England, E. B. Ehlerding, W. Cai, *Bioconjugate Chem.* **2016**, *27*, 1175-1187.
- [118] T. Nagai, K. Ibata, E. S. Park, M. Kubota, K. Mikoshiba, A. Miyawaki, *Nat. Biotechnol.* **2002**, *20*, 87-90.
- [119] Y. Chastagnier, E. Moutin, A.-L. Hemonnot, J. Perroy, *Front. Comput. Neurosci.* **2018**, *11*.
- [120] X. Chen, J. Klöckner, J. Holze, C. Zimmermann, W. K. Seemann, R. Schrage, A. Bock, K. Mohr, C. Tränkle, U. Holzgrabe, M. Decker, *J. Med. Chem.* **2015**, *58*, 560-576.
- [121] J. P. Kukkonen, J. Näsman, P. Ojala, C. Oker-Blom, K. E. Akerman, *J. Pharmacol. Exp. Ther.* **1996**, *279*, 593-601.
- [122] W. Hoss, J. M. Woodruff, B. R. Ellerbrock, S. Periyasamy, S. Ghodsi-Hovsepian, J. Stibbe, M. Bohnett, W. S. Messer, *Brain Res.* **1990**, *533*, 232-238.
- [123] F. L. Pyman, *J. Chem. Soc. Trans.* **1912**, *101*, 2260-2271.
- [124] R. A. Anderson, J. B. Cowle, *Brit. J. Ophthalmol.* **1968**, *52*, 607-611.
- [125] a) M. DeAmici, C. Dallanoce, U. Holzgrabe, C. Tränkle, K. Mohr, *Med. Res. Rev.* **2010**, *30*, 463-549; b) M. Muth, W. Bender, O. Scharfenstein, U. Holzgrabe, E. Balatkova, C. Tränkle, K. Mohr, *J. Med. Chem.* **2003**, *46*, 1031-1040.
- [126] A. DeMin, C. Matera, A. Bock, J. Holze, J. Kloeckner, M. Muth, C. Traenkle, M. DeAmici, T. Kenakin, U. Holzgrabe, C. Dallanoce, E. Kostenis, K. Mohr, R. Schrage, *Mol. Pharmacol.* **2017**, *91*, 348-356.
- [127] T. Steinfeld, M. Mammen, J. A. M. Smith, R. D. Wilson, J. R. Jasper, *Mol. Pharmacol.* **2007**, *72*, 291-302.
- [128] C. Valant, K. J. Gregory, N. E. Hall, P. J. Scammells, M. J. Lew, P. M. Sexton, A. Christopoulos, *J. Biol. Chem.* **2008**, *283*, 29312-29321.
- [129] M. C. L. Wakeham, B. J. Davie, D. K. Chalmers, A. Christopoulos, B. Capuano, C. Valant, P. J. Scammells, *ACS Chem. Neurosci.* **2022**, *13*, 97-111.
- [130] C. Valant, J. R. Lane, P. M. Sexton, A. Christopoulos, *Annu. Rev. Pharmacool. Toxicol.* **2012**, *52*, 153-178.
- [131] H. Link, K. Bernauer, *Helv. Chim. Acta* **1972**, *55*, 1053-1062.
- [132] M. Y. Berezin, J. Kao, S. Achilefu, *Chem. Eur. J.* **2009**, *15*, 3560-3566.
- [133] M. Braun, C. Bühne, D. Cougali, K. Schaper, W. Frank, *Synthesis* **2004**, 2905-2909.
- [134] U. Heywang, M. Casutt, M. Schwarz (Merck Patent GmbH), DE4033612 A1, **1992**.
- [135] J. J. Lee, L.-F. Huang, K. Zaw, L. Bauer, *J. Heterocycl. Chem.* **1998**, *35*, 81-89.

## References

- [136] M. Kirihara, Y. Asai, S. Ogawa, T. Noguchi, A. Hatano, Y. Hirai, *Synthesis* **2007**, 2007, 3286-3289.
- [137] S. Ohta, T. Yamamoto, I. Kawasaki, M. Yamashita, H. Katsuma, R. Nasako, K. Kobayashi, K. Ogawa, *Chem. Pharm. Bull.* **1992**, 40, 2681-2685.
- [138] D. Cogan, M.-H. Hao, V. M. Kamhi, C. A. Miller, M. R. Netherton, A. D. Swinamer (Boehringer Ingelheim Pharmaceuticals Inc.), WO2005090333 A1, **2005**.
- [139] R. K. Haynes, S. C. Vonwiller, M. R. Luderer, *N,N,N',N'-Tetramethylethylenediamine* in *Encyclopedia of Reagents for Organic Synthesis*, <https://doi.org/10.1002/047084289X.rt064.pub2>, John Wiley & Sons, Ltd., Hoboken, NJ, USA, **2006**.
- [140] a) T. Mukhopadhyay, D. Seebach, *Helv. Chim. Acta* **1982**, 65, 385-391; b) R. R. Dykstra, *Hexamethylphosphoric Triamide*, in *Encyclopedia of Reagents for Organic Synthesis*, (<https://doi.org/10.1002/047084289X.rh020>), John Wiley & Sons, Ltd., Hoboken, NJ, USA, **2001**.
- [141] a) S. Takano, J. Kudo, M. Takahashi, K. Ogasawara, *Tetrahedron Lett.* **1986**, 27, 2405-2408; b) H. E. Zimmerman, *Acc. Chem. Res.* **1987**, 20, 263-268; c) S. Takano, W. Uchida, S. Hatakeyama, K. Ogasawara, *Chem. Lett.* **1982**, 11, 733-736.
- [142] C. Bühne, Ph.D. thesis, Heinrich-Heine-Universität Düsseldorf **2002**.
- [143] S. G. Davies, P. M. Roberts, P. T. Stephenson, H. R. Storr, J. E. Thomson, *Tetrahedron* **2009**, 65, 8283-8296.
- [144] D. A. Horne, B. Fugmann, K. Yakushijin, G. Buchi, *J. Org. Chem.* **1993**, 58, 62-64.
- [145] E. Breitmeier, G. Jung, *Organische Chemie. Grundlagen, Stoffklassen, Reaktionen, Konzepte, Molekülstruktur*, 5th ed., Georg Thieme Verlag, Stuttgart, **2005**.
- [146] E. Reimann (Merck Patent GmbH), EP06447640 A1, **1995**.
- [147] R. Csuk, B. Woeste, *Tetrahedron* **2008**, 64, 9384-9387.
- [148] J. I. DeGraw, *Tetrahedron* **1972**, 28, 967-972.
- [149] H.-J. Deussen, M. Zundel, M. Valdois, S. V. Lehmann, V. Weil, C. M. Hjort, P. R. Østergaard, E. Marcussen, S. Ebdrup, *Org. Process Res. Dev.* **2003**, 7, 82-88.
- [150] a) R. Frlan, S. Gobec, D. Kikelj, *Tetrahedron* **2007**, 63, 10698-10708; b) M. K. Tay, E. Aboutjaudet, N. Collignon, M. P. Teulade, P. Savignac, *Synth. Commun.* **1988**, 18, 1349-1362; c) M. C. Schulbach, S. Mahapatra, M. Macchia, S. Barontini, C. Papi, F. Minutolo, S. Bertini, P. J. Brennan, D. C. Crick, *J. Biol. Chem.* **2001**, 276, 11624-11630.
- [151] A. K. Bhattacharya, G. Thyagarajan, *Chem. Rev.* **1981**, 81, 415-430.
- [152] R. J. Petroski, R. J. Bartelt, *J. Agric. Food. Chem.* **2007**, 55, 2282-2287.
- [153] ACD/Labs, *Advanced Chemistry Development Software V11.02*, via SciFinder-n, **2021**.

## References

- [154] T. J. Henderson, *Anal. Chem.* **2002**, *74*, 191-198.
- [155] R. Millet, J. Domarkas, R. Houssin, P. Gilleron, J.-F. Goossens, P. Chavatte, C. Logé, N. Pommery, J. Pommery, J.-P. Hénichart, *J. Med. Chem.* **2004**, *47*, 6812-6820.
- [156] S. G. Koenig, C. P. Vandenbossche, H. Zhao, P. Mousaw, S. P. Singh, R. P. Bakale, *Org. Lett.* **2009**, *11*, 433-436.
- [157] S. G. Davies, D. A. B. Mortimer, A. W. Mulvaney, A. J. Russell, H. Skarphedinsson, A. D. Smith, R. J. Vickers, *Org. Biomol. Chem.* **2008**, *6*, 1625-1634.
- [158] M. Baumann, I. R. Baxendale, *Org. Lett.* **2014**, *16*, 6076-6079.
- [159] C. G. Skinner, W. Shive, R. G. Ham, D. C. Fitzgerald, R. E. Eakin, *J. Am. Chem. Soc.* **1956**, *78*, 5097-5100.
- [160] A. Liljeblad, J. Lindborg, L. T. Kanerva, *Tetrahedron Asymmetry* **2000**, *11*, 3957-3966.
- [161] A. Schreiber, *Ž. Obs. Him. (via CAS)* **1969**, *39*, 1416.
- [162] N. Cohen, W. F. Eichel, R. J. Lopresti, C. Neukom, G. Saucy, *J. Org. Chem.* **1976**, *41*, 3505-3511.
- [163] J. Schmitz, E. Heller, U. Holzgrabe, *Monatsh. Chem.* **2007**, *138*, 171-174.
- [164] R. Messerer, C. Dallanoce, C. Matera, S. Wehle, L. Flammini, B. Chirinda, A. Bock, M. Irmen, C. Trankle, E. Barocelli, M. Decker, C. Sotriffer, M. DeAmici, U. Holzgrabe, *MedChemComm* **2017**, *8*, 1346-1359.
- [165] E. A. B. Kantchev, G.-R. Peh, C. Zhang, J. Y. Ying, *Org. Lett.* **2008**, *10*, 3949-3952.
- [166] B. S. Furniss, A. J. Hannaford, P. W. G. Smith, A. R. Tatchell, *Vogel's Textbook of Practical Organic Chemistry*, 5th ed., Longman Scientific & Technical, Harlow, **1989**.
- [167] M. Hieke, C. Greiner, M. Dittrich, F. Reisen, G. Schneider, M. Schubert-Zsilavecz, O. Werz, *J. Med. Chem.* **2011**, *54*, 4490-4507.
- [168] D. Menche, J. Hassfeld, J. Li, K. Mayer, S. Rudolph, *J. Org. Chem.* **2009**, *74*, 7220-7229.

## 9 Appendix

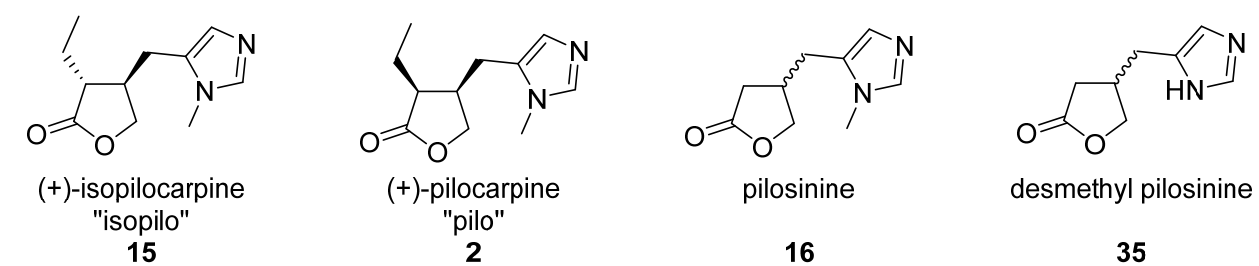


Figure 55: Overview of the synthesised orthosters.

Table 72: Overview of the synthesised hybrid molecules.

R	Molecule	n	Name
		<b>33a</b>	4 Pilo-4-naph
		<b>33b</b>	6 Pilo-6-naph
		<b>33c</b>	8 Pilo-8-naph
		<b>34a</b>	4 Isopilo-4-naph
		<b>34b</b>	6 Isopilo-6-naph
		<b>34c</b>	8 Isopilo-8-naph
		<b>69</b>	6 Desmethyl-pilosinine-6-naph
		<b>70</b>	6 Pilosinine-6-naph

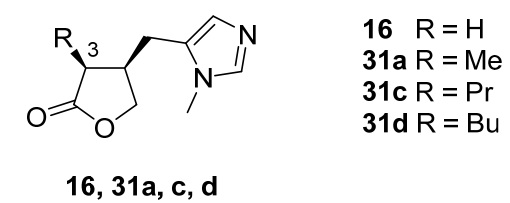


Figure 56: Overview of the targeted pilocarpine analogues.